COMPLEXATION BETWEEN CYCLODEXTRINS AND PHENYLUREA HERBICIDES IN SOLUTION AND IN THE SOLID STATE

BY: Vincent Joseph Smith M.Sc.

Thesis Presented for the Degree of

DOCTOR OF PHILOSOPHY

in the Department of Chemistry

UNIVERSITY OF CAPE TOWN

January 2009

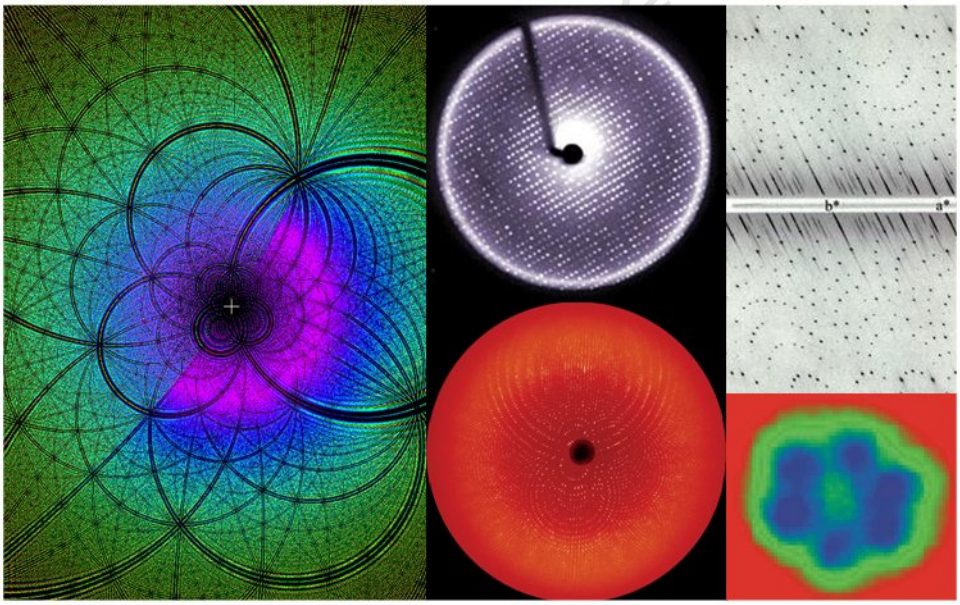

ACKNOWLEDGEMENTS

I would like to thank:
my supervisors, Professors Mino R Caira and Susan A Bourne, for their encouragement, support, excellent supervision, expertise and above all else providing the canvas on which I could express myself. I am forever grateful

Professor Luigi R Nassimbeni, for the advice, his kindness, encouragement, sense of humour and for being a constant source of knowledge

Dr Hong Su for the single crystal X-ray diffraction data collected on the Kappa CCD diffractometer

all the members of the Centre for Supramolecular Chemistry Research, UCT, for their assistance, entertainment, conversation and 'torment' during the course of this project, especially Dyanne Cruickshank and Jinjing Li

Drs Clive Oliver, Niki Báthori, Meredith Hearshaw and Andreas Lemmerer for their friendship and sense of humour

Diana Bogdan, Mircea Bogdan and Sorin Farcas at the National Institute for Research and Development of Isotopic and Molecular Technologies, Cluj-Napoca, Romania for valuable assistance and instruction on NMR analysis

The National Research Foundation, EDP and the University of Cape Town for financial support

my Friends and Family for their love, support and encouragement

Parts of this thesis have been presented at the following conferences:

Carman National Physical Chemistry Symposium, Johannesburg, 28th – 30th September 2005.

Poster presentation: Cyclodextrin inclusion of agrochemicals: complexation of the herbicide metobromuron.

Vincent J Smith, Mino R Caira and Susan A Bourne

International School of Crystallography, 39th course: "Engineering of crystalline Materials Properties: State-of-the-Art in Modeling, Design and Applications", Erice, Sicily, 7th – 17th July 2007.

Poster presentation: Multiplicity of crystal forms of a β-Cyclodextrin complex, Part I.

Vincent J Smith, Mino R Caira and Susan A Bourne

Carman National Physical Chemistry Symposium, Cape Town, 23rd – 27th September 2007.

Poster presentation: Multiplicity of crystal forms of a β-Cyclodextrin complex, Part II.

Vincent J Smith, Mino R Caira and Susan A Bourne

Fifth Conference: "Isotopic and Molecular Processes" 2007, September 20th - 22nd , Cluj-Napoca, Romania

Poster presentation: ^{1}H NMR Study of Inclusion Complexes of Phenylurea Derivatives in α-Cyclodextrin.

Vincent Smith, Diana Bogdan, Mihai Vasilescu, Mircea Bogdan, Mino R. Caira, Simion Simon.

ABSTRACT

Vincent Joseph Smith

COMPLEXATION BETWEEN CYCLODEXTRINS AND PHENYLUREA HERBICIDES IN SOLUTION AND IN THE SOLID STATE

October 2008

The author undertook the preparation of cyclodextrin inclusion complexes of four phenylurea herbicides (metobromuron, monolinuron, monuron and fenuron) using the kneading and co-precipitation methods in the solid state while also determining complex formation of the same phenylureas in solution with selected cyclodextrins. The kneading experiments were carried out first to determine whether the phenylureas would complex in the solid-state. The phenylureas were then subjected to complexation by means of co-precipitation under different conditions of crystallisation such as temperature and solvent medium in order to isolate more than one CD complex containing the same host and guest. The solution-state experiments were performed to see if the phenylurea complexes exist in solution and if so, to determine their nature.

The complexes generated from the kneading method were analysed using powder X-ray diffraction and the resulting diffractograms were interpreted by comparison with a set of pre-existing reference patterns. The comparison and subsequent matching yielded space group information and approximate unit cell dimensions. The complexes obtained from the co-precipitation method were analysed using powder X-ray diffraction, hot stage microscopy, thermogravimetric analysis, differential scanning calorimetry, ultraviolet spectrophotometry, elemental analysis and single crystal X-ray diffraction. Ultraviolet spectrophotometry and elemental analysis were used to determine the stoichiometry of the complexes while hot stage microscopy, thermogravimetric analysis and differential scanning calorimetry provided information about the thermal stability of the complexes. Single crystal X-ray diffraction was used to investigate the detailed solid-state features of the complexes while powder X-ray diffraction was used to confirm that the bulk material was the same phase as the single crystal selected for data-collection. Complex formation in solution was determined using ^{1}H-Nuclear Magnetic Resonance spectroscopy, which also provided data for the determination of the stoichiometry through chemically induced shifts of particular protons belonging to the cyclodextrin and the phenylurea guest molecule. These data were also used to determine the stability constants of the complexes formed in solution.

The results of this study are significant in the context of possible further development of pesticide-CD inclusion complexes. Furthermore, these results are significant with respect to the unprecedented isolation of as many as five crystal forms of a CD inclusion complex with the same host and guest.

TABLE OF CONTENTS

Chapter 1
INTRODUCTION

In this chapter we briefly introduce and discuss certain pertinent aspects of cyclodextrins and their inclusion complexes such as packing arrangements, crystal multiplicity, isostructurality, solution NMR and binding constants. We also provide a brief pesticide-complex review along with an outline of the motivation, aims and objectives of this thesis.

CYCLODEXTRINS

The degradation of starch by glucosyltransferase or CGTase proceeds by means of an intermolecular reaction without the participation of water to produce α(1,4)-linked cyclic end products.[1] The CGTase enzyme is isolated from the microbe *Bacillus macerans* which selectively produces these cyclic end products or cyclodextrins, Figure 1 (a). Cyclodextrins (CDs) are characterised by their truncated cone-like appearance, Figure 1 (b). The truncated cone is made up of several glucose units linked together. The cyclodextrins are named according to the number of glucose units in the macrocycle. For example, cyclodextrins which consist of 6, 7 and 8 glucose units are labelled α-, β- and γ-cyclodextrin respectively, Figure 1 (c).

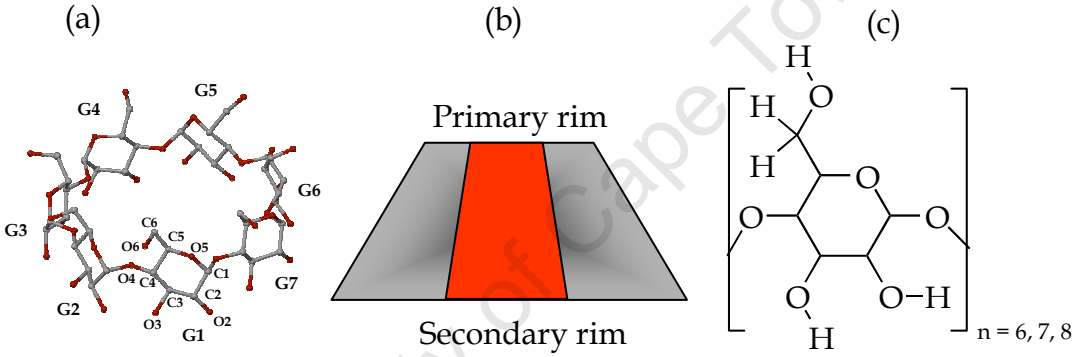

Figure 1. *(a) The macrocyclic ring of the CD and (b) the truncated cone and in parentheses in (c) a α-D-glucopyranose monomer.*

The glucose monomer units comprising cyclodextrins are α-D-glucopyranose having the $^4C_1$ chair conformation.[2,3,4] When linked together these monomer units are suitably rigid while they retain sufficient rotational flexibility around the α(1,4)-linkage (C1(n)-O4(n-1)-C4(n-1)). The truncated cone of the cyclodextrin has a hydrophobic cavity and a hydrophilic exterior. The rotational flexibility of the glucopyranose monomer orientates the methine (C3-H and C5-H) and methylene hydrogen atoms (C6-H_2) as well as the lone pairs of the bridging ethereal oxygen atoms O4(n) towards the interior of the CD cavity. The hydrophobic contribution of these hydrogens (methine and methylene) plus the additional electron density contributed by the lone pairs imposes some electrically positive character on the cavity.[5] Each rim of the cone has hydroxyl groups attached to it. Each rim is named

according to the number and type of hydroxyl groups located there. Thus, the primary rim has a single hydroxyl group (O6-H) per glucose unit while the secondary rim has two hydroxyl groups (O2-H and O3-H) per glucose unit. It follows that the primary rim is the narrower rim while the secondary rim is wider due to the natural tilt of the glucose units. The hydroxyl groups are there to promote/enhance the hydrophilicity of the cyclodextrin.[6] Hydroxyl groups O2-H and O3-H of adjacent glucose units on the secondary rim are hydrogen bonded to each other. The average hydrogen bonding distances O2(n)•••O3(n-1) for α-, β- and γ-CD are in the range 2.98 to 2.82 Å. α-CD has the weakest hydrogen bonds (average distance 2.98 Å) while γ-CD has the strongest (2.82 Å). Only β-CD (2.88 Å) has a complete set of hydrogen bonds which involves all the O2-H and O3-H atoms of the macrocyclic ring. As a consequence, β-CD is the least soluble of the three parent CDs. The solubilities of α-, β- and γ-CD in water are 14.5, 1.85 and 23.2 g per 100 cm^3 at 25 C°, respectively.[6,7]

DERIVATISED CYCLODEXTRINS

Methylation of β-cyclodextrin at the C2-OH, C3-OH and C6-OH hydroxyl positions effectively enlarges the hydrophobic surface area of the entire cyclodextrin. An additional 2 Å is added to the height of the cyclodextrin with a concomitant solubility enhancement in water. The overall effect is that the topology of inclusion is altered for these modified cyclodextrins.[6] This includes the accommodation of larger guests in the cavity as well as in the interstitial space between CD molecules. Heptakis(2,6-di-O-methyl)-β-cyclodextrin (DIMEB) and heptakis(2,3,6-tri-O-methyl)-β-cyclodextrin (TRIMEB) are two β-CD derivatives which are modified at the C2-OH, C6-OH and C2-OH, C3-OH and C6-OH hydroxyl positions respectively. As none of the O3-H hydroxyl groups is modified in DIMEB, it therefore retains the O2•••H-O3′ hydrogen bonds. The average O2•••O3′ distances are similar to those of β-CD.[8] This results in DIMEB and β-CD having similar conformations. The molecule of TRIMEB has none of the O2•••O3′

interactions that occur in DIMEB and β-CD. The conformation of TRIMEB differs from that of β-CD as it has only the C6-H•••O5 hydrogen bonds between adjacent methylglucose units which stabilise its structure.[9]

The inclusion of guest molecules in the cavity of cyclodextrin host molecules alters the three-dimensional packing arrangements of the host molecules in the solid-state.

CYCLODEXTRIN INCLUSION COMPLEXATION

Initially, it was thought that the main driving force of complexation was the replacement of the high enthalpy waters, located in the CD cavity, by a suitable guest.[1,10] The exchange process was therefore primarily driven by enthalpy and entropy changes with van der Waals forces and hydrophobic interactions regarded as secondary. However, it is claimed in a paper by Liu *et. al.*,[11] that the exclusion of cavity bound water and the release of conformational strain are not the only factors involved. In other words, the enthalpy and entropy changes during water exclusion from the cavity are not good criteria for the determination of a driving force due to the enthalpy-entropy compensation.[11] Also, according to Liu *et al.*, the primary forces of inclusion are therefore the van der Waals and hydrophobic interactions along with hydrogen bonding and steric effects.[2,12-20]

PACKING ARRANGEMENTS OF β-CYCLODEXTRIN COMPLEXES

The importance of discussing packing arrangements in this thesis is based on the fact that compounds with similar packing arrangements have grossly similar PXRD patterns. PXRD is an important technique used in the characterisation of putative complexes. An understanding of the packing arrangements therefore enables one to explain these similarities.

Generally, CDs and their inclusion complexes arrange themselves in one of two packing modes. These packing modes can best be described as cage type and channel type structures.[21] Cage structures are usually associated with

small guest molecules which are easily enveloped by the cavity, while channel structures are preferred for larger guests. Furthermore, cage structures are often monomeric arrangements while the channel type structures are dimeric, though not exclusively so.

Cage type monomeric

Cage type structures are usually arranged in such a way that the cavity is blocked off by adjacent molecules leaving no contact between guests. There are four cage type monomeric structures: herringbone (**HB**), layer (**LY**), brickwork (**BW**) and zigzag (**ZZ**). For β-CD complexes, herringbone, layer and brickwork structures usually crystallise in the space group $P2_1$, while the zigzag type crystallises in the space group $P2_12_12_1$.

HB

Herringbone is the most efficient packing arrangement as well as the preferred one for monomeric β-CD structures. The arrangement is shown here in Figure 2. The motif is characterised by CD molecules which stack along the twofold screw axis parallel to *b*. At one end the cavity is blocked by a screw related molecule while the other end is blocked by a molecule related by translation along the *b*-axis.

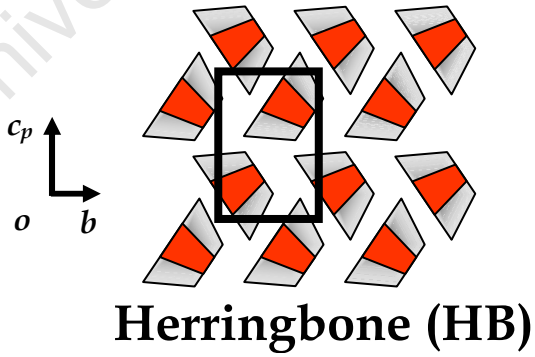

Figure 2. *The herringbone packing arrangement for monomeric β-CD complexes.*

LY

Here the molecules are arranged in layers which are parallel to the *ac*-plane but the CD molecules are inclined by ~10˚ to the plane as shown in Figure 3. The layers propagate along the *b*-axis with each layer horizontally offset by

~2.5 Å. Successive layers block off the cavity of preceding layers but not with the same efficiency as in the herringbone arrangement.

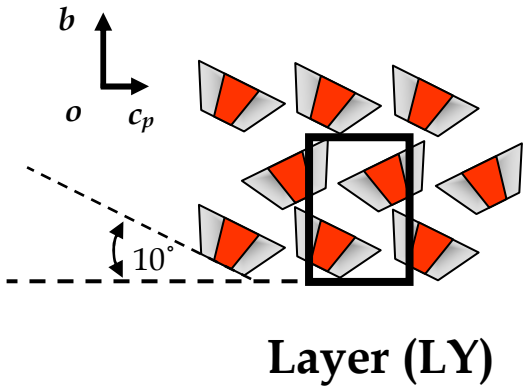

Figure 3. *The layer packing arrangement with layer propagation along the b-axis.*

BW

The cyclodextrin molecules are arranged in layers parallel to the *bc′*-plane (*c′* = 2*a* – *c*). Within each layer alternate cyclodextrins are arranged with the primary rim facing up while every other CD has the primary rim facing down. These layers propagate along *a′* (*a′* = *a* + *c*) with each layer being offset with respect to the previous layer, forming the brickwork packing shown in Figure 4.

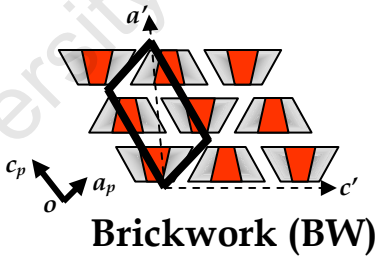

Figure 4. *Brickwork packing showing the alternating 'primary rim up' – 'primary rim down' of successive CD molecules in the direction of c′.*

ZZ

The β-CD monomers parallel to the *ab*-plane have a zigzag arrangement. Successive layers propagate along the *c*-direction. The zigzag arrangement is illustrated in Figure 5.

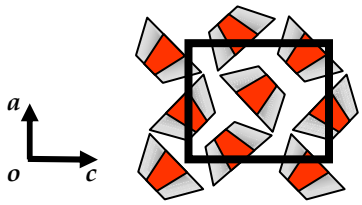

Zigzag (ZZ)

Figure 5. *The zigzag arrangement of the β-cyclodextrin monomers along the c-direction.*

Channel type monomeric

The helical channel type (**HC**) structure crystallises in the hexagonal space group $P6_1$. It is a very unusual arrangement; however, it retains the general characteristic of the monomeric motifs in that the cavity is isolated.

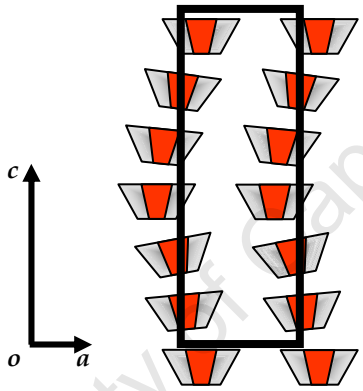

Helical channel (HC)

Figure 6. *The helical channel arrangement of β-CD monomers.*

HC

The head-to-tail arrangement of the β-CD molecules along the six-fold screw axis parallel to *c* produces a helical motif as in Figure 6. Successive molecules are rotated by 60˚ around the *c*-axis and extended by translation in layers parallel to the *ab*-plane.

Channel type dimeric

β-CD is able to form hydrogen bonded dimers in order to accommodate larger or multiple guests. These dimeric units are held together by several O-H•••O hydrogen bonds formed between O2-H and O3-H hydroxyl groups of the secondary rims of two β-CD molecules aligned in a head-to-head

manner (*i.e.* secondary rim to secondary rim). Like the monomeric unit, the dimeric unit is capable of assembling into several three-dimensional motifs.[22] A characteristic feature of the dimeric packing arrangement is the channel type motifs. If the cavities are aligned, continuous channels which span the crystal are created. However, if the cavities are slightly offset then the infinite channels become layer arrangements, as is the case here. Initially four modifications were identified by Mavridis *et al.* but more categories have since been added.[23,24] The four layer modifications are: channel (**CH**), intermediate (**IM**), screw channel (**SC**) and chessboard (**CB**). The space groups associated with these modifications are as follows: P1 and C2 with channel type, P1 with intermediate, $P2_1$ with screw channel and $C222_1$ with chessboard.

CH (P1 and C2)

The dimeric layers of the P1 structure are not parallel to the *ab*-plane. The dimers are stacked one above the other making infinite channels parallel to the *c*-axis and thus propagate along the *c*-axis as shown in Figure 7. It is noteworthy that the metric properties of the triclinic lattice are such that an alternative, monoclinic lattice can be found.[24] In other words one can, with the correct transformation matrix obtain the monoclinic unit cell (space group C2) from the triclinic cell (space group P1). The dimeric layers of the C2 structure are also parallel to the *ab*-plane but in addition the C-lattice has an extra column at (½ + x, ½ + y, z).[25] The channel is parallel to the *c-axis*.[26]

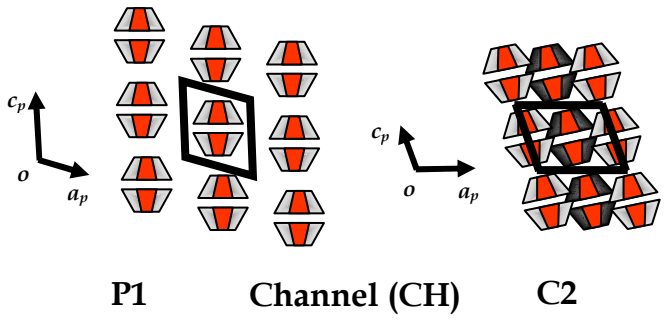

Figure 7. *A schematic representation of the channel packing arrangement for P1 (left) and C2 (right) forms. The C2 form has an extra column located at (½ + x, ½ + y, z) represented here by the darkened column.*

IM

The dimeric layer of the intermediate type is parallel to the *bc*-plane (Figure 8). The dimers are once again stacked on top of each other along the *a*-direction but the successive dimeric layers are horizontally offset to the extent of ~6 Å. For the intermediate motif the channels are not continuous.

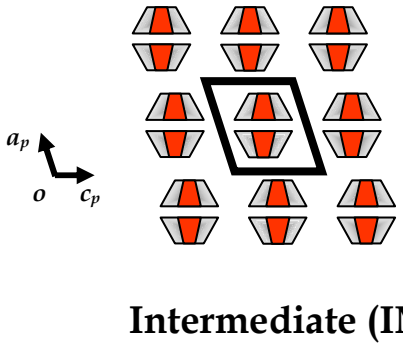

Figure 8. *The intermediate arrangement for β-CD dimers.*

SC

The dimeric layers of the screw channel arrangement are parallel to the *ac*-plane and propagate along the *b*-direction. Each layer is tilted by at least 10° to the *ac*-plane. The direction of the inclination alternates clockwise or anticlockwise for successive layers along the *b*-axis as is clearly shown in Figure 9.

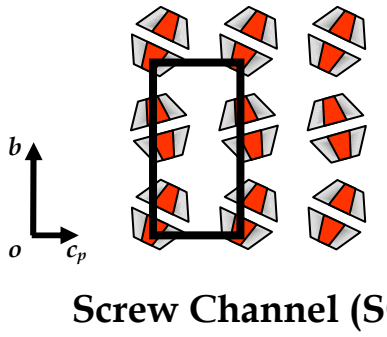

Figure 9. *Dimeric layers of the screw channel arrangement.*

CB

The dimeric layers of the chessboard arrangement are parallel to the *ab*-plane. They stack along the *c*-axis as shown in Figure 10. The consecutive layers are displaced horizontally such that they have minimal overlap with preceding layers in a chessboard motif. Owing to the displacement of the successive layers the channels are interrupted and not continuous as with the channel type.

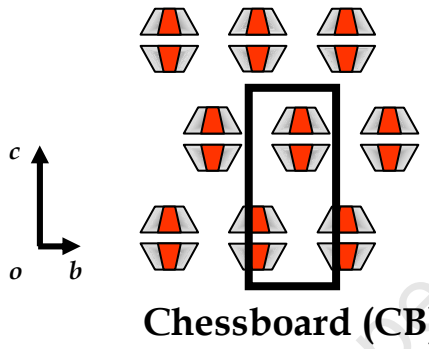

Figure 10. *A schematic diagram of the chessboard packing motif.*

Dimeric screw channel

Dimeric screw channel arrangements have two dimers in the asymmetric unit. These structures thus have dimeric layers and do not form a tetrameric arrangement. They have been previously described as disrupted channel structures.[27]

SC

The dimer at the origin is inclined at 23˚ to the *c*-axis while the dimer located at (x, ½ + y, ½ + z) makes an angle of 3˚ with the *c*-axis. The dimers are displaced laterally by ~2.45 Å. The C-centred layers of the dimers stack one above the other along the *c*-axis, Figure 11. The arrangement is not channel type as is usually found with the space group C2; the motif resembles the screw channel motif along *c*.[28*]

[*] The reader is referred to the paper by Giastas *et. al*. for a more in-depth explanation of the C2 classification as SC.[28]

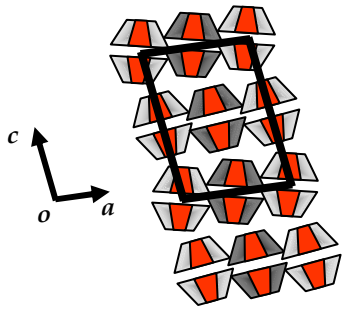

Screw channel (SC) C2

Figure 11. *Packing arrangement of the C2 screw channel type.*

Trimeric motif

The trimer comprises the usual dimer as well as an additional monomer. The interaction between the dimer and monomer is via a network of hydrogen bonds formed between the hydroxyl groups. In the dimer, the secondary rims are hydrogen bonded to each other in a head-to-head arrangement while the monomer is hydrogen bonded to the dimer in a head-to-tail manner (*i.e.* secondary rim to primary rim). The monomer is simultaneously hydrogen bonded to the next trimer in a tail-to-tail motif (*i.e.* primary rim to primary rim). Thus, the channel of the trimer extends infinitely.

TC

As mentioned previously, the trimeric channel extends infinitely along the *c*-axis. The trimers lie alongside one another in adjacent columns with parallel alignment, as shown in Figure 12. The dimer component of the trimer is exactly aligned while the monomeric part is shifted horizontally by ~0.5 Å without interrupting the channel. The trimeric channel type crystallises in the space group P1.[29]

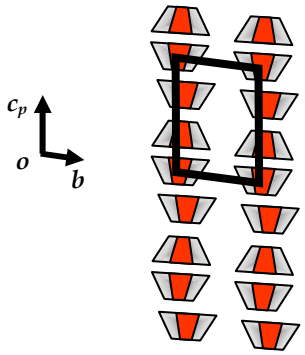

Trimeric channel (TC)

Figure 12. *A schematic representation of the trimeric channel which extends infinitely through the crystal.*

Tetrameric arrangements

The tetrameric motifs consist of two dimers stacked in a tail-to-tail manner. There are no hydrogen bonds linking the two dimers to each other. There are three tetrameric arrangements listed here: tetrameric intermediate (**TI**), tetrameric chessboard (**TC**) and tetrameric brickwork (**BW**). The space groups associated with the tetrameric arrangements are as follows: P1 and C2 with tetrameric intermediate, $P2_1$ with tetrameric chessboard, C2 with tetrameric brickwork.

TI (P1 and C2)

In the case of the P1 type tetramer, the tetramer is translated along the *b*-direction while for the C2 structure the tetramer is translated along *a*.[30] The C-lattice has an extra tetrameric column located at (½ + x, ½ + y, z), Figure 13. The tetrameric layers for the C2 type are inclined to the *ab*-plane.[31] In the case of the P1 arrangement the tetrameric layers are parallel to the *ab*-plane, as shown in Figure 13. For both arrangements the tetramer channel is not continuous as the tetrameric layers are laterally displaced with respect to each other.

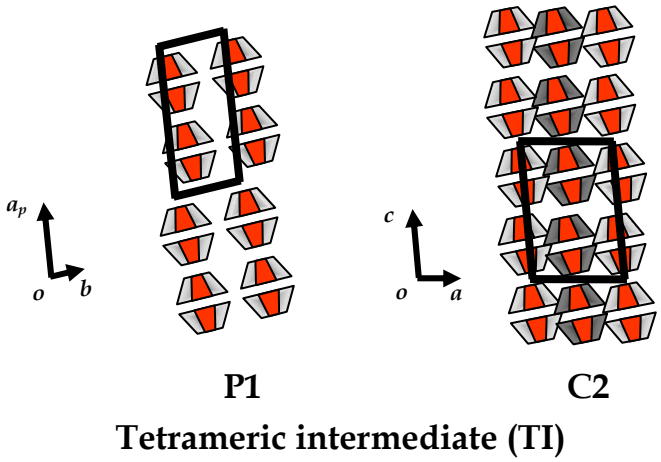

Figure 13. *The packing arrangements of the (**TI**) type for P1 and C2.*

TC

For (**a**) the tetrameric layers are stacked vertically along the *b*-axis and parallel to the *ac*-plane. Each tetrameric layer is laterally shifted such that there is no overlap between successive layers. In the case of (**b**), four dimeric layers comprise the repeating array **1**, **2**, **3** and **4** shown in Figure 14. **1** and **2** are related to **3** and **4** by the 2_1-operation along *b*. Layer **1** is horizontally displaced from layer **2** and is related to layers **3** and **4** by the screw operation. **1** and **4** are tilted by ~10˚ anticlockwise with respect to the *ac*-plane. Layers **2** and **3** are thus tilted by ~10˚ clockwise. There is no overlap between successive tetrameric layers as with (**a**). The overall motif for both (**a**) and (**b**) resembles the chessboard motif ($P2_1$).[27,32,33]

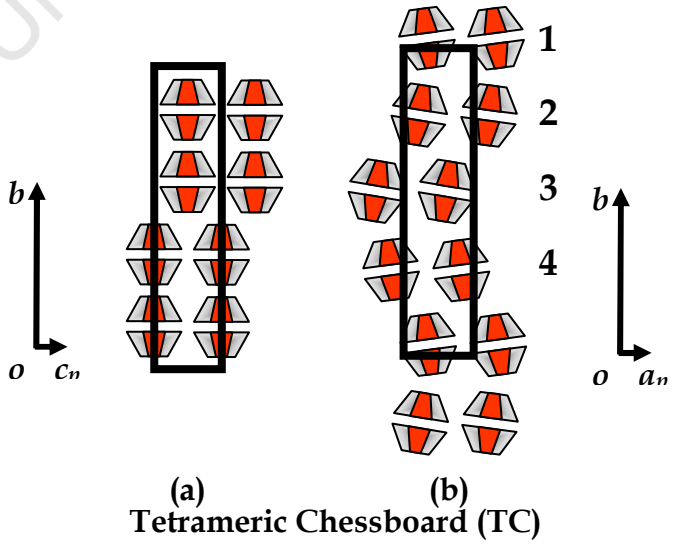

Figure 14. *Schematic diagram of the (TC) packing arrangement.*

BW

The tetrameric layers are parallel to the *ab*-plane and stack vertically along the *c*-direction. Within the tetramer, the dimeric layers are displaced laterally. The successive tetrameric layers are also displaced laterally giving an overall brickwork motif, Figure 15. The tetrameric layers are translated along *c*.[34]

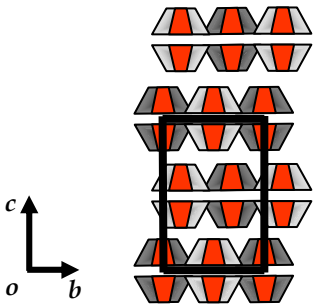

Figure 15. *The packing arrangement showing the brick type arrangement for BW.*

PACKING ARRANGEMENTS OF DIMEB COMPLEXES

DIMEB and its complexes tend mostly to crystallise in the space groups $P2_1$ and $P2_12_12_1$. The packing arrangements include channel type head-to-tail, modified brick type and modified herringbone motifs. On occasion the guest may be located in the interstitial spaces.[35]

PACKING ARRANGEMENTS OF TRIMEB COMPLEXES

TRIMEB and its inclusion complexes seem to prefer to crystallize in the space group $P2_12_12_1$ with the molecules in a screw channel type structure,[36] although structures with space group $P2_1$ have been identified.[37,38] Similarly to DIMEB complexes, the molecules are also arranged in a head-to-tail manner.

PACKING ARRANGEMENTS AND ISOSTRUCTURALITY

Two or more crystalline phases are said to be isostructural if they have similar unit cell dimensions, the same space group (this includes structures which are related by a metric transformation) and common moieties having nearly identical atomic co-ordinates.[24] The outcome of the above prerequisites is

nearly identical packing arrangements and superimposable PXRD traces. Thus, PXRD is an important tool in determining isostructurality in the absence of single crystal X-ray data.

Table 1. *Crystallographic data for dimeric β-CD complexes of the screw channel type.*[39,24]

refcode	*a* (Å)	*b* (Å)	*c* (Å)	β (°)	Guest
GETPAW	15.260	32.760	15.350	101.50	(R)-(-)-Fenoprofen
GETPEA	15.310	32.124	15.277	100.76	(S)-(+)-Fenoprofen
DUTLIN10	15.227	32.232	15.316	101.18	(RS)-Fenoprofen
NIZGUY	15.342	32.540	15.324	102.44	(L)-Menthol
QACXEX	15.454	31.693	15.255	102.92	*p*-amino-*p'*-nitrobiphenyl
BEGWEQ	15.226	31.477	15.674	104.32	paroxetine
KIFPAQ	15.428	32.545	15.437	103.56	adamantanone

Table 1 lists a set of unit cell parameters for cyclodextrin inclusion complexes. The complexes have very similar unit cell dimensions and crystallise in the monoclinic space group $P2_1$. All the structures in the series pack in the SC packing arrangement. However, despite the close similarity in the unit cell data and the identical space group not all the complexes are isostructural. For the analysis of the structures, Caira *et al.* connected the O4 atoms of a single dimeric unit forming overlapping heptagons, shown as circles in Figure 16 (a).[39] They found that the extent of overlap between these dimeric layers varied. The O4-heptagons of the inclusion complexes GETPAW, GETPEA, DUTLIN10, NIZGUY and QACXEX have nearly identical motifs (Figure 16 (b)). The motif of BEGWEQ represented by (c) did not match those in (b). Also, the motif representing KIFPAQ (**d**) did not match those of (**b**) or (**c**) either. The representative motifs of all the structures depended on the placement of the CD relative to the two-fold screw axis. The motif in (**b**) was characterised by significant overlap. There is no overlap between adjacent screw related columns. The motif propagates along the *b*-direction in a corkscrew type fashion.

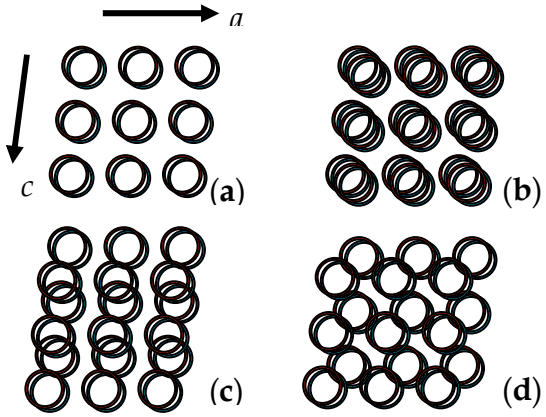

Figure 16. *In the diagram (**a**) represents a single dimeric unit, (**b**) are the consecutive dimeric layers of the isostructural series with significant overlap, (**c**) the dimeric layers for BEGWEQ featuring minor overlap between successive layers along the c-direction and (**d**) KIFPAQ with negligible overlap.*

For BEGWEQ, there was significantly less overlap, extending along the *c*-axis only. The final structure, KIFPAQ, had only negligible overlap for successive dimeric layers as shown by (**d**). The difference in overlap between (**b**) and (**c**) is ~4 Å. This series of complexes thus illustrates that close correspondence of unit cell dimensions is therefore not a sufficient condition for isostructurality.[39]

CRYSTAL FORMS

Polymorphism, as one of the topics under discussion here, has been shown to affect almost one-third of all organic compounds in the solid state while a further third is affected by solvate formation.[40,41,42] Though polymorphism is a well understood phenomenon it remains impossible to predict its occurrence or the properties associated with a new polymorph. A definition which unambiguously describes polymorphism is a synthesis of the definition offered by McCrone and the classification criterion used by Bernstein.[43,44] McCrone's definition of polymorphism states, 'a solid crystalline phase of a given compound resulting from the possibility of at least two different arrangements of the molecules of that compound in the solid state, while Bernstein's criterion is, 'classification of a system as polymorphic would be if the crystal structures are different but lead to identical liquid and vapour states.' This definition precludes solvates (hydrates are a special case, where

the solvent included is water) as polymorphs. However, this does not exclude the existence of polymorphs of solvates from occurring. An example of this is the two monohydrate forms of the antibacterial compound Nitrofurantoin; form **I** is monoclinic $P2_1/n$ while form **II** is orthorhombic Pbca.[45] Solvates have in the past been erroneously referred to as pseudopolymorphs, a term that is no longer acceptable. Strictly, the term pseudopolymorph means 'false polymorph'; the error in this is that crystal forms are not polymorphs *per se*. This terminology still persists in the literature but it has been recommended by some authors that this term be omitted from the supramolecular lexicon, undoubtedly a difficult task.[46-49]

Any discussion of polymorphism must necessarily include isostructurality. Isostructurality and polymorphism are inversely related and this relationship is illustrated in Figure 17 below.[50-52]

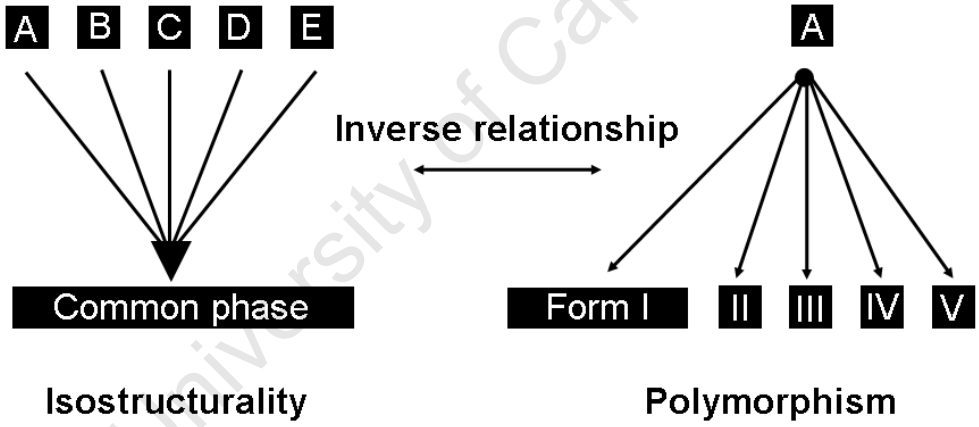

***Figure 17**. A pictorial representation of the inverse relationship between isostructurality and polymorphism.*[53]

As illustrated in Figure 17, isostructurality involves several compounds crystallising with the same phase, whereas polymorphism involves a single compound crystallising in different phases. Isostructurality also occurs amongst solvates where the included solvent differs in each case. An apt example of isostructurality amongst solvates is the macrolide antibiotic dirithromycin which forms six isostructural solvates. The solvents included in each case are ethanol, 1-propanol, 2-propanol, 1-butanol, acetone and 2-butanone.[54] An area where isostructurality has had a great impact is with

cyclodextrins, including native and modified CDs and their inclusion complexes. In a recent survey of the CSD by Caira and Lubhelwana (2005), they found 26 isostructural series for the parent CDs, including modified CDs, and cyclodextrin inclusion complexes.[23] These isostructural series span a limited number of space groups. Generally, isostructurality of cyclodextrins is limited to the more rigid host molecule and usually the guest and water molecules are excluded, though there are exceptions. Nakanishi *et al.*[30] reported an example where 13 out of a possible 19 water molecules in the structure they investigated retained the same positions as those in the fragment used to solve their structure by isomorphous replacement. Moreover they claim that these 13 water molecules are important in forming the cage type matrix.

Isostructurality has enabled the rapid identification of complex phases from the PXRD pattern.[24,30] The occurrence of multiplicity of crystal forms amongst cyclodextrins has thus far been restricted to parent CDs (native and modified). In fact, its occurrence amongst parent CDs is described here.

MULTIPLICITY OF CRYSTAL FORMS OF PARENT CYCLODEXTRINS

Crystal forms of α-cyclodextrin

For α-CD, there are four hydrated forms which all crystallise in the orthorhombic crystal system in the space group $P2_12_12_1$, Table 2. The conformations of α-cyclodextrin in forms **1** and **2** are similar to one another, both having six water molecules of crystallisation. The conformations of **3** and **4** are in turn similar, having 7.6 and 11 water molecules respectively.

Table 2. *A list of all native α-CD forms extracted from the CSD.*[35]

No.	hydration	a (Å)	b (Å)	c (Å)	α(°)	β (°)	γ(°)	T (K)	V (Å³)	refcode	Space group
1	6	14.858	34.038	9.529	90	90	90	295	4819.2	Chxamh02	$P2_12_12_1$
2	6	13.700	29.350	11.920	90	90	90	295	4792.9	Chxamh03	$P2_12_12_1$
3	7.6	14.356	37.538	9.400	90	90	90	295	5065.6	Banxuj	$P2_12_12_1$
4	11	13.839	15.398	24.209	90	90	90	295	5158.8	Goqzuh	$P2_12_12_1$
5	6	14.856	33.991	9.517	90	90	90	295	4805.8	Chxamh	$P2_12_12_1$
6	X	15.490	24.060	13.930	90	90	90	295	5191.6	Zzzriu	$P2_12_12_1$

X - the hydration values were not reported

In **1** there are two water molecules situated in the cavity and four located outside. In **2** there is a single water molecule in the cavity. In addition, there is a single hydroxyl group (O6-H) of an adjacent CD which protrudes into the cavity, a clear example of self-inclusion.[55] The remaining five water molecules are in the interstitial spaces between the CDs. In cases **1** and **2** the cyclodextrins have slightly distorted shapes differing from the usual circular or annular shape to a more elongated conformation. This conformation has previously been described as 'tense'. In **3**, there are 2.6 disordered water molecules located in the cavity, distributed over four sites. The remaining five molecules of water occupy the interstitial space. For **4** there are four water molecules outside the cavity while the remaining seven molecules occupy the cavity. These seven water molecules are severely disordered. The CD conformations for **3** and **4** are more circular in shape than those in forms **1** and **2**. The conformations of **3** and **4** are said to be 'relaxed'. The four forms have been overlaid for comparison in the stereo diagram in Figure 18.[56,57]

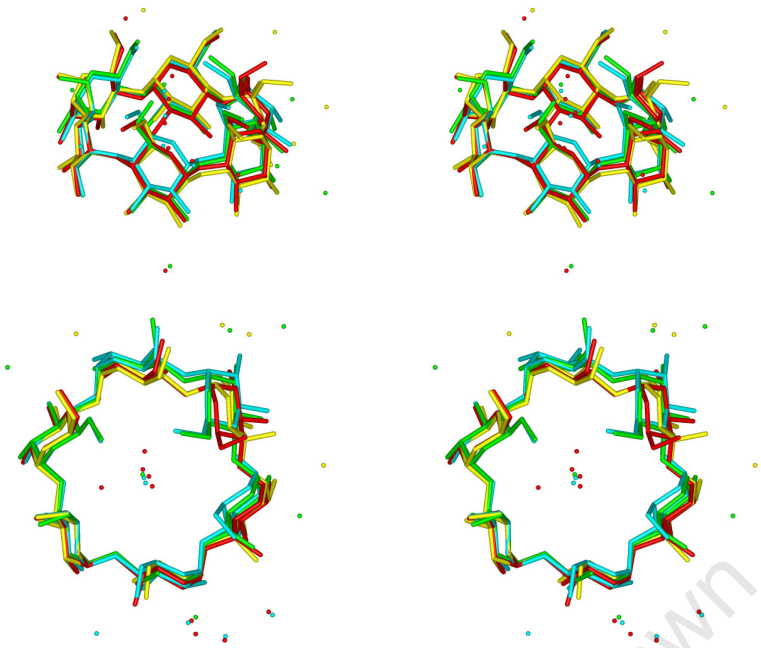

Figure 18. *A stereoview of the α-cyclodextrin host molecule for each of the four hydrates superimposed here for comparison. Key:* ***1****-blue,* ***2****-green,* ***3****-red and* ***4****-yellow.*

The major difference between these structures can be observed from their packing arrangements. **1**, **2** and **3** pack in a herringbone packing scheme while **4** takes on a brickwork arrangement. When these structures are viewed perpendicular to the mean O4 plane (represented here by the hexagonal ring consisting of the six connected O4 atoms of α - CD) these differences become clear. The view along the *b*-axis is perpendicular to the mean O4 plane, Figure 19. When viewing the packing arrangements of the four structures along the *b*-axis it is noticeable that the arrangements characterising **1** through **3** (Figure 19) show overlap to varying extents for successive layers. **2** has the greatest overlap followed by **1**. **3** shows only negligible overlap. A consequence of the overlap in **2** is the self-inclusion of a single O6-H hydroxyl group, as mentioned previously. **4** has some overlap between successive layers but the most significant aspect of this packing scheme is the pseudo-hexagonal arrangement of the O4 hexagons.[57]

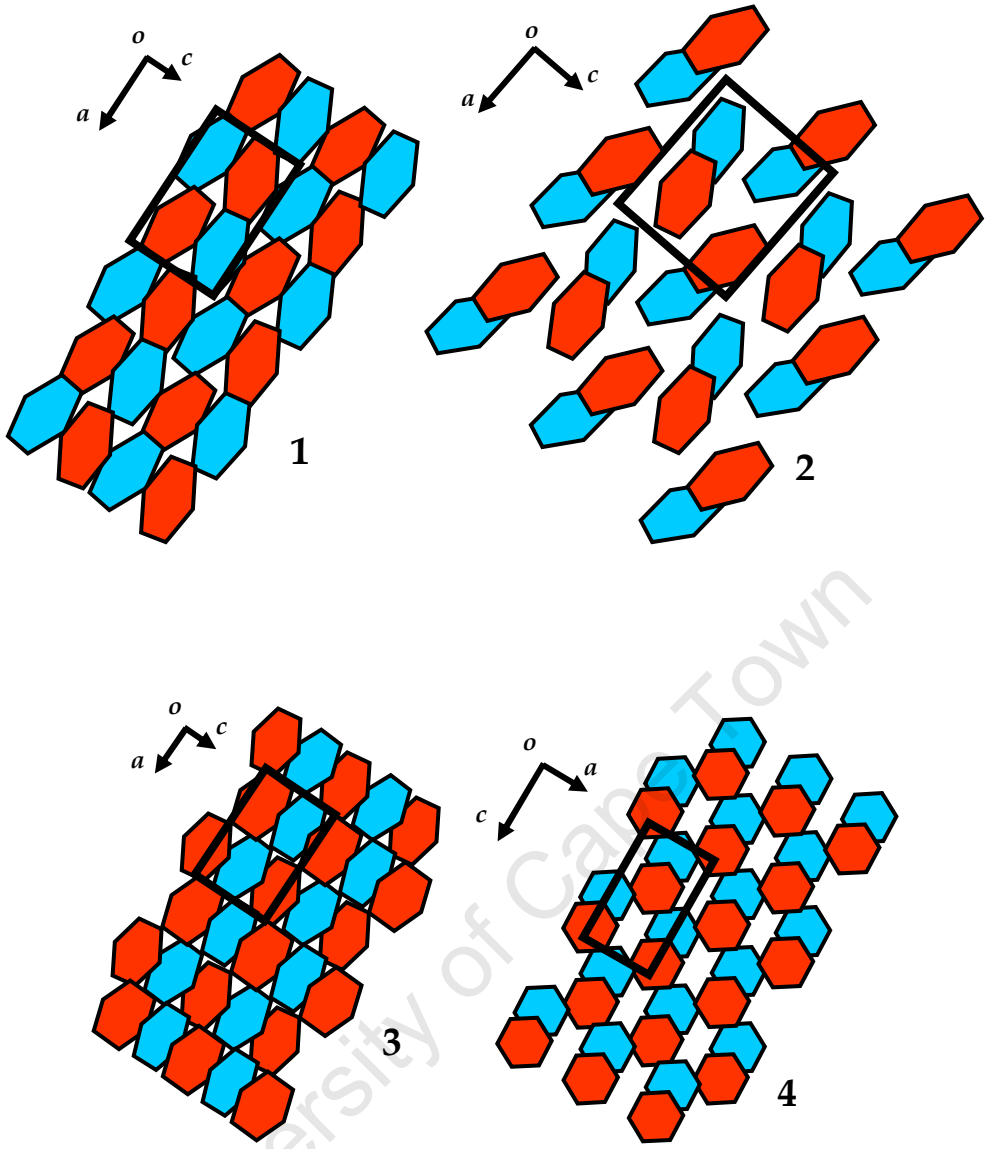

Figure 19. *The projection along the b-axis of the α–CD hydrates.*

The packing arrangements of the four hydrates are distinct and this is very significant. **1** and **2** have identical water content and are therefore true polymorphs. It is clear from the PXRD traces that forms **3** and **4** are not isostructural. The reported data in Table 2 show how significantly the unit cell parameters differ. The calculated PXRD traces are plotted in Figure 20 and it is clear that the four traces are distinct from one another.

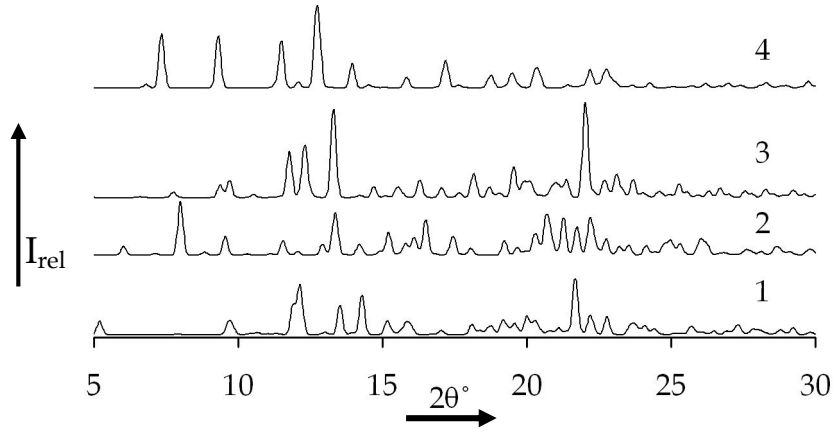

Figure 20. *Stacked computed PXRD traces for the four hydrates.*

Crystal forms of β-cyclodextrin

As with α - cyclodextrin there are several hydrates of β-cyclodextrin listed in the CSD. A search of the CSD produced 17 β-cyclodextrin structures including repeat determinations. Data for these are listed in Table 3. All of these are hydrated forms of β-cyclodextrin with the level of hydration ranging from 1 to 12.3 water molecules per molecule of cyclodextrin. Generally speaking, there are five different hydrated forms with 1, 9, 11, 11.6 and 12.3 water molecules. All 17 forms are monoclinic crystallising in the space group $P2_1$.

Table 3. *A list of all the β-CD hydrates extracted from the CSD.*[35]

No.	hydration	a (Å)	b (Å)	c (Å)	α (°)	β (°)	γ(°)	T (K)	V (Å³)	refcode	Space group
7	1	21.295	10.318	15.108	90	112.46	90	295	3067.7	Pobrut	$P2_1$
8	9.4	20.857	10.158	15.140	90	110.94	90	295	2995.8	Pobron	$P2_1$
9	11	21.085	10.212	15.123	90	111.66	90	295	3026.4	Buvseq	$P2_1$
10	12	10.310	20.860	15.090	90	109.48	90	295	3059.6	Bcdexd11	$P2_1$
11	12	20.852	10.202	14.924	90	108.81	90	120	3005.3	Bcdexd01	$P2_1$
12	12	21.271	10.321	15.104	90	112.34	90	295	3067.0	Bcdexd02	$P2_1$
13	12.3	21.283	10.322	15.092	90	112.41	90	295	3065.0	Bcdexd03	$P2_1$
14	11.6	21.161	10.254	15.110	90	111.91	90	295	3041.8	Bcdexd04	$P2_1$
15	11.9	21.233	10.294	15.103	90	112.22	90	295	3055.9	Bcdexd05	$P2_1$
16	12	21.290	10.330	15.100	90	112.30	90	295	3072.5	Bcdexd10	$P2_1$
17	11.2	21.080	10.197	15.131	90	111.58	90	295	3024.5	Buvseq01	$P2_1$
18	11	20.910	10.057	14.888	90	109.32	90	100	2954.5	Buvseq04	$P2_1$
19	9	15.107	10.242	20.911	90	110.27	90	293	3035.1	Pobron01	$P2_1$
20	X	15.180	10.250	21.120	90	111.60	90	295	3055.4	Pobron02	$P2_1$
21	1	21.265	10.314	15.097	90	112.34	90	295	3067.6	Pobrut01	$P2_1$
22	1	21.227	10.288	15.116	90	112.18	90	295	3056.8	Pobrut02	$P2_1$

X - the hydration values were not reported

The β-angle ranges from 108.8 to 112.5˚. Changes in temperature at which data collections were recorded may have been responsible for variations in the reported unit cell volumes (i.e. shrinkage associated with low temperature data collections). PXRD traces were calculated for representative structures of each of the hydrates. (Many of the atomic coordinate data were not available and PXRDs could not be calculated in those cases).

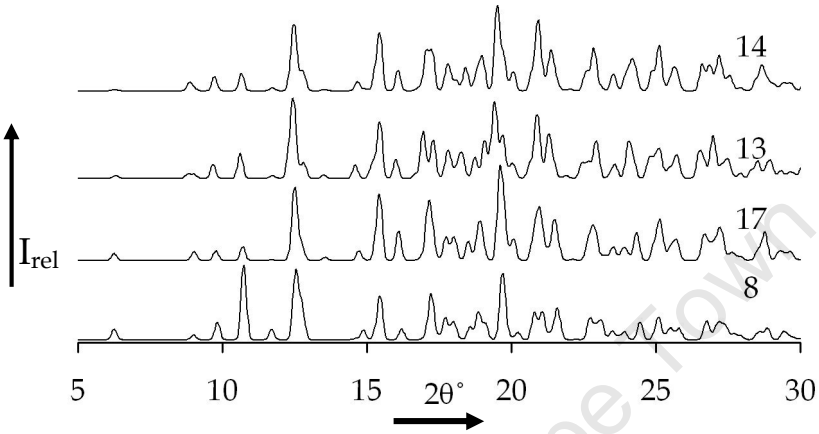

Figure 21. *PXRD patterns for nos.* ***8***, ***17***, ***13*** *and* ***14*** *of the tabulated list of β–cyclodextrin hydrates. Coordinate data were available for only four of the five hydrate types.*

It is apparent from the comparison of PXRD traces shown in Figure 21 that **8**, **17**, **13**, and **14** are isostructural. Apart from the intensity differences and variations in the β-angle, there are only slight shifts in peak angular position but these result from the variations in hydration of β-CD.

Crystal forms of γ-cyclodextrin

γ-CD presented three crystal forms having different levels of hydration: 11, 14 and 17 water molecules for **24**, **25** and **26** respectively, Table 4. The atomic coordinates for only one of the three hydrates were available and therefore further interpretations were not possible.

Table 4. *A list of all the γ-CD hydrates extracted from the CSD.*[35]

No.	*hydration*	*a* (Å)	*b* (Å)	*c* (Å)	α(˚)	β (˚)	γ(˚)	T (K)	V (Å³)	refcode	Space group
24	11	20.287	22.079	16.858	90	105.07	90	295	7291.3	Cimsas	$P2_1$
25	14	16.847	11.098	20.271	90	104.97	90	295	3661.4	Ciwmie	$P2_1$
26	17	20.253	10.494	16.892	90	105.32	90	120	3462.6	Cyocam	$P2_1$

MODIFIED CYCLODEXTRINS

Crystal forms of DIMEB

Listed in Table 5 there are 11 structures of the DIMEB parent recorded on the CSD, ten of which are hydrated forms while the remaining structure is anhydrous. Within the set of hydrates there are at least four different hydrates including several with unreported hydration values. The four classes of hydrates are: 1.1, 15, 2 and x (x represents the form with unknown or unreported water content) corresponding to **27**, **28**, **29** and several with unreported water content. The atomic coordinates for only five of the structures were provided in the CSD. These included three different hydrates and the single anhydrous form, **30**.

Table 5. *A list of all DIMEB forms extracted from the CSD.*[35]

No.	hydration	a (Å)	b (Å)	c (Å)	α (°)	β (°)	γ(°)	T (K)	V (Å³)	refcode	Space group
27	1.1	13.328	17.410	29.760	90	90	90	100	6905.5	Qiykeo	$P2_12_12_1$
28	15	14.163	20.828	29.261	90	90	90	298	8631.7	Boyfok04	$P2_12_12_1$
29	2	15.241	10.639	23.324	90	101.8	90	298	3702.2	Ceqcuw	$P2_1$
30	anhydrous	13.821	17.424	29.610	90	90	90	295	7130.6	Zulqay	$P2_12_12_1$
31	14.7	13.976	20.763	28.807	90	90	90	100	8359.3	Boyfok03	$P2_12_12_1$
32	X	13.976	20.763	28.807	90	90	90	295	8359.3	Boyfok01	$P2_12_12_1$
33	X	13.682	22.606	27.562	90	90	90	120	8524.8	Boyfok02	$P2_12_12_1$
34	15	13.976	20.763	28.807	90	90	90	120	8359.3	Boyfok11	$P2_12_12_1$
35	15	14.163	17.284	38.243	90	90	90	383	9361.7	Boyfok12	$P2_12_12_1$
36	X	13.585	17.653	29.766	90	90	90	295	7138.1	Qiykeo01	$P2_12_12_1$
37	X	13.585	17.653	29.766	90	90	90	295	7138.3	Qiykeo02	$P2_12_12_1$
38	X	13.682	22.606	27.562	90	90	90	120	8524.8	Boyfok02	$P2_12_12_1$
39	15	13.976	20.763	28.807	90	90	90	120	8359.3	Boyfok11	$P2_12_12_1$
40	15	14.163	17.284	38.243	90	90	90	383	9361.7	Boyfok12	$P2_12_12_1$

X - the hydration values were not reported

The PXRD traces for **27**, **28**, **29** and **30** were calculated from structural data extracted from the CSD and compared, Figure 22. From the stacked traces it is apparent that **27** and **30** are isostructural. **28** has a hydration number of 15 water molecules per molecule of DIMEB, a hydration level much greater than any of the other forms of DIMEB, giving rise to a unique PXRD trace.

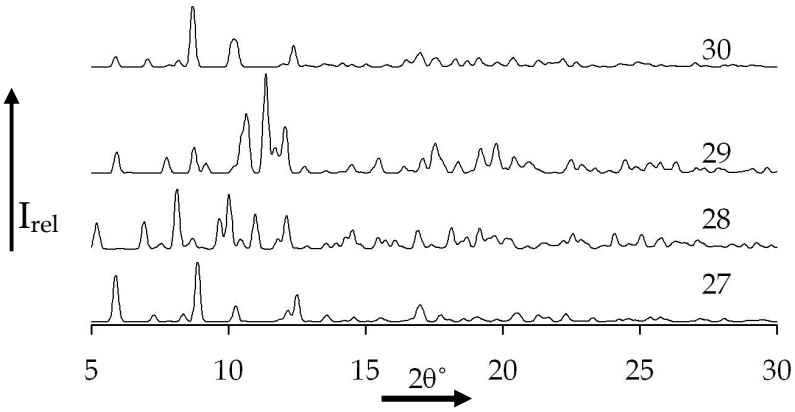

Figure 22. *Stacked PXRD traces of the four DIMEB types;* ***27*** *and* ***30*** *are isostructural while* ***28*** *and* ***29*** *are unique.*

29 is the only structure in the list which crystallizes in the monoclinic crystal system with the space group $P2_1$ and with $\beta = 101.8^{\circ}$. All the other structures are orthorhombic with the space group $P2_12_12_1$. The packing arrangement of **30** is interesting as it has the cyclodextrin molecules arranged in columns along the screw-axis parallel to the *a*-axis, seen in Figure 23. Successive cyclodextrin molecules are inclined towards the centre of the secondary rim of the upper cyclodextrin cavity adjacent to it, allowing for self-inclusion of a twofold disordered O6 methoxyl group of an adjacent CD.

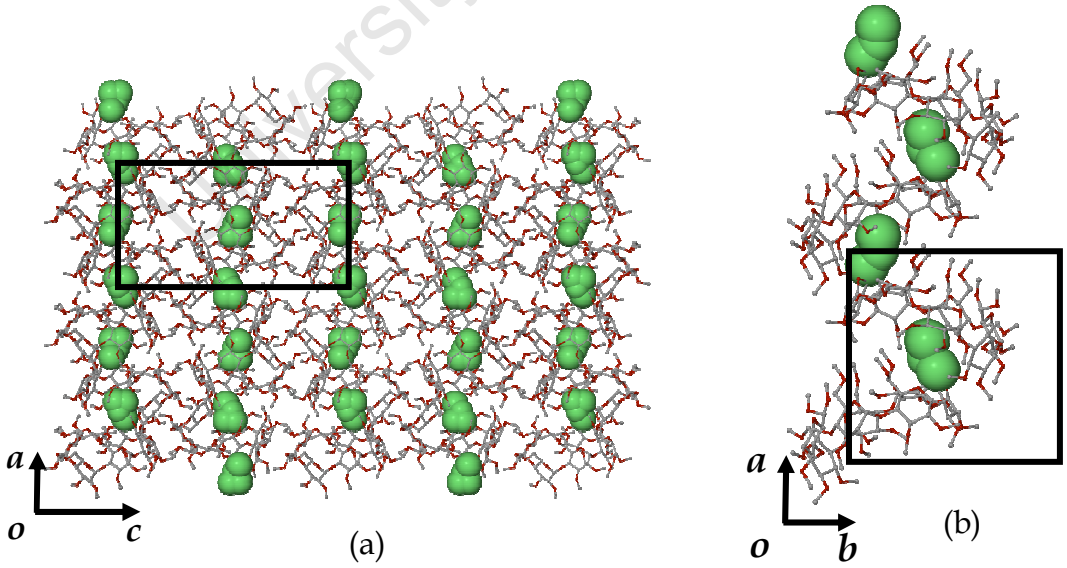

Figure 23. *(a) Self-inclusion along the screw-axis parallel to a-axis. (b) O6 methoxyl group (green) protrudes into the cavity of an adjacent CD molecule.*

The self-inclusion is propagated in the direction of the screw-axis parallel to the *a*-axis. The main difference between structures **27**, **28** and **30** is the water content. The atomic coordinates of the structures with unreported hydration number were not available. Further interpretations of these structures were not possible.

Crystal forms of TRIMEB

There are three reported forms of TRIMEB. **41** and **42** are hydrated, while **43** is anhydrous. From the calculated PXRD traces, unit cell parameters and the packing arrangements in Figures 24, 25 and Table 6 it was established that **42** and **43** are isostructural, where **43** is the dehydrated form of **42**. This is especially significant when considering the shift to lower 2θ˚ in the peak angular positions of **42** relative to **43**, a result of the slightly larger unit cell of **42**.

Table 6. *A list of all TRIMEB forms extracted from the CSD.*[35]

No.	hydration	*a* (Å)	*b* (Å)	*c* (Å)	α(˚)	β (˚)	γ(˚)	T (K)	V (Å³)	refcode	Space group
41	1	14.818	19.362	26.510	90	90	90	294	7623.2	Hezwak01	$P2_12_12_1$
42	3	16.205	16.287	30.099	90	90	90	193	7944.1	Waglog	$P2_12_12_1$
43	anhydrous	15.951	16.577	28.941	90	90	90	173	7652.7	Waglum	$P2_12_12_1$

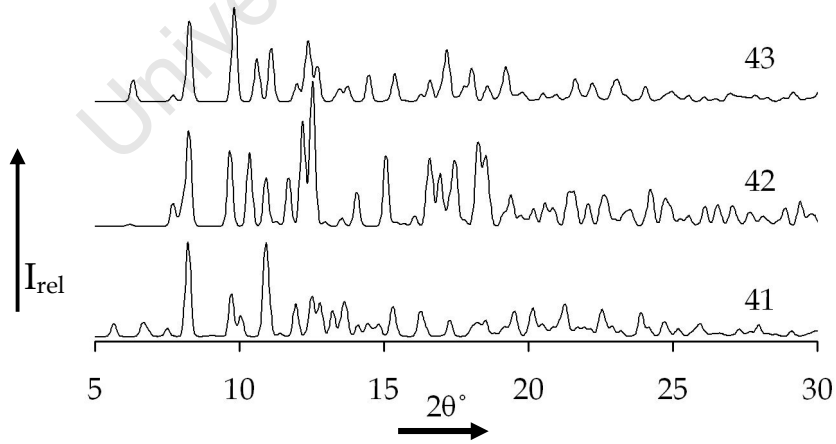

Figure 24. *Calculated PXRD patterns of TRIMEB forms* ***41****,* ***42*** *and* ***43****.*

Significantly, both forms **41** and **43** experience self-inclusion and have reduced hydration compared to the trihydrate.[58] **41** is grossly distorted due to one ring adopting the $^1C_4$ conformation. It follows that the self-inclusion

along with the overall elliptical shape aids in the reduction of the hydrophobic cavity. However, **43** does not have an elliptical shape but a circular shape instead. This is as a result of the inclusion of methoxyl groups of one CD into the cavity of another. The packing arrangements of **42** (green) and **43** (red) seen in Figure 25 are in agreement. The cyclodextrin molecules which are located near the origin of each unit cell have a near one-to-one overlap. However, as one moves further and further away from the origin in the direction along the *c*-axis this overlap diminishes and there is a sizeable displacement between the structures.[58, 59]

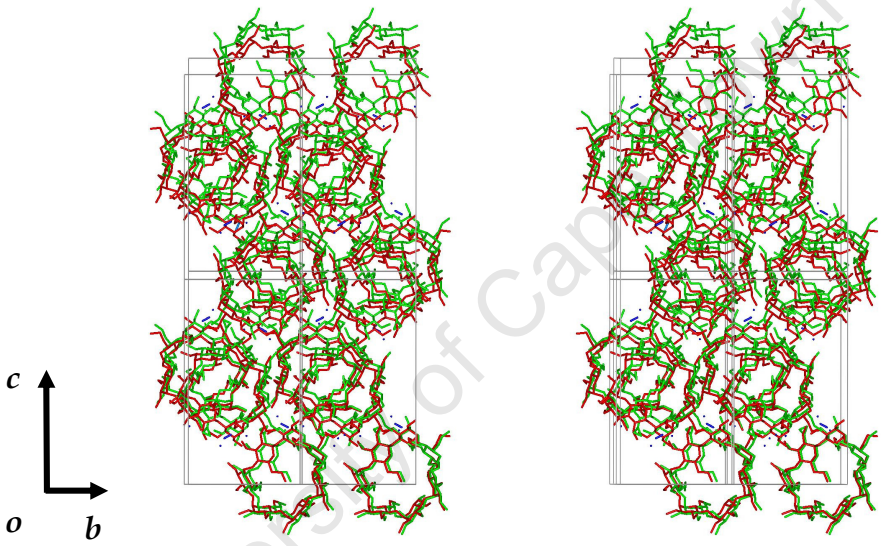

Figure 25. *A stereo diagram of the superimposed packing arrangements of* ***42*** *(green) and* ***43*** *(red), showing the level of agreement between the structures.*

The displacement between the cells is a result of the reduction in the unit cell dimensions which occurs during the dehydration of **42**. Thus all three forms of TRIMEB are unique but not polymorphic.

Crystal forms of TRIMEG

There are three different structures of Octakis(2,3,6-tri-O-methyl)-γ-cyclodextrin (TRIMEG) listed in Table 7 all of which are hydrated with 2, 4.8 and 4.5 H_2O molecules per molecule of CD. Two of the structures, **44** and **46**, crystallise in the orthorhombic crystal system in the space group $P2_12_12_1$ while the third, **45**, is monoclinic crystallising in the space group $P2_1$.

Table 7. *A list of all TRIMEG forms extracted from the CSD.*[35]

No.	hydration	a (Å)	b (Å)	c (Å)	α(°)	β (°)	γ(°)	T (K)	V (Å³)	refcode	Space group
44	2	16.730	16.875	32.172	90	90	90	298	9082.8	Giwmaa	$P2_12_12_1$
45	19.3	29.872	18.018	33.170	90	98.15	90	298	17673	Bebjat	$P2_1$
46	4.5	10.788	29.058	32.291	90	90	90	298	10122	Xersiw	$P2_12_12_1$

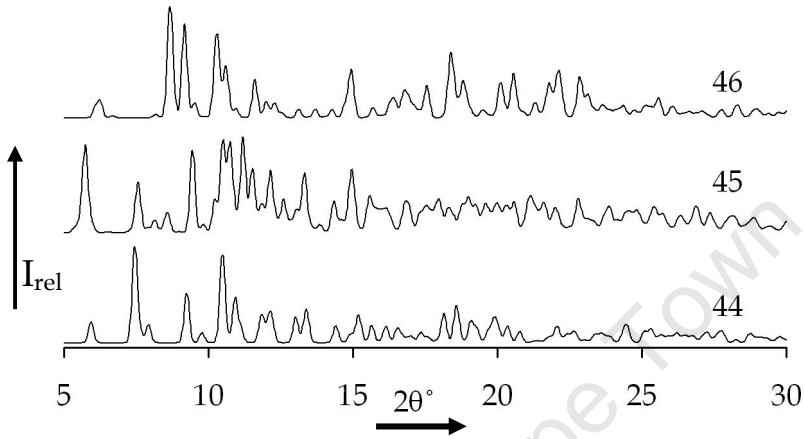

Figure 26. *The calculated PXRD patterns for three TRIMEG hydrates.*

A comparison of the calculated PXRDs for **44**, **45** and **46** shows three distinctly different traces, Figure 26. This is consistent with the significant differences in their unit cell dimensions. The structures of TRIMEG are usually characterised by self-inclusion of the O6 methoxyl groups; again all three structures are unique.

Crystal forms of peracetylated cyclodextrins

Hexakis(2,3,6-tri-*O*-acetyl)-α-cyclodextrin (TAαCD), heptakis(2,3,6-tri-*O*-acetyl)-β-cyclodextrin (TAβCD) and octakis(2,3,6-tri-*O*-acetyl)-γ-cyclodextrin (TAγCD) were recently investigated and characterised by Bettinetti *et al.*[60] The characterisation included thermal analysis (DSC and TGA), PXRD and FTIR. In their investigation they found that recrystallization of the peracetylated CDs from various solvent systems produced solvates, while hydrates and amorphous forms were obtained from spray drying or microwave-drying. Polymorphs were obtained in the process of dehydration and recrystallization from the melt of commercially available CDs.[60,61]

TAαCD

For TAαCD the crystalline anhydrous form was isolated by heating the commercially available monohydrate product from -3.5 to 103 ˚C. Recrystallising the monohydrate from 2-propanol/water (4/1, v/v) produced a dihydrate TAαCD•2H_2O, Figure 27.

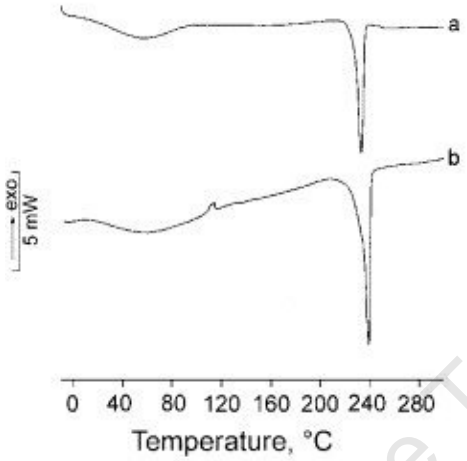

Figure 27. *DSC traces of the hydrated TAαCD which dehydrates and converts to the anhydrous form represented by (a) and the recrystallised dihydrate of TAαCD isolated from 2-propanol/water (4/1) represented here by trace (b).*[60]

TAβCD

In the case of TAβCD, two monotropically related anhydrous polymorphs are reported. Polymorph **I**, the lower melting form ($T_{fus,\ I}$ = 192.2 ± 1.8 ˚C) was isolated from the dehydration (13 to 97 ˚C) of the commercially available TAβCD. Recrystallization of polymorph **I** (at about 200 ˚C) to the higher melting polymorph **II** ($T_{fus,\ II}$ = 218.5 ± 0.8 ˚C) occurs as shown in Figure 28.

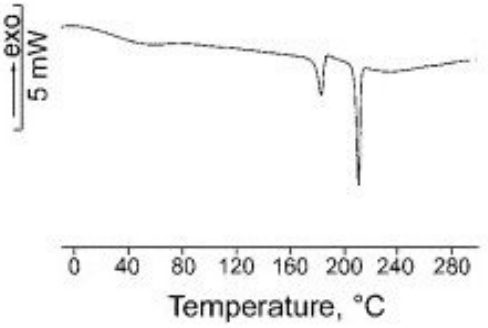

Figure 28. *A DSC trace of the commercially available TAβCD hydrate which forms polymorph **I** upon dehydration (13 to 97 ˚C, melt $T_{fus,\ I}$ = 192.2 ± 1.8 ˚C). It undergoes further recrystallization (ca. 200˚C) and forms polymorph **II** ($T_{fus,\ II}$ = 218.5 ± 0.8 ˚C).*[60]

TAγCD

For TAγCD, two anhydrous polymorphs are reported; both were isolated from a recrystallisation of the melt of solvated or hydrated forms of TAγCD, Figure 29. The polymorphs are monotropically related with the lower melting form having a melt peak at 222.5 ˚C while the higher melting form starts to melt at 225.6 ± 1.1 ˚C.[36]

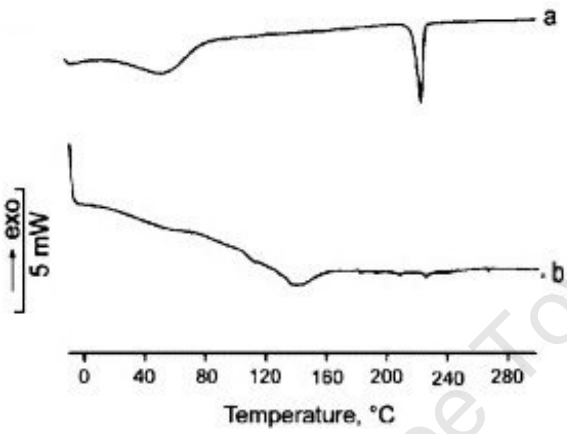

Figure 29. *DSC trace of the hydrated TAγCD which converts to the low melt polymorph (a) and the DSC of the higher melting polymorph (b) obtained from the recrystallization of an amorphous sample.*[60]

In all the cases of peracetylated CDs reported above none was characterised by means of single crystal X-ray diffraction. Recently Caira *et al.* published the structures of the peracetylated γ-CD solvates.[62]

The possibility of isolating more than one CD inclusion complex containing the same host and guest is relatively unexplored with only a few examples recorded in the literature. Here we give a brief overview of those reported in the literature and the techniques used in isolating the different forms.

MULTIPLE CRYSTAL FORMS OF INCLUSION COMPLEXES

Solvent mediated phase - transformation

In 1979 Stezowski *et al.* reported the isolation of a metastable form of a β–cyclodextrin complex with n-propanol.[63,64] The crystals were obtained by the slow cooling of a 60 : 40 (v/v) n-propanol : water solution of β-CD over 1.5 to 2 days. The crystals, designated C**II** by Stezowski, had the following unit cell parameters: a = 15.461(2) Å, b = 15.575(3) Å, c = 15.316(3) Å, α = 103.98(3)˚, β =

100.92(2)˚ and γ = 104.23(2)˚ with a unit cell volume V = 3364 Å^3. The unit cell contents reported for C**II** were $C_{96}H_{172}O_{74}$•18-19H_2O (1:2, β–CD:n-propanol) i.e. one hydrogen bonded β–CD dimer with four n-propanol molecules and between 18 and 19 water molecules. These parameters differed from crystals isolated by means of a vapour diffusion method which Stezowski *et al.* employed previously to obtain crystals of β–CD with n-propanol. The vapour diffusion crystals, named C**I**, were characterised and provided the following dimensions: a = 17.980(2) Å, b = 15.424(2) Å, c = 15.299(1) Å, α = 103.0(1)˚, β = 113.5(1)˚ and γ = 99.4(1)˚ with a unit cell volume V = 3636 Å^3. The unit cell contents for C**I** were: $C_{96}H_{174}O_{74}$•24H_2O (1:2, β–CD:n-propanol) and again there is a single β–CD dimer to four n-propanol molecules accompanied by 24 water molecules. Both structures were reported as triclinic with space group P1. The C**II** crystals were considered metastable since upon standing at room temperature for a few hours they redissolve and recrystallise as the form C**I**. Thus, the crystals undergo a solvent mediated phase – transformation, a first for cyclodextrin inclusion complexes.[64]

Similarly, in 1984 Nakanishi *et al.* isolated two forms of the dimeric β-CD inclusion complex of the barbiturate barbital.[30] Form **I** was obtained by slow cooling of an aqueous solution which contained 2.4 X 10^{-4} mol of both β-CD and barbital in a total of volume 1.5 mL. The parameters of form **I** were a = 19.716(3) Å, b = 15.497(1) Å, c = 15.549(2) Å, α = 103.63(1)˚, β = 116.65(1)˚, γ = 104.56(1)˚, Z = 1 with a unit cell volume = 3761 (1) Å^3. The crystal system was triclinic with space group P1. The unit cell contents were: $(C_{42}H_{70}O_{35})_2$•$(C_8H_{12}N_2O_3)_2$•31H_2O corresponding to a host-guest ratio of 1:1. Form **II** was isolated under similar conditions except that the volume of the solution was reduced to 0.8 mL. The parameters for form **II** were: a = 34.341(5) Å, b = 15.529(2) Å, c = 15.568(2) Å, α = 103.82(1)˚, β = 100.58(2)˚, γ = 106.67(1)˚, Z = 1 with a unit cell volume = 7434 (1) Å^3. The crystal system was triclinic with space group P1 (*i.e.* the same as that of form **I**). The unit cell

contents here were $(C_{42}H_{70}O_{35})_4 \bullet (C_8H_{12}N_2O_3)_4 \bullet 50H_2O$; the host-guest ratio was retained at 1:1. However, the authors were unable to determine which crystal was the metastable form.[30]

Phase - transition of a dimeric β–CD complex in the solid state

Rysanek *et al.* (2002) reported the solid-state phase transition of a β-CD inclusion complex observed by means of a new experimental technique.[65] The technique couples differential scanning calorimetry (DSC) with time-resolved X-ray powder diffraction as a function of temperature.[65‡] The inclusion complex whose structure was known prior to the experiment was subjected to a heating profile with range 23 -150 K and heating rate 2 K/min. The initial unit cell dimensions for the complex were: a = 19.37 Å, b = 24.45 Å, c = 15.94 Å, β = 108.72˚ and the cell volume, V = 7149 Å^3.

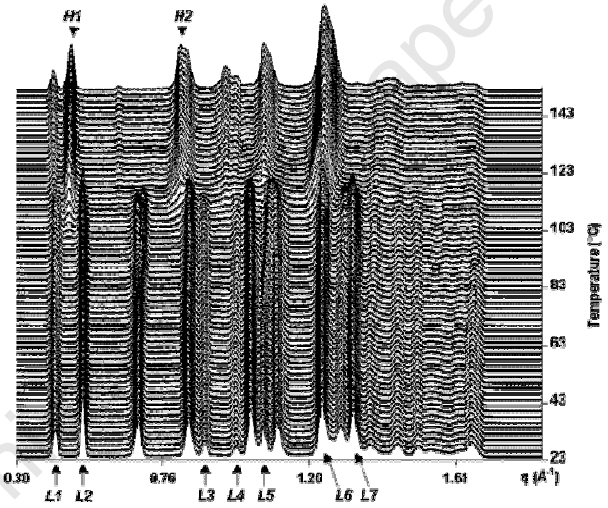

Figure 30. *The PXRD traces recorded simultaneously with DSC, showing the disappearances and appearance of the low temperature (L7 and L2) and high temperature phases (H1 and H2).*[65]

A phase change was induced at ~110 ˚C. The event was characterised by a broad endotherm on DSC and the disappearance of certain peaks (L7 and L2) from the low temperature PXRD trace and the appearance of other peaks (H1 and H2) during and after the high temperature phase change, shown in Figure 30. The fact that the sample retained a rather high level of crystallinity after the phase change enabled Rysanek *et al.* to index the new structure.

‡ The reader is referred to the paper by Rysanek *et al.* for a detailed description of the structural analysis (apparatus, data capture and interpretation).[65]

With the aid of programs such as FULLPROF[66] and PEAKFIT (Jandel Scientific, Germany) they were able to determine unit cell dimensions for the new phase. This required intimate knowledge of the dimeric packing arrangements. The data for the new phase were: monoclinic with space group C2 and unit cell dimensions a = 16.12 Å, b = 26.44 Å, c = 15.95 Å, β = 108.72˚ with the unit cell volume V = 6438 Å^3.

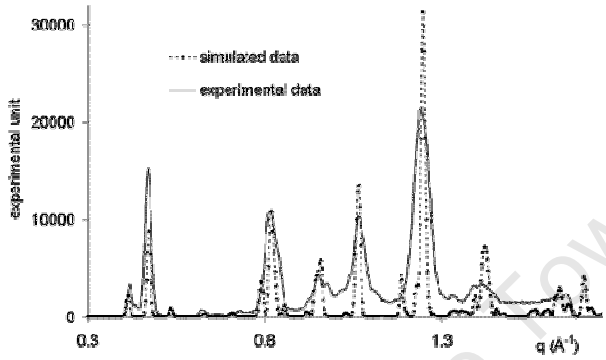

Figure 31. *The diagram shows an overlay of the simulated data and the experimental data.*[65]

As a final confirmation of the result, they calculated the PXRD pattern for the new phase and compared it to the experimental pattern, Figure 31. A high level of correspondence was obtained between the two traces.[65]

Thermal control in generating different crystal forms

In a recent paper by Caira *et al.*, the isolation of two forms of a β-cyclodextrin inclusion complex containing a common organic guest was reported.[67] These forms, crystallizing in the space group P1 (triclinic) and C2 (monoclinic), were isolated under different experimental conditions. The guest was the methyl ester of 4-hydroxybenzoic acid (also known as methylparaben). Both complexes (P1 and C2) had the same initial preparation conditions but their actual crystallization conditions were different. In the case of the P1 form the solution was allowed to cool to room temperature and thereafter it was placed in a refrigerator at *ca.* 7 ˚C to induce crystallisation. For the C2 form the solution was allowed to crystallize at room temperature *ca.* 20 ˚C. Both complexes had 1:1 stoichiometry with the molecular formulae

$(C_{42}H_{70}O_{35})_2 \bullet (C_8H_8O_3)_2 \bullet 28H_2O$ in the case of the low temperature form and $(C_{42}H_{70}O_{35}) \bullet (C_8H_8O_3) \bullet 7.2H_2O$ for the room temperature form.

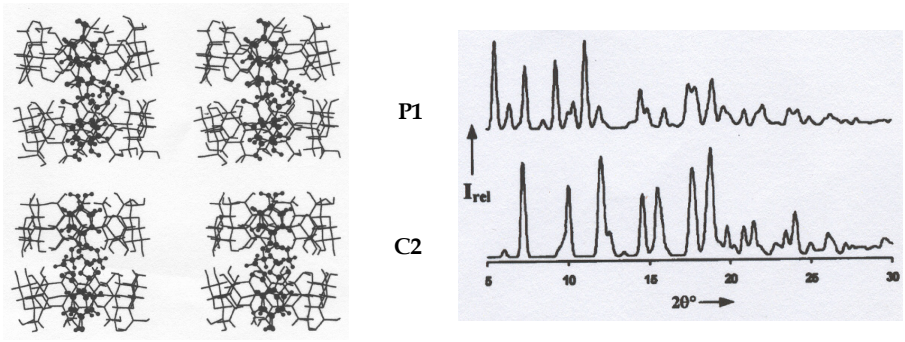

(**a**) (**b**)

Figure 32. *The stereo diagram of the two forms P1 and C2 (**a**) and the respective PXRD traces for both forms.*[67]

Both forms were characterised by single crystal X-ray diffraction, Figure 32(**a**), and they presented the following parameters: triclinic P1, a = 18.0187(3) Å, b = 15.3431(4) Å, c = 15.4140(3) Å, α = 103.464(1)˚, β = 113.122(1)˚, γ = 99.254(1)˚, unit cell volume V = 3656.65(1) $Å^3$; monoclinic C2, a = 18.8632(4) Å, b = 24.4542(5) Å, c = 15.5942(5) Å, β = 110.668(1)˚, unit cell volume V = 6730.4(3) $Å^3$.[67] For comparison the PXRDs were calculated, Figure 32(**b**); it is quite apparent that they are different.

The examples of multiplicity of crystal forms provided here are exceedingly important and underscore the need for careful control of the experimental conditions to ensure reproducible isolation of a given crystal form. More explicitly, these results have implications in the context of the pharmaceutical and agricultural industries in much the same way as polymorphism has impacted on these fields.[67]

PESTICIDE-COMPLEX REVIEW

Pesticides

The main purpose of this review is to give the reader an overview of the physicochemical properties of pesticides, their extent of usage and the benefits and pitfalls derived from their cyclodextrin inclusion.

The physicochemical properties of pesticides are often undesirable and render the formulation of pesticides for routine use extremely difficult. Some of these unwanted properties are poor solubility, chemical, thermal and physical instability, mammalian toxicity, malodour, volatility, high soil mobility, persistence and poor wettability. Each of these properties has particular knock-on effects. For instance, a compound with poor solubility may have low bioavailability and therefore reduced efficacy. Pesticides which undergo photodegradation (UV lability) may become more, or less toxic to their environment.[68] A pesticide may thus be rendered ineffective as a result of its degradation. The degradation products may be highly toxic to mammals, putting livestock at risk. Compounds with high soil mobility tend to pollute ground water sources while persistence may lead to overdosing which renders crops unusable as a result of the high levels of pesticides remaining in the soil.

The properties of pesticides mentioned here may be minimised or even totally eliminated and others may be enhanced through their inclusion in cyclodextrins. Cheap, non-toxic, biodegradable and water soluble, cyclodextrins are versatile, having the added advantage of forming inclusion compounds with a large variety of molecules. The complexes formed between cyclodextrins and pesticides are new entities and are endowed with properties which are in many instances superior to those of the pesticide. Generally, characteristics attributed to, or enhanced by CD inclusion, are: increased solubility, increased dissolution, increased bioavailability, reduced volatility, reduced overdosing, improved wettability, homogeneity and an extended half-life. Even phase-transformations, useful in the context of

pesticide formulations, can be effected by means of cyclodextrin inclusion. For example, when the starting material intended for use is an oil, it may be complexed with a cyclodextrin and transformed into a solid.[68]

One of the simplest ways in which CD inclusion can invoke change with regard to pesticide inclusion is in its physical stability. For example, the CD inclusion of sumithion, malathion and dursban resulted in an improvement in their long term stability.[68] On storage, over a nine year period, no significant change in the overall content of these pesticides was noted for the inclusion complexes while the physical mixtures showed significant loss of pesticide content on standing. The stabilisation may extend to chemical effects as well. A substantial reduction in the UV photodegradation of allethrin was achieved by its complexation with β-CD. Similarly, for 3-chloro-*p*-toluidine, its photostability was enhanced from 43% to 70% by its inclusion in β-CD. Methylparathion was likewise stabilised against chemical degradation.[69,70,71] As mentioned earlier, the solubility of the pesticides is very important as it may have a direct impact on the bioavailability of pesticides in their target area.[72] Saikosin *et al.* reported an 18-fold enhancement in the solubility of the insecticide carbaryl after its CD inclusion.[73,74] However, the cyclodextrin inclusion was accompanied by lower toxicity due to the inclusion of the insecticide, an effect which is not altogether unfavourable as its impact on the environment may also be lessened.

The environmental aspect is another way in which the use of cyclodextrins contributes, directly or indirectly. It has been reported by Villaverde *et al.* that α- and γ-CD have greatly enhanced the removal of norflurazon from contaminated soil by the formation of a soluble CD inclusion complex, aiding the remediation of soil.[72] Similar results were obtained for the pesticide 2,4-D using β-CD.[75,76] Another source of environmental contamination is the volatile pesticides which evaporate into the atmosphere where they may affect non-target crops or are returned to the ground in the form of contaminated rain water. In addition if the pesticide is expensive then losing

it to the atmosphere becomes costly. An example of a volatile pesticide is dichlorvos which has a moderate vapour pressure. After CD inclusion, its vapour pressure was barely measurable.[74,77] The catalytic effects cyclodextrins have on the pesticides are important as they provide clues to the eventual understanding of the degradation and persistence of these molecules in the soil.

Although there are substantial benefits to be gained from the inclusion of pesticides in cyclodextrins there are also pitfalls regarding strength or size of the association constant. If the association constant or binding constant is too large then the complex does not dissociate and this may inhibit the action of the pesticide. However, this could be beneficial as the half-life of the pesticide may be altered and the action of the pesticide may be extended. It is difficult to know what value for the association constant would be considered too large; an optimum value has yet to be established. The pharmaceutical industry with many more years of experience in this area has settled on $K < 10\ 000\ M^{-1}$ as a reference value for the binding constant.[78] So, if K exceeds this value then the complex is less likely to dissociate to any great extent in solution. If K is less than $10\ 000\ M^{-1}$ then it will quite easily dissociate in solution and achieve its aims.

SOLUTION NMR AND BINDING CONSTANTS

Nuclear magnetic resonance spectroscopy (NMR)

Binding may be quantitatively described by stoichiometry and binding constants. Frequently and routinely, NMR spectroscopy is used in the measurement of these parameters of host-guest systems.[79] Since Demarco and Thakkar presented direct evidence of complexation of β-CD with aromatic guest molecules in aqueous solution,[80] NMR spectroscopy has become increasingly employed to examine the mode of host-guest interaction in CD complexation phenomena.[81] As the authors state, 'the interest in such a technique is based on its ability to allow precise characterization of the non-covalent binding between the cyclodextrin and a guest molecule.'[82] Unique

features of the hydrophobic cavity of cyclodextrins are the methine hydrogens (H_3 and H_5) situated inside the cavity and the methylene hydrogens ($H_{6a,b}$) located near the primary rim. These protons are extremely sensitive to inclusion complexation and undergo measurable NMR shifts during inclusion complex formation in solution. The guest aromatic hydrogens may also undergo shifts upon inclusion. The chemically induced shifts (CIS henceforth) allow for the extraction of association constants and stoichiometries of the formed complex. The stoichiometries are obtained from the observed changes in the CIS of a particular host or guest proton H_i. These shifts are then multiplied by the concentration of the host or guest and the resulting values plotted against the mole fraction of the host or guest. The resultant curve is a Job plot. Observations of the chemically induced shifts are dependent on the exchange rate of association-dissociation of the complex in solution relative to the timescale of the NMR experiment.

Three scenarios are possible: firstly, when the exchange rate of the complex is slow relative to the timescale of the NMR experiment, then the NMR spectrum for the complex will contain peaks owing to the presence of uncomplexed host with integration intensity (m) as well as peaks for the host involved in the complex having integration intensity (n). These values of (m) and (n) may then be used along with the total concentration of the host to determine the stoichiometry of the complex. Secondly, if the exchange rate is similar or equal to the timescale of the NMR experiment, then the peaks broaden and/or disappear, and it is impossible to measure the chemically induced shifts. Finally, when the host-guest equilibrium occurs at a rate faster than the timescale of the NMR experiment, then peaks for the free host and peaks for the host involved in complex formation are fused and appear at the weighted average chemical shift in the spectrum.[83] In this case the analysis is complicated as the chemical shift in the complex cannot be observed. This problem is overcome with the method of continuous variation – in the form of an NMR titration.[80] The NMR technique used in the study reported in this

thesis was based on the shielding effects of the protons located on the interior of the cyclodextrin cavity (Figure 33).[80,81,84] The shielding and upfield movements of these protons are related to ring-current and magnetic anisotropy effects of the aromatic ring belonging to the guest,[85,86] while in the presence of the cyclodextrin (CD) the protons of the aromatic ring are deshielded and move downfield.

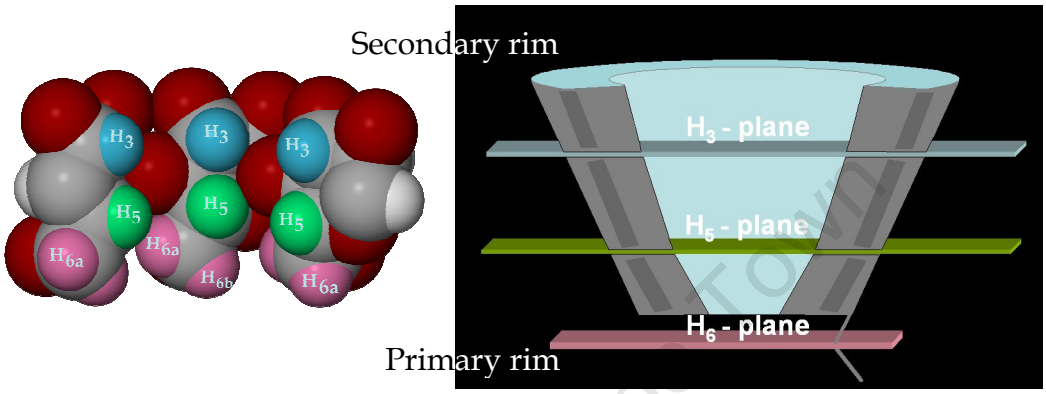

Figure 33. *The H_3, H_5 and $H_{6a,b}$ protons which line the cavity (shown in the cutaway view on the left) as well as a schematic representation of the H_3, H_5 and $H_{6a,b}$ protons represented as planes (shown on the right) dissecting the torus.*

The latter effect is probably due to the steric perturbations during inclusion.[87,88,89] The methine protons (H_3 and H_5) situated in the cyclodextrin cavity as well as the methylene protons ($H_{6a,b}$) located on the primary rim of the CD act as excellent sensors for inclusion and provide information on the interactions, position and orientation of the guest molecule.[81,90,91,92] The extent to which protons H_3, H_5 and $H_{6a,b}$ are shifted with respect to each other allows one to determine the location of the guest in the cavity. In other words if the CIS for H_3 > the CIS for H_5 then the guest is located near the wider secondary rim of the cavity and if the CIS for H_5 > the CIS for H_3 then the guest is located near the narrower primary rim.[80]

The protons located on the exterior of the CD (H_1, H_2 and H_4) remain relatively unaffected but may also show shielding effects due to hydrophobic interactions with the guest molecule.[85] The spectra obtained in the course of this work showed no evidence of new peaks being formed. Thus the

association-dissociation process is dynamic and occurs at a rate faster than the timescale of the NMR (Djedaïni et al., 1990).[91]

MOTIVATION, AIMS AND OBJECTIVES

Motivation

A series of four phenylurea analogues, metobromuron (**1**), monolinuron (**2**), monuron (**3**) and fenuron (**4**) were investigated in this study, Figure 34.

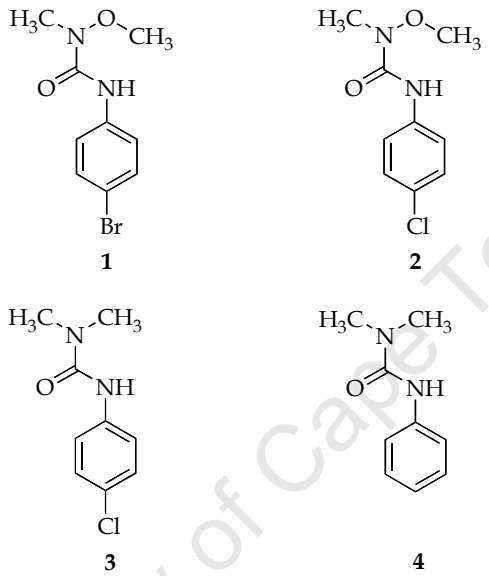

Figure 34. Guest molecules used in this study: metobromuron (**1**), monolinuron (**2**), monuron (**3**) and fenuron (**4**).

Discovered in the 1960s phenylureas represent a large and important class of herbicides which can further be divided into two main groups; the *N*-phenyl-*N*′,*N*′-methoxyureas (**1** and **2**) and *N*-phenyl-*N*′,*N*′-dialkylureas (**3** and **4**), shown in Figure 34.[93] Phenylureas are used for the control of weeds in cereals, vegetables and fruit trees through the action of inhibiting photosynthesis. Alone, phenylureas are not very toxic to animals but exposure to UV light may significantly enhance their toxicity. Phototransformation may be induced by the absorption of light resulting in the formation of more toxic intermediates.[94] In addition, it has been shown that phenylureas under suitable conditions, such as those present in humic soils, may undergo acid or base hydrolysis.[95,96] However, owing to environmental conditions these processes are slow and there is little

accumulation of these toxic by-products. Since these compounds are subject to slow transformation, with the mean persistence in the environment of 4-12 months, there are relevant risks.[97] Phenylureas are also susceptible to thermal decomposition which has significant implications for their storage, action and detection.[93,98,99,100] Cyclodextrin inclusion of many of the phenylureas has received much attention over the last two or three decades but the literature on solid-state structures of their cyclodextrin inclusion complexes is rare.

Aims and objectives

The primary aims of the project described in this thesis are listed here.

1. The preparation of cyclodextrin inclusion complexes of the four phenylurea herbicides **1**, **2**, **3** and **4** using kneading and co-precipitation methods. The characterisation of these products by TGA, DSC, HSM, and PXRD. Furthermore, using the principles of isostructurality, to determine approximate unit cell dimensions and space groups of putative complexes.
2. The determination of complex formation with selected cyclodextrins in solution using ^{1}H-NMR spectroscopy. The determination of the stoichiometry and the stability constants in solution using a specialised program for this purpose.
3. The isolation of more than one CD inclusion complex containing the same host and guest by changing the conditions of crystallisation such as the temperature of crystallisation or the solvent medium.
4. The investigation of the solid-state features of the inclusion complexes using single crystal X-ray diffraction.
5. The investigation of the thermal properties after CD inclusion.

REFERENCES

1. Frömming, K.H., Szejtli, J., *Topics in Inclusion Science – Cyclodextrins in pharmacy*, Kluwer Academic Publishers, Dordrecht, The Netherlands, **1993**, Vol. 5, Chapter 1.
2. Saenger, W., *Angew. Chem. Int. Ed. Engl.* **1980**, 19, 344-361.
3. Saenger, W., *Inclusion Compounds,* Atwood, J.L., Davies, J.E.D., MacNicol, D.D., (eds.), Oxford University Press, London, **1984**, Vol. 2, Chapter 8.
4. Harata, K., *Inclusion Compounds*, Atwood, J.L., Davies, J.E.D., MacNicol, D.D., (eds.), Oxford University Press, London, **1991**, Vol. 5, Chapter 9.
5. Cramer, F., *Einschlusverbindungen (Inclusion Compounds)*, Springer-Verlag: Berlin, **1954**.
6. Saenger, W., Jacob, J., Gessler, K., Steiner, T., Hoffman, D., Sanbe, H., Koizumi, K., Smith, S. M. and Takaha, T., *Chem. Rev.*, **1998**, 98 1787-1802.
7. Szejtli, J., In *Comprehensive Supramolecular Chemistry, Cylodextrins,* Atwood, J.L., Davies, J.E.D., MacNicol, D.D., Vogtle, F., (eds.), Pergamon: Oxford, **1996**, Vol. 3, Chapter 2.
8. Harata, K., *Seimei Kogaku Kogyo Gijutsu Kenkyushu Kenkyu Hokoku,* **1993**, 1, 1-24.
9. Harata, K., In *Comprehensive Supramolecular Chemistry, Cylodextrins,* Atwood, J.L., Davies, J.E.D., MacNicol, D.D., Vogtle, F., (eds.), Pergamon: Oxford, **1996**, Vol. 3, Chapter 9.
10. Szejtli, J., *Chem. Rev.*, **1998**, 98, 1743-1753.
11. Liu, L. and Guo, Q-X., *J. Incl. Phenom. Macrocycl. Chem*., **2002**, 42, 1-14.
12. Bender, M.L. and Komiyama, M. *Cyclodextrin Chemistry*, Springer-Verlag, Berlin, **1978**.
13. Hallen, D., Schoen, A., Shehatta, I. and Wadsoe, I. *J. Chem. Soc. Faraday Trans*., **1992**, 88, 2859-2863.
14. Rekharsky, M.V., Mayhew, M.P., Goldberg, R.N., Ross, P.D., Yamashoji, Y. and Inoue, Y. A. *J. Phys. Chem. B*., **1997**, 101, 87-100.
15. Matsui, Y. and Mochida, K. *Bull. Chem. Soc. Jpn*., **1979**, 52, 2808-2814.
16. Barone, G., Castronuovo, G., Del Vecchio, P., Elia, V. and Muscetta, M. *J. Chem. Soc. Faraday Trans. 1*, **1986**, 82, 2089-2101.
17. Fujiwara, H., Arakawa, H., Murata, S. and Sasaki, Y. *Bull. Chem. Soc. Jpn*., **1987**, 60, 3891-3894.
18. Sanemasa, I., Osajima, T. and Deguchi, T. *Bull. Chem. Soc. Jpn*., **1990**, 63, 2814-2819.
19. Harrison, J.C. and Eftink, M.R. *Biopolymers,* **1982**, 21, 1153-1166.
20. Tabushi, I., Kiyosuke, Y., Sugimoto, T. and Yamamura, K. *J. Am. Chem. Soc*., **1978**, 100, 916-919.

21. Frömming, K.H., Szejtli, J., *Topics in Inclusion Science – Cyclodextrins in pharmacy*, Kluwer Academic Publishers, Dordrecht, The Netherlands, **1993**, Vol. 5, Chapter 4.

22. Mentzafos, D., Mavridis, I.M., Le Bas, G. and Tsoucaris, G., *Acta Crystallogr.,* **1991**, B47, 746-757.

23. Lubhelwana, S., MSc Dissertation, *Crystal Isostructurality and X-ray Diffraction Studies of Cyclodextrin Inclusion Compounds,* University of Cape Town, South Africa, **2005**.

24. Caira, M. R., *Rev. Roum. Chim*., **2001**, 46, 371-386.

25. Mavridis, M. I., Hadjoudis, E. and Tsoucaris, G., *Mol. Cryst. Liq. Cryst.* **1990**, 186, 185-188.

26. Mavridis, I.M., Hadjoudis, E and Tsoucaris, G., *Carbohydr. Res.,* **1991**, 220, 11-21.

27. Dodds, D.R., PhD thesis, *Physicochemical Study of Inclusion of Drug Molecules in Cyclodextrins,* University of Cape Town, South Africa, **1999**.

28. Giastas, P., Yannakopoulou, K. and Mavridis, I.M., *Acta Crystallogr.,* **2003**, *B*59, 287-299.

29. Chatziefthimiou, S.D., Yannakopoulou, K. and Mavridis, I.M., *CrystEngComm*, **2007**, 9, 976-979.

30. Nakanishi, I., Arai, M., Fujiwara, T. and Tomita, K-I., *J. Incl. Phenom.,* **1984**, 2, 689-699.

31. Liu, Y., Zhong, R-Q., Zhang, H-Y. and Song, H-B., *Chem. Commun.,* **2005,** 2211-2213.

32. Tsorteki, F., Bethanis, K., Pinotsis, N., Giastas, P. and Mentzafos, D., *Acta Crystallogr.,* **2005**, *B*61, 207-217.

33. Vicens, J., Fujiwara, T. and Tomita, K-I., *J. Incl. Phenom.,* **1988**, 6, 577-581.

34. Shen, X-J., Chen, H-L., Yu, F., Zhang, Y-C., Yang, X-H. and Li, Y-Z., *Tetrahedron Letters*, **2004**, 45, 6813-6817.

35. Cambridge Structural Database and Cambridge Structural Database System, Version 5.29, November **2007**, Cambridge Crystallographic Data Center, University Chemical Laboratory, Cambridge, England.

36. Harata, K. *Chem. Rev.,* **1998**, 98, 1803-1827.

37. Caira, M.R., Bourne, S.A., Vilakazi, S.L. and Reddy, L., *Supramol. Chem*., **2004**, 16, 279-285.

38. Caira, M.R., Hunter, R., Bourne, S.A. and Smith, V.J., *Supramol. Chem.,* **2004**, 16, 395-403.

39. Caira, M.R., De Vries, E., Nassimbeni, L.R. and Jacewicz, V.W., *J. Inclusion. Phenom. Macrocyclic Chem.*, **2003**, 46, 37-42.

40. Threlfall, T., *The Analyst*, **1995**, 120, 2435-2460.

41. Burger, A., *Acta Pharm. Tech.,* **1979**, **Suppl.** 7, 107.

42. Kuhnert-Brandstätter, M. and Riedmann, M., *Mikrochim. Acta,* **1987**, II, 107-120.

43. McCrone, W. C., *Physics and Chemistry of the Organic Solid State*; Fox, D., Labes, M. M., Weissberger, A., Eds.; Wiley-Interscience: New York, 1965, 2, 725-767.

44. Bernstein, J., *Polymorphism in Molecular Crystals;* Oxford University Press: Oxford, **2002**, 4-8.

45. Pienaar, E. W., Caira, M. R., Lötter, A.P., *J. Crystallogr. Spectr. Res.,* **1993**, 23, 739-744.

46. Seddon, K. R., *Cryst. Growth and Des.,* **2004**, 4, 1087-1087.

47. Desiraju, G. R., *Cryst. Growth and Des.,* **2004**, 4, 1089-1090.

48. Bernstein, J., *Cryst. Growth and Des.,* **2005**, 5, 1661-1662.

49. Nangia, A., *Cryst. Growth and Des.,* **2006**, 6, 2-4.

50. Kálmán, A. and Párkányi L., *In Advances in Molecular Structure Research,* JAI Press Inc., **1997**, 189-226.

51. Fábián, L. and Kálmán, A., *Acta Crystallogr.,* **1999,** B55, 1099-1108.

52. Kálmán, A., *In Fundamental Principles of Molecular Modelling;* Gans, W., Ammon, A., Boeyens J. C. A., Eds.; Plenum Press: New York, **1996**, 209-221.

53. Smith, V. J., MSc Dissertation, *Physicochemical Study of Solid Cyclodextrin Inclusion Complexes of the Antithrombotic Ajoene,* University of Cape Town, South Africa, **2004**.

54. Stephenson, G. A., Stowell, J. G., Toma, P. H., Dorman, D. E., Greene, J. R. and Byrn, S. R., *J. Am. Chem. Soc.,* **1996**, 116, 5766-5773.

55. Lindner, K and Saenger, W., *Acta Crystallogr.,* **1982**, B38, 203-210.

56. Chacko, K. K. and Saenger, W., *J. Am. Chem. Soc.,* **1981**, 103, 1708-1715.

57. Puliti, R., Mattia, C. A and Paduano, L., *Carbohydr. Res.,* **1998**, 310, 1-8.

58. Caira, M. R., Griffith, V. J., Nassimbeni, L. R. and van Oudtshoorn, B., *J. Chem. Soc. Perkin Trans. 2,* **1994**, 2071-2072.

59. Caira, M. R., Bourne, S. A., Mhlongo, W. T. and Dean, P. M., *Chem. Commun.,* **2004**, 19, 2216-2217.

60. Bettinetti, G., Sorrenti, M., Catenacci, L., Ferrari, F. and Rossi, S., *J. Pharm. Biomed. Anal.,* **2006**, 41, 1205-1211.

61. Añibarro, M., Gessler, K., Usón, I., Sheldrick, G. M., Harata, K., Uekama, K., Hirayama, F., Abe, Y. and Saenger, W., *J. Am. Chem. Soc.,* **2001**, 123, 11854-11862.

62. Caira, M.R., Bettinetti, G., Sorrenti, M., Catenacci, L., Cruickshank, D. and Davies, K., *Chem. Commun.,* **2007**, 1221-1223.

63. Stezowski, J.J., Jogun, K.H., Eckle, E. and Bartels, K., *Nature*, **1978**, 274, 617-619.

64. Jogun, K.H. and Stezowski, J.J., *Nature*, **1979**, 278, 667-668.

65. Rysanek, N., Coquillay, M., Bourgaux, C. and Ollivon, M., *J. Phys. Chem. B,* **2002**, 106, 11870-11875.

66. Rodriguez-Carvajal, J.,Roisnel, T., *Fullprof.98* and *WinPLOTR;* new Windows 95/NT Applications for Diffraction; Newsletter No. 20; May-August, **1998**.

67. Caira, M.R., de Vries, E.J.C. and Nassimbeni, L.R., *Chem. Commun.* **2003**, 2058-2059.

68. Szente, L. and Szejtli, J., In *Comprehensive Supramolecular Chemistry, Cylodextrins,* Atwood, J.L., Davies, J.E.D., MacNicol, D.D., Vogtle, F., (eds.), Pergamon: Oxford, **1996**, Vol. 3, Chapter 17.

69. Hurley, J.C., Volz, S.A. and Johnston, J.J., *J. Agric. Food Chem.*,**1991**, 47, 2904-2907.

70. Yamamoto, I., Unai, T., Suzuki, U.Y. and Katsuda, Y., *J. Pesticide Sci.,* **1976**, 1, 41-48.

71. Yamamoto, I., Ohsawa, K. and Plapp, F.W., *J. Pesticide Sci.,* **1977**, 2, 41-49.

72. Villaverde, J., Pérez-Martínez, J.I., Maqueda, C., Ginés, J.M. and Morillo, E., *Chemosphere*, **2005**, 60, 656-664.

73. Morillo, E., In *Cyclodextrins and Their Complexes, Chemistry, Analytical Methods, Applications,* Helena Dodziuk (ed.), Weinheim:Wiley-VHC Verl., **2006**, Chapter 16.3.

74. Saikosin, R., Limpaseni, T. and Pongsawasdi, P., *J. Inclusion. Phenom. Macrocyclic Chem.,* **2002**, 44, 191-196.

75. Morillo, E., Pérez-Martínez, J.L. and Ginés, J.M., *Chemosphere*, **2001**, 44, 1065-1069.

76. Pérez-Martínez, J.I., Ginés, J.M., Morillo, E., Arias, M.J. and Moyano, J.R., *J Pesticide Sci.,* **2000**, 56, 425-430.

77. Szente, L. and Szejtli, J., *Acta Chim. Acad. Sci. Hung.,* **1981**, 107, 195-202.

78. Miller, L.A., Carrier, R.L. and Ahmed, I., *J. Pharm. Sci.,* **2007**, 96, 1691-1707.

79. Cameron, K. S., Fletcher, D. and Fielding, L., *Magn. Reson. Chem*., **2000**, 40, 251-260.

80. Demarco, P. V. and Thakkar, A. L., *J Chem. Soc., Chem. Commun.,* **1970**, 2-4.

81. Cabral Marques, H. M., Hadgraft, J., Kellaway, I. W. and Pugh, W. J., *Int. J. Pharm.,* **1990**, 63, 267-274.

82. Sicard-Roselli, C., Perly, B. and Le Bas, G., *J. Inclusion. Phenom. Macrocyclic Chem.,* **2001**, 39, 333-337.

83. Hirose, K., *J. Inclusion. Phenom. Macrocyclic Chem.,* **2001**, 39, 193-209.

84. Thakkar, A.L. and Demarco, P.V., *J. Pharm. Sci.,* **1971**, 60, 652-653.

85. De-Zhi, S., Li, L., Qiu, X-M., Liu, F., Yin, B-L. *Int. J. Pharm.,* **2006**, 316, 7-13.

86. Otagiri, M., Uekama, K., Ikeda, K., *Chem. Pharm. Bull.,* **1975**, 23, 188-195.

87. Cheney, B.V., *J. Am. Chem. Soc.,* **1968**, 90, 5386-5390.

88. Suzuki, M. and Sasaki, Y., *Chem. Pharm. Bull.,* **1979**, 27, 609-619.

89. Uekama, M., Fujinaga, T., Hirayama, F., Otagiri, M. and Yamasaki, M., *Int. J. Pharm.,* **1982**, 10, 1-15.

90. Ueda, H. and Nagai, T., *Chem. Pharm. Bull.,* **1981**, 29, 2710-2714.

91. Djedaïni, F., Zhao Lin, S., Perly, B., Wouessidjewe, D., *J. Pharm. Sci.,* **1990**, 79, 643-646.

92. Torres-Labandeira, J.J., Echezarreta-López, M., Santana-Penín, L., Vila-Jato, J.L., *Eur. J. Pharm. Biopharm.,* **1993**, 29, 255-259.

93. Mahedero, M.C., Muñoz De La Peña, A., Bautista, A. and Aaron, J.J., *J. Inclusion. Phenom. Macrocyclic Chem.,* **2002**, 42, 61-70.

94. Bonnemoy, F., Lavédrine, B. and Boulkamh, A., *Chemosphere,* **2004**, 54, 1183-1187.

95. Laudien, R. and Mitzner, R., *J. Chem. Soc., Perkin Trans. 2,* **2001**, 2230-2232.

96. Laudien, R. and Mitzner, R., *J. Chem. Soc., Perkin Trans. 2,* **2001**, 2226-2229.

97. Pramauro, E., Vincenti, M., Augugliaro, V. and Palmisano, L., *Environ. Sci. Technol.,* **1993,** 27, 1790-1795.

98. Mattern, G.C., Singer, G.M., Louis, J., Robson, M. and Rosen, J.D., *J. Assoc. Off. Anal. Chem.* **1989**, 72, 970-974.

99. Berrada, H., Font, G. and Moltó, J.C., *Chromatographia,* **2001**, 253-262.

100. Escuderos-Morenas, M.L., Santos-Delgado, M.J., Rubio-Barroso, S. and Polo-Díez, L.M., *J. Chromatogr. A.,* **2003**, 1011, 143-153.

Chapter 2

EXPERIMENTAL MATERIALS AND EXPERIMENTAL METHODS

MATERIALS

Host compounds

α-Cyclodextrin, β-cyclodextrin, γ-cyclodextrin and TRIMEB were obtained from Cyclolab (Budapest, Hungary) and were used as received.

Guest compounds

Metobromuron, monuron and fenuron were obtained from ChemService (Pennsylvania, USA) while monolinuron was obtained from Riedel-deHaën, Sigma-Aldrich (Germany). All compounds were used as received.

COMPLEX PREPARATION AND CRYSTAL GROWTH

Complexes of metobromuron, monolinuron, monuron and fenuron with β- and γ-CD were prepared by kneading equimolar amounts of host and guest with a mortar and pestle. Water was added dropwise until the product had a paste-like consistency, suitable for PXRD.

Co-precipitation

Complexes of the phenylureas with β-CD were prepared by the co-precipitation method. A solution of cyclodextrin was prepared by dissolving a known quantity of cyclodextrin in de-ionised distilled water at elevated temperature. The guest was added to the solution of cyclodextrin with prolonged stirring. Several methods were used to obtain crystals of sufficiently high quality for X-ray data-collection. These were crystallisation at low temperature, slow evaporation, slow cooling and crystal growth at elevated temperature. The solutions were left in an open vial so that the solvent (water) could evaporate slowly at room temperature. To reduce the evaporation rate even further the vials were covered with a polytop which was punctured several times.

Complexes of TRIMEB were prepared by dissolving the cyclodextrin in cold water. Once all the cyclodextrin had dissolved an equimolar amount of the

phenylurea was slowly added with stirring. The solutions were placed in a brass block on a hot plate set to *ca.* 60°C. Crystal growth occurred at elevated (*ca.* 60°C) temperature overnight.

THERMAL ANALYSIS

Thermal analysis is the measurement of changes in physical properties of a substance as a function of temperature, whilst the substance is subjected to a controlled temperature programme.[1] The main methods employed here are Hot Stage Microscopy (HSM), Thermogravimetric analysis (TGA) and Differential Scanning Calorimetry (DSC).

Hot Stage Microscopy

HSM can be used as a tool for the visual characterisation of those events which are not fully characterised by the standard techniques of TGA and DSC. Events such as colour or opacity changes in crystals which go undetected by the DSC and TGA methods are easily captured by HSM. In hot stage microscopy it is also possible to detect guest loss by immersing the complex crystal in high boiling inert oil such as silicone oil and observing the emergence of bubbles upon guest release. Most importantly, HSM plays a complementary role alongside that of the more traditional TGA and DSC methods of analysis. For this study, all crystals were immersed in silicone oil between two glass coverslips and then positioned on a Linkam THMS600 hot stage apparatus fitted with a Linkam TP92 manual temperature controller. The hot stage was mounted on a Nikon SMZ-10 stereoscopic microscope. The images were captured using a real time Sony Digital Hyper HAD colour video camera and analysed using the Soft Imaging System program, analySIS.[2]

Thermogravimetric Analysis and Differential Scanning Calorimetry

The preparation of the complex crystals for thermal analysis proceeded as follows. The single crystals were removed from their mother liquor under ambient conditions and washed in a drop of cold water to prevent the

dissolution of the crystals. This also aided in the removal of any uncomplexed cyclodextrin or guest adhering to the crystal surface. Thereafter the crystals were dried on filter paper by dabbing with another sheet of filter paper. The crystals were then placed in a pre-weighed crucible and moved inside the furnace. The measurement commenced as soon as the weight of the crystals stabilised.

TGA is the measurement of changes in the sample mass with temperature recorded using a thermobalance, which is an electronic microbalance coupled to a furnace with an associated temperature programmer. In the DSC technique, the sample (s) and a reference material (r) are maintained at the same temperature throughout ($\Delta T = T_s - T_r = 0$). In other words, the energy difference in the independent supplies to the sample and reference are recorded against the temperature programme.[2] Some of the various uses of DSC are determination of accurate melting points, measurement of onset temperature (T_{on}) for desolvation, characterisation of purity, degradation, desorption, phase transformations, polymorphic changes and thermal stability.[3]

All DSC runs were performed on a Perkin Elmer PC7-Series instrument (PE-DSC7). All TGA runs were performed on a Mettler Toledo TGA/SDTA851^e instrument using the STAR^e software version 6.10. The experimental TGA and DSC traces were recorded at a scanning rate of 10 K min^{-1} under an inert atmosphere of N_2 gas with a flow rate of 30 cm^3 min^{-1}. The sample masses ranged between 4-7 mg. In the case of the DSC, 50 µL crimped, vented aluminium pans were used while for the TGA 70 µL aluminium oxide crucibles were used. The results obtained were plotted by a Hewlett Packard Colour plotter connected to the thermal station. The calibration of the TGA instrument was performed against the Curie points of indium (156.6°C) and zinc (419.5°C). The DSC instrument was calibrated by measuring the onset

temperatures of indium (156.6°C) and zinc (419.5°C) while the heat flow was calibrated from the enthalpy of fusion of indium (28.62 J/g).

POWDER X-RAY DIFFRACTION

Powder X-ray diffraction (PXRD) patterns were recorded using a Huber Imaging Plate Guinier Camera 670 using nickel-filtered CuKα_1 radiation (λ = 1.5405981 Å) produced at 40 kV and 20 mA by a Philips PW1120/00 generator fitted with a Huber long fine-focus tube PW2273/20 and a Huber Guinier Monochromator Series 611/15. Samples for PXRD were generally not amenable to sieving. For all samples the flat sample holder with model no. 0670.000.02 was used. The sample of paste-like consistency was applied to MYLAR® polyester film (Thin-Film Sample Supports, West Chester, Pennsylvania, USA) which was suspended in the flat sample holder. A 2θ range of 4 - 100.0° was used with a step size of 0.005° 2θ. The PXRD patterns of the materials suspected to be complexes were overlaid on reference patterns of hosts and known complexes to establish (a) whether they were inclusion complexes, and if so (b) to which isostructural series they belonged.[4] For each crystal structure determined in this study by full three-dimensional X-ray analysis, refined unit cell parameters, space group symmetry, atomic co-ordinates and thermal parameters were used as input to the program LAZY PULVERIX[5] in order to generate an idealised PXRD pattern. LAZY PULVERIX uses the formula $I(hkl) = mLp\,|F(hkl)|^2$, where $I(hkl)$ is the intensity of the reflection with indices hkl, m is the reflection multiplicity, L the Lorentz factor, p the polarization factor, and $F(hkl)$ the structure factor. The homogeneity of the bulk material can be assessed by comparison with the corresponding calculated powder pattern. This comparison can also help prove the accuracy of the crystallographic model.

ULTRAVIOLET SPECTROPHOTOMETRY

For inclusion complex stoichiometry determination UV spectra were recorded on a Cintra 20 UV system over a wavelength range of 190 nm to 400 nm at a scanning rate of 1000 nm/min and a slit width of 2.0 nm.

NMR SPECTROSCOPY

Method of continuous variation (Job plot)

The stoichiometries of β-CD complexes in solution may be determined in the following way. Equimolar stock solutions of the host (H) and guest (G) are prepared in D_2O. The stock solutions are mixed together ensuring the final volume is constant. Changing the proportions of [H] and [G] ensures that the complete range ($0 < r < 1$) of ratios $r = [X] / ([H]_t + [G]_t)$ is sampled. In the preceding definition [X] is equivalent to the concentration of the host or guest for the sample and $[H]_t$ and $[G]_t$ are the total concentrations of the host and guest respectively. Thus, the total concentration of [H] and [G] is maintained constant ($[H]_t + [G]_t = M$, where M is the total concentration) for each sample. From the NMR data, the quantity $\Delta\delta_{obs} \bullet [X]$ is obtained by subtracting the observed chemical shift value for a given sample from the shift of the free X. $\Delta\delta_{obs} \bullet [X]$ is then plotted against r in a Job plot and the maximum of the curve corresponds to the complex stoichiometry.[6]

ASSOCIATION CONSTANT

The evaluation of the association constants (K) utilises the same data ($\Delta\delta_{obs}$) as used in the determination of the stoichiometry of a complex in solution. Some approximations are made during the determination of the association constant, such as the global consideration of $[H]_i >> [G]_i$ (where i counts the sample number) as well as in the graphical representation of experimental parameters. The graphical representation of the data is considered an advantage, while the use of data where the concentration of the host $[H]_i$ must be much larger than that of the guest $[G]_i$ is not always either possible or mathematically correct. The more commonly used methods for data treatment which use these approximations in the determination of K are the methods of Scatchard,[7] Benesi and Hildebrand,[8] and Scott.[9] $\Delta\delta_i$ is determined experimentally for each of the protons studied and thus the corresponding expression for K yields a different value for each proton studied.[10] Ideally, the observations of all the protons should be given the same estimate of K but

this never occurs as measurement error prevents this.[11] For example, the method for the determination of K requires $[H]_i >> [G]_i$ and when $[G]_i$ is very small then the difficulty in determining the CIS increases with its complexity (coupling). In addition, the host-to-guest ratio never exceeds 9/1, thus never coming close to the requirement of $[H]_i >> [G]_i$. Therefore, programs which utilise the $\Delta\delta_i$ for all the observed protons in the determination of K have an advantage over those which do not. CALCK,[11] EMUL,[11,12] MULTIFIT,[11,13] and CONSTEQ[14] are a few programs which determine K from all the observed protons.

The analysis of host-guest complexation is based on a simple equilibrium model in solution:

$$a{\cdot}H + b{\cdot}G \leftrightarrow H_aG_b, \text{ where } H_aG_b = C. \quad (1)$$

The association constant may then be defined as:

$$K = \frac{[C]}{[H]^a[G]^b} \quad (2)$$

$$[H]_t = [H] + a \cdot [C] \quad (3)$$

$$[G]_t = [G] + b \cdot [C] \quad (4)$$

where H represents the host, G represents the guest, C represents the complex and a, b the stoichiometry. $[H]_t$ and $[G]_t$ represent the total concentrations of the host and guest and [H], [G] and [C] are the concentrations at equilibrium. Substituting (3) and (4) into (2) we obtain:

$$K = \frac{[C]}{([H]_t - a \cdot [C])^a([G]_t - b \cdot [C])^b} \quad (5)$$

If a, b = 1 as would be established from a Job plot, equation (5) becomes:

$$K = \frac{[C]}{([H]_t - [C])([G]_t - [C])} \quad (6)$$

Experimentally the concentration of the complex C cannot be measured directly; however, it can be replaced with a parameter directly proportional to it.[14] For NMR spectroscopy this parameter is the observed chemical shift δ_{obs}. δ_{obs} is the weighted average chemical shift for the free, uncomplexed guest, δ_f, and the pure complexed state of the guest, δ_c. δ_{obs} can be written as:

$$\delta_{obs} = \frac{[G]\cdot\delta_f + b\cdot[C]\cdot\delta_c}{[G]_t} \quad (7)$$

Equation (7) may also be written as:

$$\delta_{obs} = \frac{[G]\cdot\delta_f + ([G]_t - [G])\cdot\delta_c}{[G]_t}, \text{ since } [G]_t = [G] + [C]$$

$$\delta_{obs} = \left(\frac{[G]}{[G]_t}\right)\cdot\delta_f + \left(\frac{[G]_t - [G]}{[G]_t}\right)\cdot\delta_c; \text{ if } \frac{[G]}{[G]_t} = z \text{ then}$$

$$\delta_{obs} = z\cdot\delta_f + \delta_c\cdot(1-z) \quad (8)$$

As [G] approaches 0, z approaches 0, such that $\delta_{obs} \rightarrow \delta_c$, and when $[G] = [G]_t$ or $[G]_t >> [H]_t$, then z approaches 1 and $\delta_{obs} \rightarrow \delta_f$ (similarly proven for the host). If we observe that $\Delta\delta_{obs} = \delta_f - \delta_{obs}$ and that $\Delta\delta_c = \delta_f - \delta_c$ for the free components and the pure complex then we can derive the expression:

$$\Delta\delta_{obs}^{(X)} = \frac{[C]}{[X]_t}\cdot\Delta\delta_c^{(X)} \quad (9)$$

where X = H or G for a 1:1 complex. Substituting expression (9) into equation (5) we obtain:

$$[X]_t^2\left(\Delta\delta_{obs}^{(X)}\right)^2 - [X]_t\,\Delta\delta_{obs}^{(X)}\Delta\delta_c^{(X)}\left\{[M] + \frac{1}{K}\right\} + [H]_t[G]_t\left(\Delta\delta_c^{(X)}\right)^2 = 0 \quad (10)$$

where $[M] = [H]_t + [G]_t$.

Solving equation (10) we obtain the following:

$$\Delta\delta_{obs}^{(X)} = \frac{\Delta\delta_{c}^{(X)}}{2[X]_t} \times \left\{ [M] + \frac{1}{K} \pm \left[\left([M] + \frac{1}{K} \right)^2 - 4[H]_t[G]_t \right]^{\frac{1}{2}} \right\} \quad (11)$$

For equation (11) only the negative solution is to be considered as the ratio $\Delta\delta_{obs} / \Delta\delta_c$ is always less than 1. Equation (11) must be satisfied for each sample studied. So for a set of n equations (n = no. of samples), there are two independent variables ($\Delta\delta_c$ and K) which can be solved using the experimental $\Delta\delta_{obs}$ values as reference.[14]

DETERMINATION OF THE ASSOCIATION CONSTANT

The association constants were calculated with the aid of a program called CONSTEQ.[14] It is written entirely in C^{++}, consists of about 1300 lines of code and runs under Windows 95/98/XP in DOS or Command prompt. The data are evaluated by a non-linear least-squares curve-fitting regression analysis of the observed chemical shift changes of the guest and β-CD NMR lines, as a function of concentration according to equation (11). The equation involves no approximations and correlates the total concentration of the host and guest molecules with the observed difference in the chemical shift, $\Delta\delta_{obs}$. The program is based on an iterative procedure following specific algorithms in order to fit the experimental values of $\Delta\delta_{obs}$ to the appropriate equation. Each iteration step sets up a quadratic function to determine the direction of the search and calculates the loss error function E:

$$E = \sum_{i,j} \left(\Delta\delta_{obs}^{(i,j)} - \Delta\delta_{calc}^{(i,j)} \right)^2 \quad (12)$$

E is defined as the sum of the squares of the deviations of the predicted values, until the search converges (where *i* counts the sample number and *j* the studied proton). The fitting procedure reaches convergence when the

difference between two consecutive E values is less than 10^{-6}. The treatment of the entire set of protons studied produces one single K value for the entire process and a set of calculated $\Delta\delta_{calc}$ values. $\Delta\delta_{calc}$ represents the chemical shift difference (for a given proton) between the free molecule and the pure complex.[15] The program is quite flexible as both the host and guest can be observed for spectroscopic perturbations allowing up to 15 protons to be used in the fitting process. However, the program can only be used for 1:1 host-guest stoichiometries.

APPARATUS

The NMR experiments were performed at 300 MHz and 400 MHz with Varian-Gemini 300 and Bruker AMX 400 spectrometers, respectively. The ^{1}H-NMR spectra were recorded in D_2O solution at 293 ± 0.5 K. Typical conditions were as follows: 16 K (32) data points, sweep width 4500 Hz giving a digital resolution of 0.28 Hz/point. The 90° pulse width was 13 μs and the spectra were collected by co-addition of 32 or 64 scans. The pulse width was 5μs (45°) and the spectra were collected by co-addition of 32 or 64 scans. In some cases, an appropriate Gaussian function was applied before Fourier transformation to enhance the spectral resolution. The D_2O (deuterium content 99.7 %) was purchased from INCD-ICSI (National R&D Institute for Cryogenics and Isotopic Technologies) Rm Valcea, Romania.

CRYSTAL STRUCTURE DETERMINATION

In each case single crystals of good quality were selected for their ability to extinguish plane-polarised light uniformly. Crystals were mounted on a nylon loop and coated with paratone N oil (Exxon),[16] to prevent the loss of included solvent (water) and to provide a rigid mount in the instance of low temperature data-collection. The nylon loop was mounted on a goniometer head.

Data-collection

Crystal intensity data were collected on a Nonius Kappa CCD (Charge Coupled Device) Single Crystal X-ray Diffractometer, using graphite-monochromated MoKα radiation (λ = 0.71069 Å) generated by a Nonius FR590 generator operated at 50 kV and 30 mA. Unit cell determinations were carried out both at ambient temperature (298 ± 2 K) as well as low temperature (113 ± 2 K). This check was performed to ensure there were no changes in the unit cell dimensions owing to temperature changes. All data were measured at 113 ± 2 K. The low temperatures were maintained by cooling the crystals with a constant stream of N_2 gas at a flow rate of 20 cm^3 min^{-1} with the aid of a Cryostream cooler (Oxford Cryosystems UK). Data were corrected for Lorentz-polarisation effects; unit cell refinement and data-reduction were performed using the programs DENZO and SCALEPACK.[17] All data were subjected to absorption correction using the program multi-scan*SADABS.*[18] Space group determinations were carried out by examining the systematic absences and matching the observed conditions to a known space group.[19] These assignments were confirmed by running the data through the program Xprep.[20] SHELXS-97 input files were generated with Xprep.

Structure solution and refinement

Several structures were solved by the isomorphous replacement method, using the published coordinates for selected cyclodextrin atoms of an isomorphous structure. In these cases the published coordinates of an isostructural complex were used as a trial model for refinement in the program SHELXH-97.[21] Alternatively, SHELXD was used to solve structures for which no isostructural precedent existed. All structures were refined with SHELXH-97 operating through the interface X-seed.[22]

SHELXD

SHELXD is used for the *ab initio* solution of structures from native data when a solution is not likely with SHELXS-97.[23] SHELXD is based on the dual-space

strategy first introduced in the program *Shake and Bake* by Miller *et al.*[24-28] The dual-space approach alternates between real and reciprocal space. In reciprocal space, phases are expanded in SHELXD from the 40 % most reliable using the *tangent formula* devised by Karle and Hauptman in 1956.[29,30] The real space cycles are required to impose the strong constraint that it is expected to find *N* sites with approximately equal scattering power. SHELXD makes extensive use of the Patterson function to provide better than random starting phases for the dual-space recycling. It is only limited by the requirement of atomic resolution 1.2 Å.[21]

SHELXH-97

Refinement in SHELXH-97 for larger structures involves minimisation of the function $\sum w\left(F_o^2 - F_c^2\right)^2$ using the full-matrix least-squares technique. The agreement between the observed (F_o) and calculated (F_c) structure factors is expressed by the residual index R_1, where R_1 is low for a satisfactory model and where

$$R_1 = \left(\sum \left\| F_o \right| - \left| F_c \right\|\right) / \sum \left| F_o \right| .$$

Refinement against F^2 tends to magnify the deviations of the Goodness-of-Fit, S (defined later), from unity compared with refinement against F and therefore these values are not directly comparable to structures refined against F.

The weighting scheme (w) in $wR_2 = \left[\left(\sum w\left(F_o^2 - F_c^2\right)^2\right) / \left(\sum w\left(F_o^2\right)^2\right)\right]^{1/2}$ and the parameters a and b were refined for each structure using the following expressions: $w = 1/\left[\sigma^2\left(F_o^2\right) + (aP)^2 + bP\right]$ and $P = \left[\max\left(0, F_o^2\right) + 2F_c^2\right]/3$. The terms a and b are chosen in the above weighting scheme to yield constant distributions of $\left[w\left(F_o^2 - F_c^2\right)^2\right]$ with sinθ and $(F_o/F_{max})^{1/2}$. S (Goodness-of-Fit) is defined by the expression $S = \left[\sum\left(w\left(F_o^2 - F_c^2\right)^2\right) / (n-p)\right]^{1/2}$, where *n* is the

number of reflections and p is the total number of parameters refined. Therefore, for a well-behaved structure S should be close to unity, and the over-determination ratio should be of the order $n/p \approx 10$.

ADDITIONAL RESOURCES

The Cambridge Structural Database (CSD)[31] was used to obtain coordinate data for the fragments used to solve the structures reported in this thesis. Molecular parameters and geometrical data with their associated e.s.d.s and non-bonding distances were calculated using the program PLATON.[32] WinGX[33] was used as an interface for PLATON. Molecular diagrams were created with POV-Ray for Windows.[34] Molecular packing, stereo and CPK diagrams were produced using the program Weblab ViewerPro Version 3.5.[35] Diagrams showing anisotropic thermal ellipsoids were drawn with the aid of Ortep-3 for Windows.[36] LAYER was used for the graphic display of intensity data as simulated precession photographs.[37]

Table 1 lists the final crystallographic data files pertinent to the compounds of this thesis.

Table 1. *File types found in Appendix.*

File extensions/formats	*Contents*
.HKL	Reflection data
.RES	SHELX co-ordinate data
.CIF	Crystallographic information file
.FCF	Structure factor tables
.LIS	Platon output
.XL	SHELX output file
.SUP	Tabulated supplementary data

REFERENCES

1. Brown, M.E. *Introduction to Thermal Analysis: Techniques and Applications*, Chapman and Hall, London, New York, **1998**, 1-146.
2. Soft Imaging System GmbH, *Digital Solutions for Imaging and Microscopy*, Version 3.1 for Windows © **1987-2000**.
3. Giron, D. *Thermochim. Acta*, **1995**, 248, 1-59.
4. Caira, M.R. *Roum. Chim. Rev.*, **2001**, 46, 371-386.
5. Yvon, K., Jeitschko, W. and Parthé, E., *J. Appl. Cryst.*, **1977**, 10, 73-74.
6. Job, P. *Ann. Chim. Phys.*, **1928**, 9, 113-203.
7. Scatchard, G. *Ann. N.Y. Acad. Sci.*, **1949**, 51, 660.
8. Benesi, H. A. and Hildebrand, J. H. *J. Am. Chem. Soc.*, **1949**, 71, 2703-2707.
9. Scott, R. L. *Recl. Trav. Chim. Pays-Bas*, **1956**, 75, 787-789.
10. Salvatierra, D., Díez, C. and Jaime C. *J. Incl. Phenom.*, **1997**, 27, 215-231.
11. Barrans, R. E. Jr. and Dougherty, D. A. *Supramol. Chem.*, **1994**, 4, 121-130.
12. Kearney, P. C., Mizoue, L. S., Kumpf, R. A., Forman, J. E., McCurdy, A. and Dougherty, D. A. *J. Am. Chem. Soc.*, **1993**, 115, 9907-9919.
13. Petti, M. A., Shepodd, T. J., Barrans, R. E. and Dougherty, D. A. *J. Am. Chem. Soc.*, **1988**, 110, 6825-6840.
14. Floare, C., Balibanu, F. and Bogdan, M. *Studia UBB, Physica, Special Issue*, L. 4a, **2005**, 451-454.
15. Fielding, L. *Tetrahedron.*, **2000**, 56, 6151-6170.
16. Paratone N oil (Exxon Chemical Co., Texas, USA).
17. Otwinowski, Z., Minor, W., *Processing of X-ray Diffraction Data in Oscillation Mode in Methods in Enzymology*, Vol. 276, Carter, C.W., Sweet, R.M., (eds.), Academic Press, New York, **1996**, 307-326.
18. Sheldrick, G. M., *SADABS*. University of Göttingen, Germany., **1996.**
19. *International Tables for Crystallography*, Vol. II: Mathematical Tables, Kasper, J.S. and Lonsdale, K. (eds.), Kynoch Press, Birmingham, England, **1967**, 291.
20. XPREP, *Data Preparation and Reciprocal Space Exploration*, Version 5.1, © Bruker Analytical X-ray Systems, **1997**.
21. Sheldrick, G.M. SHELXH, *Acta Crystallogr.*, **2008**, A64, 112-122.
22. Barbour, L.J. *X-Seed, A software tool for Supramolecular Crystallography, Supramol. Chem.*, **2001**, 1, 189-191.
23. Schneider, T.R. and Sheldrick, G.M., *Acta Crystallogr.*, **2002**, D58, 1772-1779.
24. Sheldrick, G.M., *Direct Methods for Solving Macromolecular Structures,* edited by Fortier, S., Dordrecht: Kluwer Academic Publishers, **1998**, 401-411.

25. Sheldrick, G.M., *Z. Kristallogr.,* **2002**, 217, 644-650.

26. Uson, I. and Sheldrick, G.M., *Curr. Opin. Struct. Biol.* **1999**, 9, 643-648.

27. Miller, R., Gallo, S.M., Khalak, H.G. and Weeks, C.M., *J. Appl. Cryst.,* **1994**, 27, 613-621.

28. Miller, R., De Titta, G.T., Jones, R., Langs, D.A., Weeks, C.M. and Hauptman, H., *Science,* **1993**, 259, 1430-1433.

29. Karle, J., *Acta Crystallogr.,* **1968**, B24, 182-186.

30. Karle, J. and Hauptman, H., *Acta Crystallogr.,* **1956**, 9, 635-651.

31. Cambridge Structural Database and Cambridge Structural Database System, Version 5.29, November **2007**, Cambridge Crystallographic Data Centre, University Chemical Laboratory, Cambridge England.

32. Spek, A.L. PLATON, *A multipurpose crystallographic tool*, Version 10500 © **1980-2000**.

33. Farrugia, L.J. WinGX, An integrated system of windows programs for the solution, refinement and analysis of single crystal X-ray diffraction data, Version 1.63, *J. Appl.Cryst*., **1999**, 32, 837-838.

34. Pov-Ray for Windows Version 3.1e.watcom.win32, The persistence of vision development team, © **1991-1999**.

35. Weblab ViewerPro Version 3.5 © **1999** by Molecular Simulations Inc., San Diego, CA.

36. Ortep-3 for Windows: Farrugia, L.J. *J. Appl. Cryst.,* **1997**, 30, 565-565.

37. Barbour, L.J., Layer - a computer program for the graphic display of intensity data as simulated precession photographs., *J. Appl. Cryst.* **1999**, 32, 351-352.

Chapter 3
^{1}H-NMR SPECTROSCOPY OF CYCLODEXTRIN INCLUSION COMPLEXES OF FOUR PHENYLUREA ANALOGUES

Here we determine inclusion complex formation between α-, β-, and γ-cyclodextrin and four phenylurea compounds in solution using ^{1}H-NMR spectroscopy. Using the same spectroscopic data, we determine the stability constants for the complexes formed in solution.

THE GUESTS

The four phenylurea analogues **1**, **2**, **3** and **4** are shown here with chemically equivalent hydrogen atoms labelled (Figure 1).

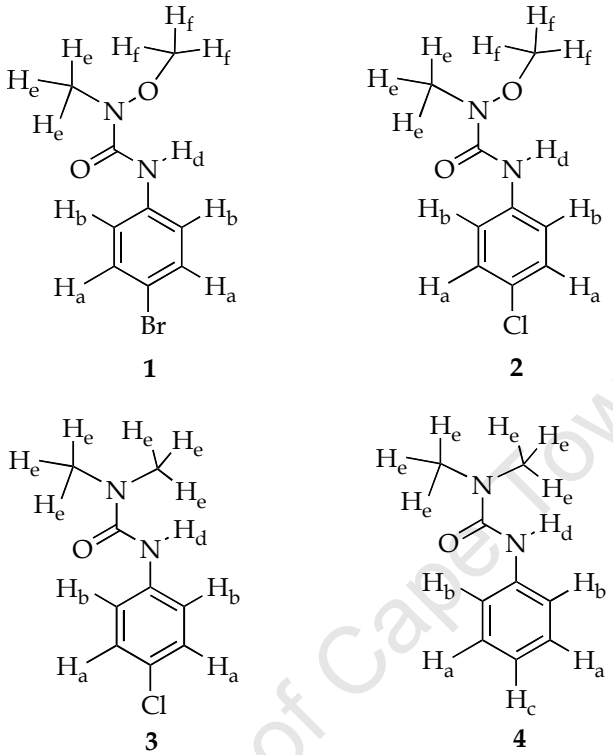

1 **2** **3** **4**

Figure 1. *Guest molecules used in this study: metobromuron (**1**), monolinuron (**2**), monuron (**3**) and fenuron (**4**).*

In general, only the guest protons which are located deep within the cyclodextrin cavity undergo chemically induced shifts. Protons which remain exposed to the bulk solvent are unaffected. Amino and hydroxyl protons are usually exchanged with D_2O and disappear from their normal position in the spectra. The large peaks at 4.70 ppm (300 MHz) and 4.78 ppm (400 MHz) seen in the spectra are due to residual HDO molecules in the D_2O solvent. They were considered as the internal standard in the measurement of the chemical shifts of the peaks of α- and β-CD in the presence and absence of the guests.

STOICHIOMETRY

α- and β-cyclodextrin

The stoichiometries for the complexes formed in solution between **1**, **2**, **3**, **4** and α-CD or β-CD were obtained by means of the continuous variation method.[1] The stock solution concentrations were 1 mM in each case. Changes in the chemical shifts of protons H_3 for α-CD and H_3, H_5, $H_{6a,b}$ for β-CD were monitored because they showed the largest CIS values, while for the guests H_a and H_b were monitored as they showed the largest CIS. Both the guest protons H_a and H_b were monitored in the case of complexation with α-CD while only H_b was monitored when the complexation was with β-CD. The Job plots for complexation with α-CD broadly maximise at r = 0.5 as shown in Figure 2.

For β-CD the plots are generally symmetrical with the maximum occurring at r = 0.5 for each complex (Figure 3). This is indicative of 1:1 stoichiometry for each complex within the range of concentrations investigated. However, (a) in Figure 3 shows evidence for the existence of a higher order complex present simultaneously with the complex of 1:1 stoichiometry. The skewed curve has a secondary maximum located in the range r = 0.7-0.8 for protons H_3, H_5, and $H_{6a,b}$ while proton H_b (belonging to the guest) has a secondary minimum in the range r = 0.2-0.3. When viewed together this suggests the existence of a complex with stoichiometry 2:1 in favour of the cyclodextrin.[2,3,4] The Job plot of the guest protons (H_a and H_b) for **4** with α-CD could not be determined as the spectra were not clearly resolved.

Mode of inclusion

Chemically induced shifts were detected for the inclusion of **1**, **2**, **3**, and **4** in α-CD with only three protons showing significant shifts.

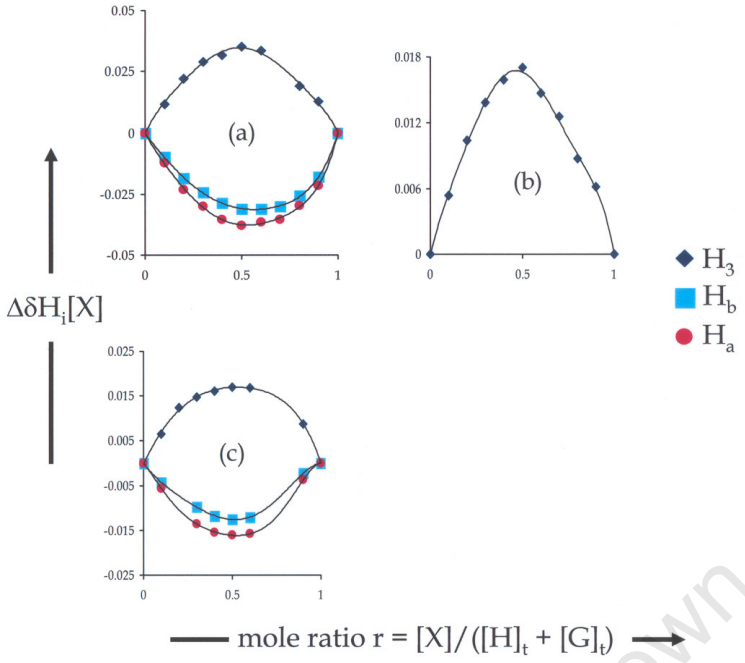

Figure 2. *Job plots for α-CD with (a)* ***1****, (b)* ***2*** *and (c)* ***3****.*

These protons are H_3 for the host α-CD, while H_a and H_b showed significant movement for the guest. Only the interactions between **1**, **2**, **3** and α-CD were significant and allowed for the Job plot to be interpreted (Figure 2). The induced shifts between **4** and α-CD were of the order < 0.01 ppm and only the data for H_3 produced a Job plot. The order of the CIS determined from the Job plots in Figure 2 for each guest with α-CD is $H_a > H_b > H_3$ for **1**, $H_3 > H_a > H_b$ for **2** and **3** while for **4** the order is $H_3 = H_b > H_a$. All CIS values are shown in Table 1, below.

Table 1. *Maximum observed CIS values for* ***1****,* ***2****,* ***3*** *and* ***4*** *with α-CD.*

α-CD	$\Delta\delta_{obs}^{max}$ H_1† (ppm)	$\Delta\delta_{obs}^{max}$ H_2† (ppm)	$\Delta\delta_{obs}^{max}$ H_3 (ppm)	$\Delta\delta_{obs}^{max}$ H_4† (ppm)	$\Delta\delta_{obs}^{max}$ H_5 (ppm)	$\Delta\delta_{obs}^{max}$ H_6† (ppm)	Guest $\Delta\delta_{obs}^{max}$ H_a (ppm)	Guest $\Delta\delta_{obs}^{max}$ H_b (ppm)
1	0.004	-0.013	0.079	-0.003	-0.009	-0.011	-0.123	-0.097
2	-0.002	0.007	0.058	-0.003	-0.015	0.003	-0.026	-0.021
3	0.018	0.020	0.065	0.017	0.016	-0.026	-0.055	-0.042
4	0.001	0.005	0.005	-0.003	0.001	0.004	-0.002	-0.005

† Job plots for these protons over the range of concentrations investigated did not give any well defined trends.

The fact that only proton H_3 of the host shows any significant CIS indicates that the guest in each case must be lodged near the secondary rim and not

located deep within the cavity. Also, the depth of penetration of each guest is slightly different. The variations in the magnitudes of the chemically induced shifts indicate the extent of intrusion into the α-CD cavity.

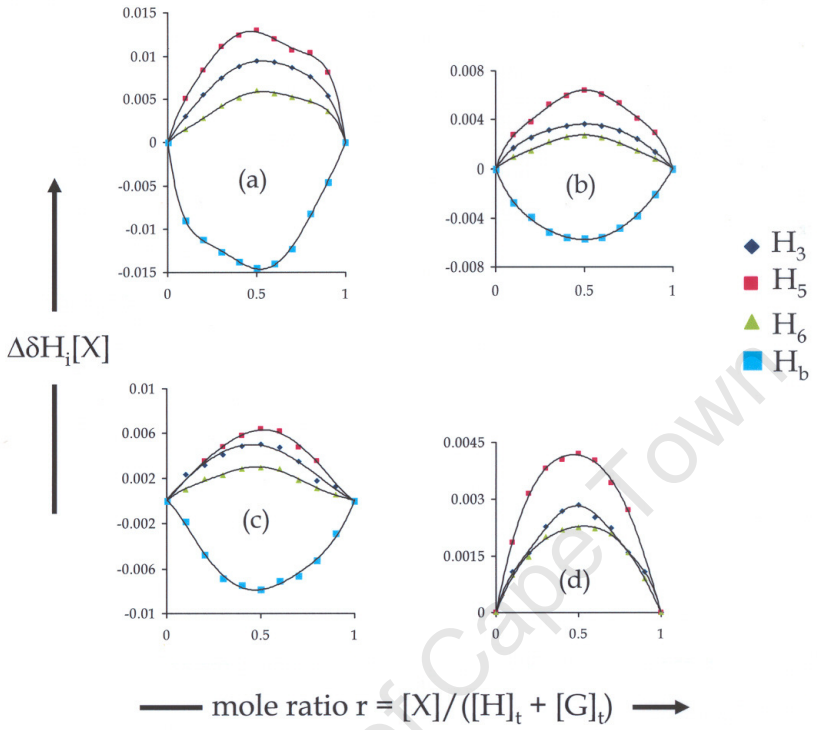

Figure 3. *Job plots for β-CD with (a)* ***1****, (b)* ***2****, (c)* ***3*** *and (d)* ***4****.*

Generally, the interactions of **1**, **2**, **3** and **4** with β-CD are similar and this similarity is reflected in the corresponding Job plots. From the Job plots shown in Figure 3 it is noticeable that the magnitudes of the CIS values for protons H_3, H_5 and $H_{6a,b}$ are in the order $H_5 > H_3 > H_{6a,b}$, suggesting that the guest (for each complex) is located near the primary rim.[5] The guest (in each case) is thus located deep within the cavity and an indication of the depth of insertion is provided by the fact that both H_3 and H_5 undergo a significant shift.[6] For the guest, the aromatic protons (labelled H_a, H_b and H_c in Figure 1) show a significant downfield movement. It is therefore concluded that the phenyl moiety interacts with the cyclodextrin. Additionally, protons H_e and H_f belonging to the methyl and methoxyl groups (for each guest molecule) show only small shifts in the range 0.001-0.009 in absolute units. This

indicates that the methyl and methoxyl moieties protrude from the torus as shown in Figure 4.[7]

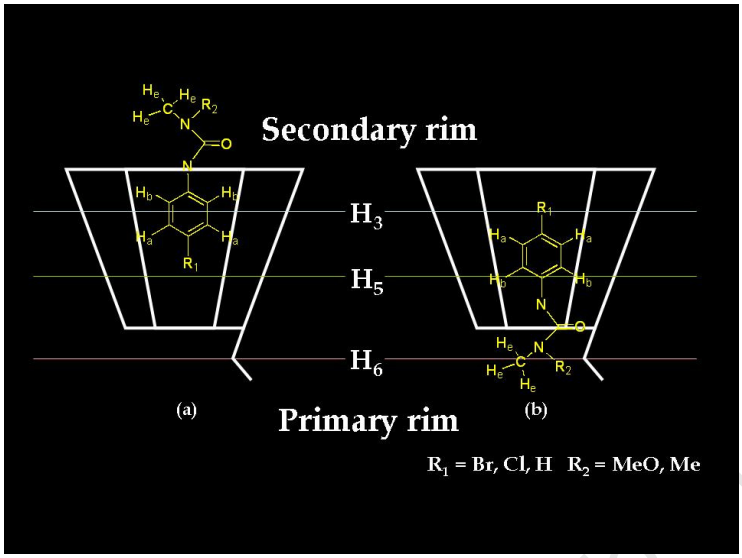

Figure 4. *Schematic diagram (not drawn to scale) depicting the possible mode of inclusion of the guest molecules deduced from the relative CIS magnitudes reported above (a) for α-CD inclusion and (b) β-CD inclusion.*

The only exception to the observed behaviour relates to the interactions of **4** with α- and β-CD. The cavity protons of the cyclodextrin have measurable upfield shifts which are comparable with those of **1**, **2** and **3** with β-CD but not with those of α-CD. Moreover, the protons located on the exterior of β-CD (H_1, H_2 and H_4) have also registered significant CIS values as shown in Table 2.

Table 2. *Maximum observed CIS values for **1**, **2**, **3** and **4** with β-CD.*

β-CD	$\Delta\delta^{max}_{obs}$ H_1† (ppm)	$\Delta\delta^{max}_{obs}$ H_2† (ppm)	$\Delta\delta^{max}_{obs}$ H_3 (ppm)	$\Delta\delta^{max}_{obs}$ H_4† (ppm)	$\Delta\delta^{max}_{obs}$ H_5 (ppm)	$\Delta\delta^{max}_{obs}$ H_6 (ppm)	Guest $\Delta\delta^{max}_{obs}$ H_b (ppm)
1	0.009	0.008	0.030	0.007	0.051	0.015	-0.046
2	0.000	-0.001	0.017	-0.001	0.027	0.010	-0.021
3	0.003	0.002	0.023	0.003	0.036	0.010	-0.029
4	-0.014	0.048	0.011	-0.075	0.019	0.010	-0.006

† Job plots for these protons over the range of concentrations investigated did not give any well defined trends.

Two of these protons experience downfield shifts (H_1 and H_4) while the third (H_2) experiences an upfield shift. This suggests that **4** interacts with the interior as well as the exterior of the β-CD. However, in the case of α-CD, protons H_1 and H_2 are shifted upfield while H_4 is shifted downfield. The chemical shifts of these protons are negligible (< 0.005 ppm). There are no significant shifts ($\Delta\delta \geq 0.01$ ppm) recorded for the aromatic protons (H_a, H_b or H_c) of **4** interacting with either α-CD or β-CD. The fact that $\Delta\delta$ for H_a, H_b, and H_c are small may be related to the ring-current effect.[7] The aromatic protons of the included guest experience deshielding while the protons interacting with the exterior of the cavity experience shielding effects, sufficient to produce only small shifts ($\Delta\delta < 0.01$ ppm).

ASSOCIATION CONSTANTS

In order to determine the extent of intermolecular binding between **1**, **2**, **3**, **4** and the CD host, the association constants were evaluated. The association constant K for a 1:1 complex was calculated using a non-linear least-squares regression analysis of the observed chemical shift changes for **1**, **2**, **3**, **4** and the cyclodextrin host (α- and β-CD) NMR lines, as a function of the CD concentration. In the case of **1**, **2** and **3**, K was evaluated using the CIS values of H_3 (host) as well as H_a and H_b of the guest for α-CD, while H_3, H_5, $H_{6a,b}$ (host) and H_b of the guest was used for β-CD. For guest **4** with β-CD, K was necessarily evaluated only on the CIS values of H_3, H_5 and $H_{6a,b}$ belonging to the host β-CD. K was not evaluated for **4** with α-CD as the observed shifts were negligible, as mentioned previously. Equation (11) was used in the evaluation, where [X] is the concentration of the host or guest of a sample and $[M] = [G]_t + [H]_t$.

$$\Delta\delta_{obs}^{(X)} = \frac{\Delta\delta_c^{(X)}}{2[X]_t} \times \left\{ [M] + \frac{1}{K} \pm \left[\left([M] + \frac{1}{K} \right)^2 - 4[H]_t[G]_t \right]^{\frac{1}{2}} \right\} \qquad (11)$$

The association constants K are listed in Tables 3 and 4 along with the correlation coefficient (R), the error loss function (E) and the calculated chemically induced shifts (CIS) Δδ.

Table 3. *K, E, R and $\Delta\delta_c$ of the α-CD complexes at 298 K.*

Guest		1	2	3	4
$K_{\alpha\text{-CD}}$	M^{-1}	1519	1085	208	-
$R_{\alpha\text{-CD}}$		0.9977	0.9991	0.9965	-
$E_{\alpha\text{-CD}}$		7.09×10^{-4}	4.3×10^{-5}	2.0×10^{-4}	-
$\Delta\delta_c H_3$	ppm	0.2076	0.1161	0.4297	-
$\Delta\delta_c H_a$	ppm	-0.2243	-0.0996	-0.3524	-
$\Delta\delta_c H_b$	ppm	-0.1814	-0.0792	-0.2647	-

Table 4. *K, E, R and $\Delta\delta_c$ of the β-CD complexes at 298 K.*

Guest		1	2	3	4
$K_{\beta\text{-CD}}$	M^{-1}	2749	368	726	715
$R_{\beta\text{-CD}}$		0.9984	0.9997	0.9987	0.9990
$E_{\beta\text{-CD}}$		4.8×10^{-5}	1.3×10^{-6}	9.8×10^{-6}	2.3×10^{-7}
$\Delta\delta_c H_3$	ppm	0.0434	0.0557	0.0446	0.0254
$\Delta\delta_c H_5$	ppm	0.0618	0.0904	0.0536	0.0385
$\Delta\delta_c H_{6a,\,b}$	ppm	0.0240	0.0386	0.0260	0.0217
$\Delta\delta_c H_b$	ppm	-0.0670	-0.0850	-0.0730	-

γ-cyclodextrin

Titration experiments with γ-CD and compounds **1**, **2**, **3** and **4** were carried out under the same conditions as those used for α- and β-CD with **1**, **2**, **3** and **4**. However, there were no observable shifts of the cavity protons or any other protons of γ-CD.

DISCUSSION

Complexes in solution may have more than one mode of guest inclusion. It is likely that stoichiometries other than 1:1 may exist in solution.[4] It is interesting to note that the experiments have shown similar modes of inclusion for all four compounds with α-CD. Similarly, the complexes with β-CD have more or less the same mode of inclusion, but different from that with α-CD. As mentioned previously, the guest in each case (**1**, **2**, **3** or **4**) is

lodged near the secondary rim of α-cyclodextrin, whereas with β-cyclodextrin the guest is located near the primary rim. These conclusions are based on the magnitudes of the CIS values for each guest with the respective host. The predominant stoichiometries for these complexes are 1:1, the only exception being guest **1** with β-CD, where both 1:1 and 2:1 host-guest stoichiometries are evident. It is generally accepted that the hydrophobicity of a guest favours its inclusion.[8] It must, therefore, directly or indirectly influence the size of the binding constant. On this basis it may be used as an indication of the strength of interaction between host and guest. The aqueous solubility of the guests is in the order **4** > **2** > **1** > **3**. However, the association constants K for the α-CD complexes do not follow this order. They are in the order **1** > **2** > **3** with association constant for **4** with α-CD not determined. The order of the association constants with β-CD differs from those for α-CD and is **1** >> **3** ≈ **4** > **2**. In fact, no trend is apparent from the data presented.

In order to compare our results for β-CD with **1**, **2**, **3** and **4** with those reported by Dupuy *et al.*,[9] we must clarify some of the theoretical aspects used in our interpretation of the data. Firstly, the chemical shift variation $\Delta\delta_{obs}$ is defined as $\Delta\delta_{obs} = \delta_{free} - \delta_{obs}$ in this work whereas Dupuy *et al.* reported the induced chemical shift as $\Delta\delta = \delta_{complex} - \delta_{free}$. Dupuy does not define the $\delta_{complex}$ term in his paper. We assume that it is equivalent to δ_{obs} for a particular H:G ratio which is not stated. According to our definition, $\Delta\delta_{complex} = \delta_{free} - \delta_{complex}$ is obtained as a fitting parameter from which we calculate the theoretical $\delta_{complex}$. This value represents the chemical shift change if only the pure complex is present in solution. Secondly, it is important to know that if the NMR signal is shifted to lower δ values then the shift is upfield. If, however, the signal is shifted to higher δ values then we have a downfield shift. Thus, in order for us to compare our results with those of Dupuy *et al.* it is necessary to change the sign of Dupuy's $\Delta\delta_{obs}$ values. So, if $\Delta\delta_{obs} > 0$ then we have an upfield shift and if $\Delta\delta_{obs} < 0$ then the shift is downfield and this is valid only if we define $\Delta\delta_{obs}$ as $\Delta\delta_{obs} = \delta_{free} - \delta_{obs}$. For **3** with β-CD, our results

as well as those reported by Dupuy *et al.* show upfield shifts for all the protons of β-CD. With our results there is a clear distinction in magnitude between $\Delta\delta_{obs}$ for H_3, H_5, $H_{6a,b}$ and $\Delta\delta_{obs}$ for H_1, H_2, H_4. In fact, there is an order of magnitude difference between them and it clearly indicates the occurrence of an interaction between guest and the interior of the host in solution. On the other hand, Dupuy's data are all of the same magnitude and therefore do not provide any clear indication of complexation. Similar trends are apparent for the signals obtained in our study and those of Dupuy for the guest protons even though the magnitudes of the shifts are different. It is also worth noting that the $\Delta\delta_{complex}$ (H_b) value (0.073 ppm) obtained from the fitting procedure used in our work (described earlier) is close to the hypothetical value (0.1 ppm) obtained by Dupuy. In the case of **4** with β-CD, Dupuy *et al.* report that all protons of the host move upfield except for proton H_2 which does not move at all. In our study all the protons are shifted, with protons H_1 and H_4 moving downfield while protons H_2, H_3, H_5 and $H_{6a,b}$ move upfield. The shift variation reported by Dupuy *et al.* for the H_4 proton of the host is larger than our reported shifts for H_3, H_5 and $H_{6a,b}$ protons. This is reflected in our results as the shift magnitudes for H_2 and H_4 are also larger than those for H_3, H_5 and $H_{6a,b}$. The only differences between Dupuy's shifts for the guest protons and ours are the magnitudes of the shifts and the fact that Dupuy *et al.* report no observable shift for H_b (Table 5).

***Table 5**. Comparison of shift variations of **4** with β-CD against those reported by Dupuy et al.*[9]

Proton‡	*Dupuy et al.* (Δδ)	Present study (Δδ)
H_a	-0.01 downfield	-0.0017 downfield
H_b	Unaffected	0.0022 upfield
H_c	-0.02 downfield	-0.0060 downfield
H_e	0.01 upfield	0.0004 upfield

‡ Protons are labelled according to Figure 2.

The two sets of data show very similar trends where the direction of the shift is concerned, the only exception being H_b. A possible reason for the reported

differences may be related to the concentrations of the solutions as most, if not all, other conditions are similar (see the experimental section, Chapter Two). However, the concentrations used in the Dupuy experiments are not reported and we are therefore unable to draw any further conclusions. From the 2-D experiments of Dupuy (for **3** and **4** with β-CD) correlation cross peaks were observed between H_3 and H_5 of the host and the *ortho*- and *meta*-protons of the guest. It is also observed that the correlation band for H_3 has greater intensity than that of H_5. Dupuy *et al.* conclude that the phenyl moiety is included in the torus while the methyl and methoxyl moieties protrude from the cavity.[9] These results correlate very well with the conclusion that we arrived at based on ^{1}H-NMR data.

REFERENCES

1. Job, P. *Ann. Chim. Phys.*, **1928**, 9, 113-203.
2. Whittaker, D., Penkler, L., Glintenkamp, L., Van Oudtshoorn, M. and Wessels, P. *J. Incl. Phenom.*, **1996**, 25, 177-180.
3. Pose-Villarnovo, B., Santana-Penin, L., Echezarreta-López, M., Perez-Marcos, M.B., Vila-Jato, J.L. and Torres-Labandeira, J.J. *S.T.P. Pharma. Sci.*, **1999**, 19, 231-236.
4. Mucci, A., Schenetti, L., Vandelli, M., Ruozi, B. and Forni, F., *J. Chem. Res.*, **1999**, (M), 1761-1795.
5. Cameron, K. S., Fletcher, D. and Fielding, L. *Magn. Reson. Chem.*, **2000**, 40, 251-260.
6. Cabral Marques, H. M., Hadgraft, J., Kellaway, I. W. and Pugh, W. J. *Int. J. Pharm.*, **1990**, 63, 267-274.
7. De-Zhi, S., Li, L., Qiu, X-M, Liu, F., Yin, B-L. *Int. J. Pharm.*, **2006**, 316, 7-13.
8. Bardelang, D., Clement, J-L., Finet, J-P., Karoui, H. and Tordo, P. *J. Phys. Chem. B*, **2004**, 108, 8054-8061.
9. Dupuy, N., Barbry, D., Bria, M., Marquis, S., Vrielynck, L. and Kister, J. *Spectrochimica Acta Part A*, **2005**, 61, 1051-1057.

Chapter 4
PXRD AND THE PRINCIPLES OF ISOSTRUCTURALITY IN THE CHARACTERISATION OF CYCLODEXTRIN INCLUSION COMPLEXES

X-ray powder diffraction is used together with the principles of isostructurality to establish complex formation and to extract space group and unit cell information for new cyclodextrin-herbicide complexes.

PREPARATION

Equimolar amounts of host and guest were used in the preparation of the inclusion complexes of α-, β- and γ-CD with **1**, **2**, **3** and **4**. Thus, for each cyclodextrin with **1**, 0.077 mmols were used, **2** required 0.093 mmols, **3** needed 0.100 mmols, while **4** required 0.122 mmols. The amounts (mg) used in each experiment are reported in Table 1. In each experiment the cyclodextrin was placed in the mortar with a few drops of water and ground to a paste. The guest was added slowly with simultaneous kneading until all of the guest was added. The process usually required between 45 minutes to one hour. During this time the paste was kept moist by the dropwise addition of water.

Table 1. *Amounts of host and guest used for each experiment.*

Guest	α-CD (mg)	β-CD (mg)	γ-CD (mg)	Guest (mg)
1	74.8	87.4	99.9	20
2	90.4	105.5	120.6	20
3	97.2	113.5	129.7	20
4	118.6	138.5	158.2	20

Complexation was confirmed by powder X-ray diffraction and the resultant traces were assigned to an isostructural series.[1] The confirmed complexes were: β-CD•**1** - **4**, and γ-CD•**1** - **4**. α-CD did not complex with any of the guests.

It is prudent to note that when the assignment of an isostructural series is undertaken, the water content, dimensions of the guest and its orientation as well as the temperature at which the data were acquired affect the peak angular positions in the PXRD trace. Thus, the tolerances within which traces are judged as isostructural are less rigid than those which are normally applied in phase identification by PXRD.

1, 2, 3 and 4 with α-CD

Attempts at forming inclusion complexes of α-CD with **1**, **2**, **3** and **4** in the solid state were unsuccessful. In solution however, these components form complexes, as described in the previous chapter. For completeness, the α-CD phases present in the failed attempts have been assigned and the results are presented below.

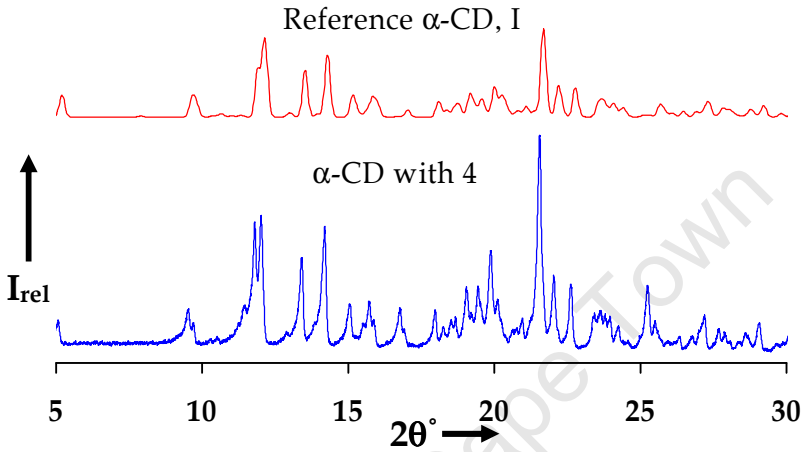

Figure 1. *A comparison between the representative trace of the kneaded product of α-CD with* ***4*** *and the reference trace for α-CD form* ***I****.*

Noticeable from the comparison in Figure 1 is the very close correspondence between the reference trace and the representative trace of the kneaded product of **4** with α-CD. In all four attempts the same phase was encountered corresponding to α-CD form **I**.

1, 2, 3 and 4 with β-CD

The resultant PXRD traces of complexes β-CD•**1** - **4** showed that all four complexes are isostructural; a representative trace (β-CD•**4**) was used for comparison with the reference traces. It was readily noticeable that the representative pattern matched very closely the reference traces for the P1 triclinic and C2 monoclinic channel type dimeric structures for β-CD complexes. Most convincing is the fact that the peak angular positions of both reference traces matched those of β-CD•**4** closely. The only notable differences between the traces are in the relative intensities of corresponding peaks (Figure 2). This is due, in part, to differences in the guest and its

orientation as well as the fact that the reference traces are averaged patterns of two or more traces.

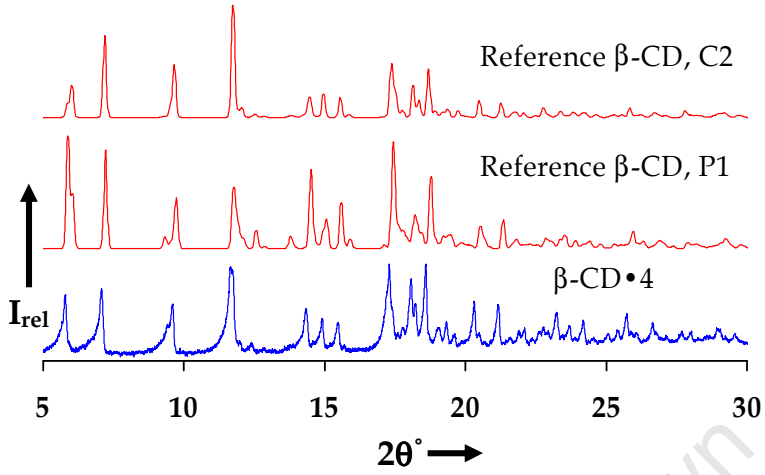

Figure 2. *PXRD traces of the two reference patterns for β-CD dimeric complexes C2 and P1 with a representative trace β-CD• 4.*

Even upon closer examination of the fine structure present in both reference traces one is unable to determine which of the traces offers a better match to that of β-CD•**4**. The metric relationship between C2 and P1 is well understood and is briefly explored here.

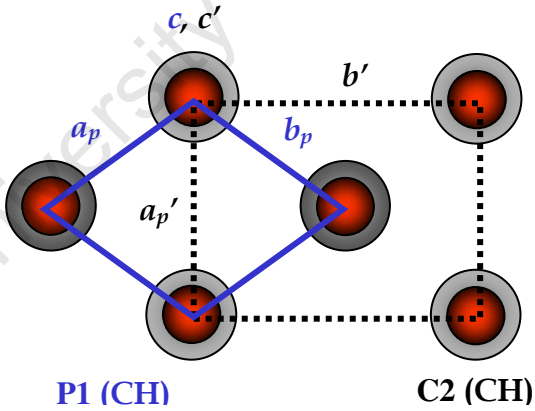

Figure 3. *Schematic diagram of the metrically related unit cells P1 (solid blue line) and C2 (broken black line).*

When we apply the metric transformation $a' = a + b$, $b' = b - a$ and $c' = c$ to the P1 unit cell we obtain a unit cell with similar dimensions as those of the C2 structure (a = ~19, b = ~24 and c = ~16).[2] Thus, according to the transformation, the two unit cells share a common axis, c, shown in Figure 3. Additionally, all dimers in both unit cells have the same orientation, as do

their guest molecules. For β-CD dimers, the space group C2 is characterised by a crystallographic diad at the interface of each dimer, whereas the P1 structure possesses only a pseudo-twofold rotation axis at its interface, (Figure 4).

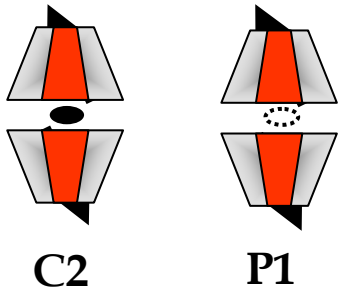

Figure 4. *A schematic showing two dimers. C2 has a crystallographic diad at the interface of the dimer and P1 has a pseudo-diad at the interface.*

The consequence of the relationship described above is virtually indistinguishable PXRD traces and in the absence of single crystal X-ray intensity data, one cannot unequivocally distinguish between C2 and P1. If, however, the unit cell data are available and if two unit cell parameters are similar (i.e. two unit cell lengths and two angles) then one would have to search for higher symmetry.[3] Here, however, one would still have to consider both options as there is no clear way of making the correct cell choice unless the Laue symmetry is unequivocal. The estimated unit cell dimensions are listed below in Table 2, along with the possible space group.

Table 2. *Possible space groups and approximate unit cell parameters for the complexes β-CD•**1 – 4.***[1]

Space group	*a* (Å)	*b* (Å)	*c* (Å)	α (˚)	β (˚)	γ (˚)	Vol. (Å³)
C2	19.3	24.5	15.9	90	109	90	7109.3
P1	15.6	15.6	15.9	101.6	101.6	103.6	3444.8

These parameters for the inclusion complexes were deduced from their isostructurality with the known inclusion complexes whose reference PXRD traces were presented in Figure 2.

1, 2, 3 and 4 with γ-CD

When comparing the PXRD trace of the representative putative γ-CD complex γ-CD•**4** with that of the reference complex, it is immediately apparent how

well the peak angular positions agree. The main difference is in the intensities, as can be seen in Figure 5.

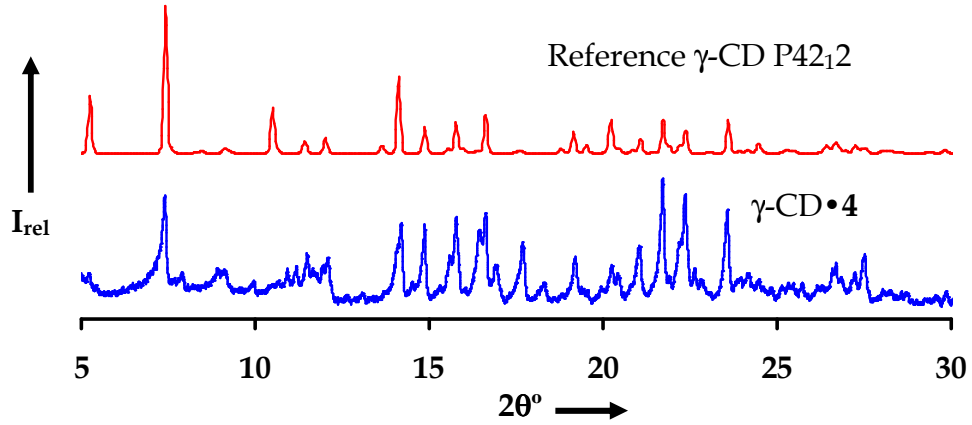

Figure 5. *The reference PXRD pattern for γ-CD complexes and the representative pattern for complexes γ-CD•**1** - **4**.*

The assignment of γ-CD complexes is probably the easiest for the cyclodextrin complexes since most γ-CD complexes crystallise in the very rare tetragonal space group P42₁2 (**CH**), Figure 6 (a). P42₁2 is a space group of high symmetry with relatively few peaks in the PXRD trace, Figure 5.

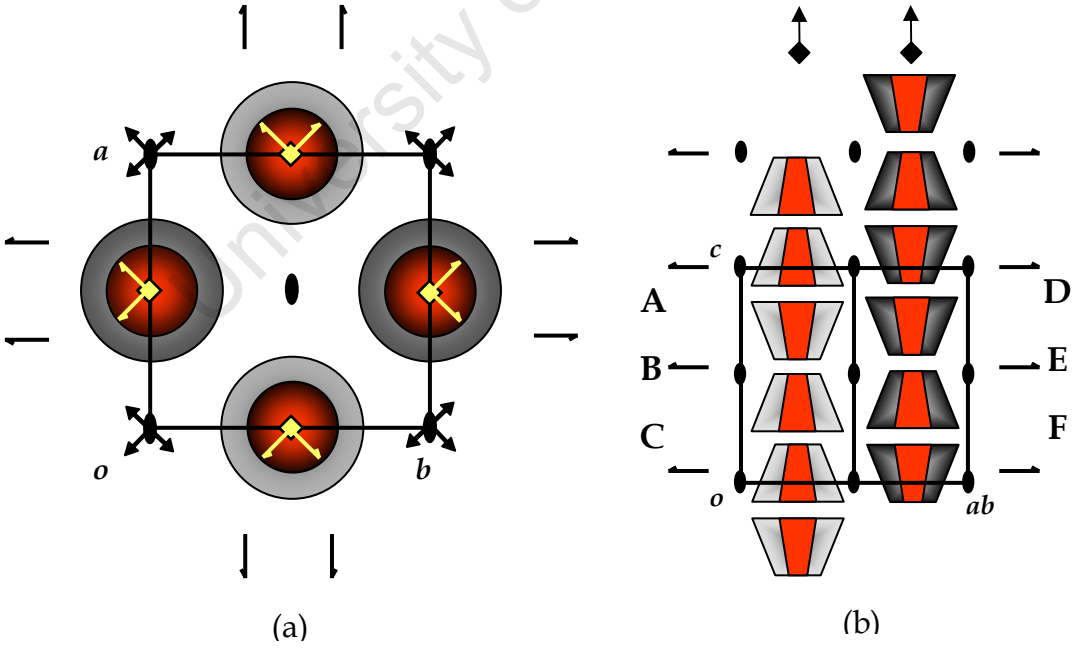

Figure 6. *Diagram (**a**) shows the packing motif of γ-CD complexes which crystallise in the space group P42₁2. The projection onto the ab-plane shows the crystallographic symmetry elements. Diagram (**b**) shows a projection along the ab-diagonal. It shows the stacking motif along the c-direction as well as the two independent columns (light and dark) parallel to c.*[4]

In the crystal, CD molecules are stacked on top of each other in columns parallel to the tetragonal *c*-axis. In fact the CD molecules are located on a fourfold axis parallel to *c*, shown by the yellow tetrad in Figure 6 (a). The channels formed by the stacked columns have an internal diameter of ~8 Å and are arranged in a square motif with the interstitial channels having a diameter of ~7 Å.[5] The repeat unit of the column is a trimer which consists of a hydrogen bonded dimer and a monomer also hydrogen bonded to it. The monomer is also hydrogen bonded to the dimer of a preceding trimeric unit. The orientations present in the trimer are thus head-to-head (A), tail-to-tail (B) and head-to-tail (C), shown in Figure 6 (b). The trimers are translated along *c*. Furthermore, the independent stacks which are adjacent to each other are in an anti-parallel arrangement and are related by a twofold rotation axis and a twofold screw axis.[4] The trimeric channel arrangement is not unique to γ-CD. Recently Chatziefthimiou *et al.* reported the trimeric channel arrangement of a β-CD complex.[6] However, the monomeric component of the β-CD trimer is offset by ~0.45 Å from the dimer, whereas the monomer in the γ-CD trimer is not offset by any significant distance. The fact that the crystallographic tetrad is at the centre of each column means that the guest located in the infinite channels of the crystal has fourfold disorder, evidenced by all the γ-CD structures ($P42_12$) reported in the CSD. The unit cell parameter values are provided in Table 3.[7]

Table 3. *Approximate unit cell parameters for the complexes γ-CD•**1** – **4**.*[1]

Space group	*a* (Å)	*b* (Å)	*c* (Å)	α (˚)	β (˚)	γ (˚)	Vol. (Å^3)
$P42_12$	23.8	23.8	23.2	90	90	90	13157.6

DISCUSSION

In this section we have confirmed the formation of eight new cyclodextrin inclusion complexes and identified their space groups. All of the complexes characterised here belong to known isostructural series. Complexes of β-CD with **1**, **2**, **3** and **4** are isostructural and their PXRD patterns matched reference traces for dimeric β-CD complexes C2 and P1. Complexes of γ-CD with **1**, **2**, **3**

and **4** are also isostructural; they belong to the isostructural series with space group $P42_12$. It was also possible to obtain the approximate unit cell dimensions for these complexes from the data corresponding to the matching reference patterns.

PXRD as used above is an efficient tool for the identification of cyclodextrin complexes but it is limited quantitatively. For example, it provides little information regarding guest orientation, crystal water content, stoichiometry and the interaction between water and the structure of the complex. In this regard single crystal X-ray diffraction is greatly superior.

REFERENCES

1. Caira, M.R, *Rev. Roum. Chim.,* **2001**, 46, 371-386.
2. Mentzafos, D., Mavridis, I.M., Le Bas, G. and Tsoucaris, G., *Acta Crystallogr.,* **1991**, B47, 746-757.
3. Herbstein, F.H. and Marsh, R.E., *Acta Crystallogr.,* **1998**, B54, 677-686.
4. Ding, J., Steiner, T. and Saenger, W., *Acta Crystallogr.,* **1991**, B47, 731-738.
5. Steiner, T. and Saenger, W., *Acta Crystallogr.,* **1998**, B54, 450-455.
6. Chatziefthimiou, S.D., Yannakopoulou, K. and Mavridis, I.M., *CrystEngComm.,* **2007**, 9, 976-979.
7. Cambridge Structural Database and Cambridge Structural Database System, Version 5.29, November **2007**, Cambridge Crystallographic Data Center, University Chemical Laboratory, Cambridge, England.

Chapter 5
β-CYCLODEXTRIN INCLUSION COMPLEXES OF TWO PHENYLUREA GUEST MOLECULES

Here we report the formation of β-cyclodextrin inclusion complexes of two phenylurea compounds (monolinuron, monuron) while we also investigate the solid-state features of the inclusion complexes using single crystal X-ray diffraction.

GUESTS: MONOLINURON AND MONURON

The structure of monolinuron (**2**) will be presented here. We report on its conformation in the solid state. The structures of monolinuron (**2**) and monuron (**3**) have been reported elsewhere.[1,2,3] In the case of **2** we thought it would be prudent to re-determine the structure at low temperature as the previous determination was carried out at room temperature (283 – 303 K as reported). The structure of **3** did not require re-determination and only the relevant torsion angles are reported here.

Preparation of single crystals of 2

20 mg of monolinuron powder was dissolved in 3 mL of ethanol at room temperature (20˚C). The solution was filtered and allowed to crystallise under ambient conditions. Crystallisation occurred within a few days of standing.

CRYSTAL STRUCTURE ANALYSIS

Space group determination

The determination of the crystal system and space group of monolinuron was carried out with the program LAYER.[4] The Laue symmetry was found to be *mmm* indicating the orthorhombic crystal system. Further investigation of the reciprocal lattice layers confirmed the reflection conditions *hkl : none; 0kl : k = 2n; h0l : l = 2n; hk0 : h = 2n*. The program XPREP was used to confirm the space group as Pbca.[5]

Structure solution and refinement

Crystal data and refinement data are presented in Table 1.

Table 1. *Crystal structure and data-collection parameters for* ***2.***

Parameters	2
Formula unit	$C_9 H_{11} Cl N_2 O_2$
Mr	214.65
Crystal system	orthorhombic
Space group	Pbca
a/Å	9.763(2)
b/Å	11.142(2)
c/Å	18.749(4)
α/°	90.00
β/°	90.00
γ/°	90.00
Vol. Å^3	2039.6(7)
Z	8
ρ_{calc} g cm^{-3}	1.398
μ (MoKα) mm^{-1}	0.350
F(000)	896
Crystal size mm^3	0.40 x 0.38 x 0.10
Temperature K	113 ± 2
Range scanned θ/°	3.52 ≤ θ ≤ 27.88
Index range	-11, 11; -13, 14; -22, 24
ϕ Scan angle °	1.0
ϕ Scan range °, no of frames	275.0, 275
ω Scan angle °	1.0
ω Scan range °, no of frames	51.0, 51; 35.0, 35
Dx mm	35
No. of reflections	20624
No. of unique reflections	2377
No. of reflections with I>2σ(I)	1613
No. of l.s. parameters	129
R_{int}, R_σ	0.0568, 0.0446
S	1.025
R_1 [$F_o > 4\sigma(F_o)$]	0.0379
wR_2	0.0957
No. of reflections omitted	4
Weighting scheme parameters	a = 0.0957, b = 0.0957
(Δ/σ)	< 0.001
Δρ excursions eÅ^{-3}	-0.339, 0.274

Unit cell refinement and data reduction were performed with program DENZO-SMN.[6] The structure solution of **2** was carried out with SHELXS-97 revealing all the non-hydrogen atoms.[7] The atoms were placed and refined isotropically on F^2 in SHELXH-97.[8] All atoms were later refined

anisotropically based on well-behaved isotropic temperature factors. All hydrogen atoms were placed in idealised positions in a riding model. The hydrogen atoms were refined isotropically and were assigned temperature factors related to the parent atom to which they were attached, namely 1.2 times those of the parent in the case of phenyl hydrogens and 1.5 times those of the parent atom for the methyl hydrogen atoms.

Molecular structure

Bond lengths and angles are provided in Table 2 and are all within the expected ranges. A drawing of the molecule showing the thermal ellipsoids at the 50 % probability level is shown in Figure 1.

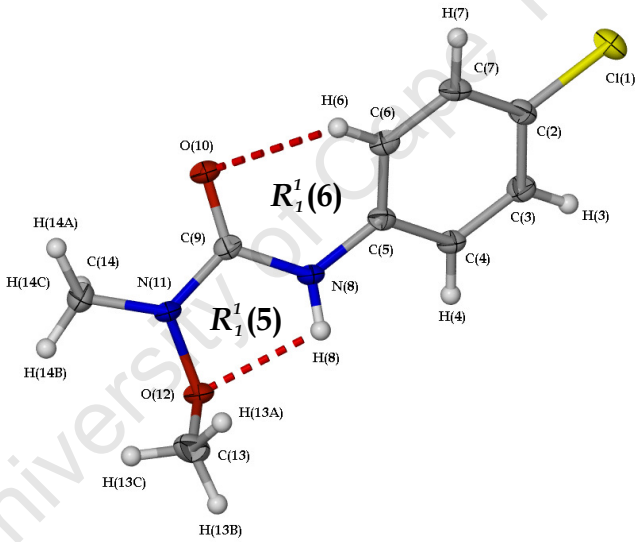

Figure 1. *The molecule of the guest monolinuron (**2**) showing the intramolecular hydrogen bonds.*

There are two intramolecular hydrogen bonds in the structure of **2**. The graph set analysis descriptors: $\boldsymbol{R_1^1(5)}$ and $\boldsymbol{R_1^1(6)}$, are shown in their respective hydrogen bonded rings.[9,10] These hydrogen bonds contribute to the stabilisation of the molecular conformation.

Table 2. *Geometrical parameters for compound* **2**

Bond	Bond lengths (Å)	Angles	Bond angles (˚)
Cl1-C2	1.747(2)	N11-O12 -C13	108.5(1)
O10-C9	1.227(2)	C5-N8-C9	123.4(1)
O12-N11	1.413(2)	O12-N11-C9	114.4(1)
O12-C13	1.429(2)	O12-N11-C14	112.5(1)
N8-C5	1.414(2)	C9-N11-C14	120.6(1)
N8-C9	1.369(2)	Cl1-C2 -C7	119.7(1)
N11-C9	1.377(2)	C3-C2-C7	121.1(2)
N11-C14	1.453(2)	Cl1-C2-C3	119.2(1)
C2-C7	1.385(2)	C2-C3-C4	119.3(1)
C2-C3	1.387(2)	C3-C4-C5	120.3(1)
C3-C4	1.382(2)	N8-C5-C4	118.1(1)
C4-C5	1.397(2)	C4-C5-C6	119.6(2)
C5-C6	1.393(2)	N8-C5-C6	122.3(1)
C6-C7	1.386(3)	C5-C6-C7	120.2(2)
		C2-C7-C6	119.4(1)
		N8-C9-N11	114.7(1)
		O10-C9-N8	125.1(2)
		O10-C9-N11	120.1(1)

Conformation

Nine torsion angles (τ_1 - τ_9) define the conformation of the 1-methoxy-1-methylurea which forms the 'spine' of the molecule. The torsion angles are shown schematically in Figure 2 and listed in Table 3. The amide group (O10-C9-N8-H8) is in the characteristic *trans* conformation.

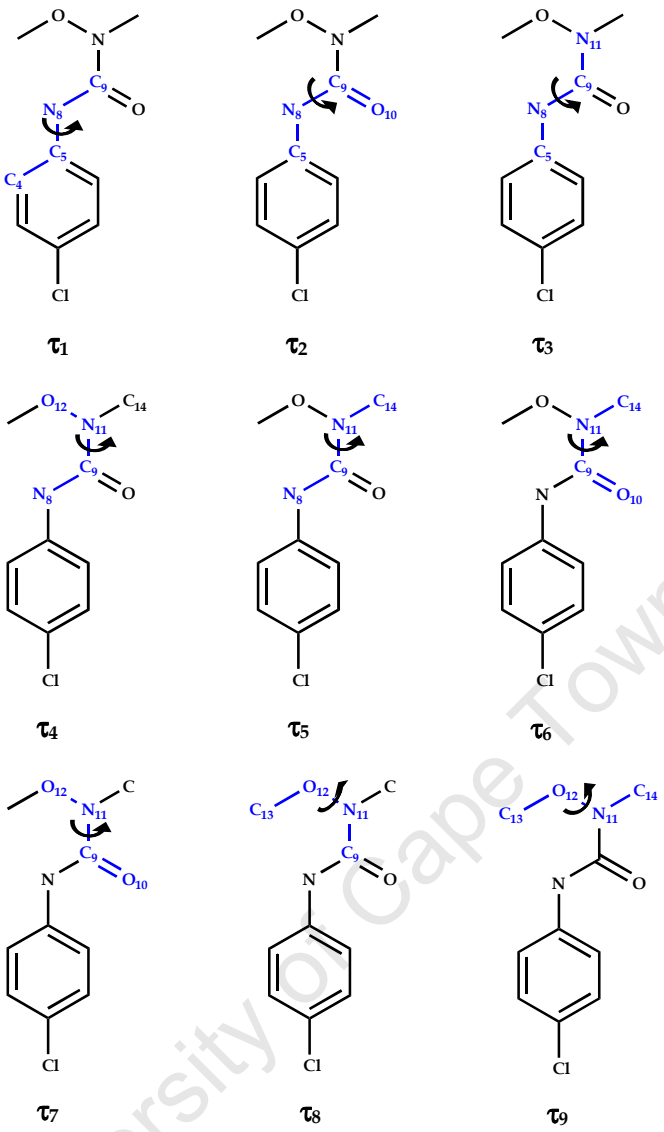

Figure 2. *Schematic diagram of the nine torsion angles of guest* ***2****.*

Torsion angle τ_1 (Figure 2) describes the rotation around bond C5-N8 and relays information about the orientation of the chlorophenyl moiety relative to the 1-methoxy-1-methylurea moiety (for simplicity, the urea moiety). τ_2 and τ_3 describe the amount of rotation around bond N8-C9 and are pertinent to the degree of 'extension' of the urea moiety. The torsion angles τ_4, τ_5, τ_6 and τ_7 describe the amount of rotation around bond C9-N11 providing information on the conformation of surrounding moieties. Finally, τ_8 and τ_9 describe the amount of rotation around bond N11-O12 and relate the disposition of bond C13-O12 relative to the mean plane through C9, N11, O12 and C14.

Table 3. *Torsion angles for* ***2****.*

Angle		Torsion angle (˚)
C4-C5-N8-C9	τ_1	-140.7(2)
C5-N8-C9-O10	τ_2	-1.9(3)
C5-N8-C9-N11	τ_3	-178.3(1)
N8-C9-N11-O12	τ_4	-18.5(2)
N8-C9-N11-C14	τ_5	-157.8(1)
O10-C9-N11-C14	τ_6	25.7(2)
O10-C9-N11-O12	τ_7	164.9(1)
C9-N11-O12-C13	τ_8	117.9(2)
C13-O12-N11-C14	τ_9	-99.5(2)

The value of τ_1 implies that the chlorophenyl moiety is rotated out of the plane of the urea moiety, in a **–ac** conformation. Torsion angle τ_2 with terminal bonds C5-N8 and C9-O10 is in a **–sp** conformation. τ_3 is very close to 180˚ and is indicative of an 'extended' conformation; bonds C5-N8 and C9-N11 are in a **–ap** conformation. Values close to zero for torsion angles τ_4 and τ_6 represent **–sp** and **+sp** conformations, respectively. On the other hand, values close to 180˚ for torsion angles τ_5 and τ_7 represent **–ap** and **+ap** conformations, respectively. The conformations indicated by the values of τ_8 and τ_9 may be described as **+ac** and **–ac** respectively; they show the disposition of bond C13-O12 as near perpendicular to the mean plane through C9, N11, O12 and C14. The monolinuron molecule essentially consists of two planes. The first is made up of N8 and the chlorophenyl ring and the second consists of the mean plane through C9, O10, N11, O12 and C14.

HYDROGEN BONDS

Table 4. *Hydrogen bonding interactions for* ***2****.*

D-H•••A	D-H (Å)	H•••A (Å)	D•••A (Å)	D-H•••A˚
N8-H8•••O12	0.88	2.17	2.565(2)	107.0
N8-H8•••O10[a]	0.88	2.35	3.094(2)	142.0
C4-H4•••O10[a]	0.95	2.44	3.223(2)	140.0
C6-H6•••O10	0.95	2.51	2.921(2)	106.0

Symmetry code: a = ½ + x, y, ½ + z

There are two intermolecular and two intramolecular hydrogen bonds in the structure of **2** (Table 4). The two intramolecular hydrogen bonds were described earlier.

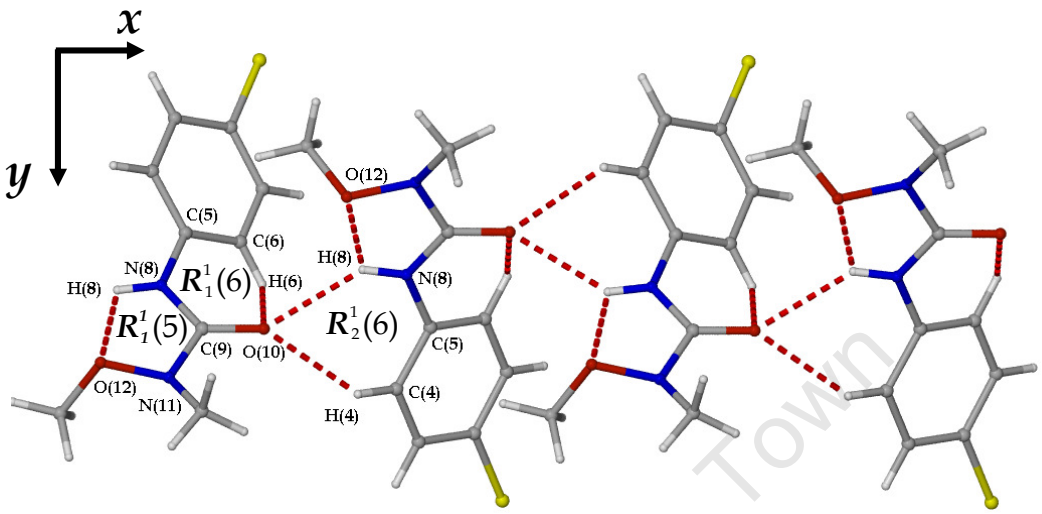

Figure 3. *The intermolecular hydrogen bonds which link adjacent molecules forming an infinite ribbon spanning the crystal. Also shown here is the graph set notation for the three rings formed by intra and intermolecular hydrogen bonding.*

The two intermolecular hydrogen bonds consist of an N-H•••O and a C-H•••O hydrogen bond. Both involve the same carbonyl oxygen of a neighbouring molecule, thus leading to the formation of hydrogen bonded ribbons parallel to the *a*-axis and extending infinitely through the crystal, as shown in Figure 3. The graph set analysis descriptors for the three rings formed by the intermolecular and intramolecular hydrogen bonds are shown in their respective rings in Figure 3.[9,10]

CRYSTAL PACKING

The unit cell contains eight symmetry related molecules arranged in two layers which have anti-parallel orientation. The layers are parallel to the *b*-axis, Figure 4. The two layers are arranged in such a way that the chlorophenyl moieties interpenetrate at *c*/2, as shown in Figure 4.

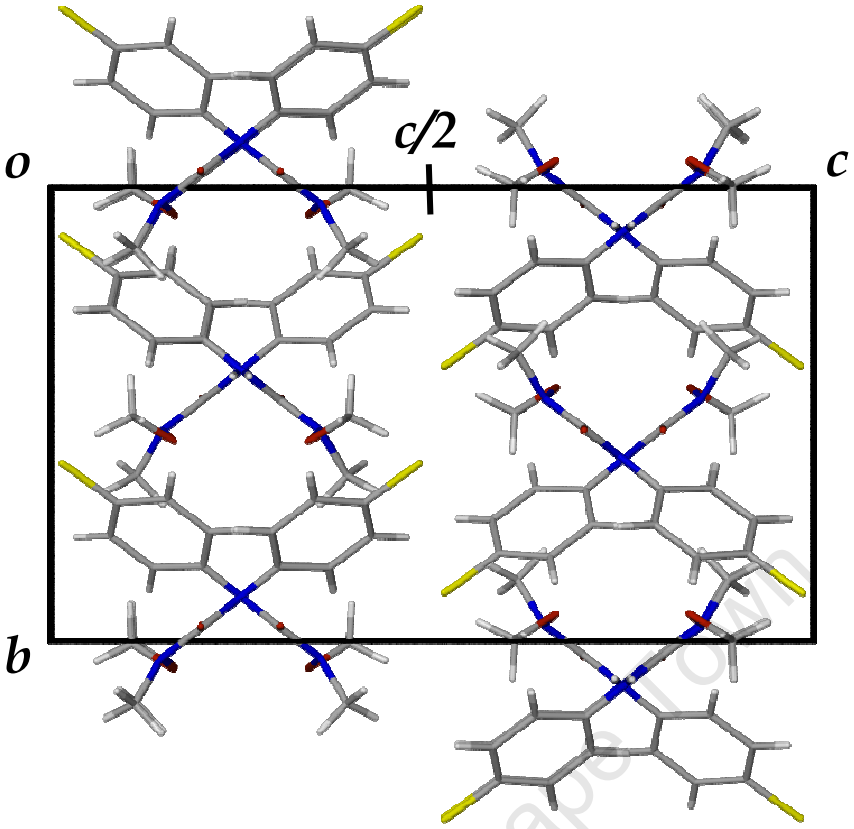

Figure 4. *The packing diagram shows the interleaved chlorophenyl groups located halfway along the c-axis.*

TORSION ANGLES OF 3

The structure of **3** has been reported elsewhere.[2] However, the torsion angles are reported here for completeness (Table 5).

Table 5. *Torsion angles for* ***3****.*

angle		Torsion angle (°)
C4/C6-C5-N8-C9	τ_1	-133.2
C5-N8-C9-O10	τ_2	-0.5
C5-N8-C9-N11	τ_3	-179.6
N8-C9-N11-C12	τ_4	10.0
N8-C9-N11-C13	τ_5	-173.1
O10-C9-N11-C12	τ_6	-169.9
O10-C9-N11-C13	τ_7	7.8

β-CYCLODEXTRIN INCLUSION COMPLEXES OF 2 AND 3

Preparation

In an attempt to isolate different crystal forms, two preparations of each guest with the host cyclodextrin were made. One preparation used only water as the crystallisation medium while the other used a water-ethanol mixture (75-25 %). For preparations containing guests **2** and **3** the host-to-guest ratio used was 2:1. For guest **2**, 212 mg (0.1864 mmol) of β-CD was dissolved in 6 mL of water. 20 mg (0.0932 mmol) of **2** was slowly added to the clear β-CD solution. In the case of guest **3**, 229 mg (0.2014 mmol) of β-CD was dissolved in 6 mL of water. 20 mg (0.1007 mmol) of **3** was slowly added to the clear β-CD solution. All preparations were carried out at elevated temperature (70 - 80˚C). The solutions were stirred until clear and filtered (0.45 μm nylon filter) while hot. To two of the preparations two mL of ethanol (96 %) was added while an extra two mL of water was added to the two remaining preparations.

Crystallisation conditions

The conditions of crystallisation were the same for all preparations. All the solutions were placed in a Dewar flask containing water at ~80˚C. The Dewar flask was covered with an insulating material to prevent rapid cooling. The water in the Dewar flask took four to five days to return to ambient temperature. Crystallisation occurred within this time. Three new complexes were obtained in this way. Guest **2** yielded crystals from the aqueous preparation as well as from the water-ethanol mixture. The phase isolated from the aqueous preparation was characterised by the composition β-CD•monolinuron•7.4(H_2O) (or (β-CD)$_2$•(monolinuron)$_2$•14.8(H_2O)) A1 (7.4 ± 0.9) while the phase isolated from the water-ethanol medium was characterised by the composition (β-CD)$_2$•(monolinuron)$_2$•22(H_2O) A2 (22 ± 1). For guest **3**, only the aqueous medium produced a new phase which was characterised by the composition (β-CD)$_2$•(monuron)$_2$•19(H_2O) A3 (19 ± 2).

Stoichiometry

The stoichiometries of the three complexes were determined by means of UV spectrophotometry (Table 6). Thermogravimetric analysis was used to determine the water content for all three crystal forms. The reported water content is the average of two measurements.

Table 6. *Stoichiometries and water content for complexes A1, A2 and A3.*

Complex	A1	A2	A3
Host:Guest ratio	1.00:0.98	1.00:1.01	1.00:0.95
H_2O^a	7.4	11	9.7

(a) H_2O molecules per CD molecule.

X-RAY STRUCTURE OF A1

Space group determination

The program LAYER was used to determine the crystal symmetry. The Laue symmetry was found to be $2/m$ indicating the monoclinic crystal system.[4] From further examination of the reciprocal lattice the reflection conditions obtained were $hkl : h + k = 2n$, $h0l : h = 2n$. The space group of A1 was confirmed with the aid of the program XPREP.[5] The space group C2 was selected as the host cyclodextrin is chiral. The inclusion complex A1 therefore crystallises in the monoclinic space group C2 with $Z = 4$ complex units per unit cell.

Structure solution and refinement

The A1 complex has a single cyclodextrin molecule in the asymmetric unit, a single guest molecule and 7.4 water molecules. Refinement parameters and crystal data are reported in Table 7. A diad parallel to the *b*-axis generates the other half of the dimeric complex. Unit cell refinement and data reduction were performed with the program DENZO-SMN.[6] A1 was found to be isostructural with the complex (β-CD)$_2$•(3,3-dimethylbutylamine)$_2$•10.7(H_2O) (refcode: VIJXAN10).[11,12] The structure of A1 was solved by isomorphous replacement using only the host coordinates of VIJXAN10. The freely rotating O6 atoms and water molecules were deleted from the refinement in order to

model any possible disorder of the O6 atoms in A1. The glucopyranose units for the host were labelled A1-A7, as shown in Figure 5. The structure was refined with SHELXH-97 with successive Fourier maps revealing the O6 atoms.[8] Several atoms of the host were disordered over two positions; these were C6A1, O6A1, O6A2, C6A6 and O6A6. Their site-occupancy factors (s.o.f.s) were refined as x, which was set to 0.5. The minor components (C6B1, O6B1, O6B2, C6B6 and O6B6) refined as 1-x. The value of x settled to 0.51. All the non-hydrogen atoms of the host were refined anisotropically except for atoms C6A1, C6B1, O6A1, O6B1, O6A2, O6B2, C6A6, C6B6, O6A6 and O6B6, which were refined isotropically. All hydrogens attached to carbon atoms were placed in idealised positions using a riding model while the hydroxyl hydrogen atoms were placed with the hydrogen bond searching model.

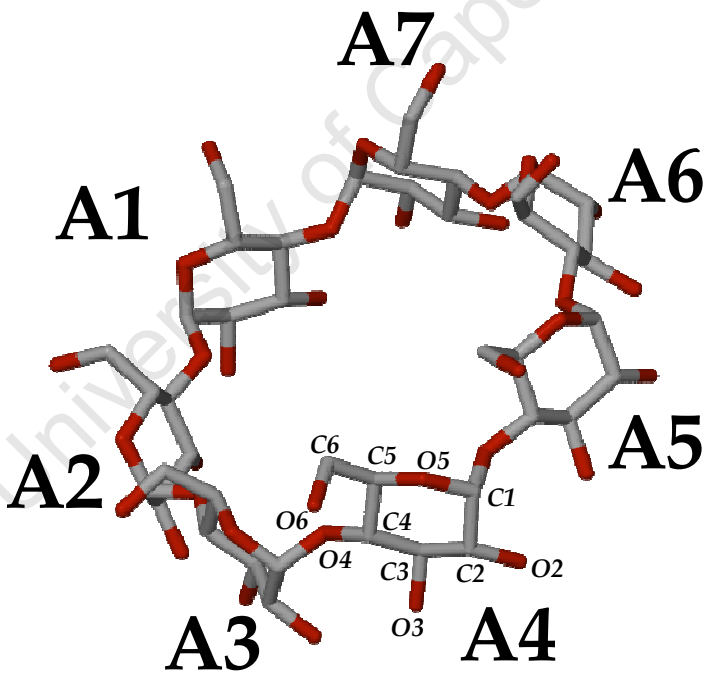

Figure 5. *Macrocyclic structure and numbering scheme of the glucose residues. Water molecules and hydrogen atoms have been omitted for clarity.*

All hydrogen atoms were assigned isotropic temperature factors of 1.2 times those of their parent atoms. 16 sites were revealed for water in the electron density map with a single water molecule having full site-occupancy while the rest had partial site-occupancies ranging between 0.26

and 0.71. The temperature factors for the water molecules with partial occupancy ranged from 0.05 to 0.12 Å^2.

Table 7. *Crystal data and data-collection parameters for A1.*

parameters	*A1*
Formula unit	$C_{42}H_{70}O_{35} \bullet C_9H_{11}N_2O_2Cl \bullet 7.4H_2O$
Mr	1482.95
Crystal system	monoclinic
Space group	C2
a/Å	19.1870(4)
b/ Å	24.5600(6)
c/ Å	15.8930(3
α/°	90.00
β/°	108.7700(1)
γ/°	90.00
Vol. Å^3	7091.0(3)
Z	4
ρ_{calc} g cm^{-3}	1.389
μ (MoKα) mm^{-1}	0.158
F(000)	3152
Crystal size mm^3	0.20 x 0.17 x 0.13
Temperature K	113 ± 2
Range scanned θ/°	2.77 ≤ θ ≤ 27.64
Index range	-24 : 24; -31 : 31; -20 : 19
ϕ Scan angle °	1.5
ϕ Scan range °, no of frames	363.0, 242
ω Scan angle °	1.5
ω Scan range °, no of frames	106.5, 71; 100.5, 67; 42.0, 28; 42.0, 28; 42.0, 28; 40.5, 27; 42.0, 28
Dx mm	30
No. of reflections	88141
No. of unique reflections	15124
No. of reflections with I>2σ(I)	8764
No. of l.s. parameters	829
R_{int}, R_σ	0.1188, 0.0887
S	1.039
R_1 [$F_o > 4\sigma(F_o)$]	0.0791
wR_2	0.2549
No. of reflections omitted	8
Weighting scheme parameters	a = 0.2549, b = 0.2549
(Δ/σ)	<0.001
Δρ excursions eÅ^{-3}	-0.47, 0.60

The 16 sites accounted for 7.8 water molecules while the thermogravimetry results accounted for 7.4 water molecules (n = 2).

Modelling of the guest

After optimisation of the host our attention turned to the guest which was disordered over two positions. After careful inspection of the difference map, two positions for chlorine were identified. This was followed by the placement of the phenyl rings that were easily identifiable by their hexagonal shape. An AFIX 66 instruction, constraining the rings as rigid hexagons, was applied once all the atoms were located in the difference map. This was followed by the careful placement and refinement of the urea moieties of both models. The two positions for the guest molecule were labelled A and B. The site-occupancy of the major component of disorder (A) was refined as x while the minor component (B) refined as 1-x. An initial value of x = 0.5 was set which refined to 0.51. Each model was assigned a global isotropic temperature factor with a starting value of 0.05 $Å^2$. The values settled between 0.09 and 0.10 $Å^2$ for models A and B. Distance restraints were imposed to ensure reasonable geometries, as the least-squares refinements were sensitive. The standard deviation for restrained bond lengths was set at σ = 0.002 Å for uniformity. Only atom Cl1B was refined anisotropically, all other atoms belonging to the guests were refined isotropically. The guest hydrogens were added in idealised positions in a riding model. Aromatic type hydrogens refined with isotropic thermal parameters 1.2 times those of their parent atoms while the methyl hydrogens refined with thermal parameters 1.5 times those of their parent atoms

STRUCTURAL DESCRIPTION

Host conformation

Several geometric parameters, which describe the host conformation, have been tabulated and placed in the appropriate appendix. However, mean values and ranges will be used here to describe the topological and conformational aspects of the macrocycle.

Primary hydroxyl torsion angles

The primary hydroxyl torsion angles **ω** (O5-C5-C6-O6) describe the rotation of the C6-O6 bond relative to the cyclodextrin cavity. A negative value for the **ω** torsion angle means that the C6-O6 atoms have *(-)-gauche* conformation and are directed away from the cavity while a positive value implies that they have *(+)-gauche* conformation and are directed toward the cavity.

All the primary hydroxyl torsion angles (**ω**) of complex A1 have *(-)-gauche* orientation except for rings A2 and A6 which are disordered. B2 and B6 have *(+)-gauche* orientation and the major components of each (A2 and A6) have *(-)-gauche* orientation. The glycosidic torsion angles **Φ** and **Ψ** as well as the pyranoid torsion angles Θ_1 and Θ_2 are in good agreement with those reported for the parent β-CD.[13,14] The glucose residues of the host are all in the $^4C_1$ conformation.

Macrocyclic symmetry

The radius **r** has a mean length of 5.14 Å and lies within a narrow range of 4.94-5.37 Å. The mean length **l** is 4.46 Å and it ranges from 4.35 to 4.61 Å. The glycosidic oxygen angle **a** has a mean of 128.5˚ and ranges from 123.5˚ to 132.6˚. None of the parameters **r**, **l** and **a** deviates substantially from the values reported for native β-cyclodextrin.

Planarity of the O4-Heptagon

The root mean square deviation (**d**) of the O4 atoms from the mean O4 plane of the host is 0.047 Å. There are four O4 atoms which have negative deviations from the mean O4 plane. They are O4A1, O4A4, O4A5 and O4A7. In addition, the torsion angles (**t**) all lie in a narrow range from -2.4 to 3.6˚.

Other useful parameters which describe the overall shape of the macrocycle are the tilt angles (τ_1 and τ_2), intersaccharidic angle (**φ**) and the O2•••O3' distances, all of which provide information about the shape of the macrocycle. For instance, τ_1 is the angle between the mean O4 plane and the six atoms of

the pyranose ring (C1, C2, C3, C4, C5 and O5) while τ_2 is the angle between the O4 mean plane and the mean plane through O4, C1, C4 and O4′. For A1, τ_1 ranges from 1.8 to 8.9˚ while τ_2 ranges from 2.6 to 10.7˚. Both are quite narrow ranges. All values of τ_1 and τ_2 are positive and the implication is that the primary rims of all the glucose residues are inclined towards the centre of the cavity. The intersaccharidic angle φ ranges from 116.5 to 119.5˚ with an average value of 118.1˚. Again this is in good agreement with those reported for β-CD.

The parameters reported here for A1 indicate that the macrocycle is highly symmetrical while the root mean square deviation **d** and torsion angle **t** show a near planar O4-heptagon. Additionally, with τ_1 and τ_2 all positive it implies that the macrocycle has a truncated cone like appearance (*i.e.* wider at the secondary rim and narrower at the primary rim).

HYDROGEN BONDING INTERACTIONS

It is prudent to note the 'flip-flop' nature of the interglucose hydrogen bonds involving the O2•••O3′ atoms of the host. This means that there is a dynamic interchange in the hydrogen bonds between O2-H•••O3′ and O3-H•••O2′, a result highlighted by Saenger *et al*.[15,16,17] It is therefore also quite plausible that such interactions may be extended to include O3•••O3′ hydrogen bonds of head-to-head hydrogen bonded hosts.

INTRA- AND INTERMOLECULAR HYDROGEN BONDS

Host intramolecular interactions

There are seven intraglucose O2-H•••O3′ hydrogen bonds which further stabilise the β-CD macrocycle. The O2-H•••O3′ interactions have hydrogen bond lengths that range from 2.81 to 2.90 Å (mean = 2.84 Å). The H-bond distances lie within a narrow band implying a round or highly symmetrical macrocycle.[15,16,17]

Host-Host intermolecular interactions

There are 25 intermolecular hydrogen bonds which stabilise the host dimer at the secondary rim interface. Twelve of the interactions are of the type O2•••O3, seven are O3•••O3 interactions with the remaining six being O2•••O2 interactions. The twelve O2•••O3 interactions have an average hydrogen bond distance of 3.12 Å and range from 3.04 to 3.17 Å. In the case of the O3•••O3 interactions the average hydrogen bonding distance is 2.88 Å ranging from 2.79 to 2.93 Å. The mean O2•••O2 hydrogen bonding distance is 3.03 Å with a range of 2.92 to 3.14 Å. It is quite clear from the average hydrogen bond lengths that the O3•••O3 interactions have a greater stabilising effect on the dimer since they have more favourable distances, a fact supported by data obtained from synchrotron experiments performed by Mavridis *et al*.[18]

INTER- AND INTRA-LAYER INTERACTIONS

The dimers are arranged in layers which stack one on top of the other. Inter-layer hydrogen bonds are formed between dimers in adjacent layers. Similarly, intra-layer hydrogen bonds are formed between dimers within the same layer.

Inter-layer interactions

There are eight inter-layer hydrogen bonds observed in this structure. All eight are O6•••O6 hydrogen bonds. The mean hydrogen bond length for the eight O6•••O6 interactions is 2.87 Å ranging from 2.61 to 3.05 Å.

Intra-layer interactions

There are two O2•••O2 intra-layer interactions and two O6•••O6 intra-layer interactions present in the structure. Both the O2•••O2 interactions have a hydrogen bond distance of 2.78 Å while both the O6•••O6 interactions have a distance of 2.83 Å. There are four long range/weak C-H•••O intra-layer hydrogen bonds between adjacent dimers. Two are of the type C2-H•••O3 while the remaining two are of the type C1-H•••O2. The hydrogen bond

distance for the C-H•••O interactions is 3.37 Å (range 3.30 to 3.45 Å) while the mean hydrogen bond angle is 151.0˚ (range 137.0 to 166.0˚).

Host-Water interactions

As mentioned previously, 16 sites were refined for 7.8 water molecules in the asymmetric unit. Six water molecules are involved in close O•••O contacts with the primary rim, with a total of 11 close contacts between the primary rim and various water molecules. The O•••OW interaction distance ranges from 2.71 - 3.19 Å for the six water molecules with the primary rim while the mean interaction distance is 2.95 Å. Nine water molecules interact with the secondary rim with 19 interactions being observed. The close contact distances between the secondary rim and the water molecules range from 2.64 to 3.23 Å with a mean distance of 2.89 Å. In addition, there are 12 water molecules involved in water-to-water interactions. Together they are involved in 22 O•••OW close contacts. The water-water close contacts range from 2.46 to 3.18 Å with a mean distance of 2.85 Å. There are also two C-H•••OW hydrogen bonds with a mean distance of 3.37 Å (range 3.34 - 3.41 Å). The interstitial water molecules are shown in Figure 6 below.

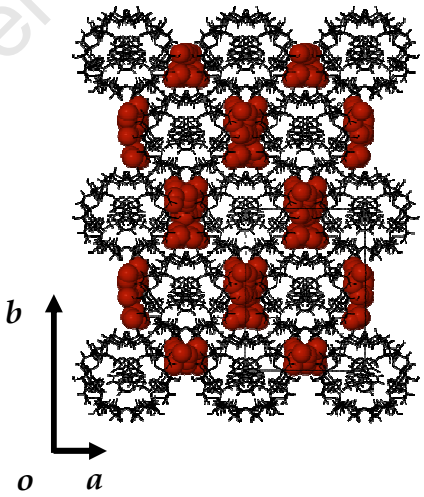

Figure 6. *Water molecules located in the interstitial spaces.*

GUEST INCLUSION

Guest disorder

In the asymmetric unit of the complex A1, a single guest molecule occupies the cyclodextrin cavity. The single guest molecule is disordered over two positions A and B. The phenyl rings of each component of disorder, A (green) and B (blue) intersect one another, as shown in Figure 7.

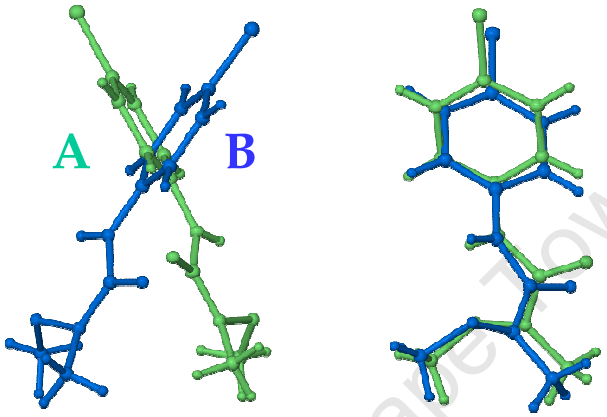

Figure 7. *A plot of the disordered components of the guest molecule in the dimer cavity. The major component is shown in green and the minor component is shown in blue.*

As it turns out, guest A is involved in unacceptably close contacts with the twofold related position. In other words the twofold related component could not be present in a single hydrogen bonded dimer. The result is that the twofold symmetry required by the space group C2 cannot always be satisfied within a single dimer. The possibility exists that the two positions are present in equal proportions in a crystal of the complex giving an average structure which maintains the C2 symmetry (Figure 8).

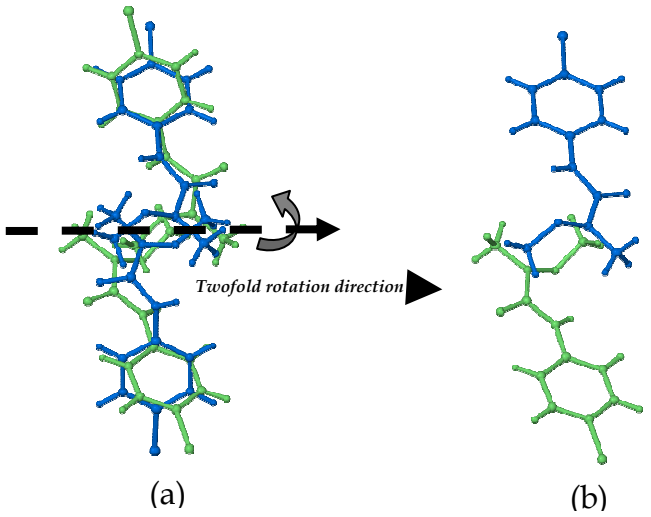

Figure 8. *Diagram (a) shows the disordered guests of complex A1. The major (green) and minor (blue) components make unacceptably short contacts with their respective twofold related counterparts as shown here. Diagram (b) shows the average contents of the dimer cavity which enables the C2 symmetry to be maintained.*

Guest location

The guest monolinuron molecule is oriented with the chlorophenyl moiety lodged at the primary rim of the cyclodextrin. The urea moiety is located at the secondary rim interface. In order to be accommodated in the cavity of the host the guest is tilted with respect to the O4-heptagon of cyclodextrin A, illustrated in Figure 9 (a). There is only partial protrusion of the chlorophenyl moiety from the primary rim. The urea moiety of the guest occupies the secondary rim interface with partial inclusion into the cavity of the other cyclodextrin which completes the hydrogen bonded dimer, as shown in Figure 9 (b).

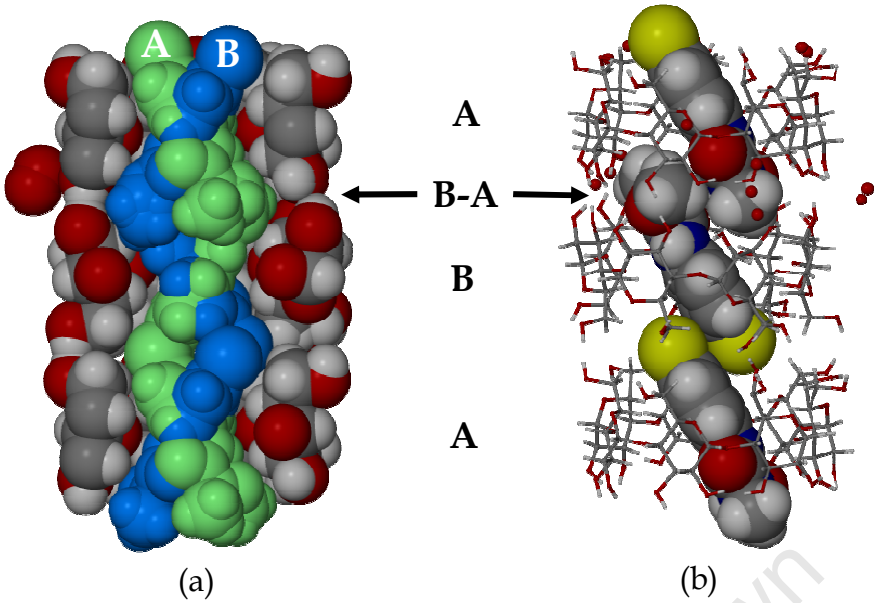

Figure 9. *Diagram (a) shows the tilted guest molecules in the dimer cavity. (b) Shows how the chlorine atoms (shown in yellow) partially include at the primary rim of an adjacent dimer and how the urea groups include into the cavity of cyclodextrins A and B at the secondary rim interface (A-B), respectively. Guest disorder has been omitted in (b) for clarity.*

The inter-dimer interface is almost completely closed off by the primary rim hydroxyl groups and interstitial water molecules surrounding it. It is effectively an extension of the dimer cavity housing the chlorine atoms, Figure 10.

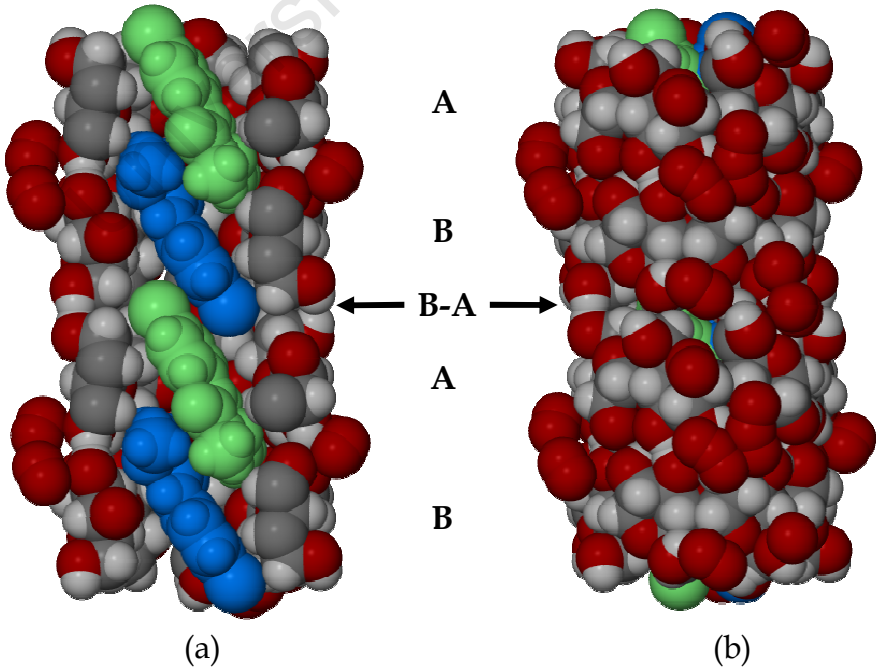

Figure 10. *(a) Shows the continuous channel formed by successive dimer cavities which effectively isolate the included guest molecules from the aqueous environment. (b) Shows how the inter-dimer interface is almost completely closed off by primary hydroxyl groups and interstitial water molecules.*

The inclinations of guest molecules A and B with respect to the O4-heptagon of cyclodextrin A are 58.2(5)˚ and 56.2(5)˚ respectively. The angle of intersection between the guests A and B is 67.6(5)˚.

Guest conformations

The torsion angle τ_1 for A and B spans the range -27.5˚ to +19.7˚. τ_2 ranges from -16.8˚ to 8.6˚ while τ_3 ranges from -167.5˚ to +172.3˚ indicating an 'extended' conformation for the two guests. The 'extended' conformation is also owing to the *trans*-planar conformation of the amide group. τ_4 ranges between -15.7˚ and +8.7˚. τ_5 spans the range -164.2˚ to +165.2˚ and is close to -180/180˚. τ_6 ranges from -4.7˚ to 19.9˚ while τ_7 ranges from -161.2˚ to +168.4˚. τ_8 and τ_9 range from -120.6˚ to +121.6˚ and -88.1˚ to +82.4˚ respectively, an indication that the disposition of bond C13-O12 is nearly perpendicular to the mean plane passing through C9, O10, N11, O12 and C14. The conformations of the included guests are shown relative to that of the uncomplexed guest in Figure 11 (a), (b), (c) and (d).

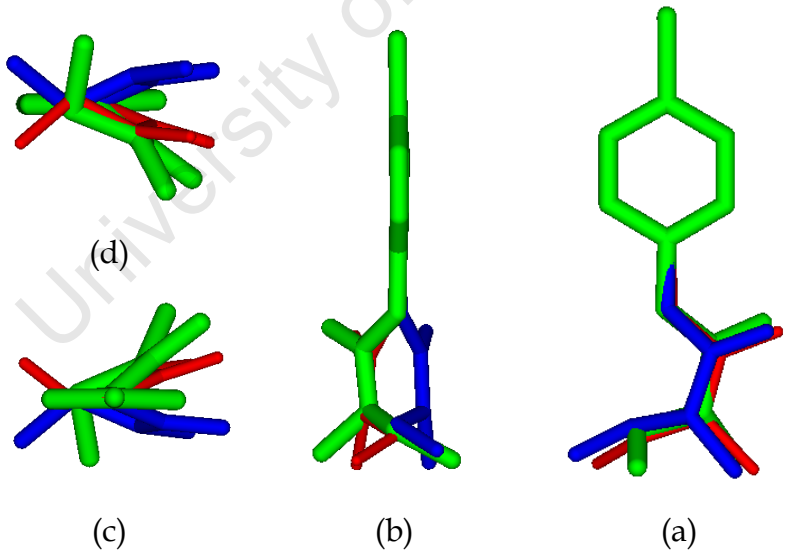

Figure 11. *Relative conformations of the included guest as compared with that of the uncomplexed guest. Guest A - blue, guest B - red and uncomplexed guest - green.*

HYDROGEN BONDING INTERACTIONS OF THE GUEST

Host-Guest intermolecular interactions

There are two C-H•••O hydrogen bonds in this structure. The average bond length of the four C-H•••O hydrogen bonds is 3.40 Å (3.38 - 3.41 Å) with an

average bond angle of 144.0° (range 135.0 - 151.0°). There are four C-Cl•••H interactions. The average C-Cl•••H distance is 2.88 Å (2.45 - 3.12 Å). Five host-guest close contacts were also observed; the mean interaction distance is 3.20 Å in the range 2.53 to 3.60 Å.

Guest intramolecular interactions

Four intramolecular hydrogen bonds were observed for the guests. Two are N-H•••O hydrogen bonds with lengths in the range 2.51-2.69 Å (mean = 2.60 Å) and the hydrogen bond angle ranging from 110.0 to 113.0° (mean = 111.0˚). For the uncomplexed guest the N-H•••O distance is 2.56 Å while the angle is 107.0˚. The two remaining bonds are C-H•••O bonds spanning a narrow range of 2.78 - 2.88 Å (mean = 2.83 Å) while the angular range is 116.0 - 120.0° (mean = 118.0˚). The C-H•••O bond length for the uncomplexed guest is 2.92 Å while the hydrogen bonding angle is 106.0˚. Inter- and intramolecular hydrogen bonds are shown Figure 12.

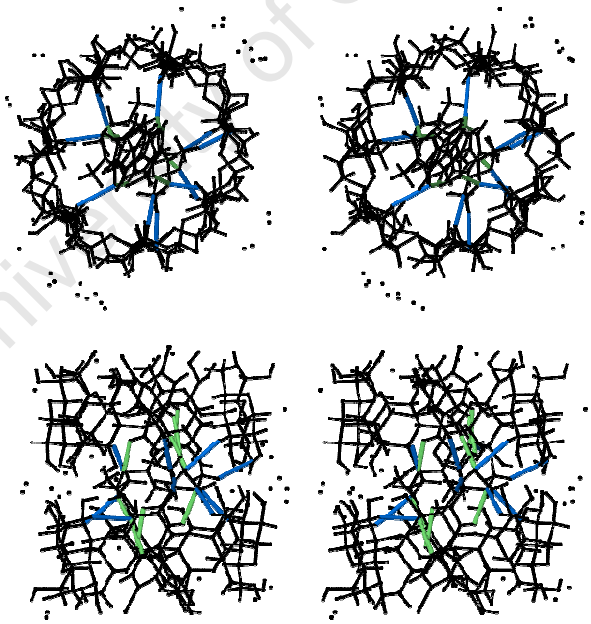

Figure 12. *Stereoview of A1, viewed from the primary (top) and side faces (bottom) showing the host-guest intermolecular hydrogen bonds (blue) and the guest-guest intramolecular hydrogen bonds (green).*

CRYSTAL PACKING

A1 packs in the channel type (**CH**) packing arrangement. There are three twofold rotation axes parallel to *b* located at 0, ½ and 1 along the *a*- and *c*-axes. A diad is located at the interface of each dimer and between two consecutive dimers in adjacent layers, Figure 13. The dimeric columns are parallel to *c* and the channels extend infinitely along *c*. The dimers are arranged in C-centred layers which propagate along the *c* direction. Successive layers are linked by inter- and intra-layer hydrogen bonds. Figure 13 shows the *b*-axis projection with the C-centred columns shown in green for clarity.

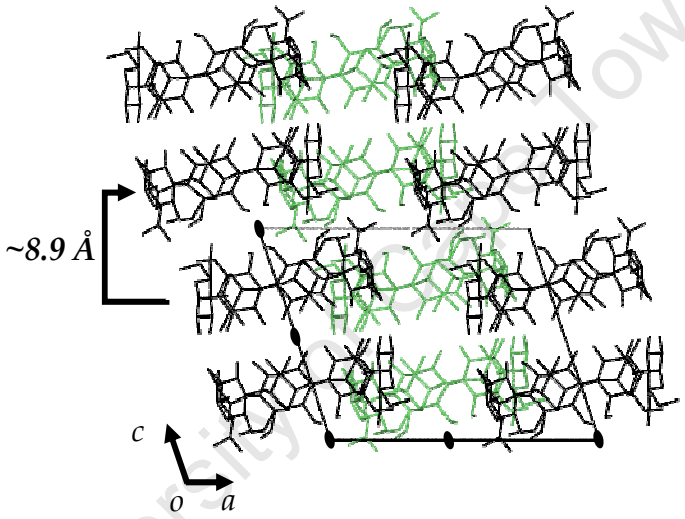

Figure 13. *Packing diagram of the A1 structure along the b-axis.*

All columns have the same orientation. The inter dimer distance, which is measured from the centroid of one CD molecule to the centroid of a symmetrically related CD molecule across the inter-dimer interface is ~8.9 Å, Figure 13. The O4-heptagons make an angle of ~10˚ with the *ab*-plane. There is an angle of 1.39(3)˚ between the O4-heptagons of two head-to-head hydrogen bonded dimers.

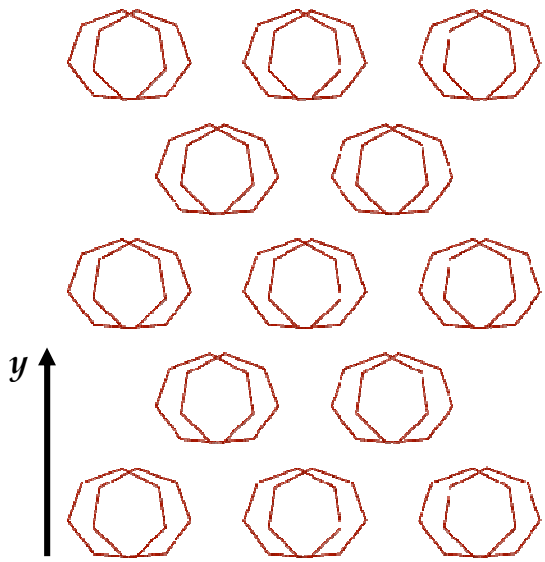

Figure 14. *O4-heptagons of adjacent dimeric layers are laterally displaced from each other.*

The lateral shift between adjacent dimers becomes more apparent when viewed perpendicular to the O4-heptagons, with successive layers laterally offset from each other by ~2.6 Å, Figure 14. The average lateral displacement for channel type structures crystallising in the space group C2 is 2.7 Å.

Comparative PXRD

Calculated and experimental traces for complex A1 are shown in Figure 15. There is a very close match in peak positions between the traces. Differences in peak intensities indicate that the experimental sample suffers from preferred orientation.

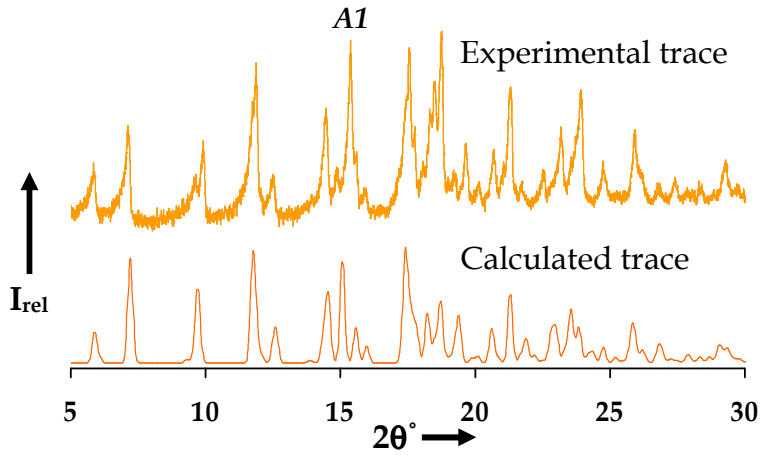

Figure 15. *Calculated and experimental PXRD traces for A1*

The match between the experimental and calculated PXRD patterns confirms the identity of the phase of the bulk material as being the same as the single crystal selected for data-collection.

X-RAY STRUCTURE OF A2

Space group determination

Program LAYER was employed to determine the crystal system and space group of A2.[1] The crystal system was found to be triclinic as the Laue symmetry was $\bar{1}$ and the space group P1 since the cyclodextrin is chiral. Confirmation of the crystal system and space group was obtained with XPREP.[2] A2 crystallises in the triclinic space group P1 with Z = 1 dimeric complex unit per unit cell.

Structure solution and refinement

Table 8 contains refinement parameters and crystal data for A2. The asymmetric unit consists of a single dimeric β-CD complex made up of two crystallographically independent cyclodextrins which are hydrogen bonded in a head-to-head manner. Each cyclodextrin molecule contains a single guest molecule. The structure was found to be isostructural with an existing complex [(β-CD)$_2$•(*p*-bromoacetanilide)$_2$•27(H_2O)] (Refcode: XADHIT) whose unit cell parameters are very similar to those of A2. Only the host coordinates were used as input fragment to solve the phase problem.[19] All guest, water molecules and O6 atoms were deleted from the trial structure in order to model any disorder which might be present. The glucopyranose units for the two host molecules in the asymmetric unit were labelled A1-A7 and B1-B7. The structure was refined with SHELXH-97 with successive difference Fourier maps revealing the O6 atoms.[5] Atoms C6A1, O6A1, C6A5 and O6A5 of the host were disordered over two positions. The major components of the disordered atoms were assigned a value of x for their s.o.f.s while the minor components (C6C1, O6C1, C6C5 and O6C5) were assigned the value 1-x. An initial value of x = 0.5 was set. It refined to 0.72 for A1 and 0.66 for A5 for the major components of the disorder.

Table 8. *Crystal data and data-collection parameters for A2.*

parameters	*A2*
Formula unit	$(C_{42}H_{70}O_{35})_2 \bullet (C_9H_{11}N_2O_2Cl)_2 \bullet 22(H_2O)$
Mr	3092.73
Crystal system	triclinic
Space group	P1
a/Ä	15.28220(1)
b/ Å	15.41640(1)
c/ Å	15.71030(1)
α/°	87.5110(1)
β/°	97.5630(1)
γ/°	103.6480(1)
Vol. Å³	3565.20(4)
Z	1
ρ_{calc} g cm^{-3}	1.440
μ (MoKα) mm^{-1}	0.164
F(000)	1646
Crystal size mm³	0.18 x 0.15 x 0.10
Temperature K	113 ± 2
Range scanned θ/°	3.94 ≤ θ ≤ 25.34
Index range	-18 : 18; -18 : 18; -18 : 18
ϕ Scan angle °	1.0
ϕ Scan range °, no of frames	363.0, 363
ω Scan angle °	1.0
ω Scan range °, no of frames	116.0, 116; 116.0, 116; 48.0, 48; 48.0, 48; 49.0, 49; 110.0, 110; 49.0, 49; 115.0, 115
Dx mm	35
No. of reflections	101707
No. of unique reflections	25465
No. of reflections with I>2σ(I)	21788
No. of l.s. parameters	1689
R_{int}, R_σ	0.0425, 0.0405
S	1.040
R_1 [$F_o > 4\sigma(F_o)$]	0.0782
wR_2	0.2233
No. of reflections omitted	146
Weighting scheme parameters	a = 0.1457, b = 4.1619
(Δ/σ)	< 0.001
Δρ excursions eÅ^{-3}	-0.85, 0.91

All hydrogen atoms attached to carbon atoms were placed and refined in geometrically calculated positions using the AFIX 43 instruction (riding model). The hydrogen atoms of the hydroxyl groups were placed using the

AFIX 83 instruction (hydrogen bond searching model). All hydrogen atoms were assigned isotropic temperature factors which were 1.2 times those of their parent atoms. 30 sites for water molecules were located in a series of difference electron-density maps accounting for 21.85 water molecules. 13 water molecules had full site-occupancy while 17 were disordered with partial occupancy. The temperature factors of the disordered water molecules range from 0.05 to 0.15 Å^2. 22 water molecules were found from TG analysis (n = 2). The site-occupancies of the disordered water molecules are listed in Table 9. 10 water molecules were refined anisotropically while the rest were refined isotropically. The 10 water molecules are OW1, OW2, OW3, OW4, OW5, OW6, OW8, OW11, OW12 and OW13. Water H atoms could not be located in the electron density maps.

Table 9. *Site-occupancies for disordered water molecules for complex A2.*

Atom	**OW9**	**OW10**	**OW14**	**OW15**	**OW16**	**OW18**	**OW20**	**OW21**	**OW22**
s.o.f.	0.69	0.51	0.65	0.57	0.57	0.54	0.54	0.74	0.55
U_{iso} (Å^2)	0.08	0.06	0.08	0.07	0.07	0.09	0.10	0.15	0.08
Atom	**OW23**	**OW24**	**OW25**	**OW26**	**OW27**	**OW28**	**OW29**	**OW30**	
s.o.f.	0.46	0.46	0.42	0.31	0.43	0.56	0.49	0.35	
U_{iso} (Å^2)	0.10	0.08	0.07	0.05	0.09	0.11	0.08	0.09	

Modelling of the guest

The two major peaks in the difference electron density map were assigned as chlorine atoms. This was followed by the placement of the phenyl rings which were easily identifiable from the hexagonal geometry. An AFIX 66 command was applied to the atoms of the rings allowing them to refine as rigid hexagons. The piecemeal assembly of the 1-methoxy-1-methylurea moieties followed. Refining this moiety was slow and painstaking as there were several possible scenarios owing to disorder. As it turns out, both independent guest molecules are disordered over two positions. The two major components of the disorder were assigned the same site-occupancy variable x while the two minor components refined as 1-x. The initial value of x was set to 0.5. The s.o.f.s of the major components settled to 0.50. The four models were assigned individual global isotropic temperature factors, which settled to 0.05, 0.07, 0.07 and 0.09 Å^2. Several distance restraints were applied

to the guest molecules to maintain reasonable geometries while the standard deviation used for restrained bond lengths was σ = 0.004 Å for uniformity. Only atom Cl1A was refined anisotropically. All other atoms belonging to the guests were refined isotropically. All the guest hydrogen atoms were placed in idealised positions in a riding model. U_{iso} for the aromatic hydrogens was 1.2 times that of the parent atom and all methyl hydrogens were assigned temperature factors 1.5 times the U_{iso} of the parent atom.

STRUCTURAL DESCRIPTION

Host conformation

Primary hydroxyl torsion angles

The primary hydroxyl torsion angles **ω** for both cyclodextrin molecules (A and B) comprising the dimer have *(-)-gauche* conformation, except for the disordered O6 atom O6C5. O6C5 has a *(+)-gauche* conformation with the C6-O6 bond pointing towards the cavity. The glycosidic (**Φ** and **Ψ**) and pyranoid (**Θ_1** and **Θ_2**) torsion angles compare well with those reported elsewhere. The conformations of the glucopyranose units are all $^4C_1$.

Macrocyclic symmetry

The mean radii **r** for CDs A and B are 5.04 and 5.01 Å respectively. Both have quite narrow ranges of 4.89 to 5.18 Å for A and 4.82 to 5.11 Å for B. The mean **l** values for CDs A and B are 4.38 and 4.36 Å respectively while the ranges are 4.29 - 4.47 Å for A and 4.30 - 4.41 Å for B. The mean glycosidic oxygen angle **a** for both CDs is 128.6˚ while the glycosidic angles for both CDs fall within the range 125.4 - 132.1˚.

Planarity of the O4-Heptagons

The root mean square deviation **d** for cyclodextrins A and B are 0.034 Å and 0.049 Å respectively. Cyclodextrin A has two O4 atoms with negative deviations (O4A1 and O4A5) while cyclodextrin B has four O4 atoms with negative deviations (O4B1, O4B4, O4B5 and O4B7). The torsion angles (**t**) for host A ranges from -2.9 to 2.8˚ while in the case of B it ranges from -3.6 to 5.4˚.

τ_1 and τ_2 for host A are all positive with τ_1 ranging from 0.9 to 8.4˚ while τ_2 ranges from 0.3 to 13.7˚. τ_1 and τ_2 for host B are also all positive with τ_1 ranging from 1.4 to 14.1˚ and τ_2 ranging from 2.0 to 13.3˚. The mean φ for CDs A and B is 117.8˚ and 118.0˚ respectively with both sets of values falling within the range 117.2 - 118.8˚.

Only small differences have been noted between cyclodextrins A and B. Most notable is the symmetrical shape of each cyclodextrin reflected in the narrow ranges of the radii, O4•••O4′ lengths and glycosidic oxygen angles. The pseudo-twofold symmetry of the dimer is evidenced by similarity in parameters mentioned here. Each cyclodextrin has a truncated cone-like appearance.

INTRA- AND INTERMOLECULAR INTERACTIONS

Host intramolecular interactions

16 intraglucose hydrogen bonds are observed in the structure. Fourteen are O2•••O3′ close contacts and two are C-H•••O hydrogen bonds. The O2•••O3′ distances range from 2.68 to 2.84 Å for CD A with a mean value of 2.78 Å while the range for CD B is from 2.65 to 2.81 Å and the mean is 2.75 Å. The two C6-H•••O5′ hydrogen bonds have a mean bond length of 3.40 Å (range 3.39 – 3.41 Å) and a mean hydrogen bond angle of 138.0˚ (range 137.0 – 140.0˚). The two C6-H•••O5 hydrogen bonds stabilise the hydroxyl groups with which they are associated.

Host-Host intermolecular interactions

There are 25 intermolecular interactions present which participate in the stabilisation of the hydrogen bonded dimer. There are seven O3•••O3 interactions with a range of 2.76 to 3.02 Å (mean = 2.84 Å). There are 14 interactions of the type O2•••O3. The mean hydrogen bonding distance is 3.06 Å in the range 2.91-3.17 Å. The six remaining interactions are O2•••O2 interactions with a mean distance of 3.01 Å in the range 2.87 to 3.21 Å.

INTER- AND INTRA-LAYER INTERACTIONS

Inter-layer interactions

Seven inter-layer interactions are observed in the structure. Six are of the type O6•••O6 with a mean hydrogen bond distance of 2.79 Å in the range 2.62 to 2.94 Å. A single C6-H•••O6 hydrogen bond is also observed with a bond length of 3.51 Å and a bond angle of 152.0˚.

Intra-layer interactions

There are 14 intra-layer interactions in the structure. These are divided into O6•••O6, O2•••O2 and C-H•••O. The mean interaction distance for the four O6•••O6 interactions is 2.81 Å with a range of 2.76 to 2.90 Å. The two O2•••O2 interactions have an interaction distance range of 2.75 to 2.77 Å and a mean distance of 2.76 Å. There are eight C-H•••O hydrogen bonds made up of four C1-H•••O2 and four C2-H•••O3 hydrogen bonds. The mean hydrogen bond distance and angle for the eight C-H•••O interactions is 3.33 Å and 150.0˚. The bond length and angular ranges are 3.29 - 3.40 Å and 130.0 - 170.0˚ respectively.

Host-Water interactions

30 sites were refined for 21.8 water molecules in the asymmetric unit. 60 interactions are observed between the water molecules and the host cyclodextrins. 14 water molecules are involved in O•••OW close contacts with the primary rim. The number of interactions between the primary rim and the water molecules amounts to 26. These interactions range from 2.57 to 3.15 Å with a mean distance of 2.81 Å. 13 other water molecules are involved in O•••OW close contacts with the secondary rim, having a total of 34 interactions. These interactions range from 2.62 to 3.23 Å with a mean value of 2.93 Å. Several water molecules that are involved in forming close contacts with the cyclodextrin also participate in water-water interactions. 65 water-water interactions are observed between 26 water molecules. They range from 2.44 to 3.23 Å and have a mean of 2.83 Å. Two water molecules only have water-water interactions. There are ten C-H•••OW hydrogen bonds

with a hydrogen bond distance of 3.31 Å (range 3.18 – 3.40 Å). Detailed values are listed in the appropriate appendices.

GUEST INCLUSION

Guest disorder

Two guest molecules occupy the dimer, each one being disordered over two positions. The disordered components have nearly equal site-occupancy. Both models are arranged in a tail-to-tail, anti-parallel orientation as shown in Figure 16. None of the atom locations of the guests is shared.

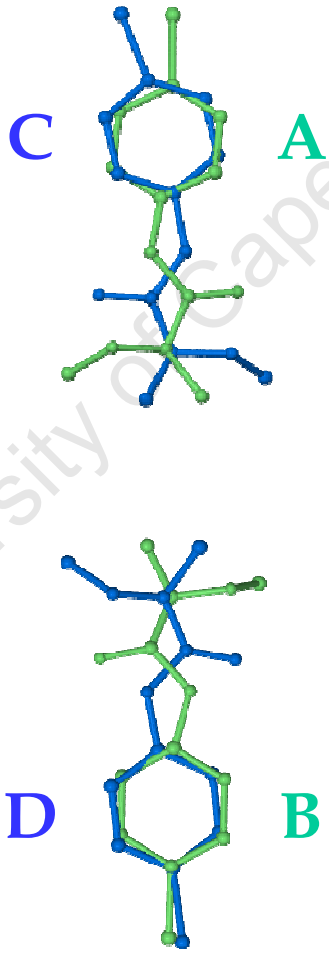

Figure 16. *Alignment of the guests in the dimeric cavity. Guests A-B (green) and C-D (blue) both have anti-parallel or tail-to-tail arrangements.*

Guests A and B (green) form one guest pair while guests C and D (blue) make up the other guest pair.

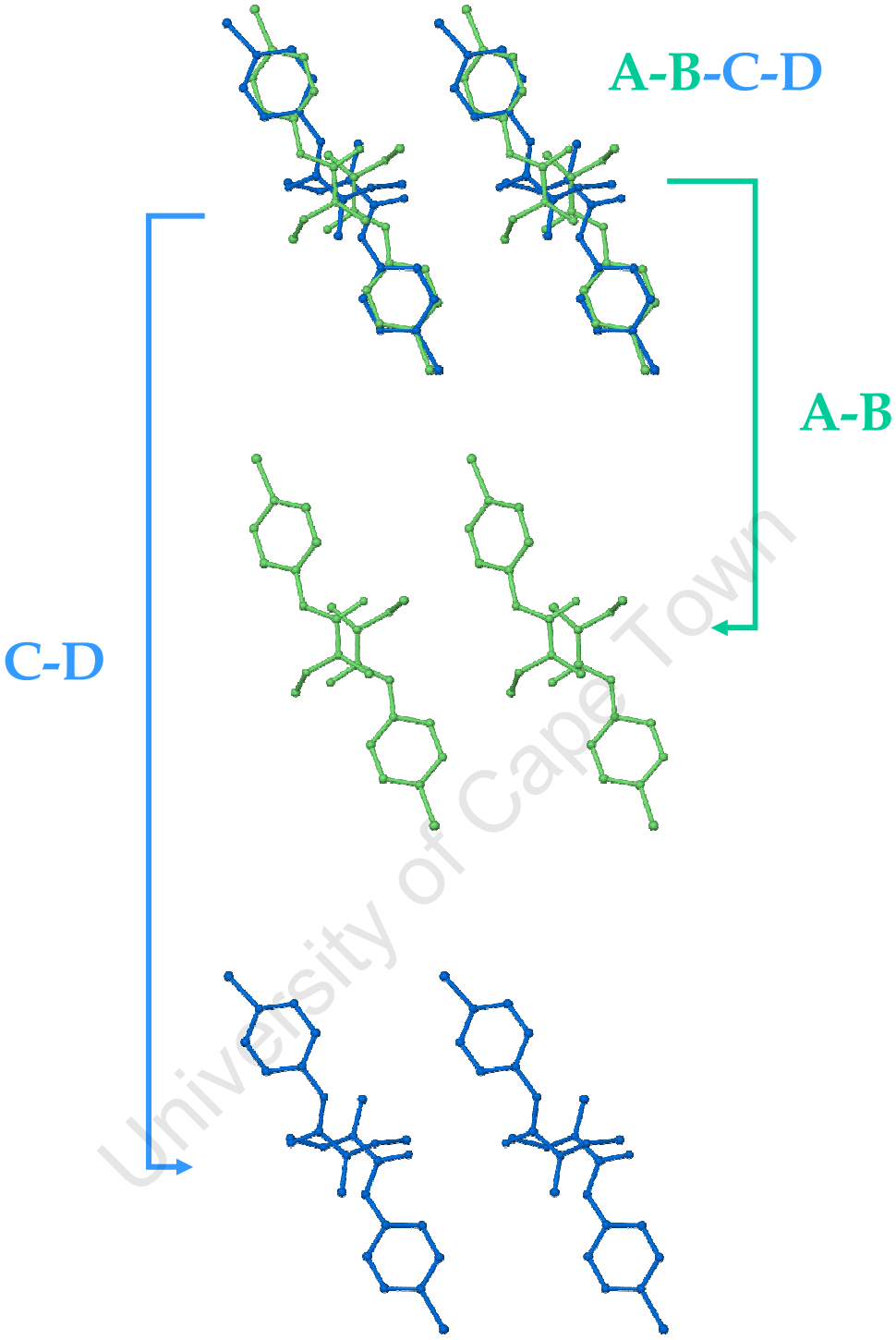

Figure 17. *Stereoview of the disordered guests A-B-C-D of A2 and the deconvoluted disordered components A-B (green) and C-D (blue).*

In the composite image shown in Figure 17, A-B-C-D represents the contents of the cavity of A2. Images A-B and C-D represent the deconvolution of the disorder.

Guest location

The dimeric complex consists of two cyclodextrin molecules containing two guest molecules, shown in Figure 18 (a). Each guest molecule is disordered over two positions inside the dimeric cavity. In order for the guests to be accommodated in the cavity they are tilted with respect to the O4-heptagon of each cyclodextrin. Thus, for guest A with host A the angle is 58.4(3)˚, guest B in host B 62.3(5)˚, guest C in host B 61.8(1)˚ and for guest D in host A 62.7(5)˚. The guests are arranged in anti-parallel manner with the chlorophenyl moiety located at the primary rim of the first CD while the urea moiety protrudes into the cavity of the second CD and is lodged at its secondary rim, as shown in the Figure 18 (b).

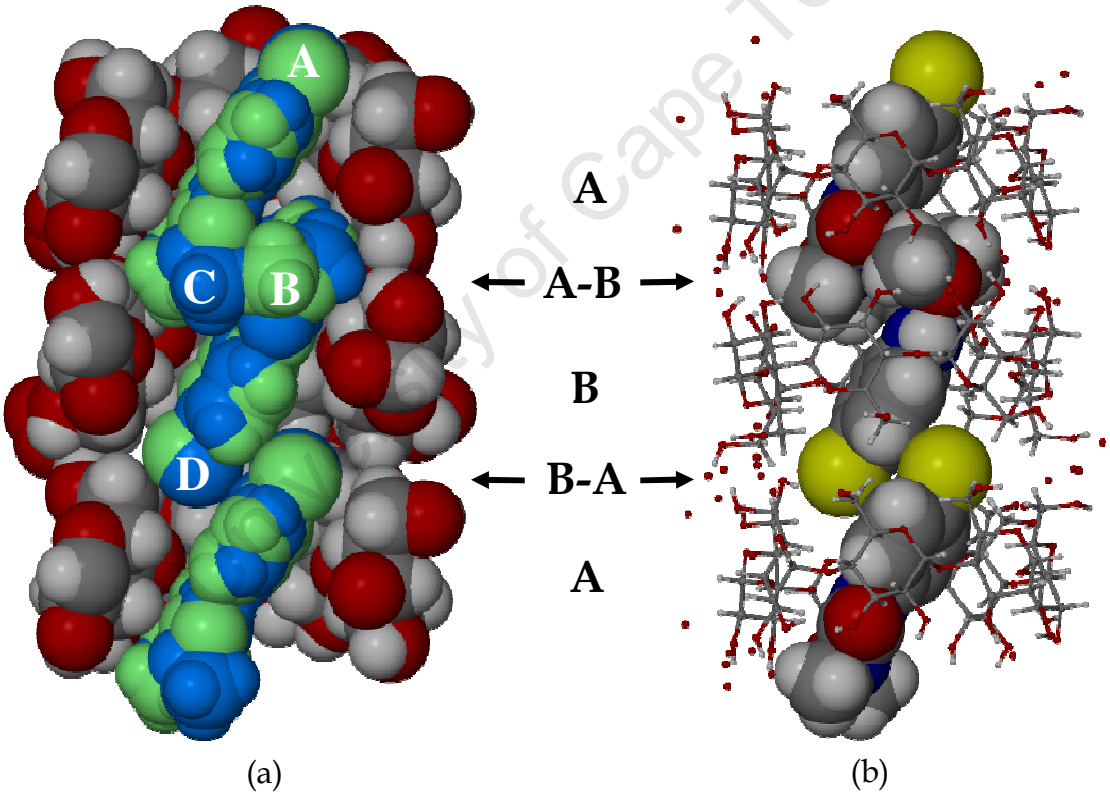

Figure 18. *Diagram (a) is a cutaway view showing the tilted guest molecules in the dimeric cavity. (b) Shows how the chlorine atoms partially include at the primary rim of an adjacent dimer and how the urea groups include into the cavity of cyclodextrins A and B at the secondary rim interface (A-B), respectively.*

Furthermore, the chlorine atom extends into the inter-dimer interface (B-A) and partially includes into the primary rim of an adjacent dimer. Two chlorine atoms therefore occupy the inter-dimer interface.

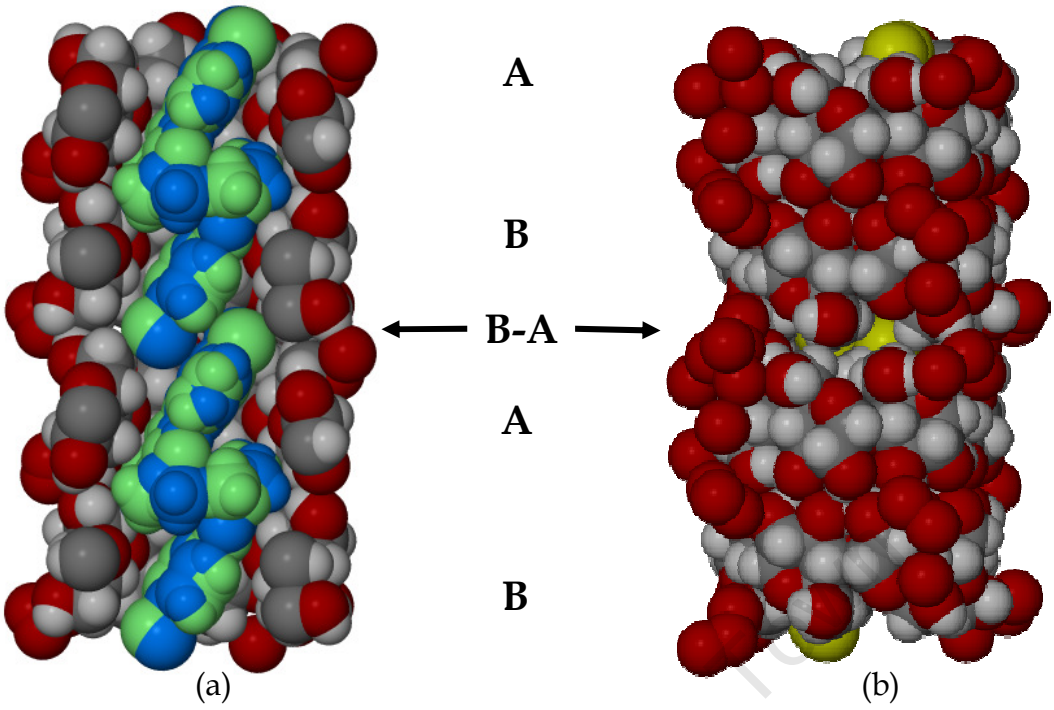

Figure 19. *(a) The disordered occupants of the continuous channel. (b) The inter-dimer interface is almost completely closed off by primary hydroxyl groups and interstitial water molecules.*

The primary hydroxyl groups of adjacent dimers and interstitial water molecules, Figure 19, close off the dimer interface. The guests are rotated away from each other. The mean planes of guests A-C and B-D are rotated by ~19˚ to each other. The interplanar angle between guests A and B is ~32˚ while C and D have an interplanar angle of ~5˚, shown in Figure 20.

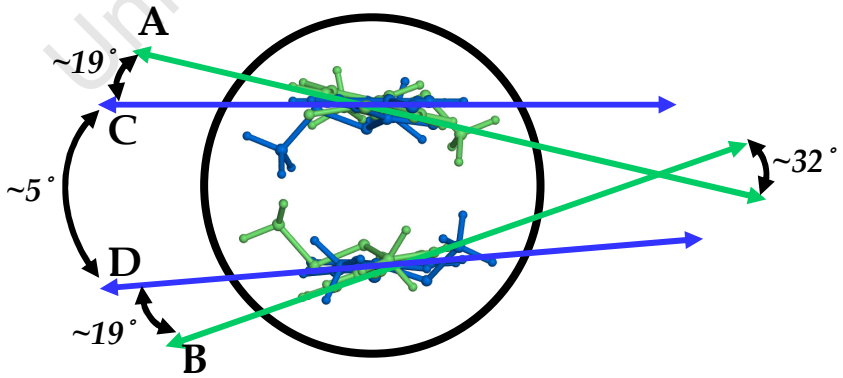

Figure 20. *The schematic diagram shows the angles of intersection between mean planes of the guest molecules.*

The close contact distances of ~3.1 Å (mean) are the result of the near parallel alignment of the guests, Figure 21.

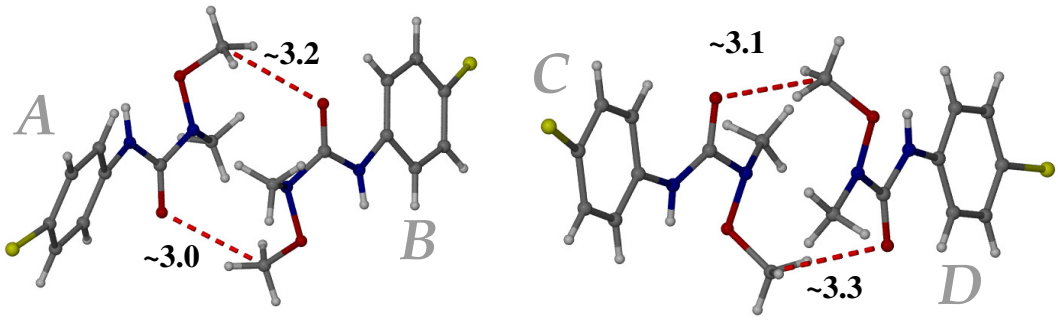

Figure 21. *The C•••O close contacts between A-B and C-D.*

Guest conformations

τ_1 for the guests of complex A2 has the greatest deviation from the torsion angles reported for the uncomplexed guest. The range is -45(3)˚ to +29(4)˚. The deviations vary in size from guest to guest and are clearly seen in the four images (a), (b), (c) and (d) presented in Figure 22. τ_2 ranges from -1(7)˚ to +20(4)˚ and has significant deviation from τ_2 for the uncomplexed guest. As with the uncomplexed guest, τ_3 is very close to -180/180˚ having a range of -177(2)˚ to +165(3)˚. This indicates an 'extended' conformation as with the uncomplexed guest.

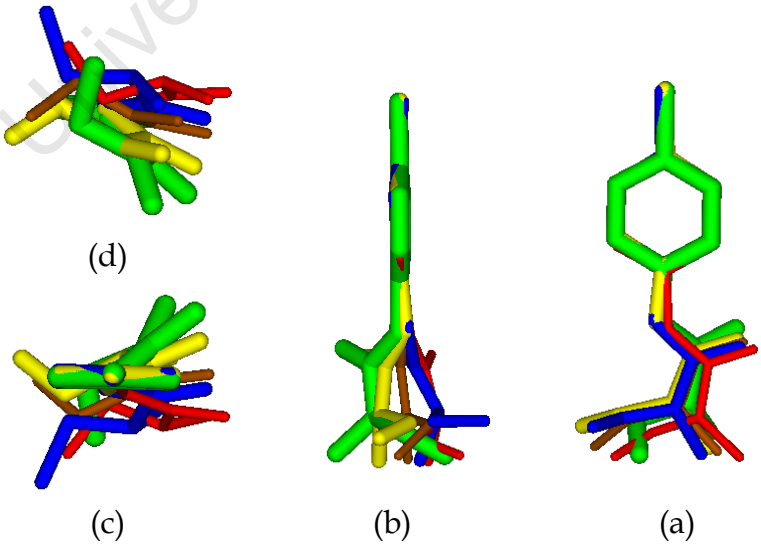

Figure 22. *The relative conformations of the included guest as compared with that of the uncomplexed guest. Guest A - yellow, guest B - blue, guest C - red, guest D - brown and uncomplexed guest - green.*

τ_4 and τ_6 have ranges of -30(1)˚ to +30(4)˚ and -43(4)˚ to +28(2)˚ respectively. τ_5 and τ_7 range from -172(1)˚ to +150(3)˚ and from -164(2)˚ to +169(2)˚, in that order. The ranges for τ_8 and τ_9 are from -123(2)˚ to +125(2)˚ and from -107(2)˚ to +109(2)˚ indicative of the C13-O12 bond being almost perpendicular to the mean plane through C9, O10, N11, O12 and C14.

HYDROGEN BONDING INTERACTIONS OF THE GUEST

Host-guest intermolecular interactions

Several intermolecular hydrogen bonds were observed in the structure. Nine are C-H•••O hydrogen bonds with a mean hydrogen bond distance of 3.38 Å ranging from 3.15 to 3.59 Å. The mean hydrogen bond angle is 147.0˚ spanning the range 124.0 to 173.0˚. There are five C-H•••Cl hydrogen bonds with a mean interaction distance of 2.90 Å and covering the range 2.77 to 3.05 Å. A number of close contacts were also observed in the structure with a mean distance of 2.82 Å in the range 3.10 - 3.58 Å. The C-H•••O interactions are shown in Figure 23.

Guest-guest intermolecular interactions

There are four intermolecular close contacts and two C-H•••O hydrogen bonds involving the guests. The mean distance is 3.30 Å in the range 3.08 to 3.57 Å. The two C-H•••O hydrogen bonds have a mean bond length of 3.12 Å (range 3.03 - 3.21 Å) and mean bond angle of 120.0° (range 113.0 - 127.0°).

Guest intramolecular interactions

There are eight intramolecular hydrogen bonds present; four are C-H•••O type while the remaining four are N-H•••O type. The C-H•••O type interactions range from 2.74 - 3.08 Å with a mean of 2.91 Å while the C-H•••O hydrogen bonding angle ranges from 100.0 to 122.0˚. The mean value is 110.0˚. These interactions are shown as green bonds in Figure 23 (bottom image). The range of distances for N-H•••O interactions is from 2.53 to 2.66 Å with a mean distance of 2.58 Å. The bond angle range is 105.0 - 109.0˚ and its mean is 107.0˚.

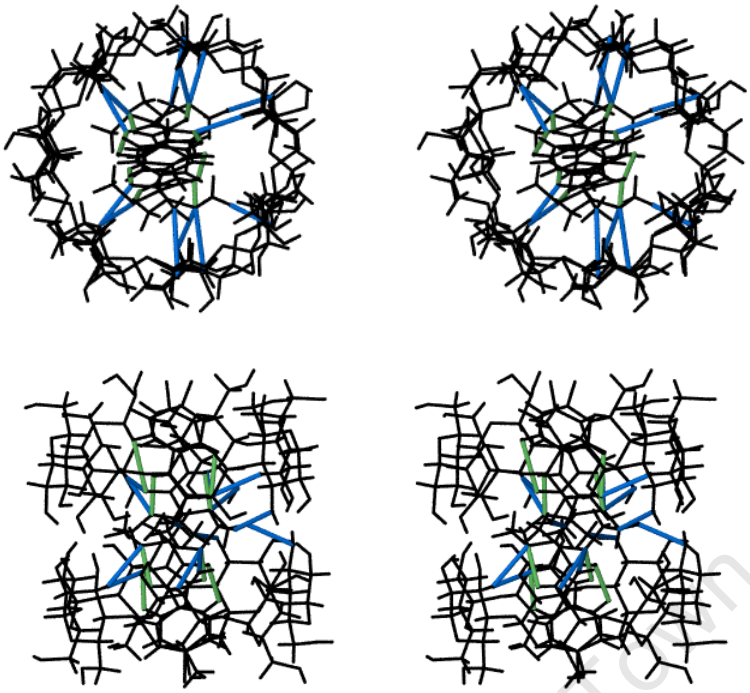

Figure 23. *(top) The stereogram shows the intermolecular hydrogen bonds (blue) between the host and guest in the cavity. (bottom) The diagram shows the intramolecular hydrogen bonds (green) in the guest molecule.*

CRYSTAL PACKING

A2 packs in the channel packing arrangement, **CH** (P1). The channel packing axis is parallel to the *c*-axis and extends infinitely, as shown in Figure 24. The O4 mean planes are inclined to the *ab*-plane by ~10˚. The layers propagate along the *c*-axis. When viewed perpendicularly to the O4 heptagons it becomes apparent that the O4-heptagons of adjacent dimers are laterally displaced (Figure 25). The size of the displacement is ~2.6 Å. The mean O4 planes of the dimer are inclined at 1.90(1)˚ to each other. The inter-dimer distance which is measured across the inter-dimer interface is ~8.7 Å.

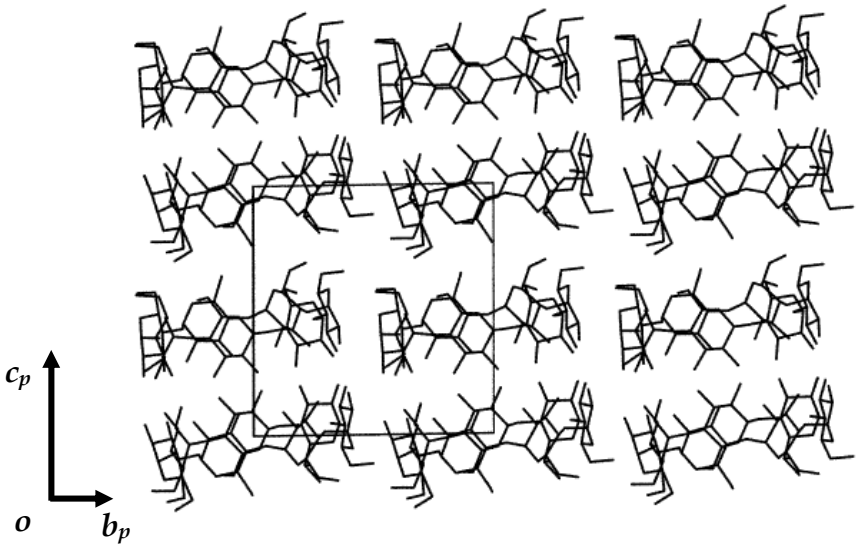

Figure 24. *Packing diagram of the A2 structure viewed along the a-axis. Only the host molecules are shown.*

The dimers are stacked on top of each other forming columns along *c* with all the columns having the same orientation (Figure 24). The orientation of the included guest is the same for all the columns in the structure.

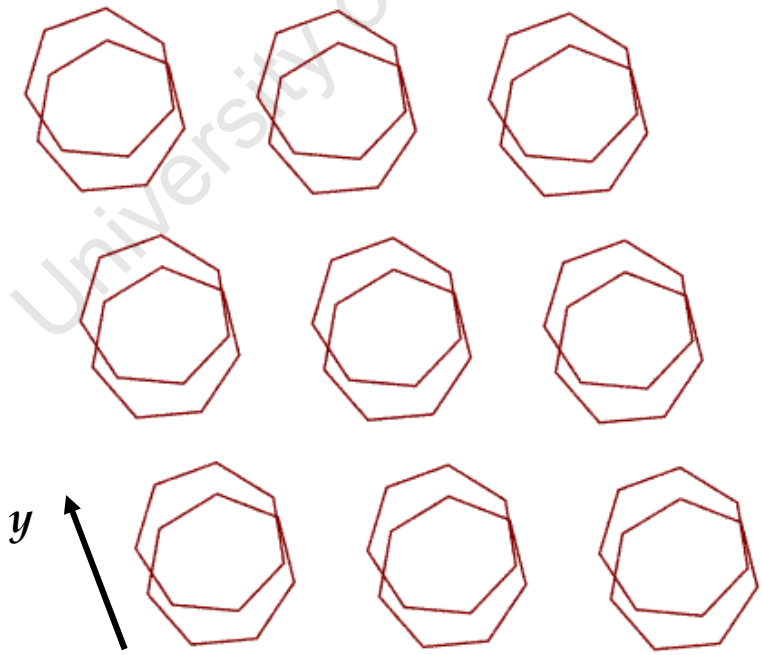

Figure 25. *The lateral displacement between dimers in adjacent layers.*

The layers and the columns are held together by a series of inter and intra-layer hydrogen bonds shown here in Figure 26.

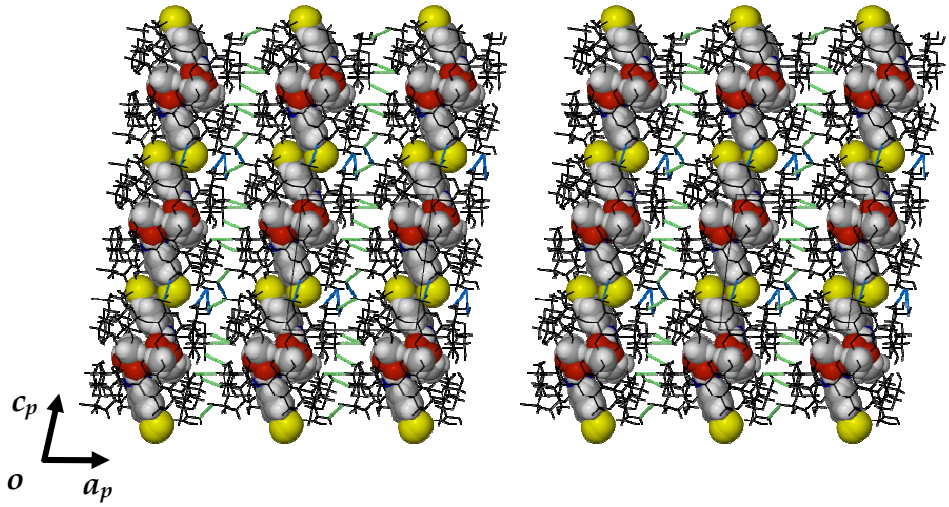

Figure 26. *The inter- and intra-layer hydrogen bonds (green and blue bonds respectively) which link the columns together viewed along b.*

Comparative PXRD

Calculated and experimental traces for A2 are shown in Figure 27. There is a slight shift in the peak positions to lower 2θ˚ for the experimental trace. This is a result of the different conditions under which the data were collected. Data for the experimental trace were collected at ambient temperature while data for the calculated trace were collected at 113 K. The level of agreement between the two traces is still very good.

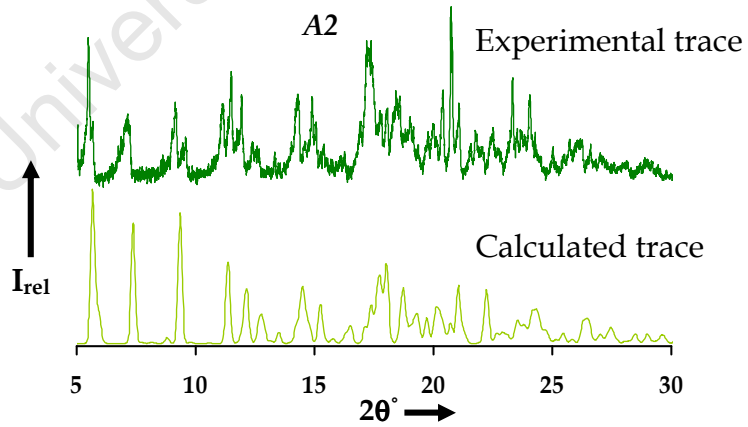

Figure 27. *Calculated and experimental PXRD traces for A2.*

The match between the calculated and experimental PXRD patterns confirms the single crystal as being representative of the bulk material. However, the extra peaks present in the experimental trace are evidence of uncomplexed guest which has crystallised and contaminates the sample.

X-RAY STRUCTURE OF A3

Space group determination

The program LAYER was employed to determine the crystal system and space group of A3.[1] The crystal system was found to be triclinic as the Laue symmetry was $\bar{1}$ and the space group P1 since the cyclodextrin is chiral. Confirmation of the crystal system and space group was obtained with XPREP.[2] A3 crystallises in the triclinic space group P1 with $Z = 1$ dimeric complex unit per unit cell.

Structure solution and refinement

Table 9 contains refinement parameters and crystal data for A3. The asymmetric unit consists of a single dimeric β-CD complex made up of two crystallographically independent cyclodextrins which are hydrogen bonded in a head-to-head manner. Each cyclodextrin molecule contains a single guest molecule, the guest being monuron. The structure was found to be isostructural with an existing complex [(β-CD)$_2$•(*p*-bromoacetanilide)$_2$•27(H_2O)] (Refcode: XADHIT) (and therefore also with complex A2 described above) whose unit cell parameters are very similar to those of A3. Only the host coordinates of XADHIT were used as input fragment to solve the phase problem.[19] All guest, water molecules and O6 atoms were deleted from the trial structure in order to model any disorder which might be present. The glucopyranose units for the two host molecules in the asymmetric unit were labelled A1-A7 and B1-B7. The structure was refined with SHELXH-97 with successive difference Fourier maps revealing the O6 atoms.[5] Atoms O3A6, C6B7 and O6B7 of the host were found to be disordered over two positions. The major components of the disordered atoms were assigned a value of x for their s.o.f.s while the minor components (O3C6, C6C7 and O6C7) were assigned the value 1-x. An initial value of x = 0.5 was set. It refined to 0.58 for B7 and 0.75 for A6 (for the major component of the disorder). All hydrogen atoms attached to carbon atoms were placed and refined in geometrically calculated positions using the AFIX 43

instruction (riding model). The hydrogen atoms of the hydroxyl groups were placed using the AFIX 83 instruction (hydrogen bond searching model).

Table 9. *Crystal data and data-collection parameters for A3.*

parameters	*A3*
Formula unit	$(C_{42}H_{70}O_{35})_2 \bullet (C_9H_{11}N_2OCl)_2 \bullet 19(H_2O)$
Mr	2984.77
Crystal system	triclinic
Space group	P1
a/Ä	15.2175(1)
b/ Å	15.4354(1)
c/ Å	15.6763(1)
α/°	87.199(1)
β/°	97.571(1)
γ/°	103.479(1)
Vol. Å^3	3548.91(4)
Z	1
ρ_{calc} g cm^{-3}	1.397
μ (MoKα) mm^{-1}	0.159
F(000)	1590
Crystal size mm^3	0.15 x 0.12 x 0.10
Temperature K	113 ± 2
Range scanned θ/°	2.95 ≤ θ ≤ 25.05
Index range	-18, 18; -18, 18; -18, 18
ϕ Scan angle °	1.5
ϕ Scan range °, no of frames	363.0, 242
ω Scan angle °	1.5
ω Scan range °, no of frames	112.5, 75; 106.5, 71; 45.0, 30; 45.0, 30;45.0, 30; 45.0, 30; 108.0, 72; 106.5,71; 45.0, 30
Dx mm	33
No. of reflections	112566
No. of unique reflections	24679
No. of reflections with I>2σ(I)	20919
No. of l.s. parameters	1605
R_{int}, R_σ	0.0806, 0.0634
S	1.025
R_1 [$F_o > 4\sigma(F_o)$]	0.0683
wR_2	0.1975
No. of reflections omitted	88
Weighting scheme parameters	a = 0.13, b = 2.9726
(Δ/σ)	< 0.001
Δρ excursions eÅ^{-3}	-0.678, 0.860

All hydrogen atoms were assigned isotropic temperature factors which were 1.2 times those of the parent atoms. 34 sites for water molecules were located in a series of difference electron-density maps accounting for 20 water molecules. 10 water molecules had full site-occupancy while 24 were disordered with partial occupancy. The temperature factors of the disordered water molecules range from 0.04 to 0.09 Å^2. 19 water molecules were found from TG analysis (n = 2). 25 water molecules were refined isotropically while the rest were refined anisotropically. Water H atoms could not be located in the electron density maps.

Modelling of the guest

The two major peaks in the difference electron density map were assigned as chlorine atoms. This was followed by the placement of the phenyl rings which were easily identifiable from their hexagonal geometry. An AFIX 66 command was applied to the atoms of the rings allowing them to refine as rigid hexagons. This was followed by the piecemeal assembly of the N,N-dimethylurea moieties. Refining the N,N-dimethylurea moiety was slow and painstaking as there were several possible scenarios owing to disorder. Each guest was disordered over two positions with major components A and B while the minor components are C and D. However, it was only possible to model the disorder of B (*i.e.* minor component C) as attempted modelling of the disordered component D proved unstable. The two major components of the disorder were assigned the same site-occupancy variable x while the two minor components refined as 1-x. The initial value of x was set to 0.5. The s.o.f.s of the major components settled to 0.80. The result of this modelling is that the guest content per β-CD dimer is 1.8 molecules, as opposed to the value of 2 suggested by the experimental analytical data. The three models were assigned individual global isotropic temperature factors, which settled between 0.04 and 0.05 Å^2. Several distance restraints were applied to the guest molecules to maintain reasonable geometries while the standard deviation used for restrained bond lengths was σ = 0.008 Å for uniformity.

Only atoms Cl1A and Cl1B were refined anisotropically. All other atoms belonging to the guests were refined isotropically, all the guest hydrogen atoms being placed in idealised positions in a riding model. U_{iso} for the aromatic hydrogens was 1.2 times that of the parent atom and all methyl hydrogens were assigned thermal parameters equal to 1.5 times the U_{iso} of the parent atom.

STRUCTURAL DESCRIPTION

Host conformation

Primary hydroxyl torsion angles

The primary hydroxyl torsion angles **ω** for both cyclodextrin molecules (A and B) comprising the dimer have *(-)-gauche* conformation, except for the disordered O6 atom O6C7. O6C7 has a *(+)-gauche* conformation with the C6-O6 bond pointing towards the cavity. Once again the glycosidic and pyranoid torsion angles compare well with those reported elsewhere. The conformations of the glucopyranose units are all $^4C_1$.

Macrocyclic symmetry

The mean radii **r** for CDs A and B are 5.02 and 5.03 Å respectively. Both have quite narrow ranges of 4.96 to 5.06 Å for A and 4.88 to 5.21 Å for B. The mean **l** values for CDs A and B are 4.36 and 4.37 Å respectively while the ranges are 4.30 - 4.42 Å for A and 4.26 - 4.50 Å for B. The mean glycosidic oxygen angle **a** for both CDs is 128.5˚ while the glycosidic angles for both CDs fall within the range 124.5 - 132.7˚.

Planarity of the O4-Heptagons

The root mean square deviation **d** for cyclodextrins A and B are 0.045 Å and 0.039 Å respectively. There are four O4 atoms with negative deviations from the mean plane of CD A; these are O4A2, O4A3, O4A5 and O4A6 while CD B has two atoms with negative deviations from the mean O4 plane, namely O4B3 and O4B7. The torsion angles (**t**) for host A ranges from -3.3 to 5.0˚ while in the case of B it ranges from -4.3 to 3.8˚. τ_1 and τ_2 for host A are all

positive with τ_1 ranging from 1.1 to 7.3˚ while τ_2 ranges from 1.2 to 12.3˚. τ_1 and τ_2 for host B are also all positive with τ_1 ranging from 1.3 to 6.9˚ and τ_2 ranging from 1.3 to 13.4˚. The mean φ for CDs A and B is 117.8˚ and 117.9˚ respectively with both sets of values falling within the range 116.7 - 119.1˚.

Both cyclodextrins are symmetrical in shape which is reflected in narrow ranges of the radii, O4•••O4 lengths and glycosidic oxygen angles. Each cyclodextrin has a truncated cone-like appearance.

INTRA- AND INTERMOLECULAR INTERACTIONS

Host intramolecular interactions

17 intraglucose hydrogen bonds are observed in the structure. Fourteen are O2•••O3′ close contacts and two are C-H•••O′ hydrogen bonds. The O2•••O3′ distances range from 2.72 to 2.82 Å for CD A with a mean value of 2.75 Å while the range for CD B is from 2.69 to 2.84 Å and the mean is 2.78 Å. The two C6-H•••O5′ hydrogen bonds have a mean bond length of 3.41 Å (range 3.40 – 3.42 Å) and a mean hydrogen bond angle of 140.0˚ (range 140.0 – 141.0˚). The three C6-H•••O5′ hydrogen bonds are similar to those found in complex A2 and therefore act in the same manner, stabilising the hydroxyl groups with which they are associated.

Host-Host intermolecular interactions

There are 25 intermolecular interactions present which participate in the stabilisation of the hydrogen bonded dimer. There are seven O3•••O3 interactions with a range of 2.75 to 2.93 Å (mean = 2.81 Å). There are 13 interactions of the type O2•••O3. The mean hydrogen bonding distance is 3.04 Å in the range 2.92 - 3.19 Å. The seven remaining interactions are O2•••O2 interactions with a mean distance of 3.01 Å in the range 2.85 to 3.15 Å.

INTER- AND INTRA-LAYER INTERACTIONS

Inter-layer interactions

Four inter-layer interactions are observed in the structure. All four are of the type O6•••O6 with a mean hydrogen bond distance of 2.89 Å in the range 2.57 to 3.30 Å.

Intra-layer interactions

There are 14 intra-layer interactions in the structure. These are divided into O6•••O6, O2•••O2, and C-H•••O. The mean distance for the four O6•••O6 interactions is 2.82 Å with a range of 2.74 to 2.94 Å. The two O2•••O2 interactions have an interaction distance range of 2.74 to 2.78 Å and a mean distance of 2.76 Å. There are seven C-H•••O hydrogen bonds made up of four C1-H•••O2 and three C2-H•••O3 hydrogen bonds. The mean hydrogen bond distance and angle for the eight C-H•••O interactions is 3.33 Å and 147.0˚. The bond length and angular ranges are 3.30 - 3.41 Å and 142.0 - 159.0˚ respectively.

Host-Water interactions

Fifty-two interactions are observed between the water molecules and the host cyclodextrins. 13 water molecules are involved in O•••OW close contacts with the primary rim. The number of interactions between the primary rim and the water molecules amounts to 28. These interactions range from 2.48 to 3.21 Å with a mean distance of 2.85 Å. Eleven other water molecules are involved in O•••OW close contacts with the secondary rim, having a total of 24 interactions. These interactions range from 2.63 to 3.22 Å with a mean value of 2.92 Å. Several water molecules that are involved in forming close contacts with the cyclodextrin also participate in water-water interactions. 74 water-water interactions are observed between 34 water molecules. They range from 2.39 to 3.18 Å and have a mean of 2.78 Å. Two water molecules only have water-water interactions. There are nine C-H•••OW hydrogen bonds with a hydrogen bond distance of 3.22 Å (range 3.15 – 3.41 Å).

GUEST INCLUSION

Guest disorder

Two guest molecules occupy the head-to head hydrogen bonded dimer, each being disordered over two positions. The major components of the disorder, guests A and B have an anti-parallel arrangement, Figure 28. Only one of the minor components of disorder could be modelled successfully (guest C). The other model was unstable during refinement owing to its very low site-occupancy (<0.3). None of the atom locations belonging to the guests are shared.

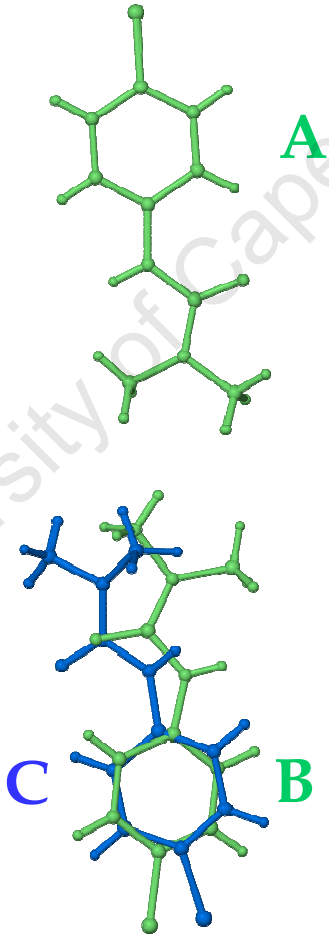

Figure 28. *Alignment of the guests in the dimer cavity. Guests A and B (green) have an anti-parallel or tail-to-tail arrangement.*

Guests A and B (green) form one guest pair while guest C (blue) is the other guest.

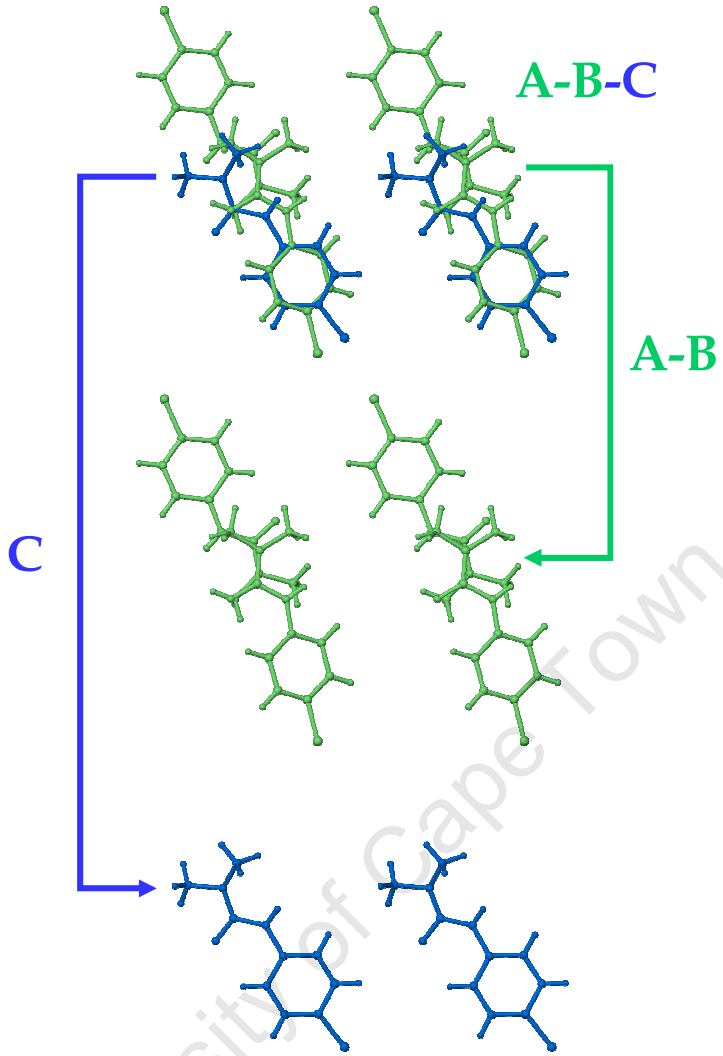

Figure 29. *Stereoview of the disordered guests A-B-C of **A3** and the deconvoluted disordered components A-B (green) and C (blue).*

In the composite image shown in Figure 29, A-B-C represents the contents of the cavity of A3. Images A-B and C represent the deconvolution of the disorder.

Guest location

The dimeric complex consists of two cyclodextrin molecules containing two guest molecules and a water molecule with partial occupancy, shown in Figure 30. Guest B is disordered over two positions while the disorder of guest A could not be modelled in the dimeric cavity. In order for the guests

to be accommodated in the cavity they are tilted with respect to the O4-heptagon of each cyclodextrin.

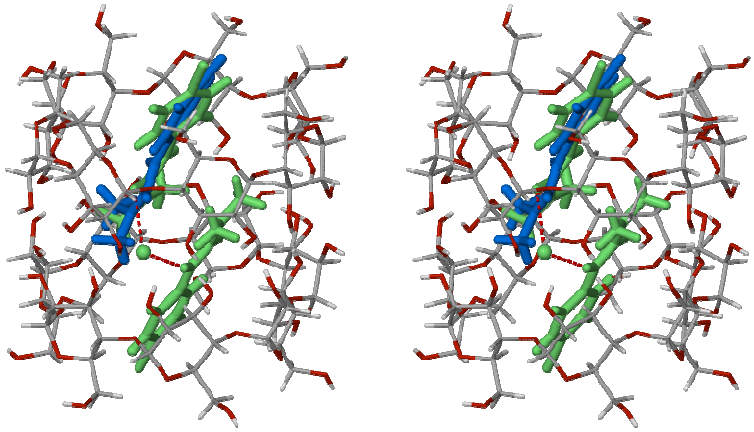

Figure 30. *The stereo view shows the guest•••OW•••guest interactions which occur in the dimer cavity. The guests and water molecules are colour-coded according to their site-occupancy.*

Thus, for guest A with host A the angle is 64.0(2)˚, guest B in host B 62.8(2)˚ and guest C in host B 64.0(1)˚. As with complex A2, the guests are arranged in anti-parallel manner with the chlorophenyl moiety located at the primary rim of the first CD molecule while the urea moiety protrudes into the cavity of the second CD molecule and is lodged at its secondary rim, as shown in Figure 31.

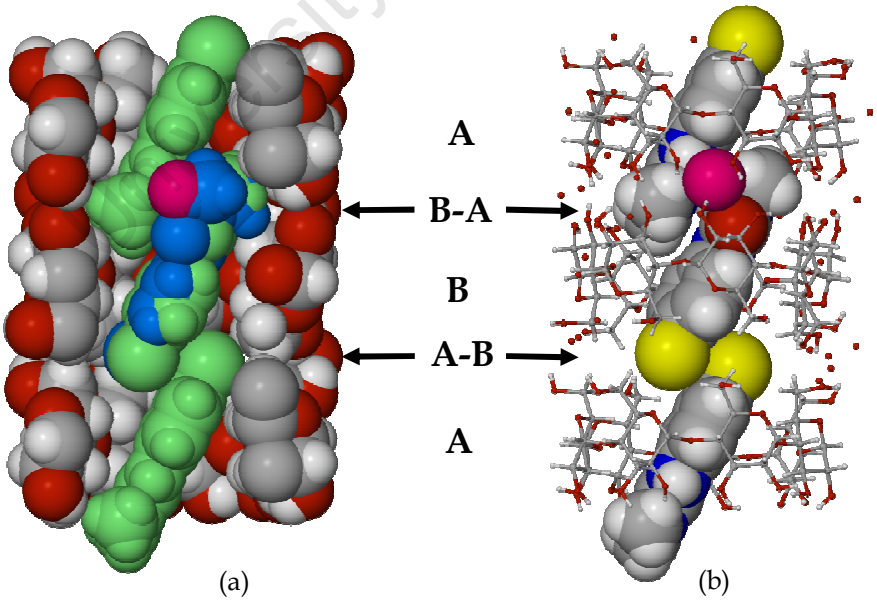

Figure 31. *(a) The tilted guest molecules in the dimer cavity. (b) Partial inclusion of the chlorine atoms at the primary rim of an adjacent dimer (A-B) and inclusion of the urea into the cavity of cyclodextrins A and B at the secondary rim interface (B-A), respectively. Guest disorder has been omitted in (b) for clarity.*

Furthermore, the chlorine atom extends into the inter-dimer interface (B-A) and partially includes into the primary rim of an adjacent dimer. Two chlorine atoms occupy the inter-dimer interface. The primary hydroxyl groups of adjacent dimers and interstitial water molecules, Figure 32, close off the dimer interface.

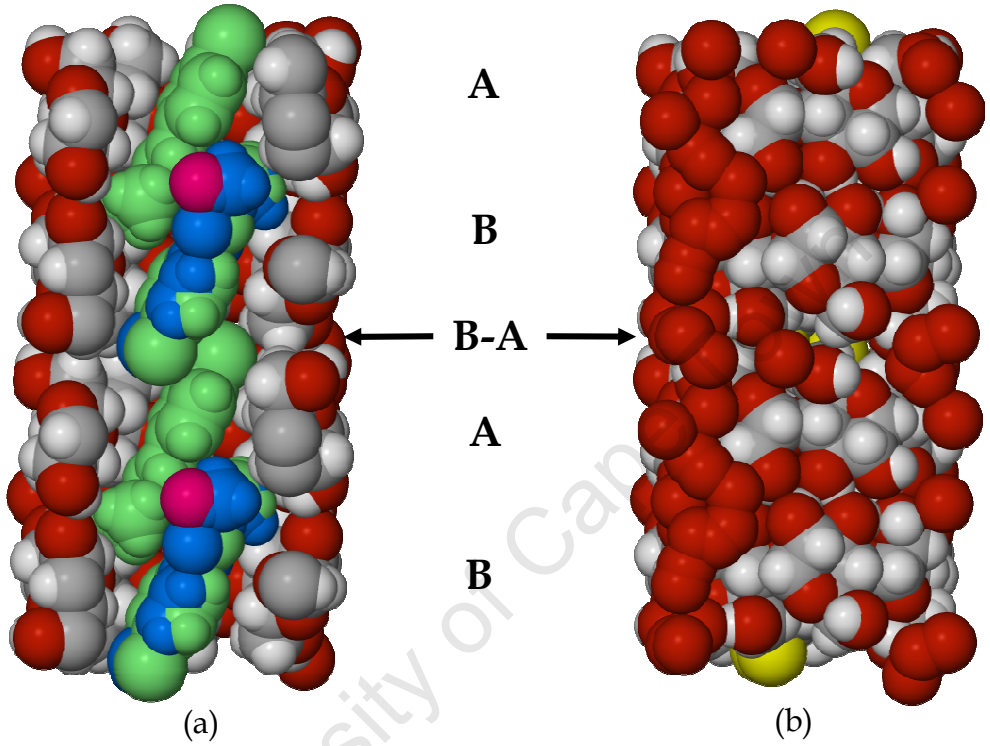

Figure 32. *(a) The water molecule (pink) is located in the dimer cavity at the secondary rim interface. (b) The inter-dimer interface is almost completely closed off by primary hydroxyl groups and interstitial water molecules.*

The guests of complex A3 are rotated away from each other so as to avoid unusually short contact distances. The mean planes of guests A and B are rotated by ~15˚ to each other while those of guests A and C are rotated by ~9˚. The interplanar angle between guests B and C is ~23˚, shown in Figure 33.

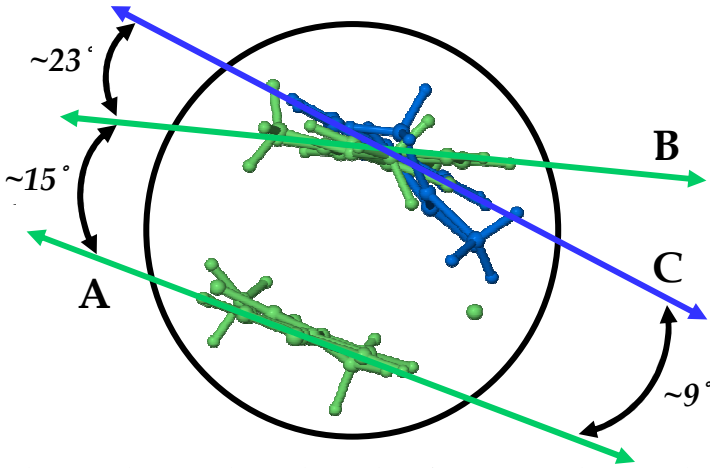

Figure 33. *The schematic diagram shows the angles of intersection between the mean planes of the guest molecules.*

The presence of a single water molecule located between guests A and B contributes to the large angle between them. Guest A makes a close O•••OW contact with the water molecule (OW11, 2.82 Å) via the carbonyl oxygen, while guest B is involved in a N-H•••OW hydrogen bond (3.05 Å, 141.0˚) via the secondary amine hydrogen, as shown in Figure 34. There is also a C-H•••OW hydrogen bond (3.21 Å, 142.0˚) which further stabilises the interactions.

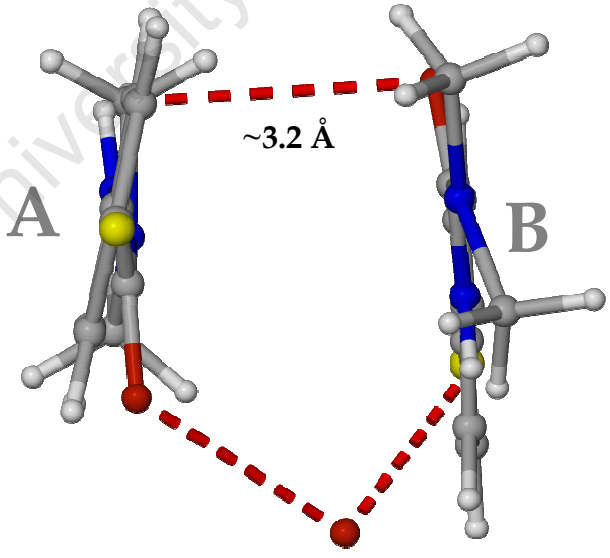

Figure 34. *The diagram shows the hydrogen bonding interactions between the water molecule and guests A and B as well as the C•••O close contact between A and B.*

The close contact distance of ~3.2 Å is a result of accommodating the water molecule between the carbonyl and amide moieties, Figure 34. Furthermore,

the N-H•••OW and O•••OW interactions must contribute to the overall stabilisation of the amido residues inside the cavity. Similar interactions have been observed in the complexes β-CD-*p*-nitroacetanilide and β-CD-*p*-bromoacetanilide where the acetylamino residues are stabilised by N-H•••OW interactions.[19,20]

Guest conformations

τ_1 for the guests of complex A3 has the greatest deviation from the torsion angles reported for the uncomplexed guest. The range is -175(7)˚ to -23(4)˚. The deviations vary in size from guest to guest and are clearly seen in the four images (a), (b), (c) and (d) presented in Figure 35. τ_2 ranges from 3(1)˚ to +11(1)˚ and has significant deviation from τ_2 for the uncomplexed guest. As with the uncomplexed guest, τ_3 is very close to -180/180˚ having a range of -180(1)˚ to +173(1)˚. This indicates an 'extended' conformation as with the uncomplexed guest.

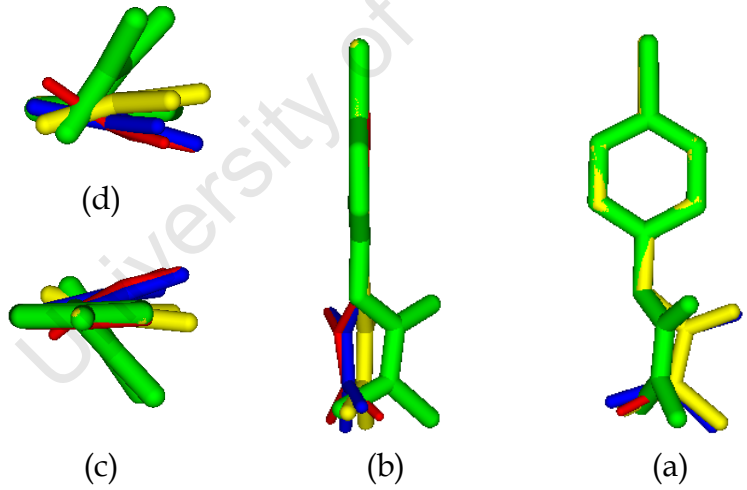

Figure 35. *Relative conformations of the included guest as compared with that of the uncomplexed guest. Guest A - yellow, guest B - blue, guest C - red and uncomplexed guest - green.*

τ_4 and τ_6 have ranges of -172(1)˚ to +14(1)˚ and -168(7)˚ to +13(9)˚ respectively. τ_5 and τ_7 range from -10(1)˚ to +178(6)˚ and from -175(6)˚ to +151(1)˚, in that order.

HYDROGEN BONDING INTERACTIONS OF THE GUEST

Host-Guest intermolecular interactions

Several intermolecular hydrogen bonds were observed in the structure. Three are C-H•••O hydrogen bonds with a mean hydrogen bond distance of 3.47 Å ranging from 3.40 to 3.57 Å. The mean hydrogen bond angle is 154.0˚ spanning the range 143.0 to 168.0˚. The C-H•••O hydrogen bonds are illustrated in Figure 36 (top image). There are two C-H•••Cl′ interactions with a mean distance of 2.93 Å and covering the range 2.90 to 2.97 Å. There are two Cl•••C close contacts with a mean interaction distance of 3.54 Å (range 3.52 – 3.57 Å).

Guest-guest intermolecular interactions

There are three intermolecular close contacts involving the guests. The mean interaction distance is 3.37 Å in the range 3.20 to 3.48 Å; see Figure 36 (top image).

Guest intramolecular interactions

There are six intramolecular hydrogen bonds present; three are C-H•••O hydrogen bonds while the remaining three are C•••O close contacts. The C-H•••O type interactions range from 2.78 - 2.85 Å with a mean of 2.82 Å while the C-H•••O hydrogen bonding angle ranges from 116.0 to 121.0˚ (mean = 118.0˚). The three C•••O close contacts have mean contact distance of 2.66 Å. These interactions are shown as green bonds in Figure 36 (bottom image). The intramolecular C-H•••O hydrogen bonds for the uncomplexed guest have a length of 3.26 Å and the angle is 133.0˚. The C•••O close contact has a mean distance of 2.72 Å in the uncomplexed guest.

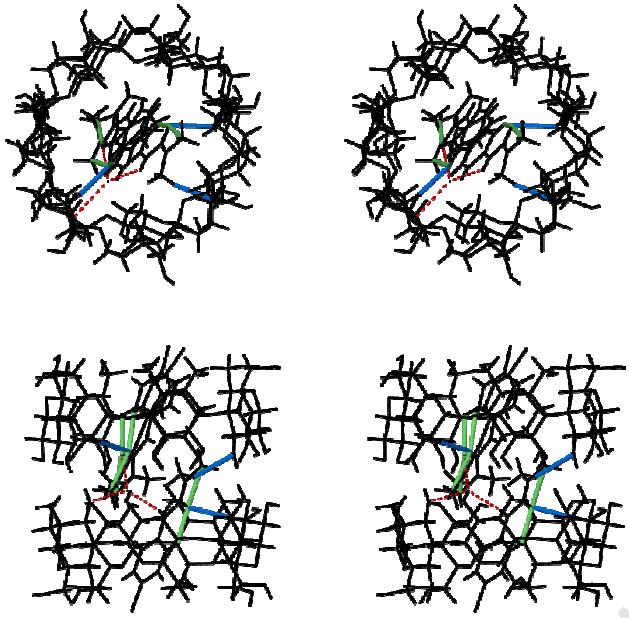

Figure 36. *(top) The stereogram shows the intermolecular hydrogen bond interactions (blue) between the host and guest in the cavity. The diagram also shows the hydrogen bonding interactions between the guests, the water molecule and the host molecule (red dashed line). (bottom) The diagram shows the intramolecular hydrogen bonds (green) in the guest molecule.*

CRYSTAL PACKING

A3 packs in the same packing arrangement as A2, **CH** (P1), with the channel axis parallel to *c* and the O4 mean planes inclined by ~10˚ to the *ab*-plane, as shown in Figure 37.

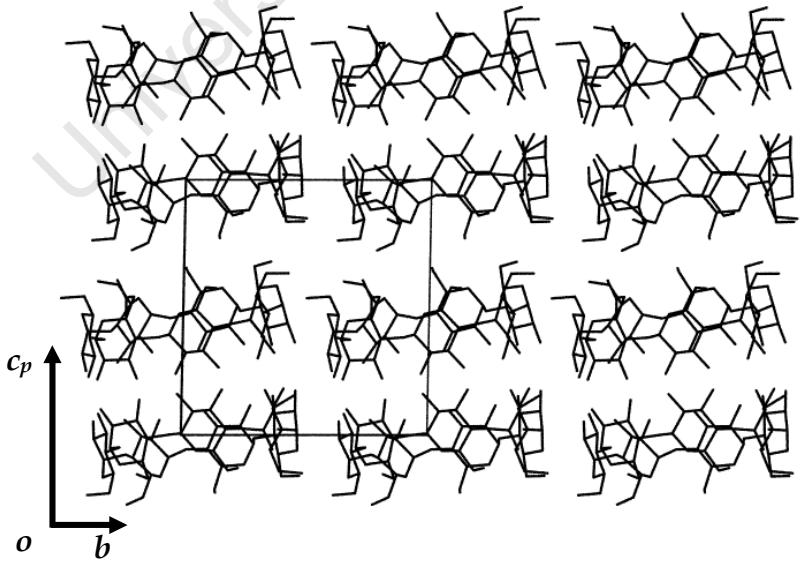

Figure 37. *Packing diagram of the A3 structure viewed along the a-axis. Guest molecules have been omitted.*

As with A2 the O4 heptagons of adjacent dimers are laterally displaced by ~2.5 Å, Figure 38. The angle of inclination between the mean O4 planes of the dimer is 1.06(1)˚ with an inter-dimer distance of ~8.7 Å.

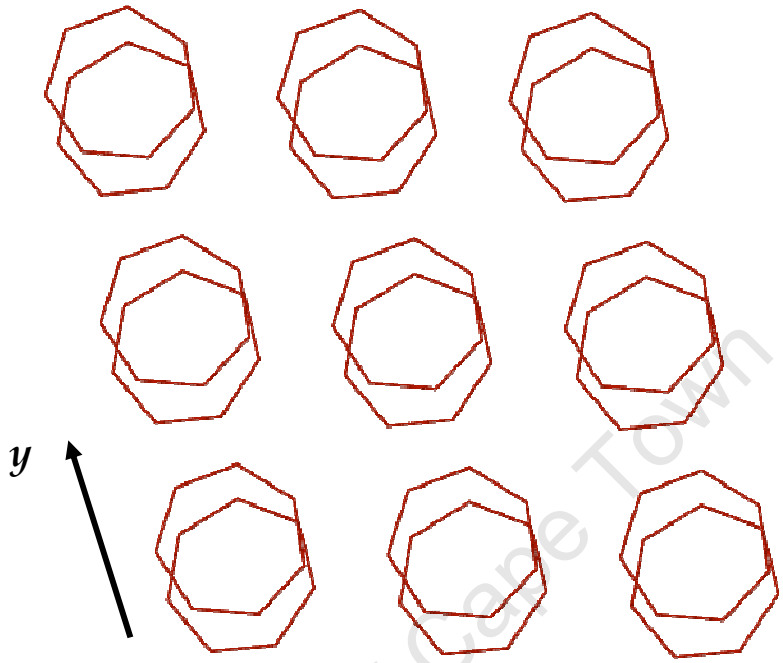

Figure 38. *The diagram shows the lateral displacement between dimers in adjacent layers.*

The orientation of the dimer and the included guest is the same throughout the structure while the columns are aligned along *c*, Figure 39.

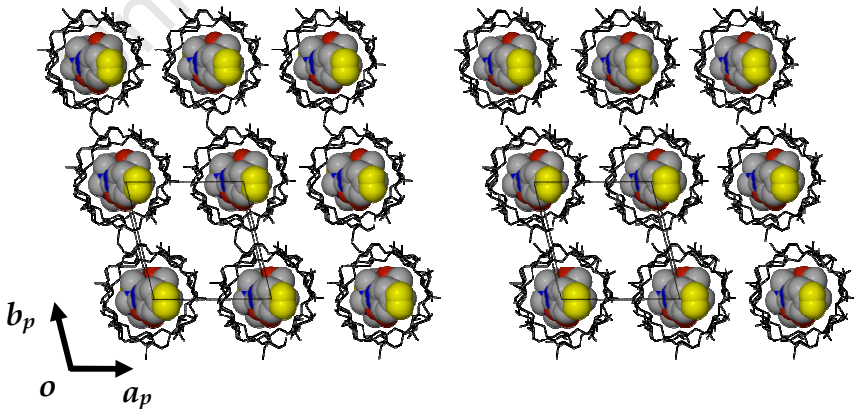

Figure 39. *The stereodiagram highlights the common orientations of the guest molecules.*

The layers and columns are held together by a series of inter and intra-layer hydrogen bonds shown here in Figure 40.

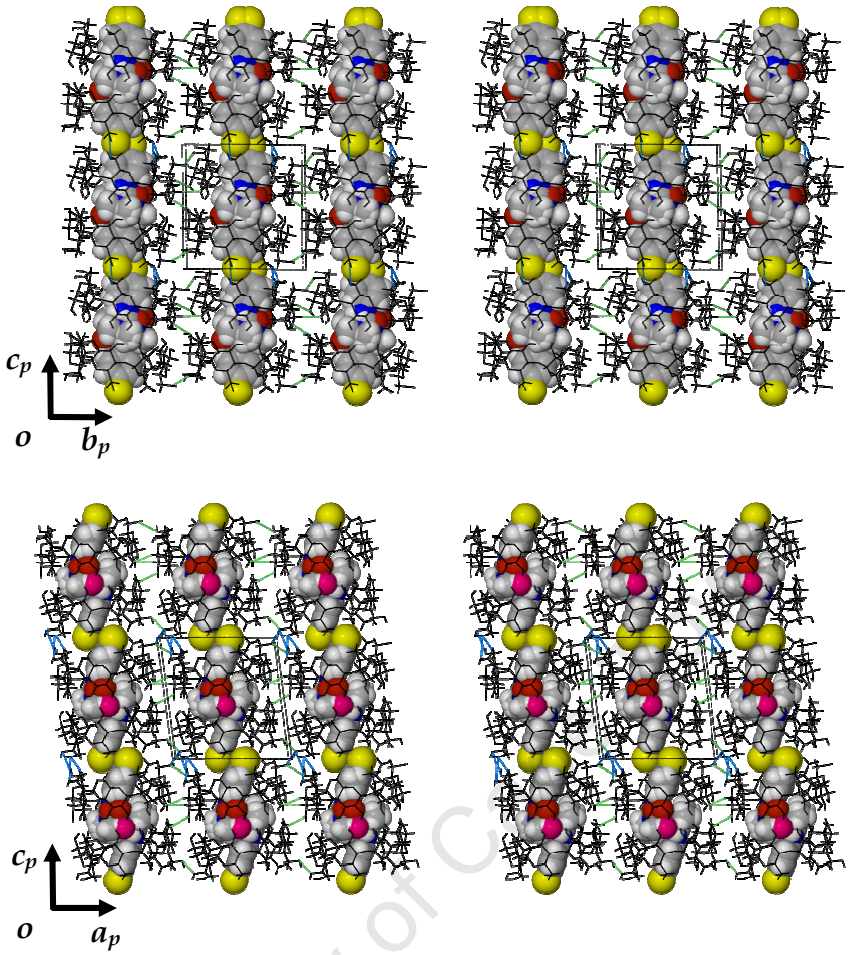

Figure 40. *The diagrams show the inter- and intra-layer hydrogen bonds (green and blue bonds respectively) which link the columns together viewed along a (top) and viewed along b (bottom).*

Comparative PXRD

The powder X-ray diffractograms (calculated and experimental) of complex A3 are shown in Figure 41. Peak positions in the experimental trace of A3 are displaced to lower 2θ˚ owing to the different conditions under which the data were collected (113 K for the calculated trace and 298 K for the experimental trace). However, the agreement between the two traces is good.

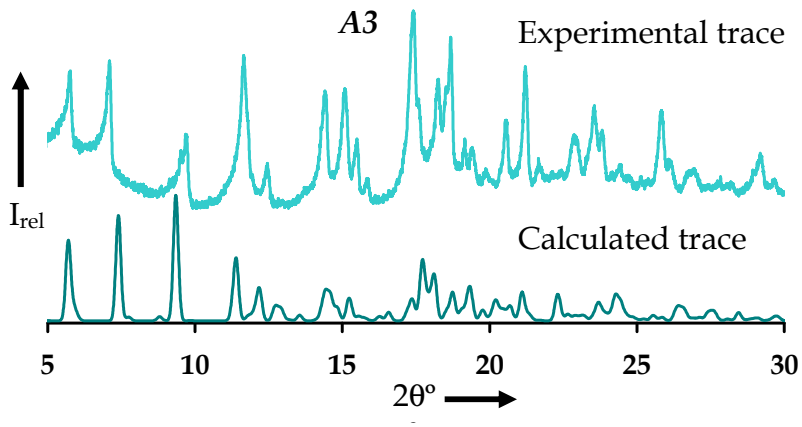

Figure 41. *Calculated and experimental PXRD traces for A3.*

General agreement between the experimental and calculated traces proves that the bulk sample is homogeneous and has the same structure as the single crystal selected for X-ray analysis.

DISCUSSION

The three experimental traces match their respective calculated PXRD traces closely with differences in peak intensities generally resulting from preferred orientation in the powdered samples. The calculated PXRD traces of the three complexes A1, A2 and A3 are shown in Figure 42. The PXRD trace of A1 shares a superficial resemblance with those of A2 and A3 especially between 5 and 13° 2θ. Closer investigation reveals differences in peak angular positions and the presence or absence of particular peaks. However, the PXRD traces of complexes A2 and A3 are nearly identical. The reasons for the similarity shall be discussed here.

Isostructurality

The similarity in the PXRD traces of A2 and A3 is based on the fact A2 and A3 crystallise in same the space group P1 having similar unit cell dimensions (a = ~15, b = ~15, c = ~15 Å, α = ~87, β= ~97, γ = ~103°), identical packing arrangements of host molecules and therefore nearly identical atomic co-ordinates for corresponding atoms. The complexes (A2 and A3) are therefore

said to be isostructural. Differences in peak intensities between the PXRD traces are primarily due to differences in the guest molecules, their orientations and crystal solvent content.

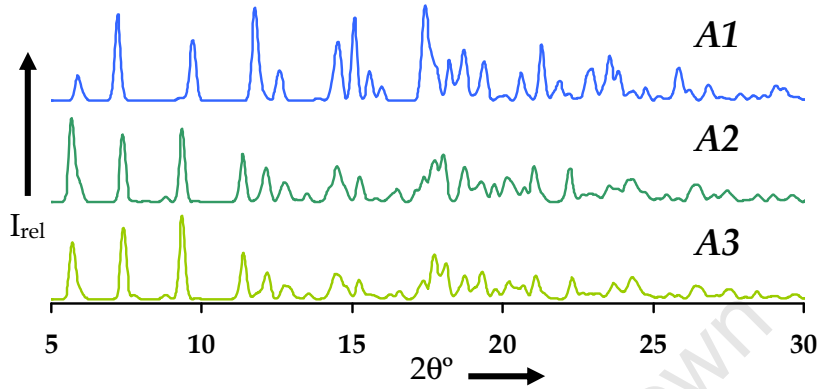

Figure 42. *Stacked calculated traces of the 1:1 β-CD inclusion complexes A1, A2 and A3.*

Conformation of the β-cyclodextrin host molecules

The host molecules in complexes A1, A2 and A3 described here display sevenfold symmetry. This is communicated by the parameters listed in Table 10. The values for **r**, **l**, and **a** have reasonably narrow ranges and are similar for the host molecules of the three complexes. The average value for **a** (128.5°) reflects the value for a regular heptagon. The root mean square deviations **d** of the O4 atoms from the least-squares mean plane through the O4-heptagons is small (Table 10). The narrow ranges for the torsion angles **t** confirm the small deviations observed for **d** and imply a nearly planar conformation for the O4-heptagons.

Table 10. *Tabulated geometric parameter ranges for inclusion complexes A1, A2 and A3.*

complex	r Å	l Å	a°	φ°	t°	τ_1°	τ_2°	[b]d Å
A1								
A	4.94 - 5.37	4.35 - 4.61	123.5 - 132.6	116.5 - 119.5	-2.4 - 3.6	1.8 - 8.9	2.6 - 10.7	0.047
A2								
A	4.89 - 5.18	4.29 - 4.47	125.4 - 132.1	117.1 - 118.8	-3.4 - 2.8	0.9 - 8.3	0.3 - 13.7	0.034
B	4.92 - 5.10	4.23 - 4.41	126.6 - 130.7	117.4 - 118.7	-3.5 - 5.4	1.4 - 14.1	2.0 - 13.3	0.049
A3								
A	4.96 - 5.06	4.30 - 4.42	127.3 - 130.1	116.7 - 118.6	-3.3 - 5.0	1.1 - 7.3	1.2 - 12.3	0.045
B	4.88 - 5.21	4.26 - 4.50	124.5 - 132.7	117.1 - 119.1	-4.3 - 3.8	1.3 - 6.9	1.3 - 13.4	0.039

(b) = root mean square deviation of O4 atoms from the O4-heptagon.

The tilt angles τ_1 and τ_2 are all positive and range from 0.9 to 14.1° for τ_1 while τ_2 ranges from 0.3 to 13.4°. The positive tilt angles are indicative of glucopyranose units whose primary sides tilt toward the centre of the cavity. The cyclodextrin host molecules therefore have a truncated cone-like appearance. The **Φ** and **Ψ** torsion angles are all within accepted values for β-CD complexes. All glucopyranose rings are in the $^4C_1$ conformation.

Intra-dimer hydrogen bonds

Three types of O•••O close contacts are responsible for the formation of the hydrogen bonded dimer. The three interactions are O2•••O3, O2•••O2 and O3•••O3 close contacts. The average strength of interaction for complexes A1, A2 and A3 is O2•••O3 < O2•••O2 < O3•••O3 with the average distances of 3.07, 3.01 and 2.83 Å respectively.

Inter- and intra-layer interactions

The inter- and intra-layer interactions involve O6•••O6, O2•••O2 and C-H•••O hydrogen bond interactions. The average inter-layer O6•••O6 close contact distance for the three complexes is 2.85 Å. The intra-layer O6•••O6 and O2•••O2 close contact distances for three complexes are 2.76 and 2.82 Å respectively. The C-H•••O hydrogen bonds have an average hydrogen bond distance of 3.33 Å and an average hydrogen bond angle of 150.0°.

Host-water interactions

The majority of the host-water interactions for the complexes A1, A2 and A3 occur at the primary and secondary rims while there are also C-H•••OW interactions that are located between the two rims. The average primary rim-water interaction for the three structures is 2.86 Å while the average distance for the secondary rim-water interaction is 2.92 Å. The weaker C-H•••OW interactions have an average distance of 3.32 Å. Furthermore, there are several water-water interactions which indirectly link the primary rim to the secondary rim. The average O•••O distance for water-water hydrogen bond interactions is 2.76 Å.

GUEST INTERACTIONS

Host-guest interactions

The host-guest complexes A1, A2 and A3 are essentially stabilised by weak C-H•••O hydrogen bonds and various close contact interactions (Table 11). Cyclodextrin inclusion complex A1 forms hydrogen bonds between the ethereal oxygen atoms of the guest and methine hydrogens of the host molecule. Complex A3 has hydrogen bonds between carbonyl oxygen atoms of the guest and methine hydrogen atoms of the host cavity. Both of these interactions are present in A2. The average distance for the hydrogen bonds involving ethereal oxygen atoms is ~3.31 Å while the average hydrogen bond angle is 133.0°. The average hydrogen bond length involving the carbonyl oxygen atom of the guest molecules is 3.47 Å with an average angle of 165.0°. All three complexes have hydrogen bonds involving the O3 atoms of the secondary rim of the host and the methyl hydrogen atoms of the guest. The average hydrogen bond distance for the complexes is 3.43 Å with a hydrogen bond angle of 145.0°.

Table 11. *Summary of host-guest interactions for A1, A2 and A3.*

Interaction	A1	A2	A3
ethereal C-H•••O	3.38 Å, 135.0°	3.15 - 3.35 Å 124.0 - 144.0°	-
carbonyl C-H•••O	-	3.35 - 3.59 Å 160.0 - 173.0°	3.42 Å, 159.0°
C-H•••O3	3.41 Å, 144.0°	3.36 - 3.38 Å 144.0 - 150.0°	3.57 Å, 143.0°
Cl•••C contacts	3.60 Å	3.36 - 3.52 Å	3.52 - 3.57 Å
C•••C contacts	3.50 Å	3.37 - 3.58 Å	3.49 Å
C•••O contacts	-	3.35 - 3.36 Å	-
O•••O contacts	-	3.10 - 3.14 Å	-
Cl•••H(C)	2.85 - 3.12 Å	2.81 - 3.05 Å	2.90 - 2.97 Å

A1, A2 and A3 also experience C•••C and Cl•••C close contacts with mean distances of 3.47 Å and 3.49 Å respectively. All three complexes have C-Cl•••H(C) halogen interactions which contribute to the stabilisation of the inclusion complexes. The mean distance for A1, A2 and A3 is 2.97 Å; as it

turns out, these interactions are on average the strongest interactions present in the complexes.

Guest intramolecular interactions

The N-H•••O and C-H•••O hydrogen bonds for the uncomplexed guest molecule **2** have hydrogen bond distances of 2.57 and 2.93 Å respectively, while the respective hydrogen bond angles are 110.0° and 107.0°. The N-H•••O and C-H•••O hydrogen bond ranges for A1 and A2 are 2.51 to 2.66 Å for A1 and 2.74 to 3.09 Å for A2. The hydrogen bond angle ranges are 105.0 to 113.0° and 100.0° to 122.0° for A1 and A2 respectively. The C-H•••O interaction for the uncomplexed guest **3** has a hydrogen bond distance of 2.92 Å and a hydrogen bond angle of 99.0°. The C-H•••O hydrogen bond distances of the guest molecules of complex A3 range from 2.78 to 2.85Å while the hydrogen bond angles range from 116.0 to 121.0°. The conformation of the guest molecules included in the cyclodextrin cavity is distorted compared to the uncomplexed guest molecules. The distortions are in response to the accommodation of the guest in the CD cavity.

Guest-guest intermolecular interactions

The primary intermolecular interactions between the guest molecules of complexes A2 and A3 are close contacts and weak C-H•••O hydrogen bonds. The contact distances for C•••O, C•••C and N•••C interactions range from 2.57 to 3.57 Å. The C-H•••O hydrogen bond interactions range from 3.02 to 3.20 Å with the hydrogen bond angle ranging from 113.0 to 129.0°. Guest-guest intermolecular interactions were not determined for complex A1.

CRYSTAL PACKING

The complex A1 crystallises in the space group C2 while A2 and A3 crystallise in P1. All the complexes pack in the **CH** (channel) arrangement with included guest molecules isolated from the interstitial water molecules. The guest molecules of the three complexes are arranged in the same tail-to-tail

arrangement with the chlorophenyl moieties located at the primary rims and the urea moieties located at the secondary rim interface.

MULTIPLICITY OF CRYSTAL FORMS

The isolation of more than one crystal form of an inclusion complex of **2** with β-CD prompted further investigation of this phenomenon. The results of our investigation are relayed in chapter six.

REFERENCES

1. Nesterova, Ya.M., Porai-Koshits, M.A. and Moev, A.G., *Zh. Strukt. Khim. (Russ.),* (*J. Struct. Chem.)*, **1981**, 22, 111-115.
2. Baughman, R.G., Hembre, R.I., Helland, B.J. and Jacobson, R.A., *Cryst. Struct. Commun.*, **1980**, 9, 749-752.
3. Lewis, R.J., Camilleri, P., Kirby, A.J., Marby, C.A., Slawin, A.A. and Williams, D.J., *J. Chem. Soc., Perkin Trans. 2,* **1991**, 1625-1630.
4. Barbour, L.J., LAYER, A computer program for the graphic display of intensity data as simulated precession photographs, *J. Appl. Cryst.,* **1999**, 32, 351-352.
5. XPREP, *Data Preparation and Reciprocal Space Exploration*, Version 5.1, (Copyright Bruker Analytical X-ray Systems, **1997**).
6. Otwinowski, Z., Minor, W., *Processing of X-ray Diffraction Data in Oscillation Mode in Methods in Enzymology*, Vol. 276, Carter, C.W., Sweet, R.M., (eds.), Academic Press, New York, **1996**, 307-326.
7. Sheldrick, G.M., *SHELXS-97, Program for Crystal Structure Solution,* Institüt für Anorganische Chemie der Universität, Tammanstrasse 4, D-3400 Göttingen, Germany, **1997**.
8. Sheldrick, G.M. *SHELXH-97*, *Acta Crystallogr.,* **2008**, A64, 112-122.
9. Etter, M.C., Macdonald, J.C. and Bernstein, J., *Acta Crystallogr.* **1990**, B46, 256-262.
10. Bernstein, J., Davis, R.E., Shimoni, L. and Chang, N-L., *Angew. Chem., Int. Ed. Engl.*, **1995**, 34, 1555-1573.
11. Cambridge Structural Database and Cambridge Structural Database System, Version 5.29 November **2007**, Cambridge Crystallographic Centre, University Chemical Laboratory, Cambridge, England.
12. Mavridis, I.M., Hadjoudis, E. and Tsoucaris, G., *Carbohydr. Res.*, **1991**, 220, 11-21.
13. Lichtenthaler, F.W. and Immel, S., *Starch*, **1996**, 48, 225-232.
14. Saenger, W. and Steiner, T., *Acta Crystallogr.,* **1998**, A54, 798-805.
15. Saenger, W., Betzel, C., Hingerty, B.E. and Brown, G.M., *Nature*, **1982**, 296, 581-583.
16. Saenger, W., Betzel, C., Hingerty, B.E. and Brown, G.M., *Angew. Chem., Int. Ed. Engl.*, **1983**, 22, 883-884.
17. Betzel, C., Saenger, W., Hingerty, B.E. and Brown, G.M., *J. Am. Chem. Soc.,* **1984**, 106, 7545-7557.
18. Makedonopoulou, S. and Mavridis, I.M., *Acta Crystallogr.*, **2000**, B56, 322-331.
19. Caira, M.R., and Dodds, D.R., *J. Inclusion Phenom. Macrocyclic Chem.*, **1999**, 34, 19-29.
20. Caira, M.R., and Dodds, D.R., *J. Inclusion Phenom. Macrocyclic Chem.*, **2000**, 38, 75-84.

Chapter 6
MULTIPLICITY OF CRYSTAL FORMS AND DIVERSE MODES OF INCLUSION OF A β-CD COMPLEX WITH A COMMON GUEST

In this chapter we report the isolation of more than one cyclodextrin inclusion complex containing the same host and guest (metobromuron). In addition, we report on the different modes of guest inclusion, the nature of guest disorder and differences in complex crystal packing modes.

THE GUEST: METOBROMURON

Key to this chapter is the structure of the guest metobromuron (**1**). The structure will be presented here with particular attention paid to its conformation in the solid state.

Preparation of single crystals

20 mg of metobromuron powder was dissolved in 2 mL of acetone at room temperature (20˚C). The solution was filtered and allowed to crystallise under ambient conditions. Crystals formed within two days of standing.

CRYSTAL STRUCTURE ANALYSIS

Space group determination

The program LAYER was used to establish the crystal symmetry as orthorhombic since the Laue symmetry was *mmm*.[1] Further inspection of the reciprocal lattice layers confirmed the reflection conditions *hkl : none; 0kl : k = 2n; h0l : l = 2n; hk0 : h = 2n*. XPREP was employed to confirm the space group as Pbca.[2] From density considerations, Z = 8 was deduced.

Structure solution and refinement

Crystal and refinement data are presented in Table 1. Unit cell refinement and data reduction were performed with the program DENZO-SMN.[3] The structure solution of **1** was carried out with SHELXS-97 which revealed all the non-hydrogen atoms.[4] The atoms were placed and refined isotropically on F^2 in SHELXH-97.[5] All atoms were later refined anisotropically based on well-behaved isotropic temperature factors. All hydrogen atoms were placed in idealised positions in a riding model except for the amide hydrogen which was located and allowed to refine freely with an N-H restraint of 0.88(1) Å applied. All hydrogen atoms were refined isotropically and were assigned temperature factors related to their parent atoms, namely 1.2 times those of the parent in the case of phenyl hydrogens and 1.5 times those of the parent atom for methyl hydrogen atoms.

Molecular structure

Bond lengths and angles are provided in Table 2 and are all within the expected ranges. A drawing of the molecule showing the thermal ellipsoids at the 50 % probability level is shown in Figure 1.

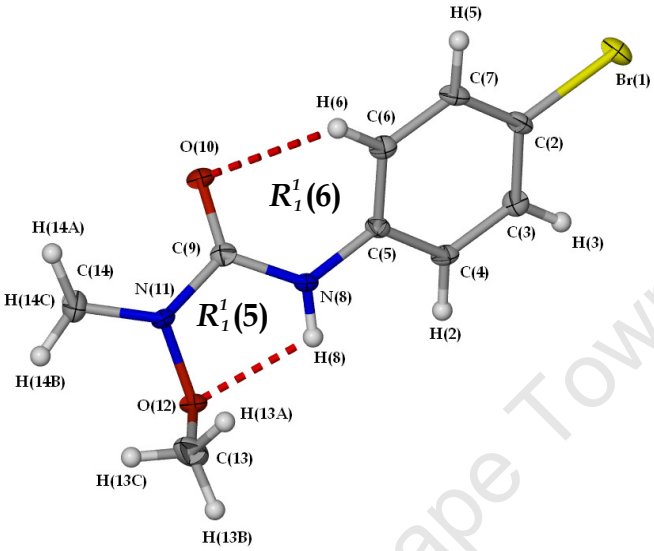

Figure 1. *The molecule of the guest metobromuron (**1**) showing the intramolecular hydrogen bonds.*

In the structure of **1** there are two intramolecular hydrogen bonds which have graph set analysis descriptors $R_1^1(5)$ and $R_1^1(6)$, as indicated in the respective hydrogen bonded rings.[6] These hydrogen bonds stabilise the molecular conformation.

Table 1. *Crystal data and data-collection parameters for* ***1***.

parameters	1
Formula unit	$C_9H_{11}N_2O_2Br$
Mr	259.1
Crystal system	orthorhombic
Space group	Pbca
a/Å	9.8071(2)
b/ Å	11.3050(3)
c/ Å	18.9632(5)
α/°	90
β/°	90
γ/°	90
Vol. Å³	2102.44(9)
Z	8
ρ_{calc} g cm^{-3}	1.637
μ (MoKα) mm^{-1}	3.887
F(000)	1040
Crystal size mm³	0.30 x 0.25 x 0.05
Temperature K	113 ± 2
Range scanned θ/°	3.0 ≤ θ ≤ 27.88
Index range	-12 : 12; -14 : 14; -24 : 24
ϕ Scan angle °	1.0
ϕ Scan range °, no of frames	251, 251
ω Scan angle °	1.0
ω Scan ranges °, no of frames	32, 32; 109, 109; 60, 60
Dx mm	32
No. of reflections	28407
No. of unique reflections	2508
No. of reflections with I>2σ(I)	1789
No. of l.s. parameters	133
R_{int}, R_σ	0.078, 0.046
S	1.005
R_1 [$F_o > 4\sigma(F_o)$]	0.0301
wR_2	0.0584
No. of reflections omitted	1
Weighting scheme parameters	a = 0.0220, b = 1.1453
(Δ/σ)	<0.001
Δρ excursions eÅ^{-3}	-0.41, 0.51

Table 2. *Geometrical parameters for compound* ***1***

Bond	Bond lengths (Å)	Angles	Bond angles (˚)
Br1-C2	1.904(2)	N11-O12 -C13	108.2(1)
O10-C9	1.231(2)	C5-N8-C9	123.8(2)
O12-N11	1.418(2)	O12-N11-C9	114.1(2)
O12-C13	1.431(3)	O12-N11-C14	112.5(2)
N8-C5	1.415(3)	C9-N11-C14	120.5(2)
N8-C9	1.363(3)	C9-N8-H8	115.7(1)
N11-C9	1.383(3)	C5-N8-H8	117.6(1)
N11-C14	1.450(3)	Br1-C2 -C7	119.9(2)
C2-C7	1.382(3)	C3-C2-C7	121.1(2)
C2-C3	1.382(3)	Br1-C2-C3	119.0(2)
C3-C4	1.383(3)	C2-C3-C4	119.4(2)
C4-C5	1.389(3)	C3-C4-C5	120.4(2)
C5-C6	1.392(3)	N8-C5-C4	118.2(2)
C6-C7	1.389(3)	C4-C5-C6	119.7(2)
		N8-C5-C6	122.1(2)
		C5-C6-C7	120.0(2)
		C2-C7-C6	119.4(2)
		N8-C9-N11	114.7(2)
		O10-C9-N8	125.3(2)
		O10-C9-N11	119.9(2)

Conformation

The amide group (O10-C9-N8-H8) forming part of the 1-methoxy-1-methylurea moiety of **1** has a *trans* conformation as is usual for these groups. Nine torsion angles (τ_1 – τ_9) define the conformation of the 1-methoxy-1-methylurea moiety. These are shown schematically in Figure 2 and listed in Table 3.

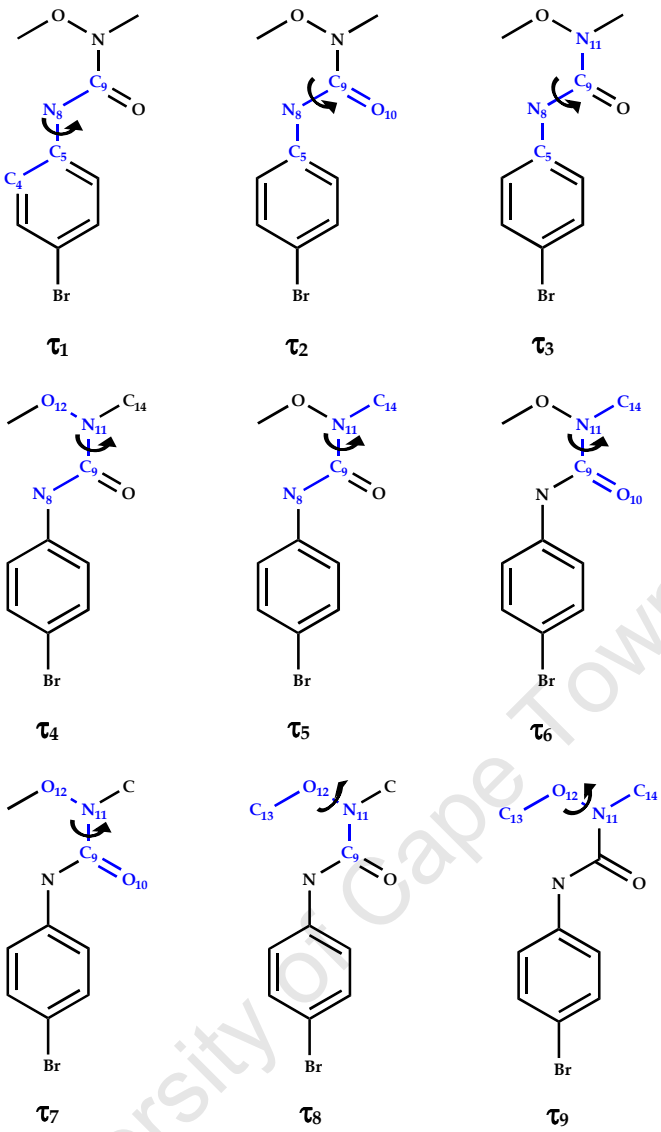

Figure 2. *Schematic diagram of the nine torsion angles of guest* ***1.***

Torsion angle τ_1 (Figure 2) describes the rotation around bond C5-N8 and relays information about the orientation of the bromophenyl moiety relative to the 1-methoxy-1-methylurea moiety (for simplicity, the urea moiety). τ_2 and τ_3 describe the amount of rotation around bond N8-C9 and are pertinent to the degree of 'extension' of the urea moiety. The torsion angles τ_4, τ_5, τ_6 and τ_7 describe the amount of rotation around bond C9-N11 providing information on the conformation of surrounding moieties. Finally, τ_8 and τ_9 describe the amount of rotation around bond N11-O12 and relate the disposition of bond C13-O12 relative to the mean plane through C9, N11, O12 and C14.

Table 3. *Torsion angles for* ***1****.*

Angle		Torsion angle (˚)
C4-C5-N8-C9	τ_1	-140.9(2)
C5-N8-C9-O10	τ_2	-1.8(3)
C5-N8-C9-N11	τ_3	-177.4(2)
N8-C9-N11-O12	τ_4	-18.8(3)
N8-C9-N11-C14	τ_5	-157.5(2)
O10-C9-N11-C14	τ_6	26.6(3)
O10-C9-N11-O12	τ_7	165.3(2)
C9-N11-O12-C13	τ_8	117.3(2)
C13-O12-N11-C14	τ_9	-100.7(2)

The value of τ_1 implies that the bromophenyl moiety is rotated out of the plane of the urea moiety, in a **–ac** conformation. Torsion angle τ_2 with terminal bonds C5-N8 and C9-O10 reflects a **–sp** conformation. τ_3 is very close to 180˚ and is indicative of an 'extended' conformation; bonds C5-N8 and C9-N11 are in a **–ap** conformation. Values close to zero for torsion angles τ_4 and τ_6 represent **–sp** and **+sp** conformations, respectively. On the other hand, values close to 180˚ for torsion angles τ_5 and τ_7 represent **–ap** and **+ap** conformations, respectively. The conformations indicated by the values of τ_8 and τ_9 may be described as **+ac** and **–ac** respectively; they show the disposition of bond C13-O12 as nearly perpendicular to the mean plane through C9, N11, O12 and C14. The metobromuron molecule essentially consists of two planes. The first is made up of N8 and the bromophenyl ring and the second consists of the mean plane through C9, O10, N11, O12 and C14.

HYDROGEN BONDING

Hydrogen bonding data are listed in Table 4.

Table 4. *Hydrogen bonding interactions for* ***1****.*

D-H•••A	D-H (Å)	H•••A (Å)	D•••A (Å)	D-H•••A˚
N8 -- H8•••O12	0.87(1)	2.14(2)	2.57 (2)	110.0
N8 -- H8•••O10[a]	0.87(1)	2.32(2)	3.12(2)	154.0
C4 -- H2 •••O10[a]	0.95	2.41	3.21(3)	141.0
C6 -- H6•••O10	0.95	2.51	2.93(3)	107.0

Symmetry code: a = ½ + x, y, ½ - z

There are two intermolecular and two intramolecular hydrogen bonds in the structure of **1**. The two intramolecular hydrogen bonds were described earlier.

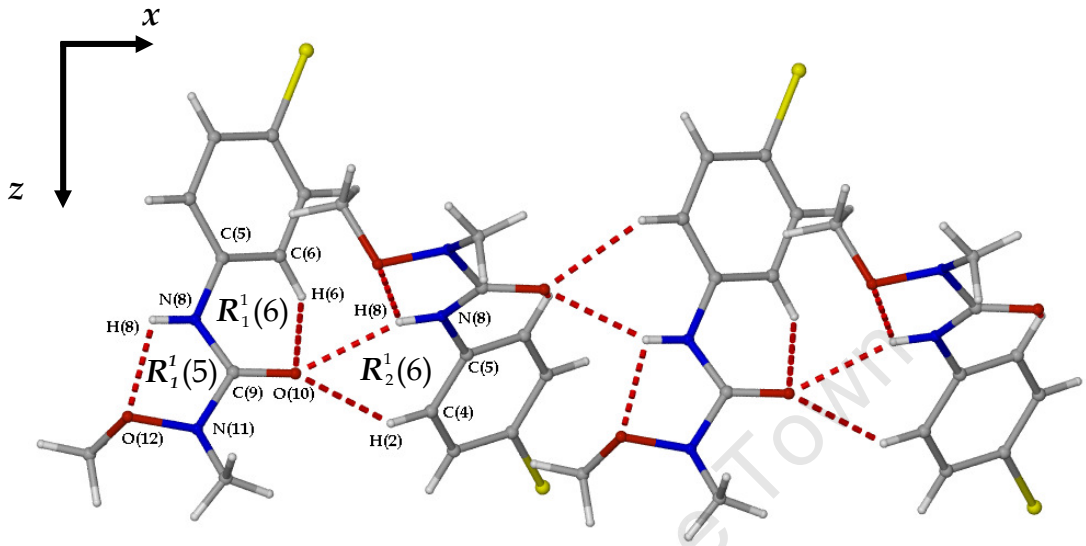

Figure 3. *The intermolecular hydrogen bonds which link adjacent molecules forming an infinite ribbon spanning the crystal. Also shown here is the graph set notation for the three rings formed by intra- and intermolecular hydrogen bonding.*

The two intermolecular hydrogen bonds consist of an N-H•••O and a C-H•••O hydrogen bond. Both involve the same carbonyl oxygen of a neighbouring molecule, thus leading to the formation of hydrogen bonded ribbons parallel to the *a*-axis and extending infinitely through the crystal, as shown in Figure 3. The graph set analysis descriptors for the three rings formed by the intermolecular and intramolecular hydrogen bonds are shown in their respective rings in Figure 3.[6,7]

CRYSTAL PACKING

The unit cell contains eight symmetry related molecules arranged in two layers which have anti-parallel orientation. The layers are parallel to the *b*-axis, Figure 4. The two layers are arranged in such a way that the bromophenyl moieties interpenetrate at *c*/2, as shown in Figure 4.

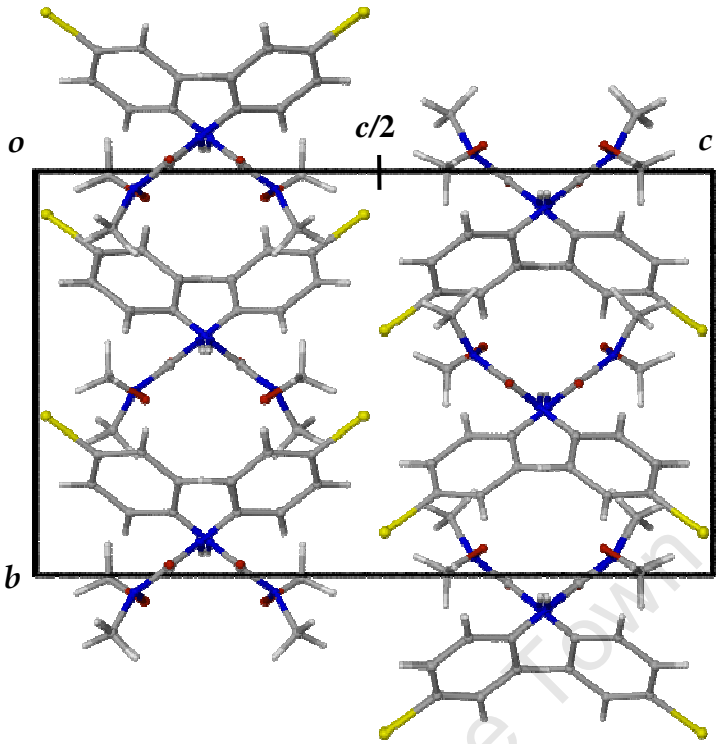

Figure 4. *The packing diagram shows the interleaved bromophenyl groups located halfway along the c-axis.*

An interesting aspect of the structures of monolinuron, monuron (chapter 5 and chapter 5 reference 2, respectively) and metobromuron is the fact that they are isostructural.

β-CYCLODEXTRIN INCLUSION COMPLEXES OF METOBROMURON

Preparation

175 mg (0.0154 mmol) of β-CD was dissolved in 6 mL of water at elevated temperature (70 - 80˚C). 20 mg (0.0077 mmol) of **1** was slowly added to the clear β-CD solution. The solutions were stirred for 3 - 4 h until clear and filtered (0.45 μm nylon filter) while hot. In an attempt to isolate different crystal forms, two complex solutions were prepared. To three of the preparations four mL of ethanol (96 %) was added while an extra two mL of water was added to the remaining preparation. Ethanol was added to three of the four preparations to prevent too rapid precipitation of the guest or complex. All preparations had a 2:1 host-guest ratio as the crystals obtained from 1:1 preparations were not of sufficiently high quality for X-ray analysis.

Crystallisation conditions

The conditions of crystallisation were different for each solution. The first preparation, which contained only water as solvent medium, was placed in a Dewar flask containing water at ~80˚C. The flask was covered with an insulating material to prevent rapid cooling and its contents returned to ambient temperature (20˚C) in four to five days, during which complex crystallisation took place. The phase obtained had composition β-CD•metobromuron•8.3(H_2O) (8.3 ± 0.6) and was labelled B1. The crystals of B1 which were initially obtained from spontaneous cooling, were not of sufficiently good quality and necessitated a repeat data collection. This resulted in the isolation/discovery of a second phase with composition (β-CD)$_2$•(metobromuron)$_2$•20(H_2O) (20 ± 1) which was labelled B2. It is not clear whether B2 results from concomitant crystallisation with B1 or whether B1 undergoes a solvent - mediated phase transformation to the new phase. Difficulty arose from the fact that these phases have virtually indistinguishable PXRD traces, making it virtually impossible to track the conversion from one phase to another or the presence of the new phase. The second solution (first of the three which contains ethanol) was kept at

elevated temperature, 38˚C. Crystallisation occurred within a week of the vial being placed at elevated temperature. A new phase was isolated here, with composition (β-CD)$_2$•(metobromuron)$_2$•21(H_2O) (21 ± 2). The new phase was labelled B3. The third solution (second of the three containing ethanol) was allowed to cool spontaneously to room temperature without precipitating and then placed in the refrigerator at ~4˚C. Crystallisation occurred after approximately three weeks; again a new phase with composition (β-CD)$_2$•(metobromuron)$_2$•25(H_2O) (25 ± 0.4) was isolated and labelled B4. The fourth preparation was placed in a Dewar flask containing water at ~80˚C. The flask was covered with an insulating material to prevent rapid cooling and its contents returned to ambient temperature in four to five days, during which complex crystallisation took place. Yet again a new phase was isolated with composition (β-CD)$_2$•(metobromuron)$_2$•25(H_2O) (25 ± 1) and was subsequently labelled B5.

Stoichiometry

The stoichiometries of the five complexes were determined by means of UV spectrophotometry (B1, B3 and B5, Table 5a) and elemental analyses (B2, B4 and B5, Table 5b). Thermogravimetric analysis was used to determine the water content for all five crystal forms. The reported water content is the average of two readings.

Table 5a. *Stoichiometries for complexes B1, B3 and B5.*

Complex	B1	B2	B3	B4	B5
Host:Guest ratio	1.00:1.03	-	1.00:0.88	-	1.00:1.07
H_2O[a]	8.3H_2O	10H_2O	10.5H_2O	12.5H_2O	12.5H_2O

(a) H_2O molecules per CD molecule.

Table 5b. *Microanalysis results for complexes B2, B4 and B5.*

		B2			B4		B5	
		Calc	Exp		Calc	Exp	Calc	Exp
% C	-	38.9	39.2	-	37.8	37.7	37.8	38.1
% H	-	6.5	6.5	-	6.6	6.6	6.5	6.4
% N	-	1.7	1.3	-	1.7	1.3	1.7	1.4

X-RAY STRUCTURE OF B1

Space group determination

The program LAYER was used to determine the crystal symmetry. The Laue symmetry was found to be 2/*m* indicating the monoclinic crystal system.[1] From further examination of the reciprocal lattice the reflection conditions obtained were *hkl : h + k = 2n, h0l : h = 2n*. The space group of B1 was confirmed with the aid of the program XPREP.[2] Three space group choices were presented, namely C2, C2/*m* and Cm. The space group C2 was selected as the host cyclodextrin is chiral. The inclusion complex B1 crystallises in the monoclinic space group C2 with $Z = 4$ complex units per unit cell.

Structure solution and refinement

The B1 complex has a single cyclodextrin molecule in the asymmetric unit, a single guest molecule and 8.3 water molecules. Refinement parameters and crystal data are reported in Table 6. A diad parallel to the *b*-axis generates the other half of the dimeric complex. Unit cell refinement and data reduction were performed with the program DENZO-SMN.[3] B1 was found to be isostructural with the complex (β-CD)$_2$•(methyl-4-hydroxybenzoate)$_2$•7.2(H_2O) (refcode: AJUVEG).[8,9] The structure of B1 was solved by isomorphous replacement using only the host coordinates of AJUVEG. The freely rotating O6 atoms and water molecules were deleted from the refinement in order to model any possible disorder of the O6 atoms in B1. The glucopyranose units for the host were labelled A1-A7, as shown in Figure 5. The structure was refined with SHELXH-97 with successive Fourier maps revealing the O6 atoms.[5] Several atoms of the host were disordered over two positions; these were C4A3, C5A3, O5A3, C6A3, O6A3 and O6A7. Their site-occupancy factors (s.o.f.s) were refined as x, which was initially set to 0.5. The minor components (C4B3, C5B3, O5B3, C6B3, O6B3 and O6B7) refined as 1-x. The value of x settled to 0.51.

Table 6. *Crystal data and data-collection parameters for B1.*

parameters	***B1***
Formula unit	$C_{42}H_{70}O_{35} \bullet C_9H_{11}N_2O_2Br \bullet 8.3H_2O$
Mr	1543.62
Crystal system	monoclinic
Space group	C2
***a* / Å**	19.221(4)
***b* / Å**	24.5082(5)
***c* / Å**	15.865(3)
α / °	90
β / °	109.96(3)
γ / °	90
Vol. Å³	7024.45(2)
Z	4
ρ_{calc} g cm^{-3}	1.460
μ (MoKα) mm^{-1}	0.692
F(000)	3260
Crystal size mm³	0.15 x 0.15 x 0.20
Temperature (K)	113 ± 2
Range scanned θ / °	1.4 ≤ θ ≤ 23.5
Index range	-21 : 21; -27 : 27; -17 : 17
ϕ Scan angle / °	0.3
ϕ Scan range / °, no of frames	363.0, 1210
ω Scan angle / °	0.3
ω Scan range / °, no of frames	114.6, 382; 111.9, 373; 45.6, 152; 46.2, 154; 45.9, 153; 108.9, 363; 46.8, 156; 45.9, 153; 45.3, 151
Dx mm	38
No. of reflections	62313
No. of unique reflections	10198
No. of reflections with I>2σ(I)	5160
No. of l.s. parameters	690
R_{int}, R_σ	0.172, 0.135
S	1.306
R_1 [$F_o > 4\sigma(F_o)$]	0.1550
wR_2	0.4103
No. of reflections omitted	2
Weighting scheme parameters	a = 0.2000
(Δ/σ)	<0.001
Δρ excursions eÅ^{-3}	-0.47, 0.91

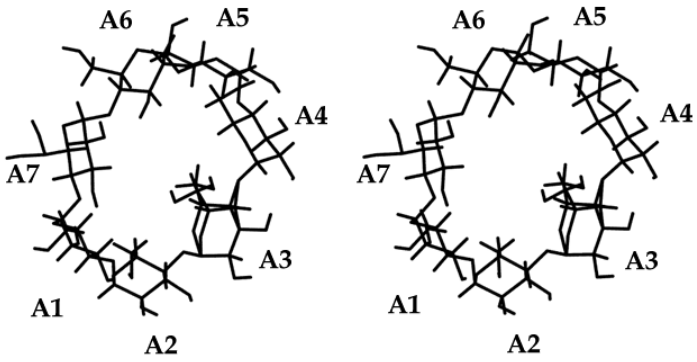

Figure 5. *Labelling of the glucopyranose units of the macrocycle.*

All atoms were refined anisotropically except those listed in Table 7.

Table 7. *Isotropically refined atom list for B1.*

O6A1	C5A3	C4B3	C1A4	O6A5
C6A1	O5A3	C5B3	O6A4	C5A6
C5A1	C6A3	O5B3	C5A5	C1A7
O6A2	O6A3	C6B3	O5A5	C6A7
C4A3	C4A3	O6B3	C6A5	O6A7
O6B7				

All hydrogen atoms of the host were placed in idealised positions using a riding model, except for hydroxyl hydrogen atoms which were refined using a hydrogen bond searching model. All hydrogen atoms refined with U_{iso} = 1.2 times those of the parent atoms. Twelve sites for water molecules were located in the difference map with only three sites having full site-occupancy. The other nine water molecules had only partial occupancy. The temperature factors and s.o.f.s are reported in Table 8. The sum of the site-occupancies for these twelve water molecules with full and partial site-occupancy amounted to 8.5 water molecules while 8.3 water molecules were accounted for from TGA (n = 2). Water H atoms could not be located. None of the water molecules was refined anisotropically.

Table 8. *Site-occupancies for disordered water molecules for complex B1.*

Atom	OW3	OW5	OW6	OW7	OW8	OW9	OW10	OW11	OW12
s.o.f.	0.42	0.92	0.63	0.49	0.91	0.36	0.89	0.56	0.52
U_{iso} (Å^2)	0.09	0.19	0.17	0.18	0.20	0.17	0.20	0.21	0.20

Modelling of the guest and guest inclusion

The electron density in the cavity of the cyclodextrin host was particularly weak or diffuse and ranged between 0.6 and 1.6 e $Å^{-3}$. This was not a particularly good sign when considering the presence in the guest molecule of the heavy atom, bromine. In addition, abnormal distances and angles between electron density peaks did not allow for guest placement. Several attempts were made at resolving the guest position from the electron - density maps but these were unsuccessful. Moreover, the fact that a significant number of atoms belonging to the host could not be refined anisotropically was not favourable either. The resultant high R-factor (R_1) and weighted R-factor (wR_2) are due to these many complicating factors. It is noteworthy that the case presented here is the best of a number of data-collections carried out on several different crystals of B1 at low temperature. Added to this is the inherently poor diffraction of β-CD complexes. In mitigation, there are several cases of β-CD inclusion complexes reported in the literature crystallising in this space group where the guests could not be modelled.[9] The residual electron density in the cavity is shown in Figure 6. The presence of the guest as well as the stoichiometry were established using UV spectrophotometry as mentioned previously.

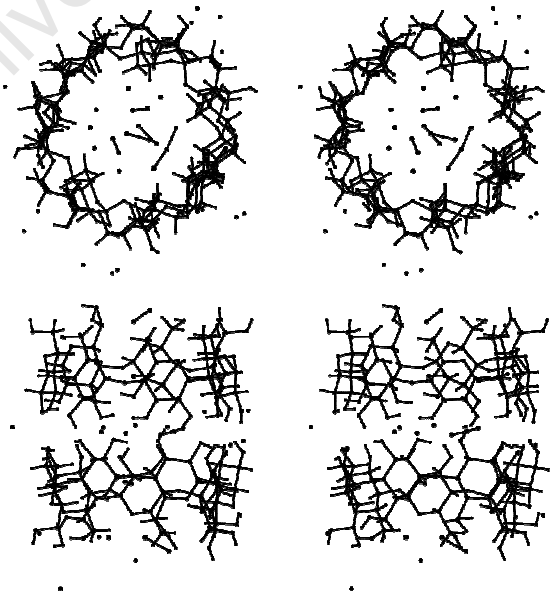

Figure 6. *Stereoview of B1, viewed from the primary (top) and side faces (bottom) showing the highest electron density peaks in the dimer cavity.*

It is noteworthy that in the isostructural complex containing monolinuron (chapter 5, complex A1), it *was* possible to model the guest.

STRUCTURAL DESCRIPTION

Detailed tables of the parameters summarised below are available in the Appendices.

Host conformation

Primary hydroxyl torsion angles

All the primary hydroxyl torsion angles (**ω**) of B1 indicate a *(-)-gauche* orientation except for A3 and A7 which are disordered. A3 and A7 have *(+)-gauche* orientation and the minor components of each (B3 and B7) have *(-)-gauche* orientation. The glycosidic torsion angles **Φ** and **Ψ** as well as the pyranoid torsion angles Θ_1 and Θ_2 are in good agreement with those reported for the parent β-CD.[10,11] The glucose residues of the host are all in the $^4C_1$ conformation.

Macrocyclic symmetry

The radius **r** has a mean length of 5.05 Å and lies within a narrow range of 4.70-5.30 Å. The mean length **l** is 4.37 Å and it ranges from 4.26 to 4.47 Å. The glycosidic oxygen angle **a** has a mean of 128.5˚ and ranges from 126.1˚ to 131.2˚. None of the parameters **r**, **l** and **a** deviates substantially from the values reported for native β-cyclodextrin.

Planarity of the O4-Heptagon

The root mean square deviation (**d**) of the O4 atoms from the mean O4 plane of the host is 0.036 Å. There are four O4 atoms which have negative deviations from the mean O4 plane. They are O4A2, O4A3, O4A6 and O4A7. In addition, the torsion angles (**t**) all lie in a narrow range from -2.7 to 2.5˚.

For B1, the tilt angle τ_1 ranges from 1.0 to 12.5˚ while τ_2 ranges from 3.0 to 11.7˚. All values of τ_1 and τ_2 are positive and the implication is that all the glucose residues are inclined towards the centre of the cavity. The

intersaccharidic angle **φ** ranges from 112.5 to 120.1˚ with an average value of 117.3˚; again this is in good agreement with those reported for β-CD.

The parameters reported here for B1 indicate that the macrocycle is highly symmetrical while **d** and torsion angle **t** show a near planar O4 heptagon. Additionally, with τ_1 and τ_2 all positive it implies that the macrocycle has a truncated cone-like appearance (*i. e.* wider at the secondary rim and narrow at the primary rim).

INTRA- AND INTERMOLECULAR HYDROGEN BONDS

Host intramolecular interactions

There are seven intraglucose O2•••O3′ hydrogen bonds which further stabilise the β-CD macrocycle. The O2•••O3′ interactions have hydrogen bond lengths which range from 2.81 to 2.89 Å. The H-bond distances lie within a narrow band implying a round or highly symmetrical macrocycle (as mentioned previously).[12,13,14]

Host-Host intermolecular interactions

There are 25 intermolecular hydrogen bonds which stabilise the host dimer at the secondary rim interface. Eleven of the interactions are of the type O2•••O3, seven are O3•••O3 interactions with the remaining seven being O2•••O2 interactions. The eleven O2•••O3 interactions have an average hydrogen bond distance of 3.09 Å and range from 3.03 to 3.13 Å. In the case of the O3•••O3 interactions the average hydrogen bonding distance is 2.81 Å ranging from 2.76 to 2.85 Å. The mean O2•••O2 hydrogen bonding distance is 3.06 Å with a range of 2.97 to 3.18 Å. The average values of the O3•••O3 hydrogen bonds reflect the assertions made by Mavridis *et al*.[15]

Inter-layer interactions

Eleven inter-layer H-bonds are observed in the structure. All eleven are O•••O interactions. Two are O6•••O5 interactions and nine are O6•••O6 interactions. The two O6•••O5 interactions have an average hydrogen bond length of 3.33 Å (range 3.27 – 3.40 Å) and an average hydrogen bond angle of

151.0˚ (range 145.0 – 158.0˚). The O6•••O5 bond involves the disordered glycosidic units of the cyclodextrin. This interaction also adds to the overall stability of the complex. The interactions are shown in Figure 7. The remaining O6•••O6 interactions have a mean hydrogen bond length of 2.93 Å in the range 2.76 to 3.08 Å.

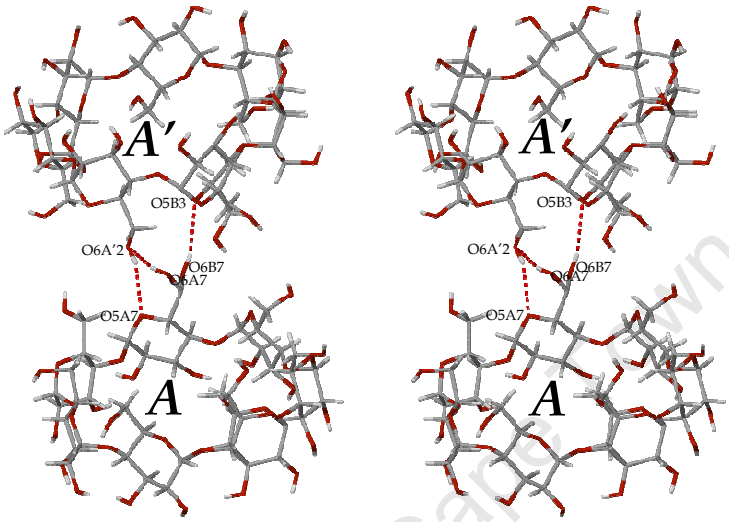

Figure 7. *The stereo diagram shows the hydrogen bonds between host molecules of adjacent dimers. The disordered hydroxyls O6A7 and O6B7 are involved in hydrogen bond formation.*

Intra-layer interactions

There are two O2•••O2 intra-layer interactions and two O6•••O6 intra-layer interactions present in the structure. The mean O2•••O2 interaction distance is 2.73 Å while the mean O6•••O6 interaction distance is 2.88 Å. There are four long range/weak C-H•••O intra-layer hydrogen bonds between adjacent dimers. Two are of the type C2-H•••O3 while the remaining two are of the type C1-H•••O2. The hydrogen bond distance for the C-H•••O interactions is 3.40 Å (range 3.32 to 3.58 Å) while the mean hydrogen bond angle is 151.0˚ (range 136.0 to 167.0˚).

Host-Water interactions

As mentioned previously, 12 sites were refined for 8.3 water molecules in the asymmetric unit. Six water molecules are involved in close O•••O contacts with the primary rim, with a total of nine close contacts between the primary rim and various water molecules (OW1, OW2, OW3, OW5, OW7 and OW11).

The O•••OW distance ranges from 2.60 to 3.04 Å for the six water molecules interacting with the primary rim while the mean interaction distance is 2.82 Å. The remaining six water molecules interact with the secondary rim with 12 interactions involving OW4, OW6, OW8, OW9, OW10 and OW12 being observed. The close contact distances between the secondary rim and the water molecules range from 2.64 to 3.12 Å with a mean distance of 2.89 Å. In addition, there are seven water molecules (OW1, OW2, OW4, OW6, OW8, OW9 and OW10) involved in water-to-water interactions. Together they are involved in nine OW•••OW close contacts. The water-water close contacts range from 2.69 to 3.20 Å with a mean distance of 2.87 Å.

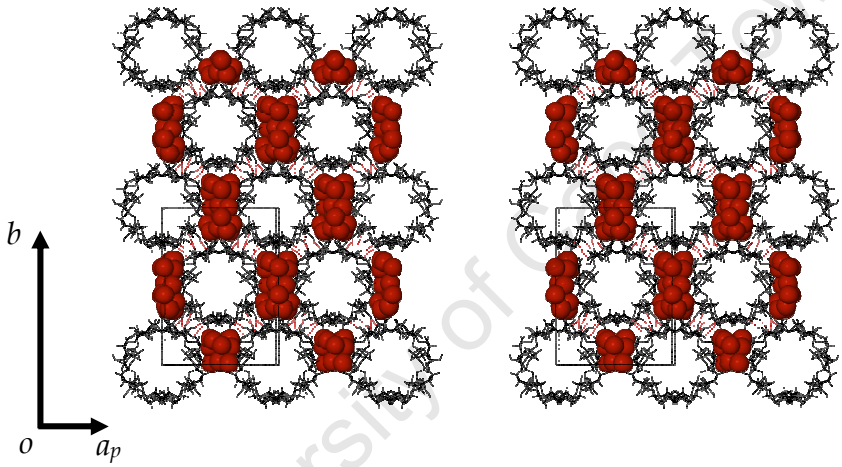

Figure 8. *Water molecules located in the interstices and the inter- and intra-molecular hydrogen bonds (red lines) which isolate the interstitial water molecules.*

The water molecules are all located in the interstitial spaces between the cyclodextrin host molecules and are isolated in the interstices by the inter-layer and intra-layer hydrogen bonds, as shown in Figure 8. The water molecules form 'water-bridges' by hydrogen bonding adjacent dimers (inter-layer) to each other, adding to the overall stability of the crystal structure, Figure 9.

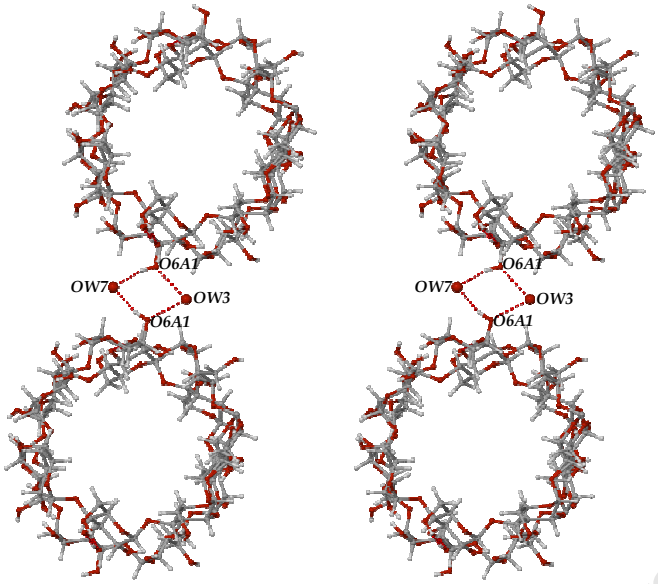

Figure 9. *Two hydrogen bonded water molecules linking host molecules of adjacent dimers.*

CRYSTAL PACKING

B1 is characterised by the channel type (**CH**) packing arrangement. There are three twofold rotation axes parallel to *b* located at 0, ½ and 1 along the *a*- and *c*-axes. A diad is located at the interface of each dimer and between two consecutive dimers in adjacent layers, Figure 10. The dimeric columns are parallel to *c* and the channels extend infinitely along *c*. The dimers are arranged in C-centred layers which propagate along the *c* direction. Successive layers are linked by inter- and intra-layer hydrogen bonds. Figure 10 shows the *b*-axis projection with the C-centred columns shown in green for clarity.

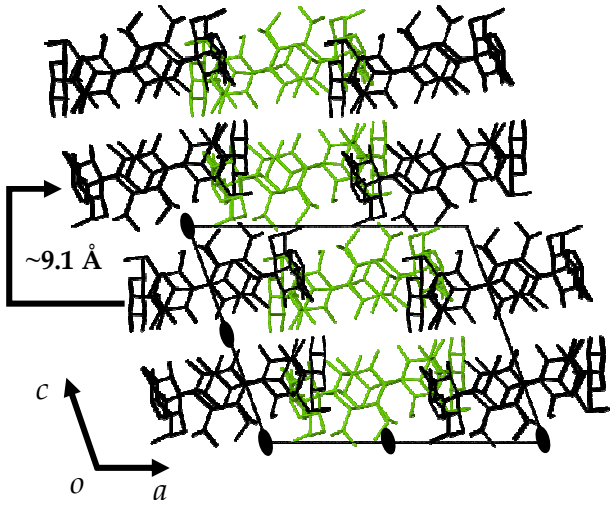

Figure 10*. Packing diagram of the B1 structure along the b-axis.*

All columns have the same orientation. The inter-dimer distance, which is measured from the centroid of one CD to the centroid of a symmetrically related CD across the inter-dimer interface, is ~9.1 Å, Figure 10. The O4 heptagons make an angle of ~10˚ with the *ab*-plane. There is an angle of 0.90(2)˚ between the O4 heptagons of two head-to-head hydrogen bonded dimers.

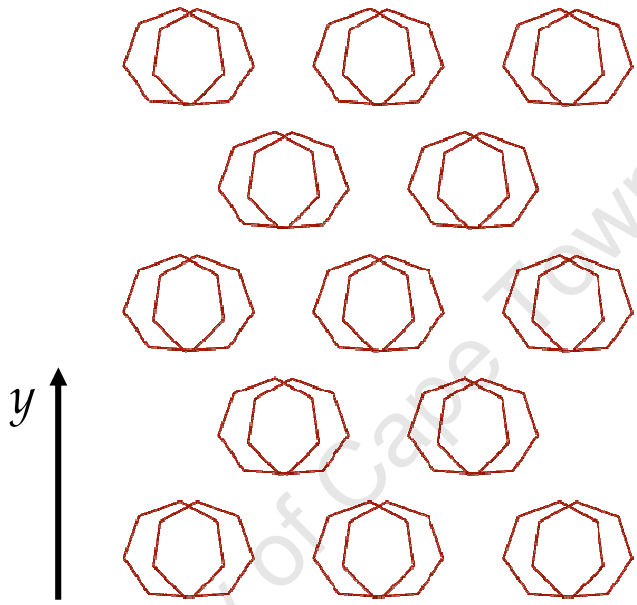

Figure 11. *O4 heptagons of adjacent dimeric layers are laterally displaced from each other.*

When viewed perpendicular to the O4 heptagons of the dimer it is apparent that successive layers are laterally offset from each other by ~2.8 Å, Figure 11. The average lateral displacement for channel type structures crystallising in the space group C2 is 2.7 Å.[15]

Comparative PXRD

Calculated and experimental traces for B1 are shown in Figure 12. There is a very close match in peak positions between the traces. Differences in peak intensities indicate that the experimental sample suffers from preferred orientation.

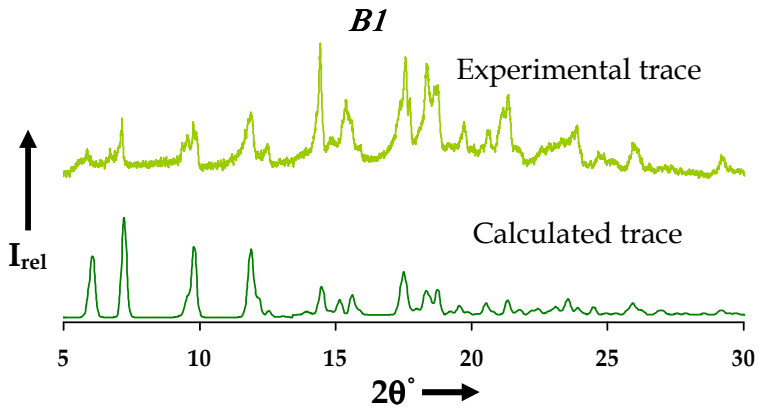

Figure 12. *Calculated and experimental PXRD traces for **B1**.*

General agreement between the experimental and calculated traces proves that the bulk sample is homogeneous and has the same structure as the single crystal selected for X-ray analysis. The extra peaks present in the experimental trace are evidence of uncomplexed guest which has crystallised and contaminates the sample.

X-RAY STRUCTURE OF B2

Space group determination

The crystal system and space group determination of B2 was carried out with the program LAYER. Examination of the reciprocal lattice in LAYER revealed the monoclinic crystal system owing to the 2/*m* Laue symmetry.[1] Further checks of the reciprocal lattice established the reflection conditions *hkl : none; 0k0 : k = 2n*. The two space group choices were $P2_1$ and $P2_1/m$. The space group $P2_1$ was chosen on the basis of the host cyclodextrin being chiral. XPREP confirmed both the monoclinic crystal system and the space group as $P2_1$.[2] The inclusion complex B2 crystallises in the monoclinic space group $P2_1$ with $Z = 2$ dimeric complex units per unit cell.

Structure solution and refinement

B2 has a single hydrogen bonded dimer consisting of two crystallographically independent cyclodextrin molecules, two guest molecules and 20 water molecules in the asymmetric unit. Refinement parameters and crystal data are reported in Table 9. SHELXD was used to solve the structure from *ab initio* methods as no isostructural precedent existed.[16-18] The resultant solution revealed most of the non–hydrogen atoms belonging to the host molecules as well as atoms assigned as water. The O6 atoms and water molecules were deleted to prevent model bias; refinement proceeded in SHELXH-97.[5] All the O6 atoms were located in successive difference Fourier maps. The glucopyranose units of the host molecules were labelled A1-A7 and B1-B7. All the non-hydrogen atoms of the host were refined anisotropically. All hydrogens attached to carbon atoms were placed in idealised positions using a riding model while the hydroxyl hydrogens were placed with the hydrogen bond searching model. All hydrogen atoms were assigned isotropic temperature factors of 1.2 times those of their parent atoms. The successive electron density maps revealed 24 sites for water with 22 sites fully occupied and two with partial site-occupancy, accounting for a total of

23 water molecules while with thermogravimetry only 20 water molecules were found (n = 2).

Table 9. *Crystal data and data-collection parameters for B2.*

parameters	B2
Formula unit	$(C_{42}H_{70}O_{35})_2 \bullet (C_9H_{11}N_2O_2Br)_2 \bullet 20H_2O$
Mr	3148.51
Crystal system	monoclinic
Space group	$P2_1$
a /Å	19.0127(2)
b / Å	24.4425(4)
c / Å	16.0965(2)
α / °	90
β / °	108.648(1)
γ / °	90
Vol. Å^3	7087.62(2)
Z	2
ρ_{calc} g cm^{-3}	1.475
μ (MoKα) mm^{-1}	0.689
F(000)	3328
Crystal size mm^3	0.06 x 0.15 x 0.15
Temperature K	113 ± 2
Range scanned θ / °	$3.2 \leq \theta \leq 24.1$
Index range	-21 : 21; -25 : 25; -15 : 15
ϕ Scan angle / °	0.5
ϕ Scan range / °, no of frames	289.5, 579
ω Scan angle / °	-
ω Scan range / °, no of frames	-
Dx mm	35
No. of reflections	55308
No. of unique reflections	19083
No. of reflections with I>2σ(I)	16665
No. of l.s. parameters	1675
R_{int}, R_σ	0.057, 0.060
S	1.098
R_1 [$F_o > 4\sigma(F_o)$]	0.0997
wR_2	0.2904
No. of reflections omitted	55
Weighting scheme parameters	a = 0.1785, b = 22.0330
(Δ/σ)	<0.001
Δρ excursions eÅ^{-3}	-1.73, 1.52

The site-occupancies and temperature factors for the disordered water molecules were respectively 0.60 and 0.06 Å^2 for OW23, 0.40 and 0.16 Å^2 for OW24. The site-occupancies of OW23 and OW24 were linked to the site-occupancies of the guests. All water molecules except OW23 and OW24 were refined anisotropically. None of the water molecules was refined with H atoms as the latter could not be located in the difference map.

Modelling of the guest

With the host refined and optimised the guests still required attention. The highest remaining peaks in the difference map were assigned and refined as bromine. Next, the phenyl rings were revealed in the difference map. An AFIX 66 instruction, constraining the ring as a rigid hexagon, was applied once all the atoms of the ring were located in the difference map. This was followed by the tedious placement and refinement of the atoms making up the urea group. At this point in the refinement it became evident that the guests were disordered. Each guest was disordered over two positions with major components A and B while the minor components are C and D. However, it was only possible to model the disorder of B (*i.e.* minor component C) as attempted modelling of the disorder related to A proved unstable. The site-occupancy factors of the major components of disorder were refined as x while their counterparts were refined as 1-x. An initial value of x = 0.5 was set and refined to 0.68. Global isotropic temperature factors were set for each component of disorder with starting values of 0.05 Å^2. These values settled between 0.04 and 0.11 Å^2 for the three components. Distance restraints were imposed to ensure reasonable geometries as the least-squares refinements were sensitive. The standard deviation for restrained bond lengths was set at σ = 0.004 Å for uniformity. Only atoms Br1A and Br1B were refined anisotropically; all other atoms belonging to the guests were refined isotropically, the guest hydrogens being added in idealised positions in a riding model. Aromatic type hydrogens refined with 1.2 times the U_{iso} of their parent atoms while the methyl hydrogens refined with 1.5

times the U_{iso} of their parent atoms. Major electron density peaks (1.5 e $Å^{-3}$) were located within 0.8 Å of atom OW23 and were ascribed to inadequate absorption correction and anisotropic motion.

STRUCTURAL DESCRIPTION

Host Conformation

Primary hydroxyl torsion angles

The primary hydroxyl torsion angles **ω** for both cyclodextrins (A and B) which make up the dimer reflect a *(-)-gauche* conformation. Thus, all the C6-O6 bonds are directed away from the cavity. The glycosidic torsion angles **Φ** and **Ψ**, as well as the pyranoid torsion angles Θ_1 and Θ_2 are in good agreement with those for B1. All the glucopyranose units for both cyclodextrins are in the $^4C_1$ conformation.

Macrocyclic symmetry

The mean radii **r** for CDs A and B are 5.04 and 5.05 Å and lie in the range 4.81 to 5.26 and 4.97 to 5.18 Å respectively. The mean length **l** of A is 4.37 Å (range 4.20-4.48 Å) while B has a mean length of 4.38 Å (range 4.28-4.47 Å). The mean glycosidic oxygen angle **a** of both CDs is 128.5˚ while the ranges are 123.9-132.6˚ for A and 125.6-130.6˚ in the case of B.

Planarity of the O4-Heptagons

The root mean square deviation **d** of the O4 atoms from the mean O4 plane of host molecules A and B is 0.032 Å and 0.052 Å respectively. The torsion angles **t** range from -4.7 to 3.9˚ for A and -3.9 to 4.4˚ for host B. Tilt angles (τ_1 and τ_2) for host A, are all positive and range from 2.0 to 13.6˚ for τ_1 and from 3.0 to 13.7˚ for τ_2. Similarly for host B, the tilt angles are positive ranging from 1.5 to 8.8˚ for τ_1 and from 2.6 to 11.5˚ for τ_2, indicative of the primary rims of the glucose residues being inclined towards the cavity, as with B1. The mean **φ** (intersaccharidic angle) value for the hosts is 118.4˚ for A and 118.0˚ for B with ranges 116.7-120.7˚ and 116.6-121.0˚ respectively.

When comparing the mean values for the parameters reported here (for hosts A and B), it is notable that the differences are small. Little variation in **l** distances results from a fairly symmetrical macrocycle. This is reinforced by the fact that **r** has little variation and is confined to a fairly narrow band and is symptomatic of a round macrocycle. The truncated cone-like appearance of both cyclodextrin molecules is confirmed by an entire set of positive tilt angles.

INTRA- AND INTERMOLECULAR INTERACTIONS

Host intramolecular interactions

17 intramolecular hydrogen bonds are observed in the dimer. There are fourteen intraglucose O2•••O3′ interactions and the rest are C-H•••O hydrogen bonds. The average hydrogen bond length for the seven O2•••O3′ bonds belonging to CD A is 2.79 Å in the range 2.73 to 2.88 Å. The seven interactions belonging to CD B have an average length of 2.81 Å in the range 2.72 to 2.84 Å. For the C-H•••O hydrogen bonds the average bond length is 3.42 Å (range 3.41 – 3.42 Å) and the average bond angle is 143.0˚ (range 142.0 - 144.0˚). The three C-H•••O hydrogen bonds stabilise the conformations of the hydroxyl group with which they are associated.

Host-Host intermolecular interactions

There are 27 intermolecular O•••O close contacts in the structure which help stabilise the head-to-head hydrogen bonded dimer. Thirteen are O2•••O3 interactions which range from 3.02 to 3.19 Å with a mean value of 3.1 Å. Seven are O2•••O2 type interactions with a mean interaction distance of 2.99 Å and a range of 2.82 to 3.11 Å. The seven remaining hydrogen bonds are indicated by O3•••O3 interactions. Their mean hydrogen bond length is 2.80 Å and they range from 2.75 to 2.93 Å.

INTER- AND INTRA-LAYER INTERACTIONS

Inter-layer interactions

There are four inter-layer interactions present in the structure; all four are O6•••O6 type interactions. The mean hydrogen bonding distance for these is 2.80 Å in the range 2.75 to 2.86 Å.

Intra-layer interactions

There are four O2•••O2 intra-layer interactions in the structure; all have interaction distances of 2.75 Å. Four O6•••O6 intra-layer interactions are also present in the structure. The mean O6•••O6 interaction distance is 2.91 Å and the range is 2.87 to 2.97 Å. Four long range intra-layer interactions were observed in the structure, all of which are C-H•••O interactions. The four interactions can further be divided into two C1-H•••O2 hydrogen bonds and two C2-H•••O3 hydrogen bonds. The C-H•••O hydrogen bonds have a mean hydrogen bond distance of 3.33 Å in the range 3.25 to 3.39 Å with a mean hydrogen bond angle of 152.0˚, these angles spanning the range 129.0 - 173.0˚.

Host-Water interactions

24 sites were refined for 21 water molecules in the asymmetric unit. 13 water molecules make O•••OW close contacts with the primary rim. 32 interactions are observed for the 13 water molecules (OW1, OW4, OW5, OW6, OW7, OW8, OW9, OW11, OW13, OW17, OW18, OW19 and OW21). The interaction distance ranges from 2.65 to 3.23 Å with a mean distance of 2.87 Å. Seven other water molecules (OW2, OW3, OW10, OW14, OW15, OW16 and OW20) make close contacts with the secondary rim; a total of 17 interactions is observed. The close contact distances range from 2.65 to 3.19 Å with a mean distance of 2.89 Å. Several of these water molecules mentioned here are also involved in water-water contacts. In fact, 16 water molecules (OW1, OW2, OW3, OW5, OW7, OW8, OW9, OW10, OW11, OW12, OW13, OW14, OW15, OW16, OW17 and OW18) are involved in the water-water contacts with a total of 26 interactions between them. The water-water contact distances

range from 2.68 to 3.16 Å and have a mean of 2.80 Å. Further, four C-H•••OW (OW = water) hydrogen bond interactions were also observed, the average interaction distance being 3.38 Å (range 3.18 – 3.46 Å) and the average angle 146.0˚ (range 126.0 – 161.0˚).

The water molecules are located both in the interstices and in the inter-dimeric interface between adjacent dimers. The interstitial water molecules are isolated on two sides by the inter- and intra-layer hydrogen bonds which run in a zigzag pattern parallel to the *b*-axis, as shown in Figure 13.

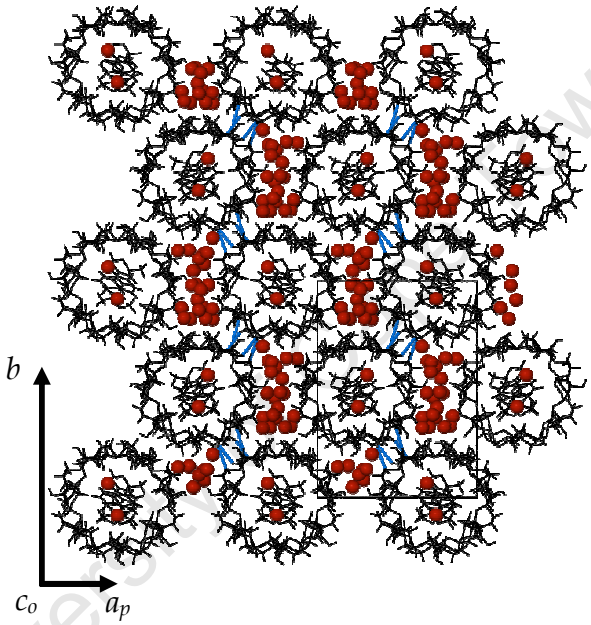

Figure 13. *Water molecules located in the interstitial spaces. Also shown is the zigzag pattern of the inter- and intra-layer hydrogen bonds (blue) which run along the b-axis. The inter- and intra-layer hydrogen bonds do not isolate the interstitial space as in **B1**. The water molecules are shown at 50% of the van der Waals radius for clarity.*

As with the previous structure, the water molecules form hydrogen bonded bridges to aid in the stabilisation of the structure.

GUEST INCLUSION

Estimated Standard Deviation (**e.s.d.**): It is noteworthy that the estimated standard deviations of the guest atoms are approximately 10 times those of the host owing to the disorder of the guests. The result is that the **e.s.d.s** of the torsion angles for the guests are unusually large.

Guest disorder

In the head-to-head hydrogen bonded dimer, two guest molecules occupy the cavity. Each guest molecule is disordered over two positions. The major components of the disorder, guests A and B (green) have an anti-parallel arrangement, Figure 14. Only one of the minor components could be modelled (blue). The other model was unstable during refinement owing to its very low site-occupancy (<0.2). Further attempts to include it in the model were therefore not warranted.

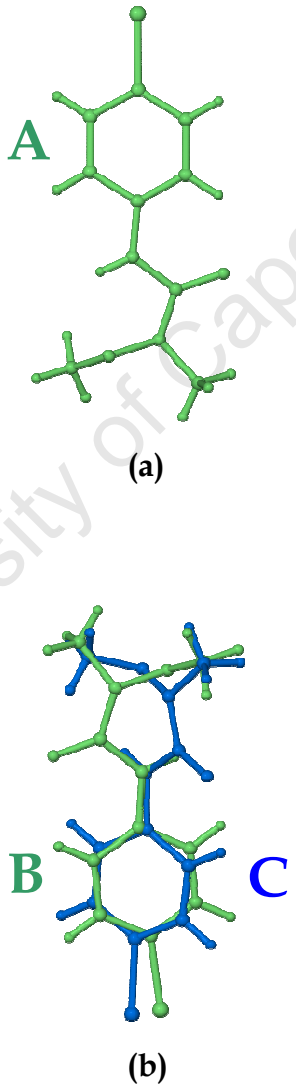

Figure 14. *Alignment of the guests in the dimeric cavity. Guests A and B (green) have an anti-parallel or tail-to-tail arrangement.*

A composite image A-B-C of the guest disorder is presented in Figure 15, representing the contents of the dimeric cavity of inclusion complex B2. The disordered images are separated and shown as models A-B and C.

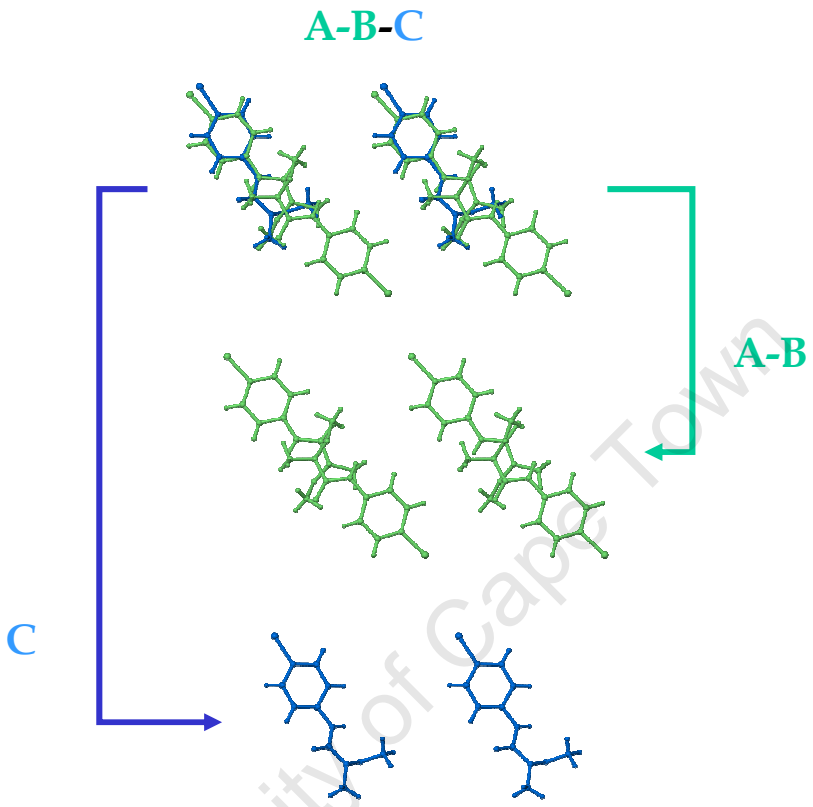

Figure 15. *Stereoview of the disordered guests A-B-C of B2 and the deconvoluted disordered components A-B (green) and C (blue).*

Guest location

For B2, the dimeric cavity accommodates two guest molecules that are arranged in an anti-parallel fashion with the bromine atoms located at opposite ends of the dimer. The guest metobromuron molecule is substantially longer than the depth of a single cyclodextrin cavity and is tilted, allowing the bromophenyl moiety to lodge at the primary rim of cyclodextrin A. The urea moiety is lodged deep within the cavity at the secondary rim interface of A, protruding into the cavity of B, as shown in Figure 16 (a).

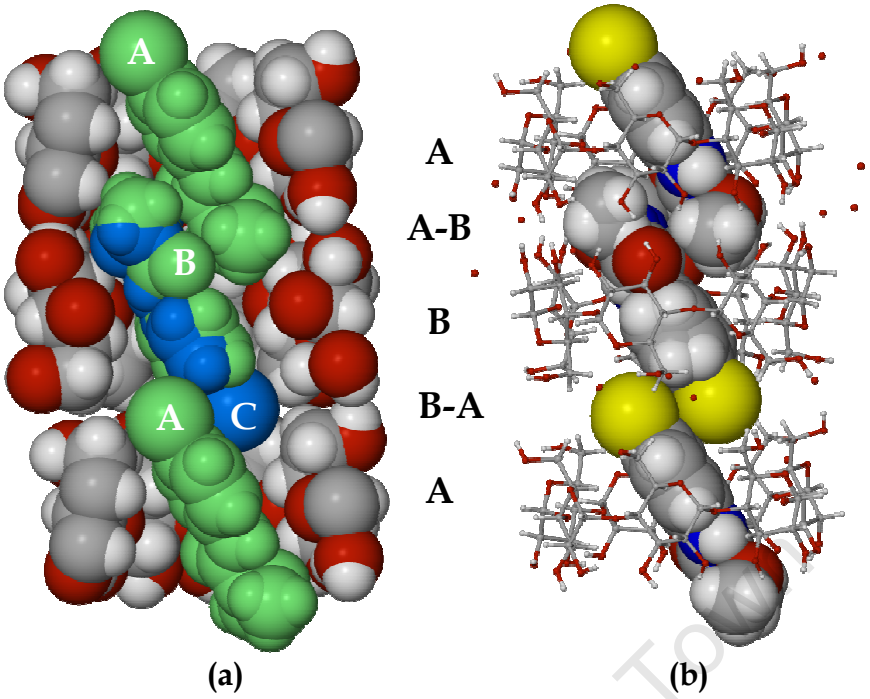

Figure 16. *Diagram (a) is a cutaway view showing the tilted guest molecules in the dimeric cavity. (b) Shows how the bromine atoms partially include at the primary rim of an adjacent dimer and how the urea groups include into the cavity of cyclodextrins A and B at the secondary rim interface (A-B), respectively.*

The bromine atoms partially include at the primary rim (B-A) of an adjacent dimer, as shown in Figure 16 (a) and (b).

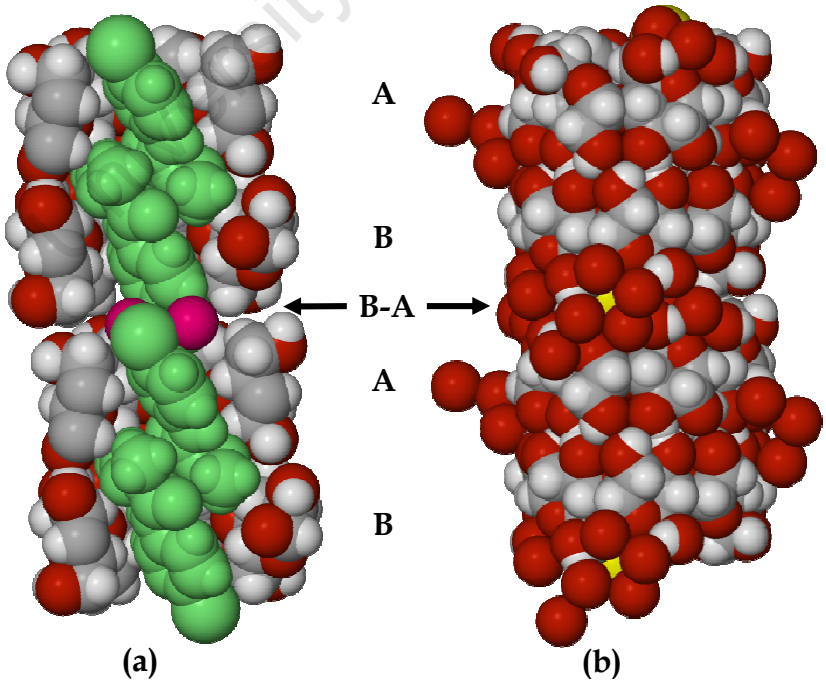

Figure 17. *(a) Shows the water molecules (pink) located in the inter-dimer interface along with the bromine atoms of the guest. (b) Shows how the inter-dimer interface is almost completely closed off by primary hydroxyl groups and interstitial water molecules.*

Further, the inter-dimer interface is almost completely closed off by the primary hydroxyl group and interstitial water molecules surrounding it. It is effectively an extension of the dimer cavity housing the bromine atoms and two water molecules, Figure 17 (a) and (b). The water molecules are shown in pink in Figure 17 (a).

The amount of tilt of each guest molecule is measured by the angle between the phenyl ring (mean plane) of each guest molecule (A, B and C) and the mean O4 plane of the cyclodextrin in which it is included. For guest A included in host A the angle is 61.7(5)˚, for guest B in host B the angle is 65.4(4)˚ and for guest C in host B the angle is 58.0(2)˚. In addition, the guest molecules are rotated with respect to each other such that the angle between the mean planes of molecules B and C is ~29˚ whereas the angle between A and B is ~15˚ and between A and C is ~ 14˚ as shown in Figure 18 (left).

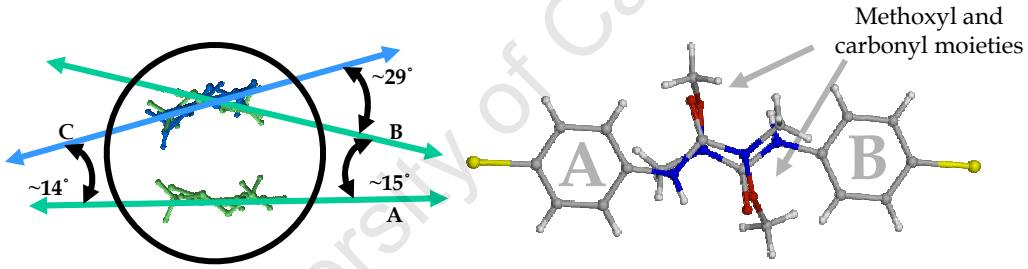

Figure 18. *The schematic diagram on the left shows the angles of intersection between mean planes of the guest molecules while the diagram on the right shows the moieties which overlap in the cavity.*

The angle formed between guest molecules A and B is such that the distance between the methoxyl and carbonyl moieties of the guest molecules is maximised. This prevents unacceptable close contacts between guests A and B (Figure 18). The shortest contact distance between guests A and B is 3.01 Å (O10A•••C13B).

Guest conformations

Inclusion of the guest within the cavity of the cyclodextrin has an effect on the guest conformation. These effects are communicated through changes to the torsion angles of the guest. Some of the torsion angles are more responsive to

the confined environment of the cavity and therefore show greater deviations in their values when compared to those of the uncomplexed guest. We have therefore selected only pertinent torsion angles to report and compare against those of the uncomplexed guest. Also, the two intramolecular hydrogen bonds are present in this structure of the complexed guest. This is an indication that the overall conformation has not deviated too far from that of the uncomplexed guest (**1**). A complete list of the torsion angles selected for comparison is reported in the appendix. Torsion angle τ_1 which involves atoms C4/6-C5-N8-C9 of the included guests A, B and C has the largest deviation from τ_1 (-140.9(2)˚) for the uncomplexed guest. τ_1 for A, B and C spans the range -25(6)˚ to +2(3)˚ and the effect can clearly be seen in Figure 19 (c). Figures 19 (a), (b) and (d), offer alternative views to the one presented in Figure 19 (c). τ_2 ranges from -4(7)˚ to -1(4)˚, a narrow range of values which are close to the value of τ_2 for the uncomplexed guest. τ_3 ranges from -170(1)˚ to +173(4)˚ indicating an 'extended' conformation for the three guests. The 'extended' conformation is also owing to the *trans*-planar conformation of the amide group. τ_4 ranges between -29(2)˚ and +21(4)˚.

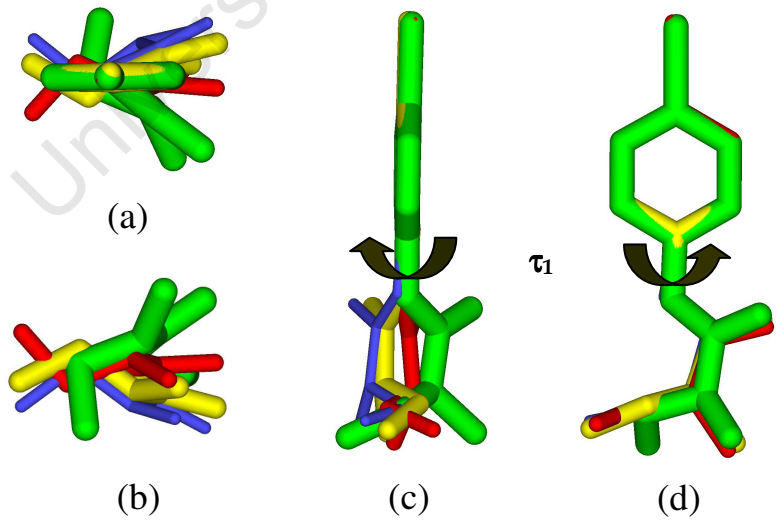

Figure 19. *Relative conformations of the included guest as compared with that of the uncomplexed guest. Guest A - yellow, guest B - blue, guest C - red, and uncomplexed guest - green.*

τ_5 spans the range -170(4)˚ to +159(2)˚ and is close to -180/180˚. τ_6 ranges from -27(3)˚ to 33(2)˚ while τ_7 ranges from -164(3)˚ to

+171(3)˚. τ_8 and τ_9 range from -116(2)˚ to +123(1)˚ and -105(2)˚ to +100(2)˚ respectively, an indication that the disposition of bond C13-O12 is nearly perpendicular to the mean plane passing through C9, O10, N11, O12 and C14.

HYDROGEN BONDING INTERACTIONS OF THE GUEST

Host-Guest intermolecular interactions

Eleven intermolecular host–guest interactions were observed. Five are C-H•••O hydrogen bonds with an average bond length of 3.34 Å covering the range 3.22 - 3.43 Å. The average hydrogen bond angle is 147.0° in the range 127.0 to 170.0˚. Three C-Br•••H(C) interactions were observed with a mean distance of 3.18 Å and a range from 3.17 to 3.19 Å. Three host-guest close contacts (O•••O, C•••C and Br•••C) were also observed; the mean interaction distance is 3.43 Å in the range 3.20 to 3.62 Å.

Guest-guest intermolecular interactions

Four intermolecular close contacts (C•••O, C•••C and Br•••C) were observed between the guests. The mean interaction distance is 3.35 Å covering the range from 3.01 to 3.58 Å.

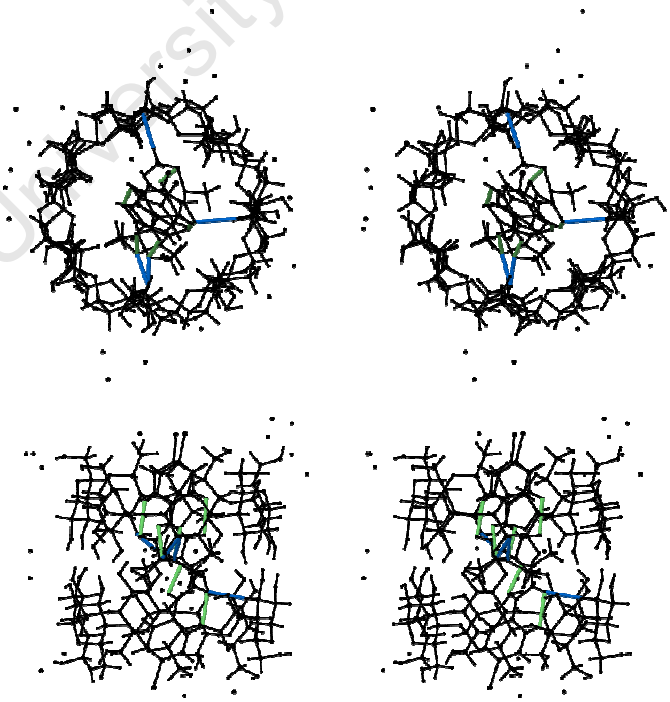

Figure 20. *The stereogram shows the intermolecular hydrogen bond interactions between the host and guest (blue) in the cavity (top). The diagram also shows the intramolecular hydrogen bonds (green) of the guest (bottom).*

Guest intramolecular interactions

Six intramolecular hydrogen bonds were observed for the guests. Three are N-H•••O hydrogen bonds with lengths in the range 2.52 - 2.61 Å (mean = 2.57 Å) and the hydrogen bond angle ranging from 100.0 to 109.0° (mean = 106.0˚). For the uncomplexed guest the N-H•••O distance is 2.57 Å while the angle is 110.0˚. The three remaining bonds are C-H•••O bonds spanning a narrow range of 2.77 - 2.89 Å (mean = 2.81 Å) while the angular range is 112.0 - 118.0° (mean = 116.0˚). The C-H•••O bond length for the uncomplexed guest is 2.93 Å while the hydrogen bonding angle is 107.0˚.

The intermolecular bonds serve to stabilise the host-guest interaction while the guest intramolecular interactions stabilise the guest conformation. The host-guest intermolecular hydrogen bonds are shown in green in Figure 20.

Guest-Water interactions

Four close contacts between the guest and included water were observed, one C-H•••OW (water) hydrogen bond and the others are Br•••OW interactions. The hydrogen bond length for the C-H•••OW type is 2.94 Å while the hydrogen bond angle is 134.0˚. The Br •••OW interaction distance ranges from 2.74 to 3.39 Å. The interactions are shown in Figure 21.

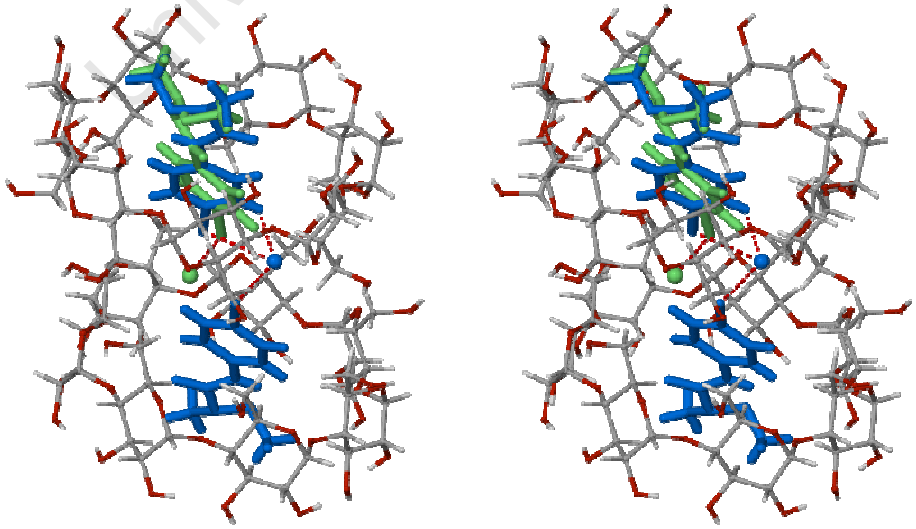

Figure 21. *The stereo view shows the Br•••OW interactions which occur in the inter-dimer interface. The guests and water molecules are colour coded according to their site-occupancy.*

CRYSTAL PACKING

B2 is also characterised by the channel packing arrangement **CH** ($P2_1$). The channels extend infinitely along the *c*-axis. The mean O4 planes of the dimer are inclined at ~10˚ to the *ab*-plane and are stacked on top of each other in columns which propagate in layers along the *c*-axis. When viewed perpendicular to the O4 heptagons it is noticeable that consecutive layers are laterally offset by 2.25 Å (Figure 22) with O4 heptagons inclined by 1.70(3)˚ to each other. The inter-dimer distance measured across the inter-dimer interface is ~9.2 Å.

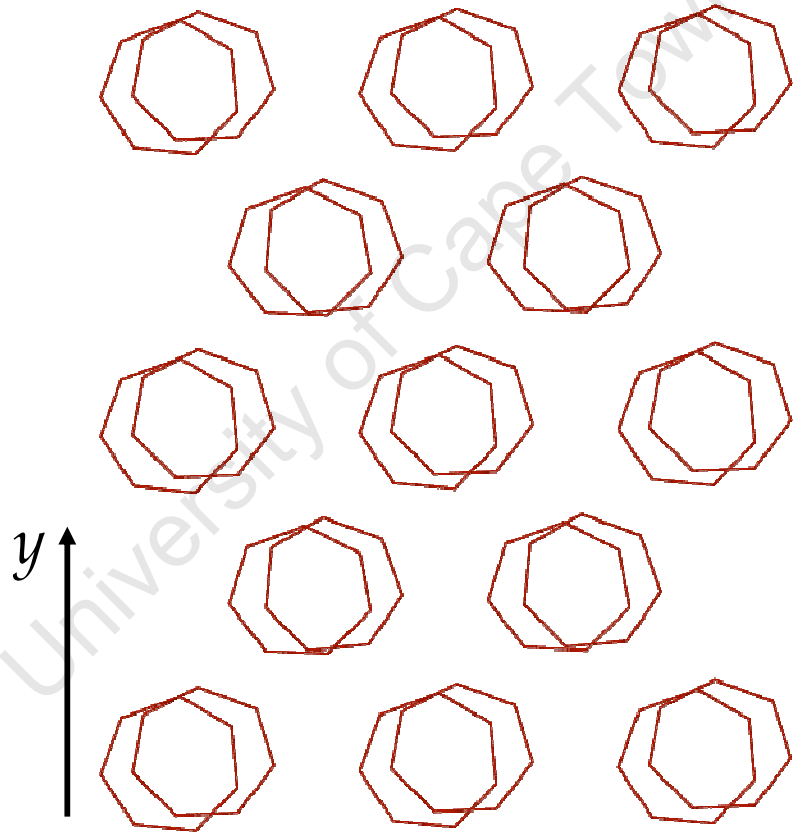

***Figure* 22.** *Lateral displacement of O4-heptagons of dimers in adjacent layers when viewed perpendicular to the mean O4 plane.*

There are three screw axes parallel to the *b*-axis, located at 0, ½ and 1 along the *a*- and *c*-axes, Figure 23. The columns along the *b*-axis have a zigzag arrangement with alternate columns having opposite orientation (shown in green).

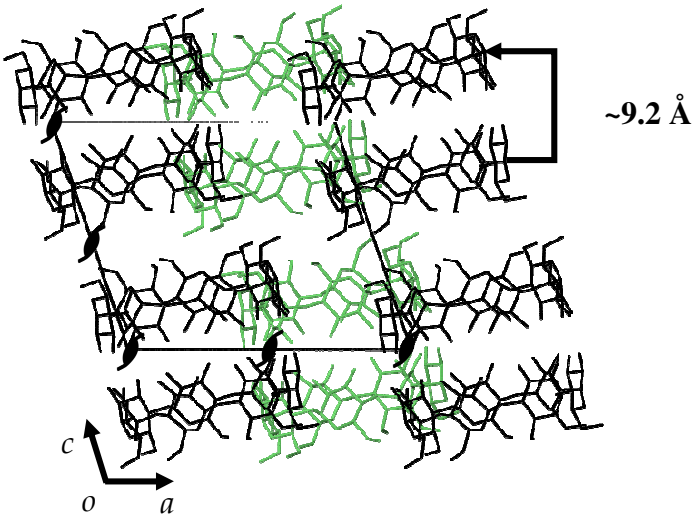

Figure 23. *Packing of the host molecules in B2.*

The $P2_1$ **CH** type packing arrangement has a dimer located at (-x, ½ + y, -z) and therefore has a pseudo-C-centred appearance. It is not C-centred since the orientation of the column located at (-x, ½ + y, -z) is reversed. This is shown more clearly in Figure 24 (a) and (b) below.

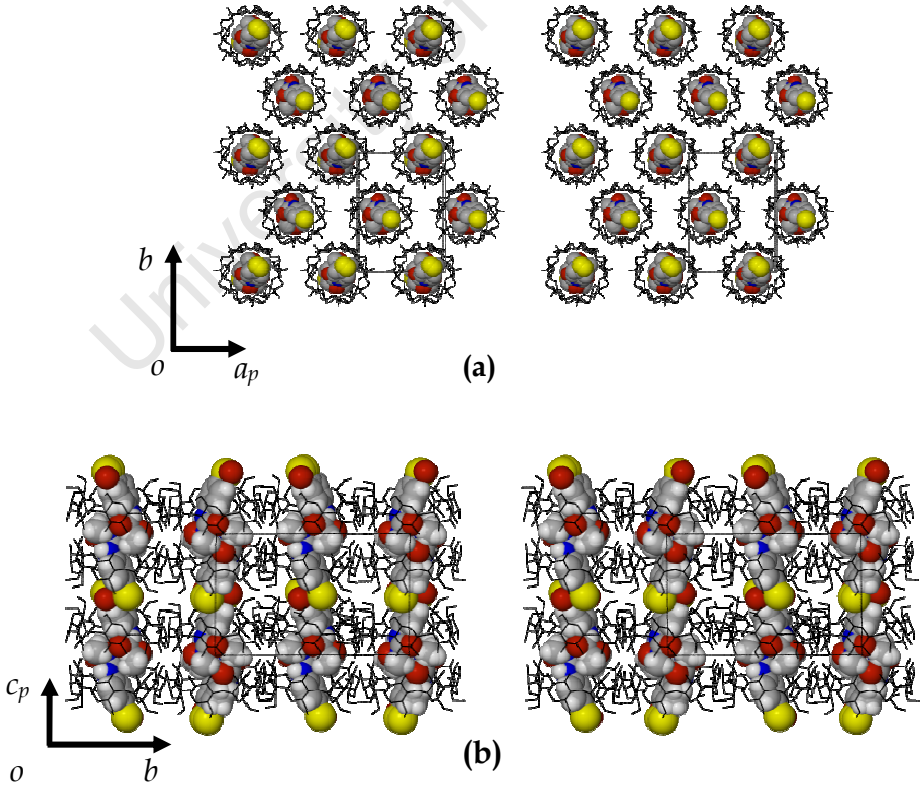

Figure 24. *The stereo diagram (a) shows clearly the opposite orientation of the columns located at -x, ½+ y, -z. The stereo diagram (b) shows an alternative projection along the a-axis.*

Comparative PXRD

Calculated and experimental traces for B2 are shown in Figure 25. There is a very close match in peak positions between the traces, differences in peak intensities being due to preferred orientation in the powdered sample. The general shift of peaks in the calculated PXRD pattern to higher 2θ values is due to the low temperature of the data-collection for the single crystal X-ray analysis. The match between the calculated and experimental PXRD patterns confirms the single crystal as being representative of the bulk material.

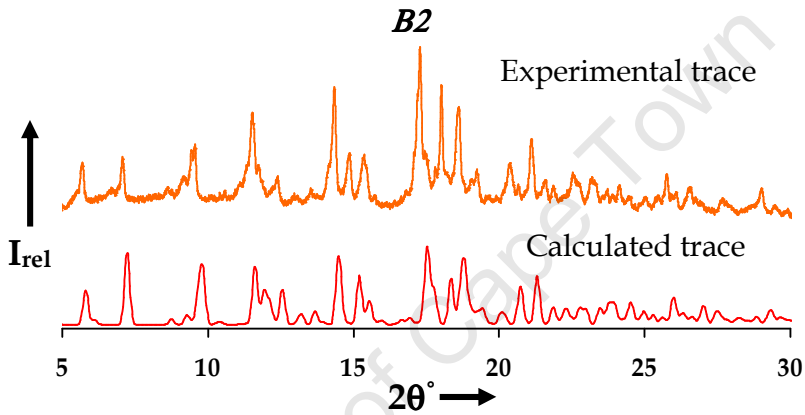

Figure 25. *Calculated and experimental PXRD traces for B2.*

X-RAY STRUCTURE OF B3

Space group determination

LAYER was employed to determine the crystal system and space group of B3.[1] The crystal system was found to be triclinic as the Laue symmetry was $\bar{1}$ and the space group P1 since the cyclodextrin is chiral. Confirmation of the crystal system and space group was obtained using XPREP.[2] B3 crystallises in the triclinic space group P1 with $Z = 1$ dimeric complex unit per unit cell.

Structure solution and refinement

Table 10 contains refinement parameters and crystal data for B3. The asymmetric unit consists of a single dimeric β-CD complex made up of two crystallographically independent cyclodextrins which are hydrogen bonded in a head-to-head manner and 21 water molecules. Each cyclodextrin molecule contains a single guest molecule. The structure was found to be isostructural with an existing complex [2(β-CD)•2(*p*-bromoacetanilide)•27(H_2O)] whose unit cell parameters are very similar to those of B3. Only the host coordinates were used as input fragment to solve the phase problem.[19] All guest, water molecules and O6 atoms were deleted from the trial structure in order to model any disorder which might be present. The glucopyranose units for the two host molecules in the asymmetric unit were labelled A1-A7 and B1-B7. The structure was refined with SHELXH-97 with successive difference Fourier maps revealing the O6 atoms.[5] Atoms C6A1, O6A1, C6A5, O6A5, C2B1, O2B1 and O3B1 of the host were disordered over two positions. The major components of the disordered atoms were assigned a value of x for their s.o.f.s while the minor components (C6C1, O6C1, C6C5, O6C5, C2C1, O2C1 and O3C1) were assigned the value 1-x. An initial value of x = 0.5 was set. It refined to 0.54 for A1, 0.63 for A5 and 0.76 for the major components of the disorder. All hydrogen atoms attached to carbon atoms were placed and refined in geometrically calculated positions using the AFIX 43 instruction (riding model). The hydrogen atoms of the

hydroxyl groups were placed using the AFIX 83 instruction (hydrogen bond searching model).

Table 10. *Crystal data and data-collection parameters for B3.*

parameters	*B3*
Formula unit	$(C_{42}H_{70}O_{35})_2 \bullet (C_9H_{11}N_2O_2Br)_2 \bullet 21H_2O$
Mr	3166.53
Crystal system	triclinic
Space group	P1
a/Å	15.2246(3)
b/ Å	15.3951(3)
c/ Å	15.7047(3)
α/°	87.71(3)
β/°	97.407(3)
γ/°	103.677(3)
Vol. Å^3	3546.54(1)
Z	1
ρ_{calc} g cm^{-3}	1.483
μ (MoKα) mm^{-1}	0.690
F(000)	1674
Crystal size mm^3	0.10 x 0.10 x 0.08
Temperature K	113 ± 2
Range scanned θ/°	3.6 ≤ θ ≤ 25.4
Index range	-18 : 18; -18 : 18; -18 : 18
ϕ Scan angle °	1.0
ϕ Scan range °, no of frames	363, 363
ω Scan angle °	1.0
ω Scan range °, no of frames	101.0, 101; 63.0, 63; 99.0, 99; 43.0, 43; 43.0, 43; 32.0, 32
Dx mm	31
No. of reflections	56849
No. of unique reflections	20653
No. of reflections with I>2σ(I)	12696
No. of l.s. parameters	1650
R_{int}, R_σ	0.131, 0.185
S	0.989
R_1 [$F_o > 4\sigma(F_o)$]	0.1148
wR_2	0.2939
No. of reflections omitted	68
Weighting scheme parameters	a = 0.1813
(Δ/σ)	<0.001
Δρ excursions eÅ^{-3}	-0.88, 0.98

All hydrogen atoms were assigned isotropic temperature factors which were 1.2 times those of their parent atoms. 24 sites for water molecules were located in a series of difference electron-density maps accounting for 21.8 water molecules. 18 water molecules had full site-occupancy while six were disordered with partial occupancy. The temperature factors of the disordered water molecules range from 0.07 to 0.20 Å^2. 21 water molecules were found from TG analysis (n = 2). The site-occupancies of the disordered water molecules are listed in Table 11. 13 water molecules were refined isotropically while the rest were refined anisotropically. The 13 water molecules are OW4, OW7, OW11, OW14, OW15, OW16, OW17, OW18, OW19, OW20, OW21, OW22 and OW24. Water H atoms could not be located in the electron density maps.

Table 11. *Site-occupancies for disordered water molecules in complex B3.*

Atom	OW4	OW15	OW18	OW20	OW22	OW23
s.o.f.	0.44	0.55	0.45	0.87	0.80	0.73
U_{ISO} (Å^2)	0.11	0.07	0.04	0.13	0.15	0.11

Modelling of the guest

The two major peaks in the electron density map were assigned as bromine atoms. This was followed by the placement of the phenyl rings which were easily identifiable from the hexagonal geometry. An AFIX 66 command was applied to the atoms of the ring allowing it to refine as a rigid hexagon. This was followed by the piecemeal assembly of the 1-methoxy-1-methylurea moieties. Refining the methoxyl-1-methylurea moiety was slow and painstaking as there were several possible scenarios owing to disorder. As it turns out, both guest molecules are disordered over two positions. The two major components of the disorder were assigned the same site-occupancy variable x while the two minor components refined as 1-x. The initial value of x was set to 0.5. The s.o.f.s of the major components settled to 0.51. The four models were assigned individual global isotropic temperature factors, which settled to 0.06, 0.07, 0.07 and 0.08 Å^2. Several distance restraints were applied to the guest molecules to maintain reasonable geometries while the standard

deviation used for restrained bond lengths was σ = 0.004 Å for uniformity. Only atoms Br1A and Br1C were refined anisotropically; all other atoms belonging to the guests were refined isotropically. All the guest hydrogen atoms were placed in idealised positions in a riding model. U_{iso} for the aromatic hydrogens was 1.2 times that of the parent atom and all methyl hydrogens were given thermal parameters 1.5 times the U_{iso} of the parent atom. Major electron density peaks (0.97 e $Å^{-3}$) were located near Br1B and Br1D. The peaks were ascribed to residual anisotropic motion which was not modelled.

STRUCTURAL DESCRIPTION

Host conformation

Primary hydroxyl torsion angles

The primary hydroxyl torsion angles **ω** for both cyclodextrin molecules (A and B) comprising the dimer indicate a *(-)-gauche* conformation, except for the disordered O6 atom O6C5. The torsion angle O5A5-C5A5-C6C5-O6C5 has a *(+)-gauche* conformation with the C6-O6 bond pointing towards the cavity. The glycosidic (**Φ** and **Ψ**) and pyranoid (Θ_1 and Θ_2) torsion angles compare well with those measured for B1 and B2. The conformations of the glucopyranose units are all $^4C_1$.

Macrocyclic symmetry

The mean radii **r** for CDs A and B are 5.04 and 5.02 Å respectively. Both have quite narrow ranges of 4.80 to 5.24 Å for A and 4.72 to 5.24 Å for B. The mean **l** values for CDs A and B are 4.37 and 4.35 Å respectively while the ranges are 4.26-4.49 Å for A and 4.31-4.41 Å for B. The mean glycosidic oxygen angle **a** for both CDs is 128.5˚ while the glycosidic angles for both CDs fall within the range 125.2-132.5˚.

Planarity of the O4-Heptagons

The root mean square deviations **d** for the O4-heptagons of cyclodextrins A and B are 0.036 Å and 0.045 Å respectively. Each cyclodextrin has two O4

atoms with negative deviations; these are O4A1 and O4A5 for CD A while O4B4 and O4B7 for CD B have negative deviations. The torsion angle (**t**) for host A ranges from -3.6 to 2.5˚ while in the case of B it ranges from -3.4 to 4.8˚. τ_1 and τ_2 for host A are all positive with τ_1 ranging from 1.1 to 9.3˚ while τ_2 ranges from 1.5 to 15.6˚. τ_1 and τ_2 for host B are also all positive with τ_1 ranging from 0.1 to 13.2˚ and τ_2 ranging from 1.8 to 14.4˚. The mean φ for CDs A and B is 117.5˚ and 118.3˚ respectively with both sets of values falling within the range 115.4-119.5˚.

Differences between the parameters of the two independent CD molecules are small, with the symmetrical shape of each cyclodextrin reflected in narrow ranges of the radii, O4•••O4′ lengths and glycosidic oxygen angles. The similarity in these values for the two cyclodextrins reinforces the pseudo-twofold symmetry of the dimer. Each cyclodextrin has a truncated cone-like appearance, as is the case with B1 and B2.

INTRA- AND INTERMOLECULAR INTERACTIONS

Host intramolecular interactions

17 intraglucose hydrogen bonds are observed in the structure. Fourteen are O2•••O3′ close contacts and three are C-H•••O hydrogen bonds. The O2•••O3′ distances range from 2.67 to 2.84 Å for CD A with a mean value of 2.78 Å while the range for CD B is from 2.68 to 2.81 Å and the mean is 2.75 Å. The three C6-H•••O5 hydrogen bonds have a mean bond length of 3.39 Å (range 3.38 – 3.40 Å) and a mean hydrogen bond angle of 139.0˚ (range 137.0 – 141.0˚). The three C6-H•••O5 hydrogen bonds are similar to those found in B2 and therefore act in the same manner, stabilising the hydroxyl groups with which they are associated.

Host-Host intermolecular interactions

There are 30 intermolecular interactions present which participate in the stabilisation of the hydrogen bonded dimer. There are seven O3•••O3 interactions with a range of 2.76 to 3.00 Å (mean = 2.83 Å). There are 13

interactions of the type O2•••O3. The mean hydrogen bonding distance is 3.06 Å in the range 2.91-3.17 Å. The ten remaining interactions are O2•••O2 interactions with a mean distance of 3.03 Å in the range 2.96 to 3.13 Å.

INTER- AND INTRA-LAYER INTERACTIONS

Inter-layer interactions

Five inter-layer interactions are observed in the structure. Four are of the type O6•••O6 with a mean hydrogen bond distance of 2.79 Å in the range 2.55 to 2.90 Å. A single C6-H•••O6 hydrogen bond is also observed with a bond length of 3.48 Å and a bond angle of 154.0˚.

Intra-layer interactions

There are 14 intra-layer interactions in the structure. These are divided into O6•••O6, O2•••O2, C-H•••O. The mean interaction distance for the seven O6 •••O6 interactions is 2.83 Å with a range of 2.75 to 2.93 Å. The five O2•••O2 interactions have an interaction distance range of 2.73 to 2.85 Å and a mean distance of 2.76 Å. There are eight C-H•••O hydrogen bonds made up of four C1-H•••O2 and four C2-H•••O3 hydrogen bonds. The mean hydrogen bond distance and angle for the eight C-H•••O interactions are 3.31 Å and 150.0˚. The C•••O distance and C-H•••O angular ranges are 3.26-3.42 Å and 128.0-172.0˚ respectively.

Host-Water interactions

24 sites were refined for 21 water molecules in the asymmetric unit. 78 interactions are observed between the water molecules and the host cyclodextrins. 12 water molecules are involved in O•••OW close contacts with the primary rim. The number of interactions between the primary rim and the water molecules amounts to 26. These interactions range from 2.66 to 3.21 Å with a mean distance of 2.97 Å. Nine other water molecules are involved in O•••OW close contacts with the secondary rim, having a total of 21 interactions. These interactions range from 2.61 to 3.22 Å with a mean value of 2.78 Å. Several water molecules which are involved in forming close contacts with the cyclodextrin also participate in water-water interactions. 30

water-water interactions are observed among the 22 water molecules. The O•••O distances range from 2.44 to 3.24 Å and have a mean of 2.86 Å. Two water molecules only have water-water interactions. There is also a single C-H•••OW hydrogen bond with a hydrogen bond distance of 3.43 Å and a bond angle of 148.0˚.

GUEST INCLUSION

Guest disorder

The dimer is occupied by two guest molecules, each disordered over two positions. The disordered components have near equal site-occupancy. Both models are arranged in a tail-to-tail, anti-parallel orientation as shown in Figure 26. None of the atom locations of the guests is shared between disordered components.

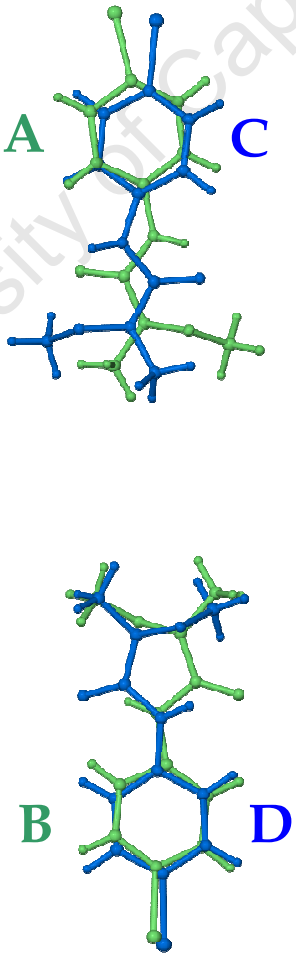

Figure 26. *The diagram shows the alignment of the guests in the dimer cavity. Guests A and B (green) and C and D (blue) have an anti-parallel or tail-to-tail arrangement.*

Guests A and B (green) form one guest pair while guests C and D (blue) comprise the other guest pair.

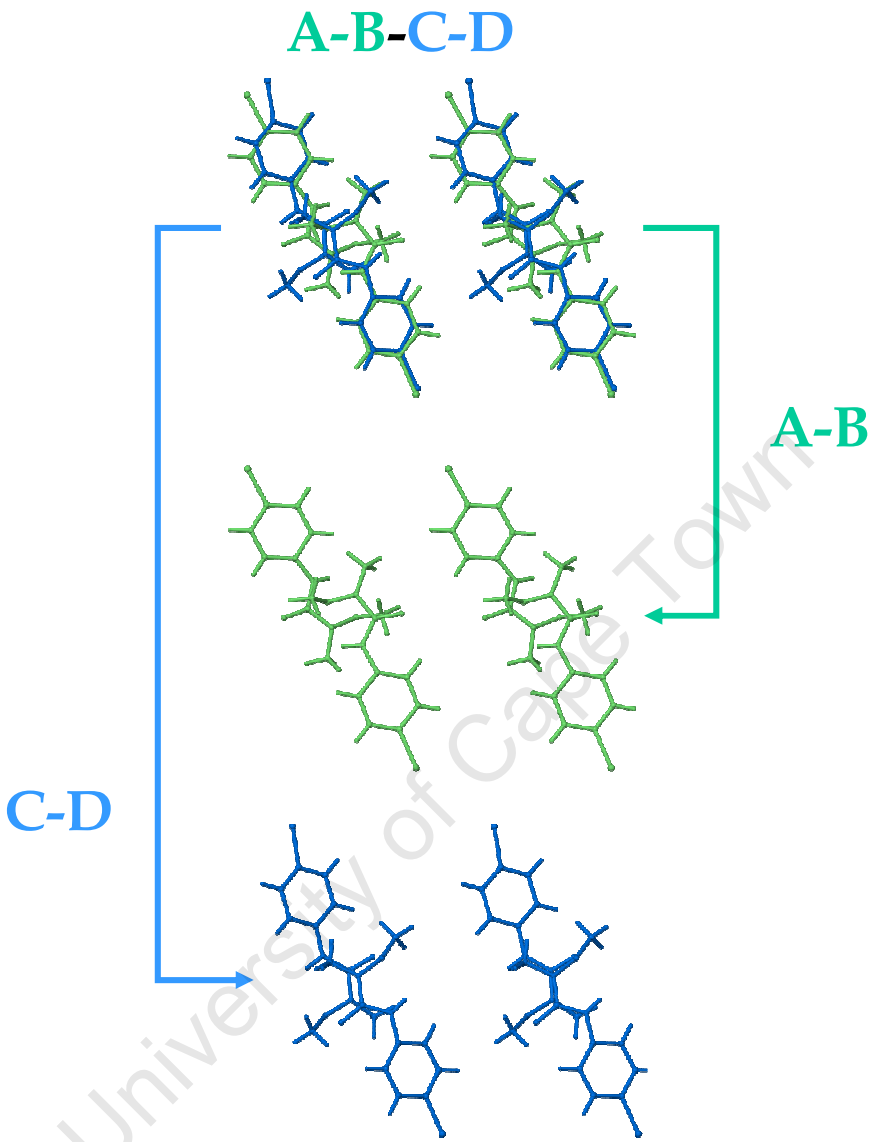

Figure 27. *Stereoview of the disordered guests A-B-C-D of **B3** and the deconvoluted disordered components A-B (green) and C-D (blue).*

In the composite image shown in Figure 27, A-B-C-D represents the contents of the cavity of B3. Images A-B and C-D represent the deconvolution of the disorder.

Guest location

The dimeric complex consists of two cyclodextrin molecules containing two guest molecules and a water molecule with half occupancy, shown in

Figure 28 (a). Each guest molecule is disordered over two positions inside the dimeric cavity. In order for the guests to be accommodated in the cavity they are tilted with respect to the O4 heptagon of each cyclodextrin. Thus, for guest A with host A the angle is 59.2(6)˚, guest B in host B 65.1(7)˚, guest C in host A 60.0(8)˚ and for guest D in host B 58.9(3)˚. As with B2, the guests are arranged in anti-parallel manner with the bromophenyl moiety located at the primary rim of the first CD molecule while the urea moiety protrudes into the cavity of the second CD molecule and is lodged at its secondary rim, as shown in the Figure 28 (b).

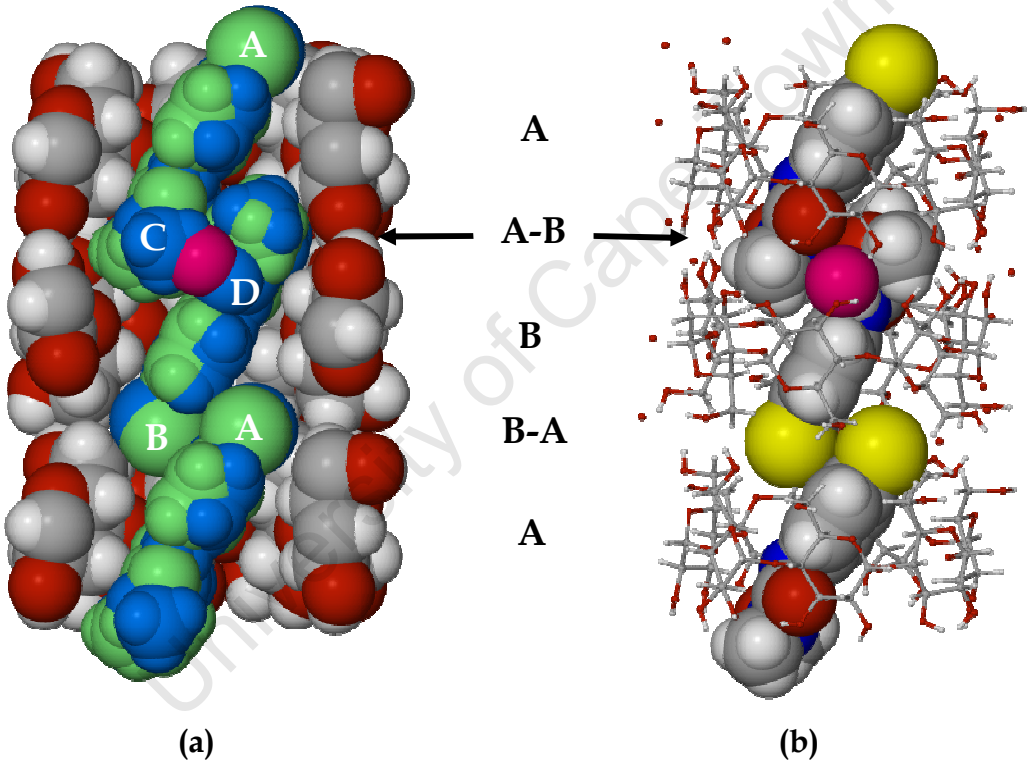

Figure 28. *Diagram (a) shows the tilted guest molecules in the dimer cavity. (b) Shows how the bromine atoms partially include at the primary rim of an adjacent dimer and how the urea groups include into the cavity of cyclodextrins A and B at the secondary rim interface (A-B), respectively. Guest disorder has been omitted in (b) for clarity.*

Furthermore, the bromine atom extends into the inter-dimer interface (B-A) and partially includes into the primary rim of an adjacent dimer. The inter-dimer interface is therefore occupied by two bromine atoms as with the previous structure. The dimer interface is closed off by the primary hydroxyl

groups of adjacent dimers and interstitial water molecules, Figure 29 (a) and (b).

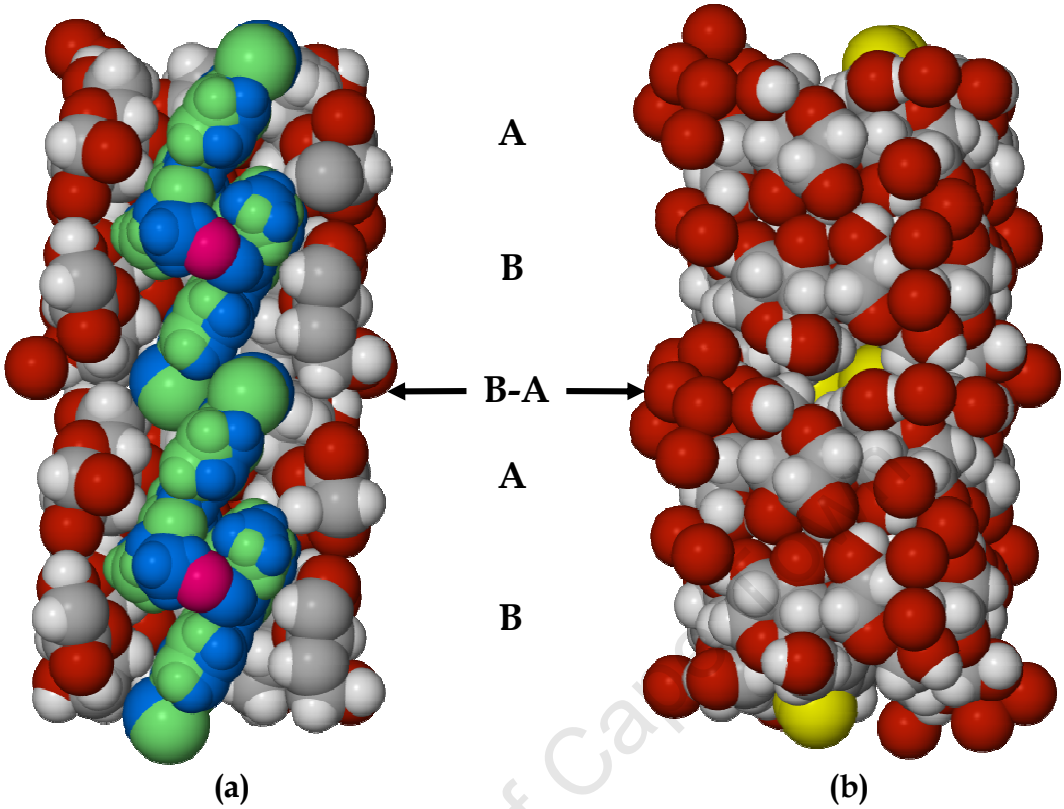

Figure 29. *(a) Shows the water molecule (pink) located in the dimer cavity just below the secondary rim interface. (b) Shows how the inter-dimer interface is almost completely closed off by primary hydroxyl groups and interstitial water molecules.*

The guest molecules are rotated away from each other. The mean planes of guests A and B are rotated by ~17˚ to each other while those of guests C and D are rotated by ~1˚ only. The interplanar angle between guests B and D is ~17˚ while A and C have an interplanar angle of ~29˚, shown in Figure 30.

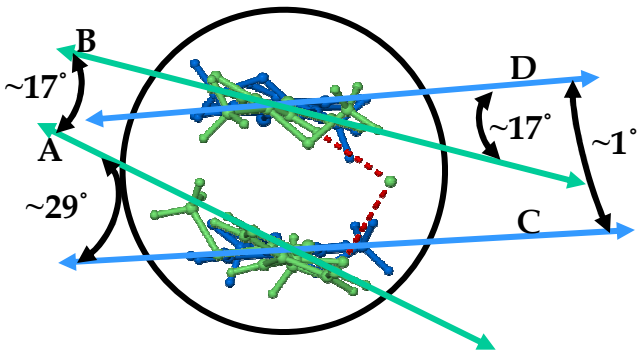

Figure 30. *The schematic diagram shows the angles of intersection between the mean planes of the guest molecules.*

The presence of a single water molecule located between guests A and B contributes to the large angle between them. Guest A makes a close O•••OW contact with the water molecule (OW4, 2.78 Å) via the carbonyl oxygen, while guest B is involved in a N-H•••OW hydrogen bond (3.25 Å, 171.0˚) via the secondary amine hydrogen, as shown in Figure 31 (a).

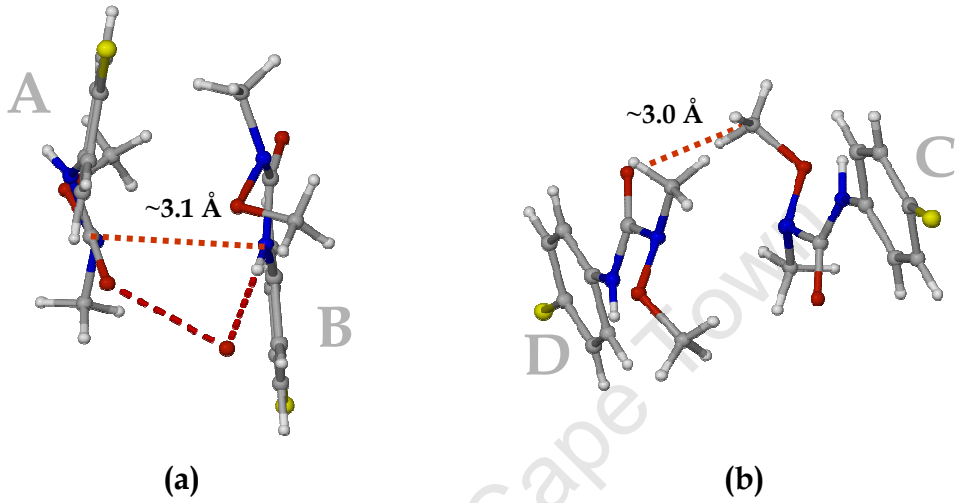

Figure 31. *Diagram (a) shows the hydrogen bonding interactions between the water molecule and guests A and B. (b) Shows the near parallel alignment of the mean planes of guests C and D with close contact distance of ~3.0 Å.*

The close contact distance of ~ 3.0 Å is a result of the nearly parallel alignment of guests C and D, Figure 31 (b). Furthermore, the N-H•••OW and O•••OW interactions act in a similar way as those reported in chapter five of this thesis and elsewhere.[19,20]

Guest conformations

τ_1 for the guests of B3 has the greatest deviation from the torsion angles reported for the uncomplexed guest. The range is -45(3)˚ to +29(4)˚. The deviations vary in size from guest to guest and are clearly seen in the four images (a), (b), (c) and (d) presented in Figure 32. τ_2 ranges from -1(7)˚ to +20(4)˚ and deviates significantly from τ_2 for the uncomplexed guest. As with the uncomplexed guest, τ_3 is very close to -180/180˚ having a range of -177(2)˚ to +165(3)˚. This indicates an 'extended' conformation as with the uncomplexed guest.

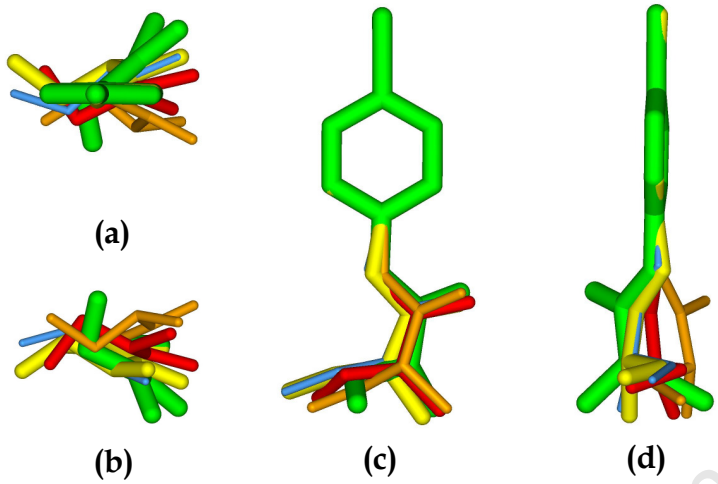

Figure 32. *The diagram shows the relative conformations of the included guest as compared with that of the uncomplexed guest. Guest A - yellow, guest B - blue, guest C - red, guest D - brown and uncomplexed guest - green.*

τ_4 and τ_6 have ranges of -30(1)˚ to +30(4)˚ and -43(4)˚ to +28(2)˚ respectively. τ_5 and τ_7 range from -172(1)˚ to +150(3)˚ and from -164(2)˚ to +169(2)˚, in that order. The ranges for τ_8 and τ_9 are from -123(2)˚ to +125(2)˚ and from -107(2)˚ to +109(2)˚ indicative of the C13-O12 bond being almost perpendicular to the mean plane through C9, O10, N11, O12 and C14.

HYDROGEN BONDING INTERACTIONS OF THE GUEST

Host-Guest intermolecular interactions

Several intermolecular hydrogen bonds were observed in the structure. Seven are C-H•••O hydrogen bonds with a mean hydrogen bond distance of 3.34 Å ranging from 3.18 to 3.52 Å. The mean hydrogen bond angle is 144.0˚ covering the range 126.0 to 175.0˚. There are also several C-H•••Br interactions with a mean interaction distance of 3.05 Å and covering the range 2.85 to 3.25 Å. A number of close contacts were also observed in the structure with a mean interaction distance of 3.25 Å in the range 2.71-3.58 Å. The C-H•••O interactions are shown in Figure 33.

Guest-guest intermolecular interactions

There are four intermolecular close contacts involving the guests. The mean interaction distance is 3.15 Å in the range 3.05 to 3.32 Å. There is a single weak C-Br•••π interaction with a distance Br•••ring centroid of 3.98 Å and an angle of 121.0˚. C-Br•••π interactions are considered as strong if the interaction distance is less than or equal to the sum of the van der Waals radii. Weak interactions have an interaction distance equal to the sum of the van der Waals radii plus 10%.[21,22]

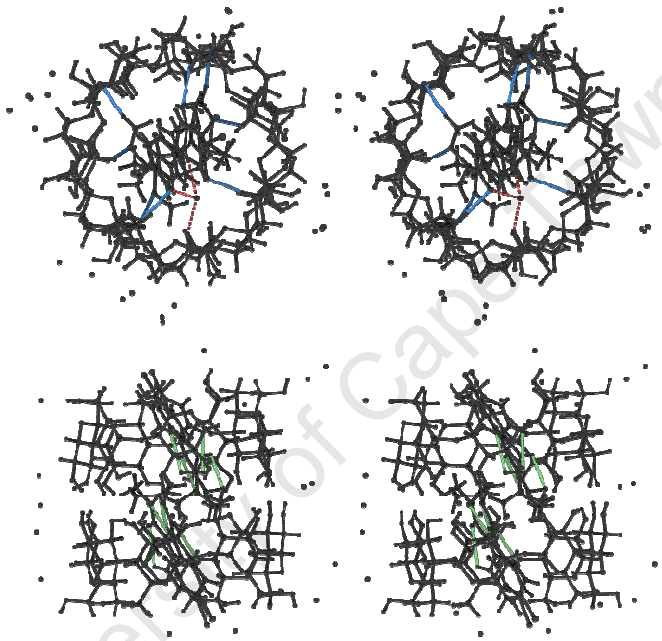

Figure 33. *(top) The stereogram shows the intermolecular hydrogen bond interactions (blue) between the host and guest in the cavity. The diagram also shows the hydrogen bonding interactions between the guests, the water molecule and the host molecule (red dashed line). (bottom) The diagram shows the intramolecular hydrogen bonds (green) in the guest molecule.*

Guest intramolecular interactions

There are eight intramolecular hydrogen bonds present; four are C-H•••O type while the remaining four are N-H•••O type. The C•••O distances for the C-H•••O type interactions range from 2.93 to 3.03 Å with a mean of 2.96 Å while the C-H•••O hydrogen bonding angle ranges from 108.0 to 118.0˚. The mean value is 112.0˚. These interactions are shown as green bonds in Figure 33 (bottom image). The range of distances for N-H•••O interactions is from 2.56 to 2.73 Å with a mean distance of 2.61 Å. The bond angle range is 104.0-108.0˚ and its mean is 106.0˚.

CRYSTAL PACKING

B3 packs in the channel packing arrangement, **CH** (P1). The channel packing axis is parallel to the *c*-axis and extends infinitely, as shown in Figure 34. The O4 mean planes are inclined to the *ab*-plane by ~10˚. The layers propagate along the *c*-axis. When viewed perpendicular to the O4 heptagons it becomes apparent that the O4 heptagons of adjacent dimers are laterally displaced, Figure 35. The size of the displacement is ~2.3 Å. The mean O4 planes of the dimer are inclined at 1.79(4)˚ to each other. The inter-dimer distance which is measured across the inter-dimer interface is ~8.7 Å.

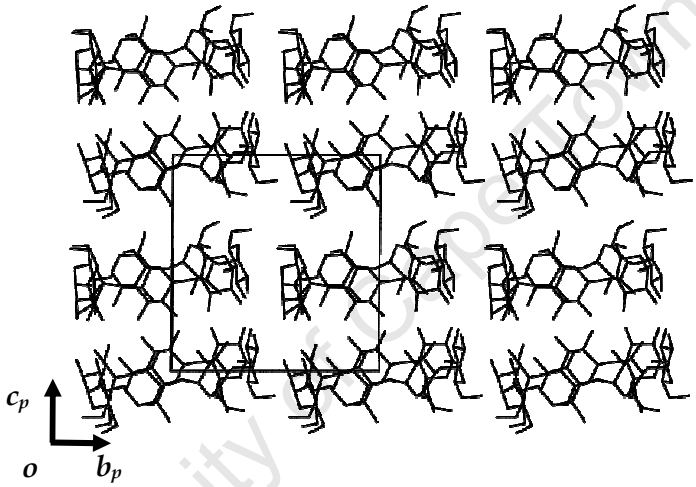

Figure 34. *Packing diagram of the B3 structure viewed along the a-axis. Guest molecules omitted.*

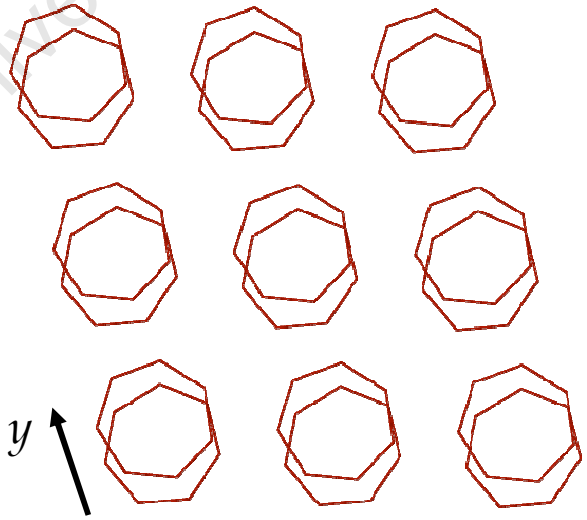

Figure 35. *The diagram shows the lateral displacement between dimers in adjacent layers. The shift becomes more evident when viewed perpendicular to the mean O4 plane.*

The dimers are stacked on top of each other forming columns along *c* with all the columns having the same orientation (Figure 36). The orientation of the included guest is the same for all the columns in the structure.

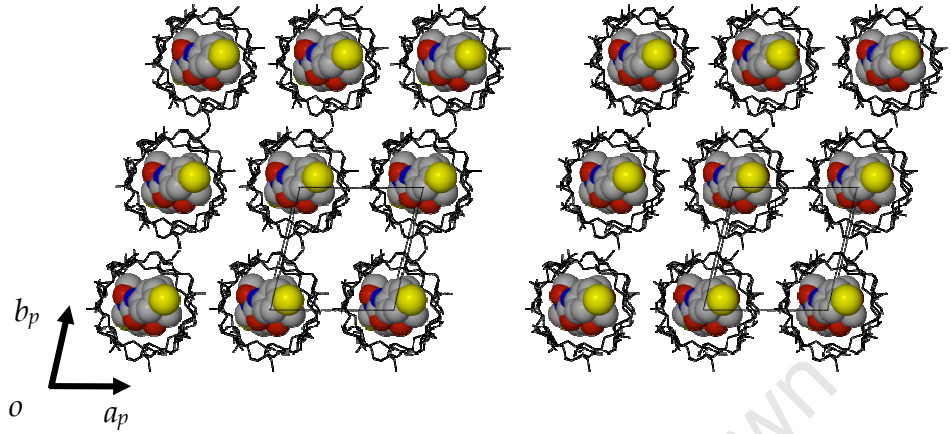

Figure 36. *The stereo diagram highlights the common orientations of the guest molecules.*

The layers and the columns are held together by a series of inter and intra-layer hydrogen bonds shown here in Figure 37.

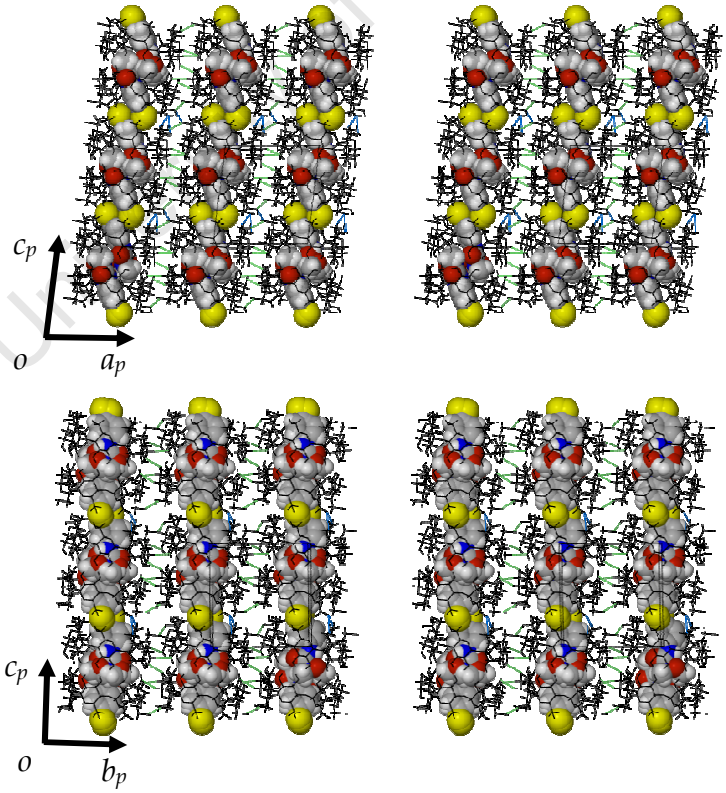

Figure 37*. The diagrams show the inter- and intra-layer hydrogen bonds (green and blue bonds respectively) which link the columns together viewed along b (top) and viewed along a (bottom).*

Comparative PXRD

Calculated and experimental traces for B3 are shown in Figure 38. There is a slight shift in the peak positions to lower 2θ˚ for the experimental trace. This is a result of the different conditions under which the data were collected. Data for the experimental trace were collected at ambient temperature while data for the calculated trace were collected at 113 K. The level of agreement between the two traces is still very good.

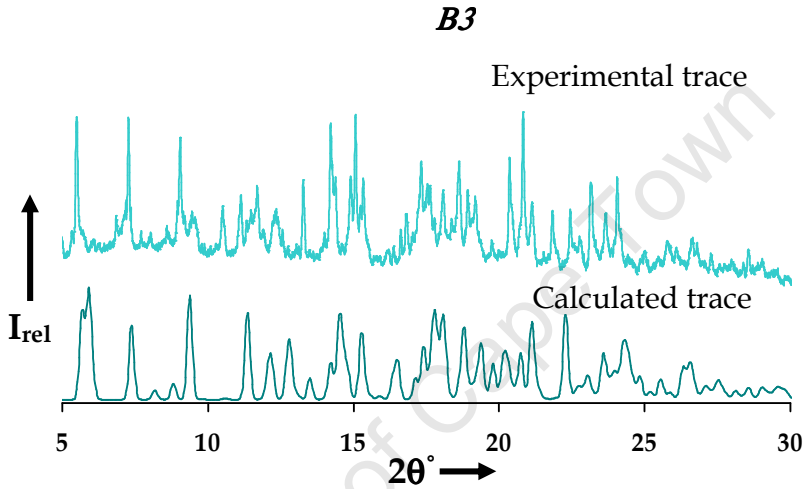

Figure 38. *Calculated and experimental PXRD traces for B3.*

General agreement between the experimental and calculated traces proves that the bulk sample is homogeneous and has the same structure as the single crystal selected for X-ray analysis. The extra peaks present in the experimental trace are evidence of uncomplexed guest which has crystallised and contaminates the sample.

It is worth mentioning that complexes A2, A3 and B3 are isostructural.

X-RAY STRUCTURE OF B4

Space group determination

The determination of the crystal system and space group of the β-CD inclusion complex B4 was carried out with the program LAYER.[1] The examination of the reciprocal lattice layers yielded the Laue symmetry 2/*m* while the reflection conditions were *hkl : none; 0k0: k = 2n*. The two space group choices were $P2_1$ and $P2_1/m$. The space group $P2_1$ was chosen on the basis of the host cyclodextrin being chiral. The crystal system and space group were confirmed with XPREP.[2] B4 crystallises in the monoclinic space group $P2_1$ with $Z = 2$ dimeric complex units in the unit cell.

Structure solution and refinement

Crystallising in the monoclinic space group $P2_1$, the asymmetric unit consists of a dimer made up of two crystallographically independent cyclodextrin molecules, two guest molecules and 25 water molecules. Refinement parameters and crystal data are reported in Table 12. Unit cell refinement and data reduction were performed with the program DENZO-SMN.[3] B4 was found to be isostructural with an existing inclusion complex 2(β-CD)•2[(*R*)-(-)-2-(3-phenoxyphenyl)propionic acid]•26H_2O (refcode: GETPAW).[23] The structure of B4 was solved by means of isomorphous replacement using only the host coordinates of GETPAW as input fragment to overcome the phase problem. The freely rotating O6 atoms were omitted from the trial structure in order to facilitate the modelling of any possible disorder. The glucopyranose units for the two host molecules in the asymmetric unit were labelled A1-A7 and B1-B7. The structure was refined with SHELXH-97 and successive difference Fourier maps revealed the O6 atoms.[5] As it turns out, C6B4 and O6B4 are disordered over two positions (their disordered counterparts are C6C4, O6C4). The s.o.f.s of the disordered components were refined as x and 1-x with an initial value of x = 0.5. It so happens that the disorder of C6B4 and O6B4 of one host molecule is related to the disorder of the included guest and so the free variable used for the guest

Table 12. *Crystal data and data-collection parameters for B4.*

parameters	B4
Formula unit	$(C_{42}H_{70}O_{35})_2 \bullet (C_9H_{11}N_2O_2Br)_2 \bullet 25H_2O$ (B4)
Mr	3238.58
Crystal system	monoclinic
Space group	$P2_1$
a/Å	15.2613(1)
b/ Å	31.747(2)
c/ Å	15.4396(1)
α/°	90
β/°	102.105(1)
γ/°	90
Vol. Å^3	7314.16(8)
Z	2
ρ_{calc} g cm^{-3}	1.471
μ (MoKα) mm^{-1}	0.673
F(000)	3428
Crystal size mm^3	0.09 x 0.12 x 0.12
Temperature K	113 ± 2
Range scanned θ/°	1.0 ≤ θ ≤ 25.1
Index range	-18 : 18; -37 : 37; -18 : 18
ϕ Scan angle °	0.8
ϕ Scan range °, no of frames	363.2, 454
ω Scan angle °	0.8
ω Scan range °, no of frames	38.4, 48; 37.6, 47; 126.4, 158; 78.4, 98; 119.2, 149; 124.0, 155; 75.2, 94; 111.2, 139
Dx mm	40
No. of reflections	176721
No. of unique reflections	25737
No. of reflections with I>2σ(I)	18654
No. of l.s. parameters	1730
R_{int}, R_σ	0.069, 0.071
S	1.036
R_1 [$F_o > 4\sigma(F_o)$]	0.0845
wR_2	0.2320
No. of reflections omitted	62
Weighting scheme parameters	a = 0.1226, b = 18.6351
(Δ/σ)	<0.001
Δρ excursions eÅ^{-3}	-1.98, 2.77

was extended to C6B4 and O6B4. The disorder of the guests will be dealt with later in this chapter. The value of x for the disordered components (C6B4, O6B4 and the guest) refined to 0.64. All the host atoms except C6B4, O6B4, C6C4 and O6C4 were refined anisotropically. All the hydrogen atoms of the

host molecules were placed in idealised positions using a riding model, except for those of the hydroxyl hydrogen atoms, which were refined using a hydrogen bond searching model (AFIX 83). All the hydrogen atoms of the host refined with U_{iso} = 1.2 times those of the parent atoms. Refinement continued and 27 sites were located for water molecules. 22 positions were assigned full site-occupancy while five other water molecules were assigned partial occupancy. Four of the five water molecules with partial occupancy had site-occupancies assigned according to the initial electron density and were fixed accordingly. These values are listed in Table 13. The temperature factors for the disordered water molecules were allowed to refine, settling in the range 0.03 – 0.19 Å^2. All except eight water molecules were refined anisotropically. The eight water molecules which were refined isotropically are O13W, O14W, O15W, O16W, O21W, O23W, O24W and O27W. The total number of water molecules accounted for in the refinement amounted to 24.9. 25 water molecules were accounted for from TG analysis (n = 2). Water H atoms could not be located.

Table 13. *Site-occupancies for disordered water molecules for complex B4.*

Atom	O13W	O15W	O14W	O23W	O27W
s.o.f.	0.65	0.35	0.37	0.63	0.87
U_{iso} (Å^2)	0.03	0.05	0.08	0.05	0.19

Modelling of the guest

After the refinement and optimisation of the cyclodextrin host structure and placing of the water molecules, the focus shifted to locating the guest molecules in the difference Fourier map. The two most prominent peaks in the difference map were assigned as bromine. Subsequently, two phenyl rings were clearly identifiable from their hexagonal geometry and were constrained as rigid hexagons using the AFIX 66 instruction. With careful manipulation and refinement one could also discern the urea groups in the difference map. Only at this stage in the refinement did it become evident that both guests were disordered over two positions. The major component of each model was assigned a variable site-occupancy x and global isotropic

temperature factors. The s.o.f.s settled to 0.65 (for the major components) while the temperature factors settled to 0.06 Å^2 and 0.09 Å^2. The secondary (disordered) components of each guest were tediously located in successive difference maps and were painstakingly refined. The global temperature factors for the secondary or minor components settled to 0.10 and 0.11 Å^2. The least-squares refinement was sensitive and several distance restraints were imposed on the guest molecules to ensure reasonable geometries. The standard deviation employed for restrained bond lengths was σ = 0.002 Å for uniformity. All atoms of the guests were refined isotropically except for atoms Br1A and Br1C as guest disorder did not warrant anisotropic refinement. All guest hydrogen atoms were added in idealised positions in a riding model. U_{iso} for aromatic type hydrogen atoms was 1.2 times those of their parent atoms while methyl hydrogen atoms were assigned U_{iso} equal to 1.5 times the U_{iso} of their parent atoms. Relatively large residual electron density peaks were found within 0.68 Å of atom Br1B and were ascribed to limitations in the absorption correction routine as well as the anisotropic model employed.

STRUCTURAL DESCRIPTION

Host conformation

Primary hydroxyl torsion angles

Except for primary hydroxyl groups of glucopyranose units A7 and B4 (with ring B4 being disordered over two positions) all the primary hydroxyl torsion angles (**ω**) of B4 indicate a *(-)-gauche* conformation. The minor component of the disordered primary hydroxyl group B4 (*i.e.* primary hydroxyl group C4) has a *(-)-gauche* conformation while the conformation of the major component is *(+)-gauche*. Glycosidic torsion angles **Φ** and **Ψ** as well as pyranoid torsion angles Θ_1 and Θ_2 are in good agreement with those reported elsewhere. All the glucose residues are in the $^4C_1$ conformation.

Macrocyclic symmetry

The mean **r** of both CDs is 5.03 Å ranging between 4.99 and 5.12 Å for A and between 4.70 and 5.40 Å for B. The mean **l** for A and B is 4.37 Å in the range 4.31 to 4.41 Å for A and 4.27 to 4.54 Å for B. The mean glycosidic oxygen angle **a** for both CDs is 128.5˚ while the ranges for both sets of angles are within the range 122.0-132.0˚. It is interesting to note that the ranges reported for cyclodextrin B are larger than those reported for cyclodextrin A.

Planarity of the O4-Heptagons

The root mean square deviations of the O4 atoms comprising the O4-heptagons of the host molecules A and B are 0.036 Å and 0.019 Å respectively. There are four O4 atoms with negative deviations for A (A1, A2, A5 and A6) and three O4 atoms with negative deviations for B (B3, B6 and B7). The torsion angle **t** of A ranges from -4.7 to 4.1˚ while for B it ranges from -2.4 to 2.3˚. The tilt angles τ_1 and τ_2 of both CDs are all positive with the angular values for A ranging from 2.3 to 7.1˚ for τ_1 and for τ_2 the range is from 1.8 to 10.7˚. The ranges for B are 1.7 to 9.3˚ for τ_1 and 5.0 to 17.9˚ for τ_2. The mean φ value for cyclodextrins A and B are 118.2˚ and 118.0˚, respectively. φ ranges from 116.9 to 119.2˚ for A and from 116.6 to 120.2˚ for B.

These parameters indicate that the cyclodextrins involved in dimer formation are symmetrical. Also, both CDs have maintained their toroidal shape.

INTRA- AND INTERMOLECULAR INTERACTIONS

Host intramolecular interactions

The stabilisation of the conformation of the cyclodextrins is maintained by the intraglucose hydrogen bonds. 17 intraglucose interactions are accounted for in the structure of B4, made up of O2•••O3′ and C-H•••O interactions. The fourteen O2•••O3′ distances of cyclodextrin A range from 2.71 to 2.89 Å with a mean length of 2.78 Å. For cyclodextrin B the O2•••O3′ interactions range from 2.72 to 2.92 Å with a mean length of 2.81 Å. The three C-H•••O hydrogen bonds involve the hydroxyl groups of the cyclodextrin. Their

function is the stabilisation of the hydroxyl groups. The mean H-bond length for the C-H•••O interactions is 3.40 Å (range 3.35 – 3.49 Å) with a mean angle of 140.0˚ (range 133.0 – 151.0˚).

Host-Host intermolecular interactions

28 intermolecular hydrogen bonds are involved in the formation of the dimer. Seven interactions are of the type O3•••O3 with a mean interaction distance of 2.78 Å (range 2.70 to 2.87 Å). There are seven O2•••O2 intra-dimer interactions with a mean interaction distance of 2.98 Å in the range 2.91 to 3.05 Å. Fourteen O2•••O3 interactions complete the set of 28 hydrogen bond interactions. The mean O2•••O3 length is 3.07 Å in the range 2.97-3.17 Å.

INTER- AND INTRA-LAYER INTERACTIONS

Inter-layer interactions

There are three inter-layer interactions in the structure of B4. Two are O6•••O6 interactions with a mean distance of 2.63 Å. There is also a single long range C6-H•••O6 hydrogen bond with a length of 3.47 Å and hydrogen bond angle of 164.0˚.

Intra-layer interactions

There are 17 intra-layer interactions in the structure. Seven are O6•••O6 interactions with a mean length of 2.71 Å in the range 2.47 to 3.01 Å. There are also four O2•••O2 intra-layer interactions present in the structure with a mean distance of 2.72 Å in the range 2.70 to 2.74 Å. The six remaining hydrogen bonds present are weak C-H•••O interactions. Three are C1-H•••O2 hydrogen bonds and three are C2-H•••O3 hydrogen bonds. The mean interaction distance is 3.32 Å (range 3.26 – 3.40 Å) and the mean hydrogen bond angle is 152.0˚ (range 137.0 – 165.0˚). The hydrogen bond distances and angles range from 3.26 to 3.40 Å and from 137.0 to 165.0˚ respectively.

Host-Water interactions

27 sites were refined for 25 water molecules in complex B4. Ninety O•••OW close contacts between the cyclodextrin dimer and water molecules were observed, including water-water contacts. 14 water molecules are involved in O•••OW contacts with the primary rim forming a total of 29 interactions. The average length for these interactions is 2.74 Å (range 2.29 - 3.21 Å). Eleven other water molecules are involved in close contacts with the secondary rim. There are 25 interactions observed between the secondary rim and the interstitial water molecules. The average length for interactions at the secondary rim is 2.88 Å (range 2.66 - 3.19 Å). 26 water molecules take part in water-water interactions; some also interact with the cyclodextrin dimer. There are 36 interactions with an average contact distance of 2.81 Å ranging from 2.51 to 3.23 Å.

GUEST INCLUSION

Guest disorder

The hydrogen bonded dimer contains two guests disordered over two positions with the major components arranged in a head-to-tail parallel orientation while the minor components are arranged in a tail-to-tail, anti-parallel fashion. The major components are guests A and B (green coloured guests in Figure 39) while guests C and D are the minor components (blue coloured molecules in Figure 39).

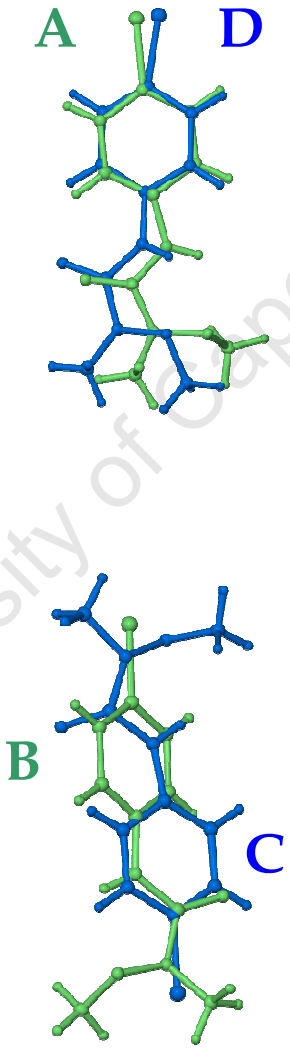

Figure 39. *Alignment of the guests in the dimeric cavity. Guests A and B (green) have parallel (head-to-tail) arrangement. Guests C and D (blue) have anti-parallel (tail-to-tail) alignment.*

The stereo diagram in Figure 40 is a composite image of the disorder of guests A, B, C and D present in the cavity of B4. The different disordered models are drawn separately and are indicated with the colour-coordinated arrows.

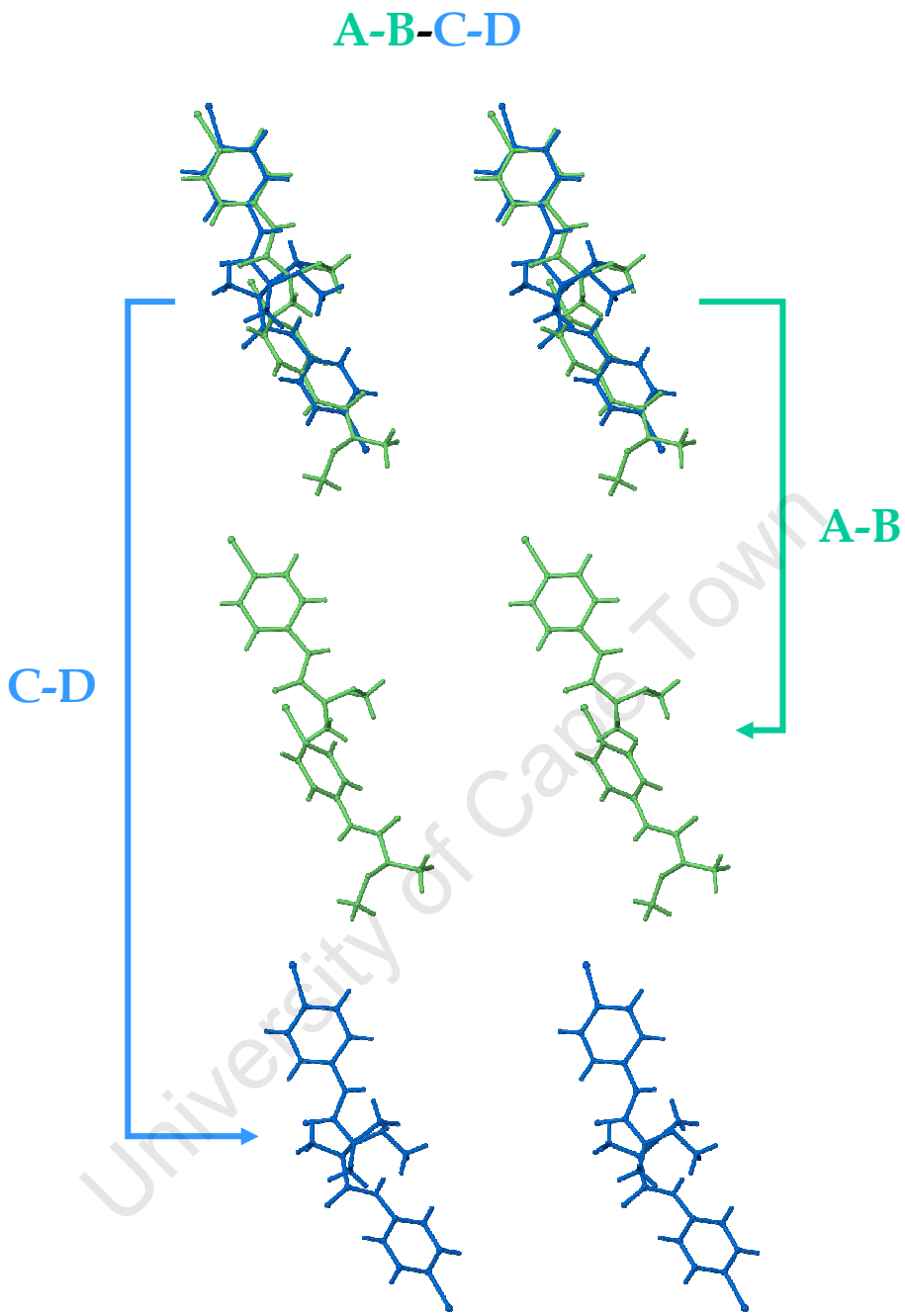

Figure 40. *Stereoview of the disordered guests A, B, C and D of **B4** and the deconvoluted disordered components A-B (green) and C-D (blue).*

Guest location

Each cyclodextrin making-up the head-to-head hydrogen bonded dimer is occupied by a twofold disordered guest shown in Figure 41 (a). The accommodation of the guest within the cavity is facilitated by its tilting diagonally across the cavity. In this way it occupies as much of the available

cavity as possible. The amount of tilt is measured between the plane of the phenyl moiety and the O4 heptagon of the respective host. Guest A makes an angle of 64.8(5)˚ with O4 heptagon A and guest B makes an angle of 67.5(5)˚ with O4-heptagon B. Guests C and D make angles of 62.2(5)˚ and 65.6(5)˚ with the O4-heptagons of CD molecules B and A respectively.

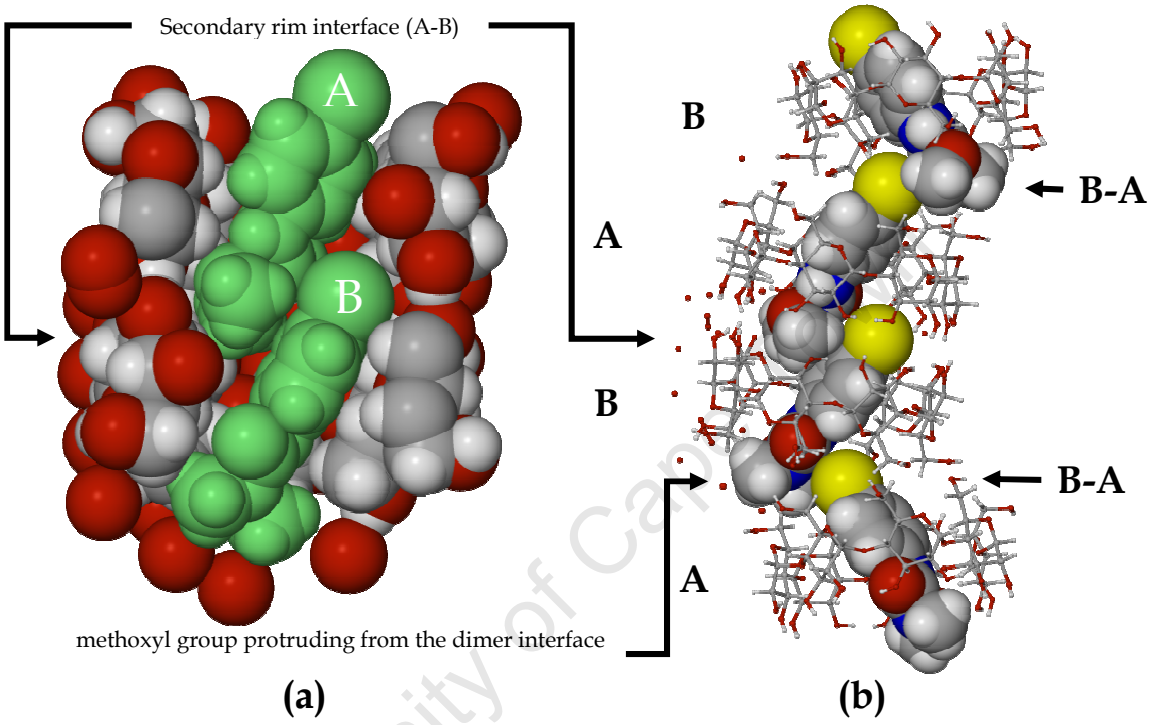

Figure 41. *(a) Shows major guest components A and B included in the cavity with parallel alignment. (b) Shows the urea moiety protruding from the inter-dimer interface into the interstitial ('extra-cavity') space.*

Guests A and B lie in a head-to-tail parallel orientation, Figure 41 (a). The bromophenyl moiety of guest A protrudes from the primary rim of cyclodextrin A and the urea moiety is lodged at the secondary rim interface with partial inclusion into the cavity of cyclodextrin B. Guest B has its bromophenyl moiety located at the secondary rim interface with partial inclusion into the cavity of host A while the urea moiety is lodged at the primary rim of host B. The urea group of guest B protrudes from the inter-dimer interface, Figure 41 (b). Consecutive dimers are inclined by ~20˚ allowing the urea group to protrude into the interstitial spaces where it is surrounded by water molecules.

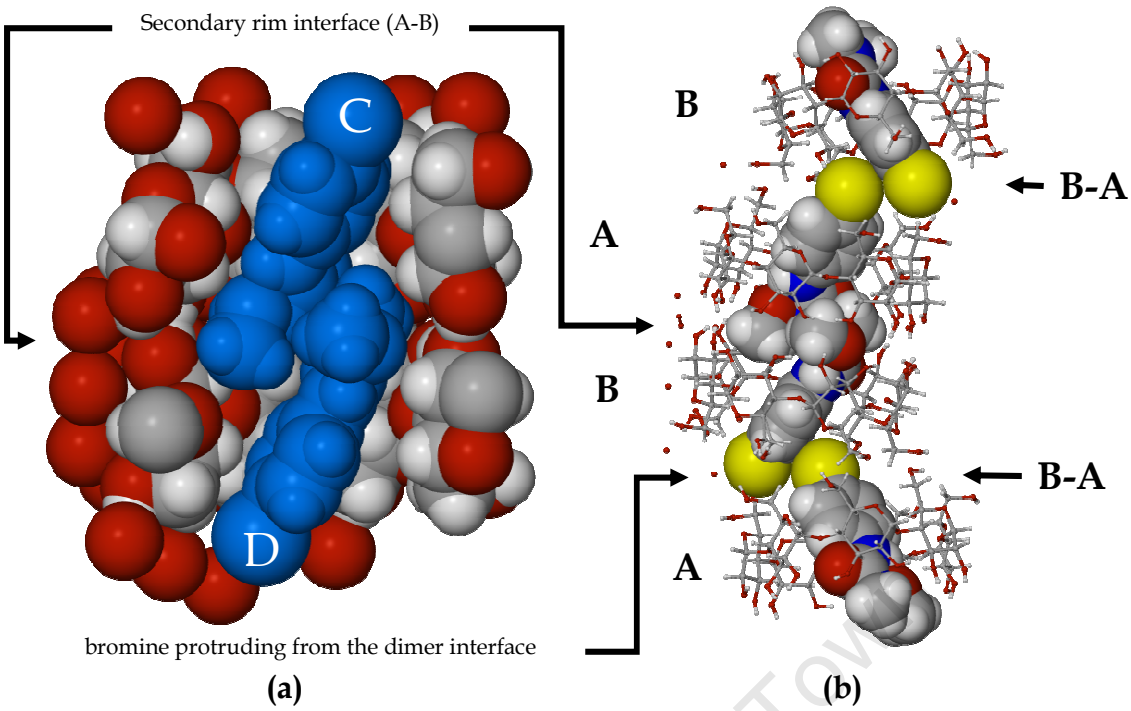

Figure 42. *(a) Shows minor guest components C and D included in the cavity with anti-parallel alignment. (b) Shows the bromine moiety protruding from the inter-dimeric interface into the interstitial space.*

Guests C and D are arranged in an anti-parallel manner, Figure 42 (a). The bromophenyl moiety of C is located at the primary rim of host A while the urea moiety is lodged at the secondary rim interface with partial inclusion into the cavity of host B. The bromophenyl moiety of guest D is located at the primary rim of host B with the bromine partially protruding from the dimer interface into the interstitial spaces where it is partially surrounded by interstitial water molecules, Figure 42 (b). The urea moiety of guest D is located at the secondary rim interface, including partially into the cavity of host A. The dimer interface (B-A) is not completely closed off by the primary rim hydroxyls or the interstitial water molecules, Figure 43 (a).

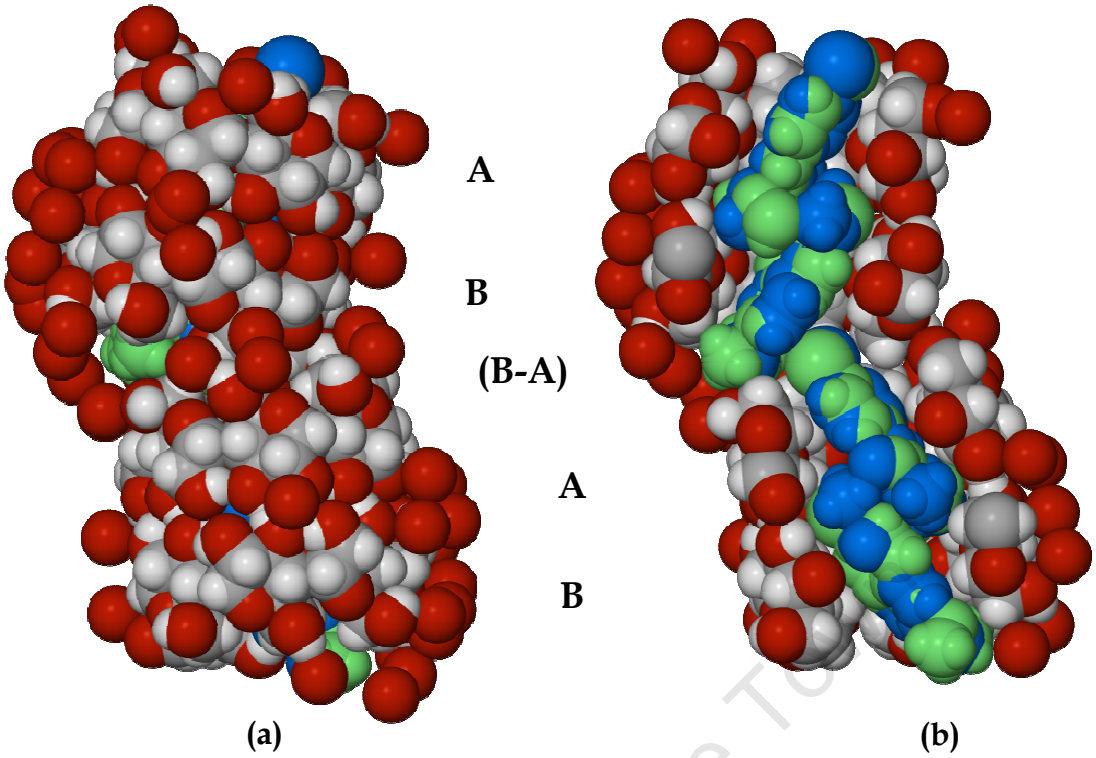

Figure 43. *(a) Shows that the inter-dimer interface is not completely closed off by primary hydroxyl groups and interstitial water molecules. (b) Shows how the urea and bromine moieties are surrounded by interstitial water molecules at the inter-dimeric interface.*

Owing to the disorder, the dimer interface is either occupied by the bromine of guest A and the urea moiety of guest B (Figure 43 (b)) or by two bromine moieties belonging to guests C and D, as shown in Figure 42 (b).

In addition to the tilt, the guests are rotated relative to each other. The amount of rotation of each guest pair (*i.e.* A and B or C and D) is influenced by the orientation of the guests in the cavity.

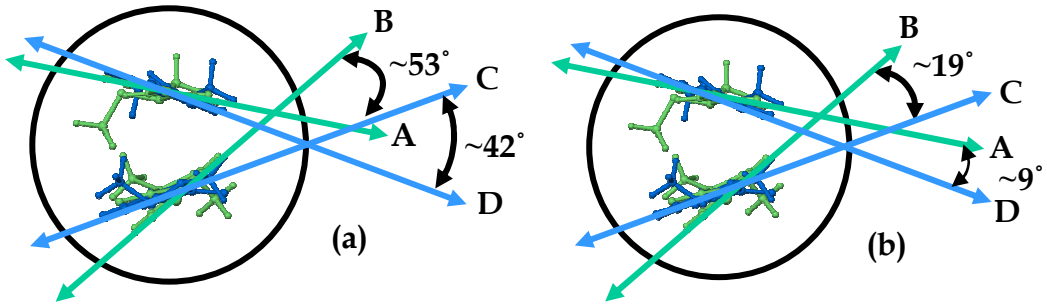

Figure 44. *The schematic diagram shows the angles of intersection between the mean planes of guests A, B, C and D.*

The angle between the mean planes of guests A and B is ~53˚ while the angle between C and D is ~42˚ Figure 44 (a). The angles of intersection between mean planes of the guests B and C is ~19˚ while the angle between A and D is ~9˚ as shown in Figure 44 (b). In the case of the guests C and D, rotation around C9-N11 and N11-O12 optimises the distance between the methoxyl groups of the respective guests, Figure 45 (a).

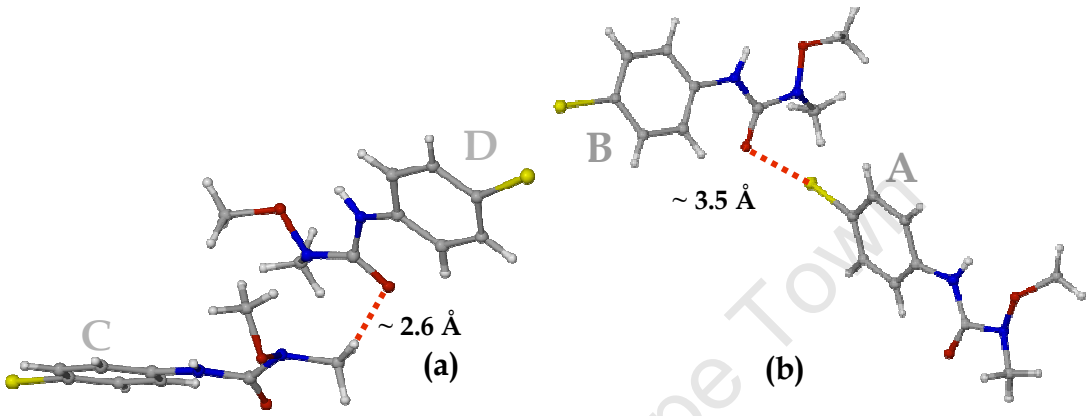

Figure 45. *(a) Shows the C-H•••O interaction between guests C and D. Diagram (b) shows close contacts between guests A and B.*

Distances between guests are maintained by the tight fitting environment found inside the dimeric cavity. There are close contact distances between guests A and B of approximately 3.5 Å for Br•••O, Figure 45 (b). For guests C and D there is a C-H•••O hydrogen bond between the methyl group of guest C and the carbonyl oxygen of guest D (2.60 Å, 126.0˚ Figure 45 (a)). Other close contact distances have been tabulated and are reported in the appropriate appendix.

Guest conformations

Generally, the values reported for the torsion angles of the guests of B4 have rather large deviations from those reported for the uncomplexed guest. τ_1 ranges from -19(2)˚ to +28(2)˚ while τ_2 ranges from -28(3)˚ to +5(2)˚. τ_3 ranges from -179(1)˚ to +178(1)˚ indicating an 'extended' conformation for all guests.

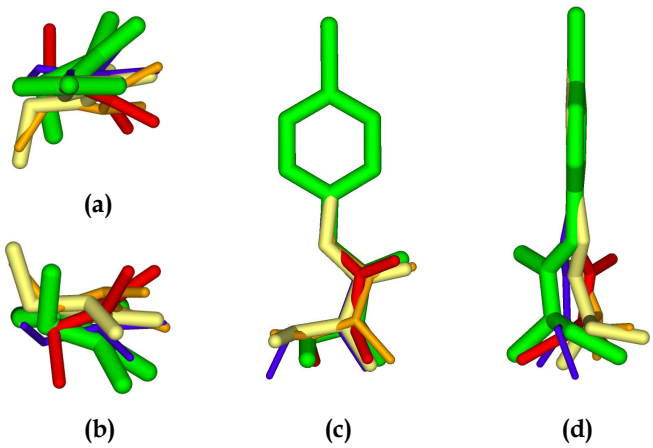

Figure 46. *The diagram shows the relative conformations of the included guest as compared with that of the uncomplexed guest. Guest A - yellow, guest B - blue, guest C - red, guest D - brown and uncomplexed guest - green.*

τ_4 ranges from -12(2)˚ to +35(1)˚ and τ_6 ranges from -39(4)˚ to +28(2)˚. τ_5 and τ_7 have ranges from -157(2)˚ to +173(1)˚ and from 171(1)˚ to +168(2)˚ respectively. The ranges for τ_8 and τ_9 are -160(3)˚ to +122(1)˚ and -96(1)˚ to +109(1)˚ respectively. The disposition of bond C13-O12 varies from nearly perpendicular to the mean plane through C9, O10, N11, O12 and C14 to being approximately coplanar with the mean plane, as shown in Figure 46 (blue model).

HYDROGEN BONDING INTERACTIONS OF THE GUEST

Host-guest intermolecular interactions

There are nine intermolecular hydrogen bonds in the structure; four are C-H•••O hydrogen bonds, four are C-Br•••H interactions and there is a single O-H•••O hydrogen bond. There are also several close contacts between the host and guest. The C-H•••O hydrogen bonds have a mean length of 3.28 Å (range 2.88 – 3.52 Å) and a mean hydrogen bond angle of 145.0˚ (range 133.0˚ - 160.0˚). The mean C-H•••Br interaction distance is 3.17 Å. The O-H•••O hydrogen bond length is 2.81 Å and the H-bond angle is 160.0˚. The mean close contact interaction distance is 3.39 Å. The C-H•••O interactions are shown in Figure 47.

Guest-guest intermolecular interactions

There are eight intermolecular close contacts between the guests. The mean distance for the eight interactions is 3.22 Å. There is also a single weak C-Br•••π interaction in the structure with a Br•••ring centroid distance of 3.82 Å and an angle of 162.0˚.[21,22]

Guest intramolecular interactions

Eight intramolecular hydrogen bonds are present in the structure. Four are C-H•••O hydrogen bonds and four are N-H•••O hydrogen bonds. The four C-H•••O hydrogen bonds have a mean length of 2.87 Å and range from 2.79 to 2.92 Å. The mean angle for the hydrogen bonds is 121.0˚ and the range is 115.0-127.0˚.

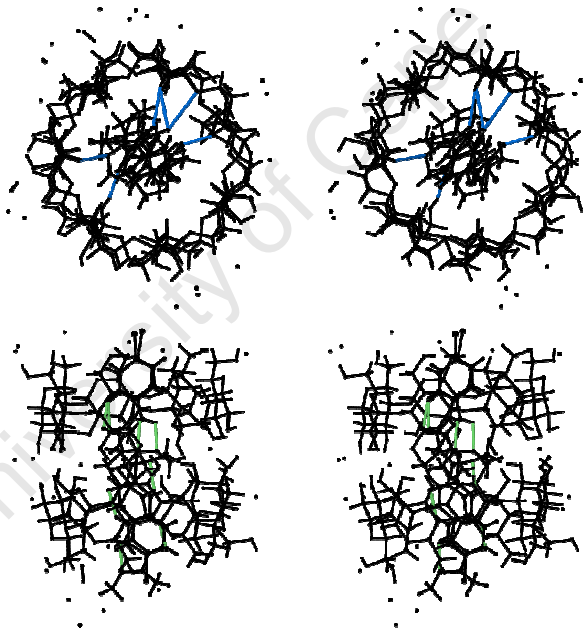

Figure 47. *(top) The stereogram shows the intermolecular hydrogen bond interactions (blue) between the host and guest in the cavity. (bottom) The diagram shows the intramolecular hydrogen bonds (green) of the guest molecules.*

The mean length of the four N-H•••O hydrogen bonds is 2.54 Å and the mean angle is 110.0˚. The range for the H-bond length is 2.48-2.57 Å and the range for the H-bond angle is 109.0-114.0˚. The intramolecular hydrogen bonds are shown in green in Figure 47 (bottom image).

CRYSTAL PACKING

Crystallising in the space group $P2_1$, B4 packs in the screw channel motif, **SC**. The dimeric layers of the screw channel are parallel to the *ac*-plane and propagate by means of the 2_1-operation along the *b*-axis (Figure 48). The distance from the centroid of cyclodextrin B to the centroid of cyclodextrin A measured across the inter-dimer interface is 9.87 Å.

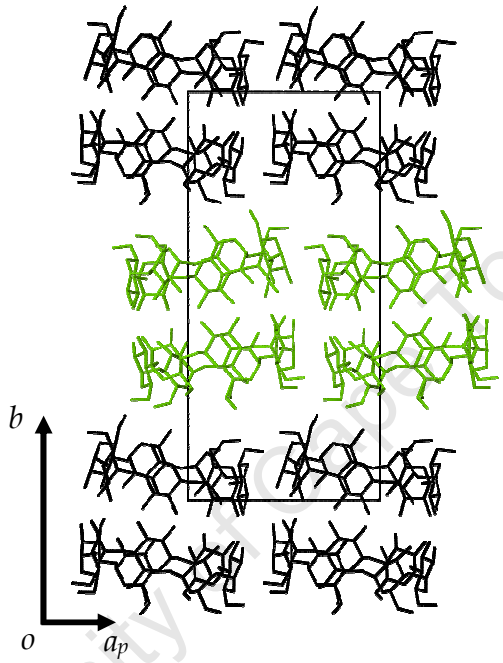

Figure 48. *Propagation of the dimeric layers along the b-axis by means of the 2_1-operation.*

Each layer is inclined by ~10˚ to the *ac*-plane with the direction of inclination alternating between clockwise and anticlockwise for consecutive layers, as mentioned previously (Figure 48). The lateral offset between consecutive layers is ~2.7 Å, Figure 49. The angle between the O4 heptagons of a single dimer is 1.33(2)˚.

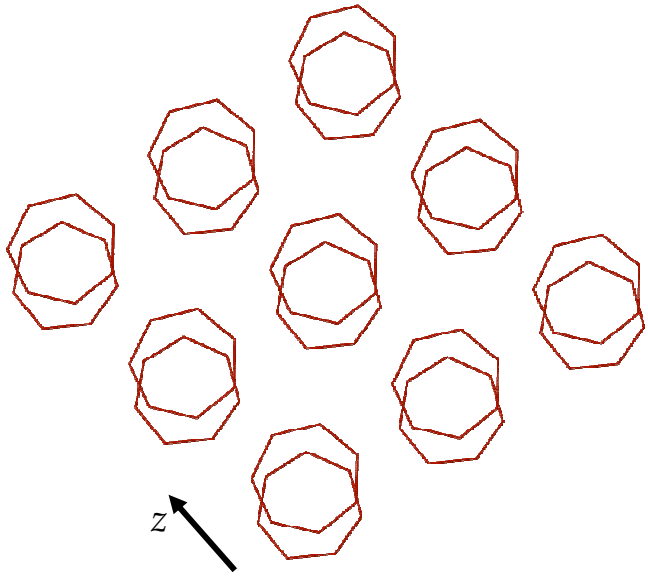

Figure 49. *Lateral displacement between O4-heptagons of dimers in adjacent layers.*

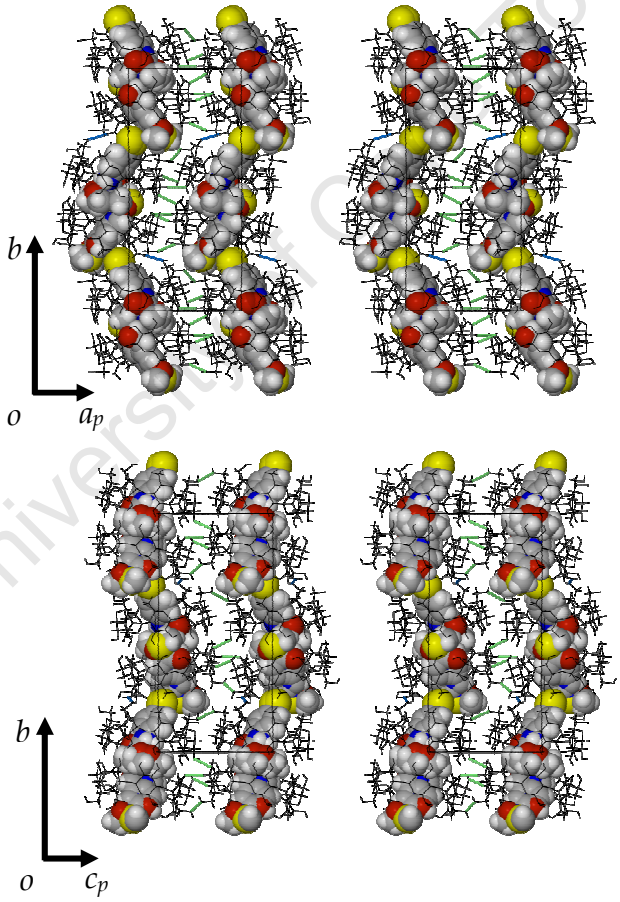

Figure 50. *Intra-layer interactions along the a- and c-axes, top and bottom respectively. The intra-layer hydrogen bonds are shown in green while the inter-layer hydrogen bonds are shown in blue.*

The parallel, undulating columns which stack along *b* are held together by a series of inter and intra-layer hydrogen bonds (Figure 50).

Comparative PXRD

Calculated and experimental traces for B4 are shown in Figure 51. There is a slight shift in the peak positions to lower 2θ˚ for the experimental trace. This results from the different conditions under which the data were collected. Data for the experimental trace were collected at ambient temperature while data for the calculated trace were collected at 113 K. There are also differences in intensity between the calculated and the experimental traces resulting from preferred orientation in the experimental sample.

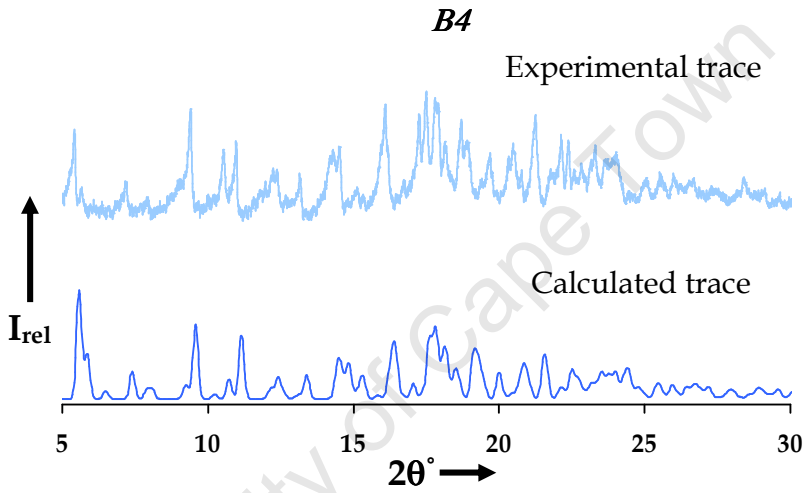

Figure 51. *The calculated and experimental PXRD traces for **B4**.*

The match between the experimental and calculated PXRD patterns confirms the identity of the phase of the bulk material as being the same as the single crystal selected for data-collection.

X-RAY STRUCTURE OF B5

Space group determination

The program LAYER was used to examine the reciprocal lattice layers. The examination yielded 2/*m* Laue symmetry indicating the monoclinic crystal system.[1] The reflection conditions were *hkl : none; 0k0 : k = 2n*. The space group choice was $P2_1$ as the host is chiral. The choice of the monoclinic crystal system and the space group $P2_1$ was confirmed using the program XPREP.[2] $Z = 4$ dimeric complex units in the unit cell.

Structure solution and refinement

The complex B5 crystallising in the monoclinic space group $P2_1$ has two crystallographically independent dimers, four guest molecules and 50 water molecules making up the asymmetric unit. Refinement parameters and crystal data are reported in Table 14. SHELXD was employed to solve the structure of B5 from *ab initio* methods, as there were no isostructural precedents for isomorphous replacement. The resulting solution revealed all the non-hydrogen atoms of both the host and guest including some of the water molecules. Prior to refinement with SHELXH-97, all O6 atoms, water molecules and guest atoms were deleted to prevent model bias due to any unmodelled disorder. The glucopyranose units of the independent host molecules were labelled A1-A7, B1-B7, C1-C7 and D1-D7. From several successive Fourier difference maps it was possible to locate and place all O6 atoms. O6C7 was disordered over two positions and its minor component was labelled O6E7. The site-occupancies were refined as x and 1-x, x having an initial value of 0.5 and eventually refining to 0.56. All atoms belonging to the hosts, except for C5C7, O6C7 and O6E7, were refined anisotropically. All hydrogen atoms attached to carbon atoms were placed in geometrically calculated positions (riding model) using the AFIX 43 command while the hydrogen atoms of the hydroxyl groups were placed using the hydrogen bond searching model (AFIX 83). The isotropic temperature factors assigned to the hydrogen atoms were 1.2 times those of their parent atoms.

Table 14. *Crystal data and data-collection parameters for B5.*

parameters	B5
Formula unit	$(C_{42}H_{70}O_{35})_2 \bullet (C_9H_{11}N_2O_2Br)_2 \bullet 25H_2O$
Mr	3238.58
Crystal system	monoclinic
Space group	$P2_1$
a/Å	15.3079(2)
b/ Å	31.676(5)
c/ Å	31.053(5)
α/°	90
β/°	102.353(1)
γ/°	90
Vol. Å^3	14708.8(4)
Z	4
ρ_{calc} g cm^{-3}	1.462
μ (MoKα) mm^{-1}	0.669
F(000)	6856
Crystal size mm^3	0.18 x 0.22 x 0.10
Temperature K	113 ± 2
Range scanned θ/°	2.5 ≤ θ ≤ 25.4
Index range	-18 : 18; -38 : 38; -37 : 37
ϕ Scan angle °	0.4
ϕ Scan range °, no of frames	298, 745
ω Scan angle °	0.4
ω Scan range °, no of frames	79.6, 199; 130, 325; 108.4, 271; 120.4, 301; 130, 325; 58.8, 147; 56.8, 142
Dx mm	40
No. of reflections	231281
No. of unique reflections	52134
No. of reflections with I>2σ(I)	27855
No. of l.s. parameters	3534
R_{int}, R_σ	0.101, 0.152
S	1.022
R_1 [$F_o > 4\sigma(F_o)$]	0.0879
wR_2	0.2633
No. of reflections omitted	93
Weighting scheme parameters	a = 0.1528
(Δ/σ)	<0.001
Δρ excursions eÅ^{-3}	-1.20, 2.60

55 water molecules were located in successive electron density maps. 46 water molecules have full site-occupancy while the remaining nine have partial site-occupancies. The temperature factors for the nine disordered

water molecules were in the range 0.03 – 0.17 Å^2. The s.o.f.s for the disordered water molecules are listed in Table 15. Eleven water molecules were refined isotropically while the rest of the water molecules were refined anisotropically. The eleven isotropically refined water molecules are OW33, OW35, OW39, OW42, OW45, OW46, OW49, OW51, OW52, OW53, OW54 and OW55. The refinement accounted for 50 water molecules. This was in agreement with 50 water molecules determined from TG analysis (n = 2). Water H atoms could not be located in the difference electron density maps.

Table 15. *Site-occupancies for disordered water molecules of complex B5.*

Atom	OW35	OW39	OW46	OW49	OW51	OW52	OW53	OW54	OW55
s.o.f.	0.83	0.76	0.66	0.76	0.63	0.37	0.24	0.60	0.34
U_{iso} (Å^2)	0.06	0.13	0.06	0.11	0.08	0.06	0.03	0.17	0.07

Modelling of the guest

With the refinement well-advanced, evidence for 1:1 stoichiometry was clear with each cyclodextrin dimer containing two guest molecules. The four most prominent peaks in the difference map were assigned as bromine and refined. As with previous refinements the phenyl rings were easily identifiable in the difference map and refined as rigid hexagons using the AFIX 66 instruction. This was followed by the intricate and challenging refinement of the urea moieties of each guest. Each guest presented disorder of differing complexity with one guest completely disordered over two positions (guest A with minor component E) while another shared a common bromine atom (guest D with minor component G) and the remaining two guests had only particular moieties disordered over two positions (B with minor component F, and C with minor component H). The s.o.f.s of the major guest components were refined with a free variable x while the minor components refined as 1-x. The initial value of x was set to 0.5 and it eventually settled to 0.61 for A-B and 0.76 for C-D. Each model was assigned separate global temperature factors, which ranged between 0.05 and 0.12 Å^2. As with all the other refinements the least-squares refinement was sensitive, requiring several distance restraints to be imposed on the guest molecules to ensure reasonable geometries. The

standard deviation used for restrained bond lengths was σ = 0.002 Å for uniformity. Only certain atoms of the guests were refined anisotropically, namely Br1A, Br1B, Br1C, Br1D, Br1E, Br1F, C9B, O10B, O12B, C13B, C14B, C2C, C3C, C4C, C5C, C6C, C7C, and N8C. All guest hydrogen atoms were added in idealised positions in a riding model. U_{iso} for aromatic type hydrogen atoms were assigned values of 1.2 times those of the parent atoms while methyl hydrogen atoms were given 1.5 times the U_{iso} of their parent atoms. Major electron density peaks were located near C14G (within 0.34 Å) and were ascribed to residual absorption and anisotropic motion.

STRUCTURAL DESCRIPTION

Host conformation

Primary hydroxyl torsion angles

The hydroxyl groups E7 and C5 have *(+)-gauche* **ω** torsion angles while all other hydroxyl groups belonging to the four cyclodextrins in the asymmetric unit of B5 have *(-)-gauche* **ω** torsion angles. The glycosidic torsion angles **Φ** and **Ψ** as well as the pyranoid torsion angles Θ_1 and Θ_2 are in agreement with those reported elsewhere for the parent. All 28 crystallographically independent glucose residues are in the $^4C_1$ conformation.

Macrocyclic symmetry

The mean radii **r** for the host cyclodextrins A, B, C and D are 5.05, 5.02, 5.04 and 5.04 Å respectively. They span the respective ranges 4.99-5.18 Å, 4.86-5.23 Å, 4.96-5.12 Å and 4.94-5.25 Å. The mean distances **l** for the four host molecules are 4.38 Å (range 4.34-4.42 Å), 4.35 Å (range 4.30-4.44 Å), 4.37 Å (range 4.34-4.44 Å) and 4.37 Å (range 4.29-4.52 Å) for A, B, C and D, respectively. The average glycosidic oxygen angle for the four cyclodextrins is 128.5˚ while the set of glycosidic oxygen angles of all four cyclodextrins fall within the range 123.7 - 131.6˚.

Planarity of the O4-Heptagons

The root mean square deviations **d** of the O4 atoms from the respective O4-heptagons in the cyclodextrin molecules A, B, C and D are 0.028, 0.037, 0.031 and 0.028 Å respectively. Three O4 atoms (A2, A3 and A6) of cyclodextrin molecule A have negative deviations from the mean O4 plane of cyclodextrin A while four O4 atoms belonging to cyclodextrin molecules B, C and D (B1, B4, B5, B7, C1, C3, C6, C7, D1, D3, D4 and D6) have negative deviations from the mean O4 planes of their respective cyclodextrin. The torsion angle **t** ranges from -3.3 to 2.4˚ for CD A, -4.0 to 3.5˚ for B, -3.9 to 4.2˚ for C and -3.4 to 3.1˚ for D. The tilt angles τ_1 and τ_2 for the quartet of cyclodextrin molecules are all positive with angular ranges from 2.7 to 8.6˚ for τ_1 (A) and 1.9 to 11.5˚ for τ_2 (A), 2.2 to 6.0˚ for τ_1 (B) and 3.9 to 13.2˚ for τ_2 (B), 2.3 to 9.7˚ for τ_1 (C) and 1.0 to 13.0˚ for τ_2 (C), 1.8 to 17.3˚ for τ_1 (D) and 3.5 to 17.2˚ for τ_2 (D). The intersaccharidic angles φ for the four CDs range from 117.6 to 119.5˚ for A, 116.7 to 119.5˚ for B, 116.1 to 118.9˚ for C and 116.7 to 119.4˚ for D.

All the parameters here point to the fact that all the CDs are round, symmetrical and toroidal in shape. The CDs have near planar O4 heptagons and are geometrically similar to those of the parent β-CD.

INTRA- AND INTERMOLECULAR INTERACTIONS

Host intramolecular interactions

The asymmetric unit of complex B5 contains two independent β-CD dimers (AB and CD). In dimer AB there are fourteen O2•••O3′ interactions with a mean hydrogen bond distance of 2.80 Å in the range 2.71 to 2.94 Å for A and a mean distance of 2.81 Å covering the range from 2.74 to 2.88 Å for B. In dimer CD there are also fourteen O2•••O3′ interactions with a mean distance of 2.80 Å (range 2.71 - 2.90 Å) for C and a mean interaction distance of 2.80 Å (range 2.74 - 2.90 Å) for D. Dimer AB has two C6-H•••O5′ hydrogen bonds with a mean distance of 3.33 Å and a mean angle of 143.0˚. Dimer CD has three C6-H•••O5′ hydrogen bonds with a mean interaction distance of 3.37 Å and a mean angle of 142.0˚.

Host-Host intermolecular interactions

Dimer AB has 28 intermolecular hydrogen bonds which stabilise the head-to-head arrangement of the two cyclodextrin molecules. Dimer CD also has 28 intermolecular hydrogen bonds involved in its formation. For AB, seven of the 28 interactions are O3•••O3 interactions with a mean length of 2.80 Å (range 2.71 to 2.90 Å). In the case of dimer CD, the mean interaction distance for the seven O3•••O3 interactions is 2.79 Å (range from 2.72 to 2.94 Å). Each dimer has a full set of seven intra-dimer O2•••O2 interactions. For both dimers the mean O2•••O2 distance is 2.98 Å with the respective ranges 2.94 to 3.07 Å for AB and 2.88 to 3.11 for CD. AB also has fourteen O2•••O3 interactions with a mean length of 2.98 Å with a range of 3.00 to 3.19 Å. The fourteen O2•••O3 interactions for dimer CD have a mean distance of 2.97 Å with a range 3.00 to 3.18 Å.

INTER- AND INTRA-LAYER INTERACTIONS

Inter-layer interactions

Five O6•••O6 interactions are present in the structure. The average interaction distance for these is 2.70 Å (range 2.66 - 2.72Å). There is also a single C6-H•••O6 bond belonging to the AB dimer. It has a hydrogen bond distance of 3.52 Å and a hydrogen bond angle of 166.0˚.

Intra-layer interactions

25 interactions are observed in the structure; ten interactions are O6•••O6 interactions with a mean distance of 2.78 Å and a range of 2.73-2.86 Å. There are also five intra-layer O2•••O2 interactions with mean distance of 2.68 Å in the range 2.66 to 2.72 Å. The remaining ten interactions are C-H•••O hydrogen bonds and can be divided equally between the C1-H•••O2 and C2-H•••O3 interactions. The mean distance for the C-H•••O interactions is 3.33 Å (range 3.24 - 3.43 Å) while the mean hydrogen bond angle is 152.0˚ (range 139.0-165.0˚).

Host-Water interactions

171 O•••OW close contacts were observed for 50 water molecules refined over 55 sites. 26 water molecules are involved in 59 close contacts with the primary rims of both dimers. The mean interaction distance between the water molecules and the primary rims is 2.99 Å (range 2.60-3.20 Å). Fourteen other water molecules are involved in close contacts with the secondary rims making a total 46 contacts. The mean contact distance is 2.91 Å with a range 2.64-3.24 Å. 26 water molecules are engaged in water-water interactions resulting in 66 contacts. The close contacts have a mean distance of 2.71 Å and range from 2.41 to 3.12 Å. Furthermore, four C-H•••OW interactions are present in the structure. The mean hydrogen bond distance is 3.29 Å in the range 2.96-3.45 Å. The mean hydrogen bond angle for the four H-bonds is 143.0˚ and the range is 134.0-153.0˚.

GUEST INCLUSION

Guest disorder

Two head-to-head hydrogen bonded dimers are arranged in two parallel columns (I and II) which make-up the asymmetric unit of the complex B5. Each dimer has two guest molecules included in the cavity while each guest molecule is disordered over two positions, to various extents, Figure 52. Guest A is completely disordered over two positions with the minor component labelled E, Figure 52 (a). Guests B and F share atoms C9B, O10B, N11B, O12B, C13B and C14B as shown in Figure 52 (b) represented by the light blue/cyan coloured portion of the molecules.

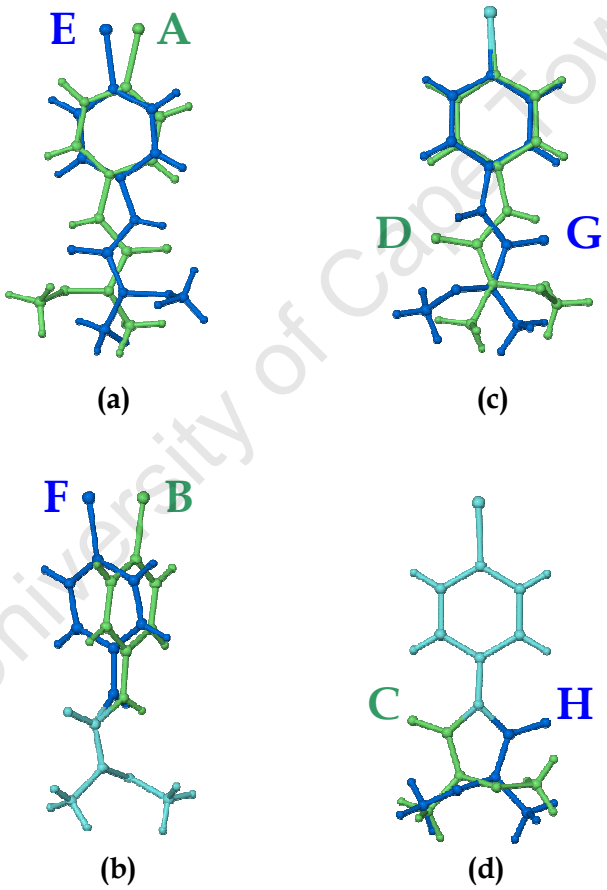

Figure 52. *The image shows the guests A, B, C and D (green) along with the associated disordered components E, F, G and H (blue). Parts of molecules represented in light blue/cyan have full site-occupancy and are shared between models.*

Guest D shares a bromine atom with its minor component G as shown in Figure 52 (c). For guest C, the urea moiety is disordered over two positions shown by the green and blue coloured components in Figure 52 (d). The

green coloured molecule is the major component of the molecule, Figure 52 (d). The disordered guests appear to have pseudo-twofold symmetry. However, the pseudosymmetry is not reflected in the host molecules.

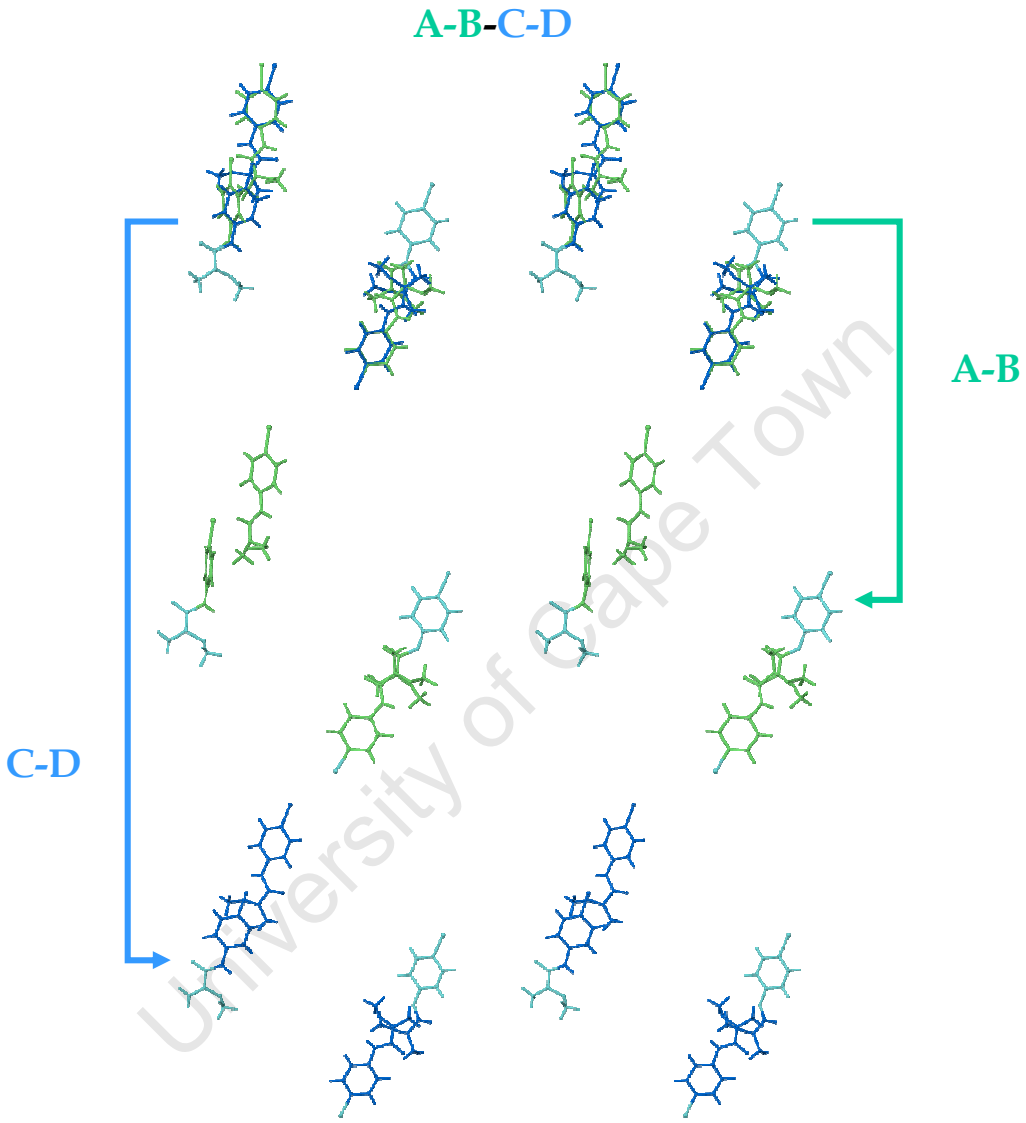

Figure 53. *A composite image showing guest disorder in the complex B5.*

Figure 53 is a stereoview showing the composite image for the disordered guests found in the cavity of the two dimers. The deconvoluted models are presented with colour-coordinated arrows. The light blue/cyan coloured moieties represent shared atoms.

Guest location

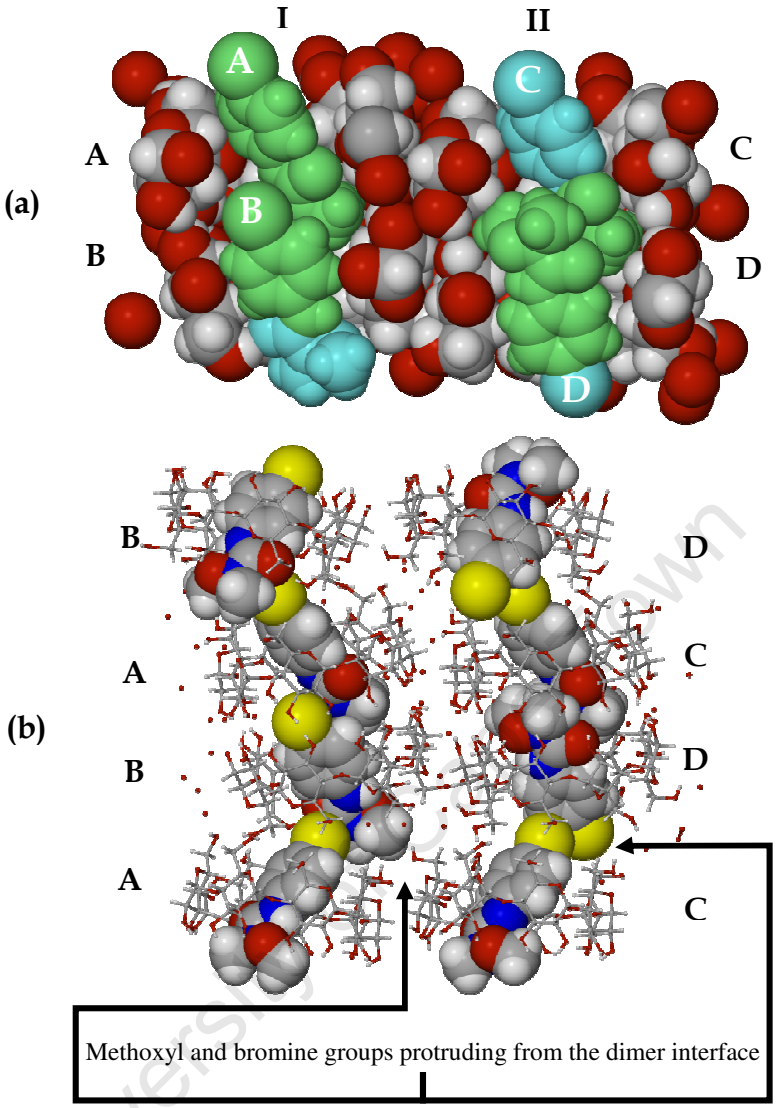

Figure 54. *The top diagram shows the major components of disorder A, B, C and D which are included in the cavities of the two independent host dimers. Guests A and B (column I) have parallel alignment while guests C and D (column II) have an anti-parallel alignment. (b) The bottom diagram shows the urea moiety (column I) and the bromine moiety (column II) protruding from the inter-dimeric interface into the interstitial space.*

As with all the preceding complexes the guests are tilted so that they may be optimally accommodated in the cavity of the cyclodextrin molecules. The angles between phenyl rings and the respective O4-heptagons for guests A, B, C and D are 64.0(4)˚, 65.0(3)˚, 60.5(2)˚ and 62.7(7)˚ respectively. Guests A and B (column I), are arranged in a parallel manner (head-to-tail). The bromophenyl moiety of A is located at the primary rim of cyclodextrin A while the urea moiety is located at the secondary rim interface with partial

inclusion into the cavity of cyclodextrin B. On the other hand, the bromophenyl moiety of guest B is located at the secondary rim interface with partial inclusion into the cavity of cyclodextrin A while the urea moiety of guest B is lodged at the primary rim of cyclodextrin B (Figure 54). Guests C and D (column II) are arranged in an anti-parallel orientation (tail-to-tail) with the bromophenyl moieties of both guests located at the primary rims of the cyclodextrin in which they are included.

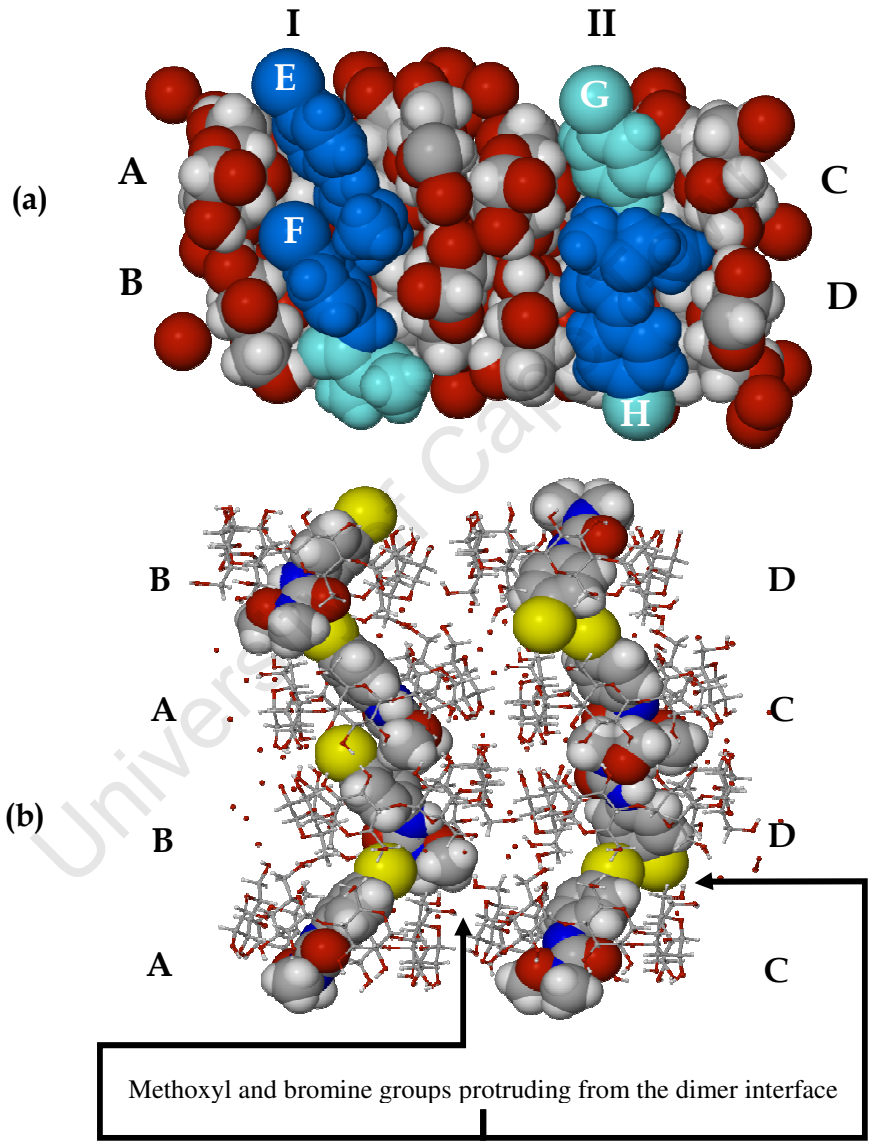

Figure 55. *The top diagram shows the minor components of disorder E, F, G and H which are included in the cavity. Guests E and F (column I) have parallel alignment while G and H (column II) have an anti-parallel alignment. (b) The bottom diagram shows the urea moiety (column I) and the bromine moiety (column II) protruding from the inter-dimeric interface into the interstitial space.*

The secondary rim interface is occupied by the urea moieties of both guests. Successive dimers are inclined by ~24˚, column I and ~17˚, column II. This inclination allows parts of the guest to protrude from the inter-dimer interface into the interstitial space, as shown in Figure 55. Guests E, F and G have inclinations of 61.8(1)˚, 62.0(9)˚ and 60.8(1)˚ with respect to the O4-heptagon planes, that for guest H remaining the same as that for guest C since the bromophenyl moiety has full site-occupancy. The modes of inclusion of guests E, F, G and H are similar to those displayed by guests A, B, C and D (Figure 55).

The dimer interfaces B-A and D-C are not completely closed off from the interstitial spaces, Figure 56 (a). The dimer interface B-A is occupied by the urea moiety of guest A or the disorder-related urea moiety of guest E and the bromine of guest B or the disorder-related bromine moiety of guest F. In turn, the dimer interface D-C is occupied by two bromine moieties belonging to guests C and D since both bromine atoms have full occupancy, as shown in Figure 56 (b).

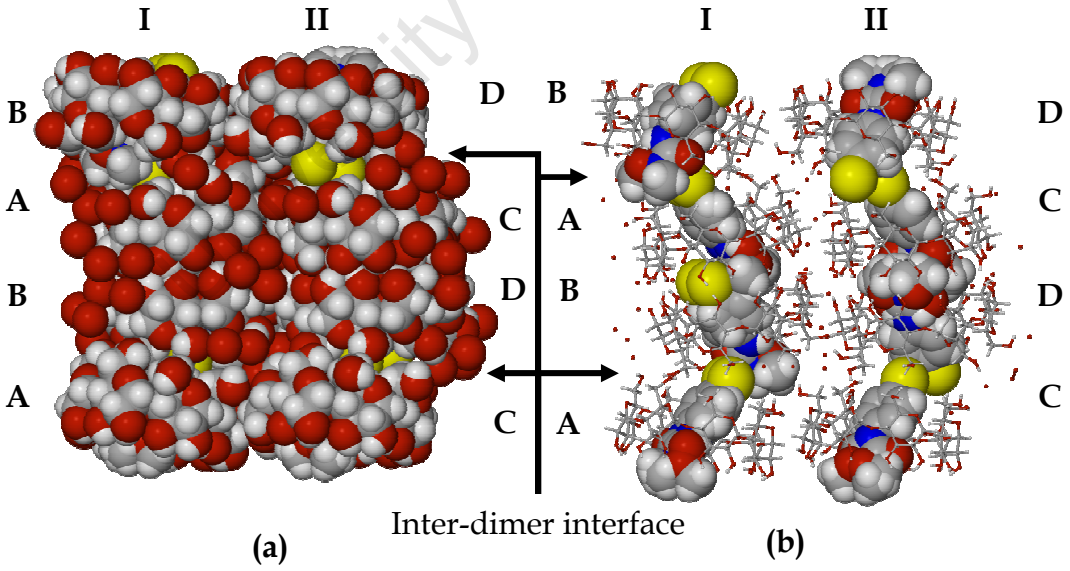

Figure 56. *Diagram (a) shows the partly exposed urea and bromine moieties in the B-A and D-C interfaces of columns I and II. In diagram (b) the occupants of the respective inter-dimer interfaces are visible. Interface D-C is occupied by two bromine atoms while interface B-A is occupied by a urea moiety and a bromine moiety.*

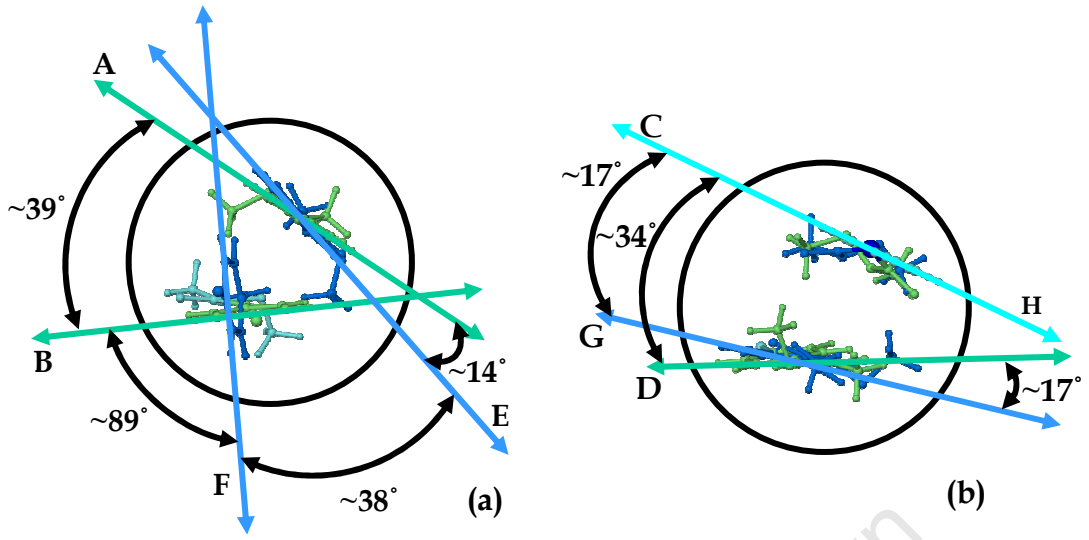

Figure 57. *The schematic diagram shows the angles of intersection between the mean planes of guests A, B, C and D in (a) and E, F, G and H in (b).*

In addition to the tilting of the included guests, they are rotated relative to each other in order to avoid short contact distances. The extent of rotation of each guest pair (A-B, E-F, D-C and G-H) is influenced by the alignment of the guests (parallel or anti-parallel). Guests A-B and E-F have a parallel arrangement with their respective average interplanar angles of ~39˚ and ~38˚, shown in Figure 57 (a). Guests D-C and G-H have anti-parallel arrangements with angles of ~34˚ and ~17˚ respectively (Figure 57 (b)). Interplanar angles between the disordered guest pairs A-E, F-B and D-G are approximately 14, 89 and 17˚ respectively. The rotation maximises the distances between certain guest moieties. For instance, the methoxyl group of guest A is approximately 4 Å from the centroid of the bromophenyl moiety of guest F. The minimum distance between the tertiary amine N atom of guest E and a phenyl hydrogen on guest B is ~3.4 Å (Figure 58 (a) and (c) respectively). Guests C and G are rotated so as to maximise the distance between their urea moieties. A similar situation applies to guests D-H. The minimum distance between these moieties is ~3.1 Å, Figures 58 (b) and (d).

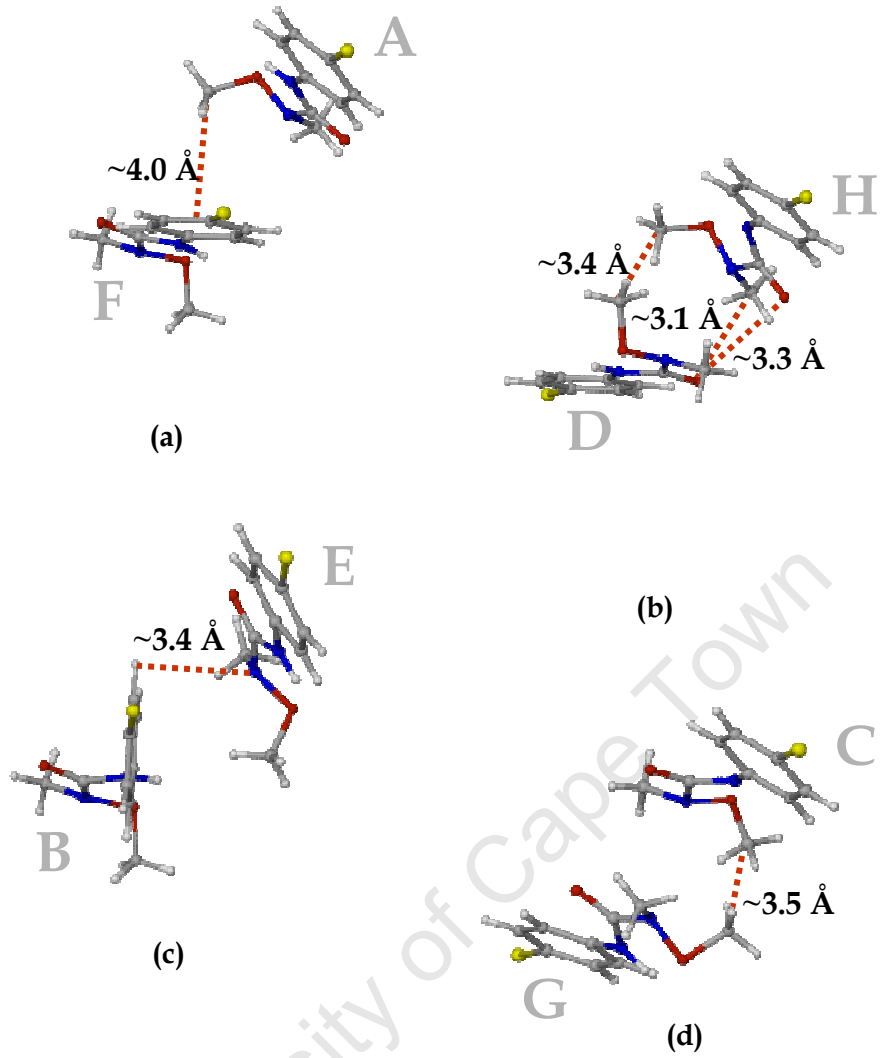

Figure 58. *Minimum distances between related guest molecules.*

Guest conformations

τ_1 for the guests of complex B5 spans the range from -35(2)˚ to +80(4)˚. Figure 59 shows clearly the contribution made by τ_1, visible in all the views shown. τ_2 ranges from -5(4)˚ to +17(4)˚. τ_3 ranges from -174(1)˚ to 175(1)˚ and as with the guests of the previous complexes τ_3 is close to -180/180˚ implying an 'extended' conformation. τ_4 and τ_6 range from -23(3)˚ to +21(2)˚ and from -38(2)˚ to +30(3)˚ respectively. τ_5 ranges from -170(1)˚ to +162(2)˚ while τ_7 ranges from -178(2)˚ to +171(1)˚. τ_8 and τ_9 range from -113(1)˚ to +125(2)˚ and from -114(3)˚ to +123(2)˚. The relative sizes of τ_8 and τ_9 indicate that the C13-O12 bond is orientated above the mean plane through C9, O10, N11, O12 and C14.

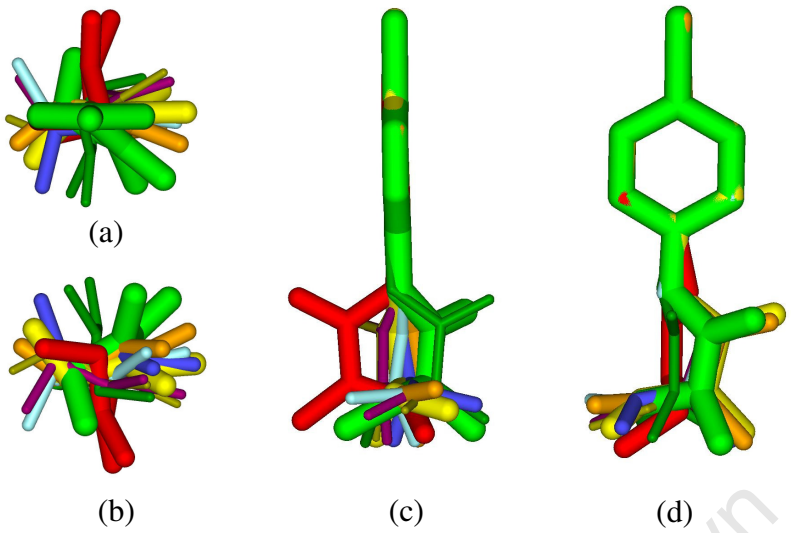

Figure 59. *The diagram shows the relative conformations of the included guest as compared with that of the uncomplexed guest. Guest A - yellow, guest B - blue, guest C - red, guest D - brown, guest E – light blue, guest F – dark green, guest G - purple, guest H – greenish-brown and uncomplexed guest - green.*

HYDROGEN BONDING INTERACTIONS OF THE GUEST

Host-guest intermolecular interactions

There are six host-guest intermolecular hydrogen bonds observed in the structure; five are C-H•••O hydrogen bonds while the sixth is an O-H•••O hydrogen bond. The C-H•••O bonds have a mean distance of 3.43 Å (range 3.35 - 3.51 Å) and a mean H-bond angle of 146.0˚ (range 128.0 - 167.0˚). The O-H•••O hydrogen bond length is 2.80 Å and its hydrogen bond angle is 163.0˚. Six C-Br•••H interactions were also observed in the structure. The mean distance for the six interactions is 3.17 Å. Several close contacts are also present in the structure. The mean close contact distance is 3.58 Å. The C-H•••O interactions are shown in Figure 60.

Guest-guest intermolecular interactions

There are several intermolecular close contacts present in the structure. The mean interaction distance for the close contacts is 3.32 Å. There is also a single weak C-Br•••π interaction in the structure. The interaction distance is 3.94 Å and the angle is 177.0˚.[21,22]

Guest intramolecular bonds

There are 15 intramolecular interactions present in the structure (Figure 60, bottom). Seven are C-H•••O interactions and eight are N-H•••O interactions. The mean hydrogen bond length for the C-H•••O interactions is 2.91 Å (range 2.82-3.04 Å) while the mean hydrogen bond angle is 116.0˚ (range 102.0-124.0˚). The N-H•••O hydrogen bonds have a mean hydrogen bond length of 2.58 Å (range 2.52-2.64 Å) and the mean hydrogen bonding angle is 108.0˚ (range 106.0-111.0˚). The hydrogen bond angle for the C-H•••O interaction is larger than those reported for the uncomplexed guest (107.0˚). The hydrogen bond lengths are closer to that of the uncomplexed guest (2.93 Å). On the other hand, the values for the N-H•••O interactions are very close to the values for the uncomplexed guest (2.57 Å and 110.0˚). The differences in the values reported for the uncomplexed guest can be attributed to the distortions of the conformations of the guest molecules which occur upon complexation.

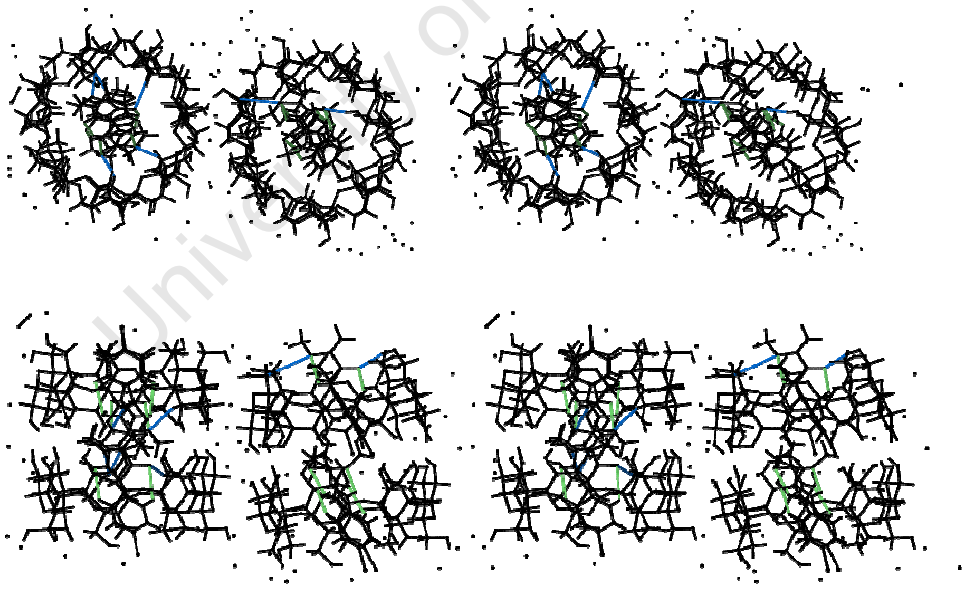

Figure 60. *(top) The stereogram shows the intermolecular hydrogen bond (blue) interactions between the host and guest in the cavity. (bottom) The diagram shows the intramolecular hydrogen bonds (green) of the guest molecules.*

Guest-water interactions

There is a single C13B•••OW21 water-guest interaction in the structure. The close contact distance is 3.31 Å.

CRYSTAL PACKING

B5 crystallises in the screw channel packing arrangement **SC** with two cyclodextrin dimers parallel to each other. Both dimers are inclined by ~10˚ to the *ac*-plane. As with B4, the inclination alternates clockwise or anti-clockwise for consecutive layers along the *b*-axis, Figure 61 (a). The distance from the centroid of CD A to the centroid of CD B measured across the dimer interface is ~9.9 Å while the distance from the centroid of C to the centroid of D is ~9.8 Å. Successive layers are offset by ~2.7 Å for both columns I and II (Figure 61 (b)). The O4 heptagons of dimer AB are inclined to each other by 0.70(3)˚ while those for dimer CD are inclined by 1.73(2)˚.

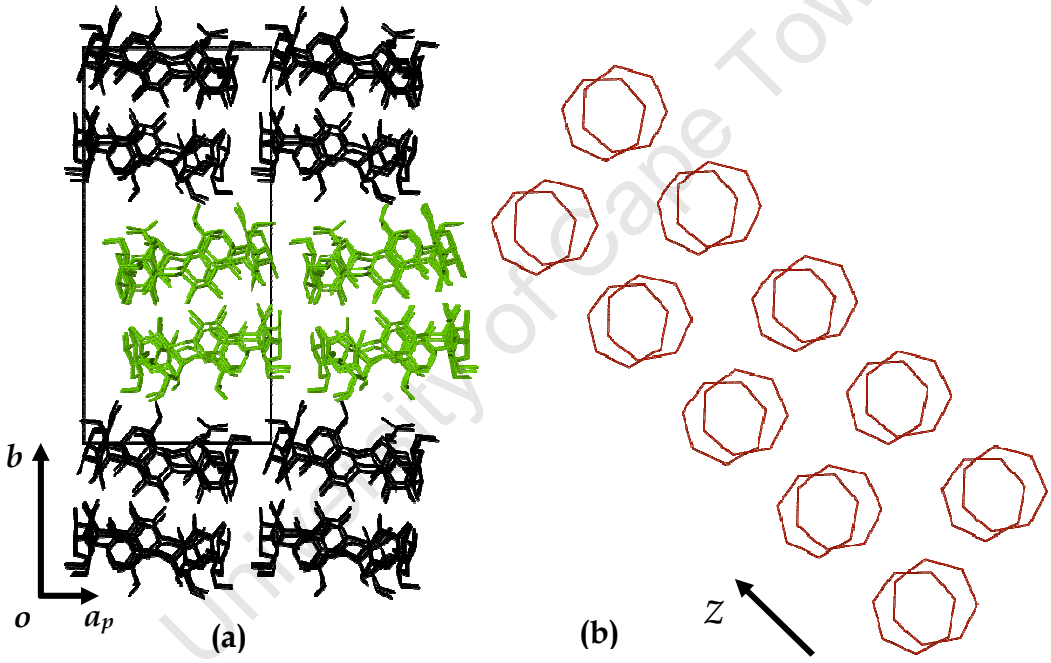

Figure 61. *Diagram (a) shows the alternating clockwise and anti-clockwise inclination of the dimeric layers. Diagram (b) shows the lateral shift between adjacent dimeric layers in column I as representative.*

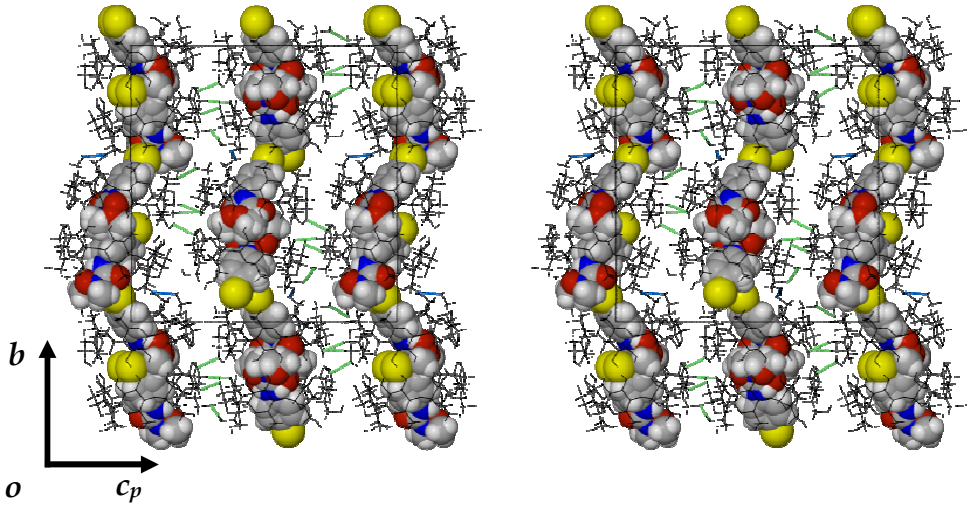

Figure 62. *The stereo diagram shows the inter-layer (green) and intra-layer (blue) hydrogen bonds which hold the columns together.*

The parallel dimeric columns are stabilised by a series of inter- and intra-layer hydrogen bonds shown in Figures 62 and 63.

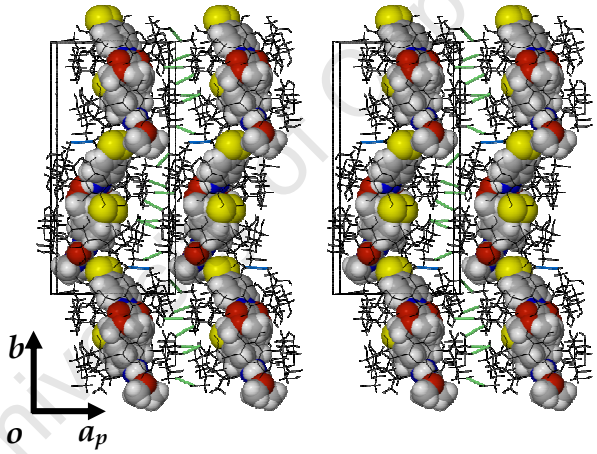

Figure 63. *An alternative view of the inter- and intra-layer hydrogen bonds present in the structure.*

Comparative PXRD

Calculated and experimental traces for B5 are shown in Figure 64. There is a slight shift in the peak positions to lower 2θ˚ for the experimental trace. This results from the different conditions under which the data were collected. Data for the experimental trace were collected at ambient temperature while those for the calculated trace were collected at 113 K. There are also differences in intensity between the calculated and the experimental traces resulting from preferred orientation in the experimental sample.

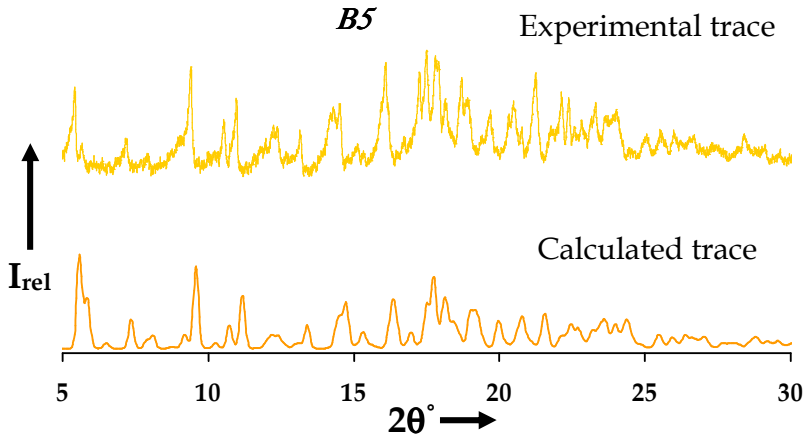

Figure 64. *The calculated and experimental PXRD traces for B5.*

The match between the PXRD patterns confirms the phase of the bulk material and that of the single crystal selected for data-collection as being the same.

DISCUSSION

Powder X-ray Diffraction

Calculated PXRD patterns

The experimental PXRD traces for the five complexes were successfully matched to their respective calculated traces which were based on single crystal X-ray data. The calculated traces are presented here in a stacked format for comparison, Figure 65. In general, the five PXRD traces share similar characteristics such as the four most intense peaks residing between 5 and 12˚ 2θ.

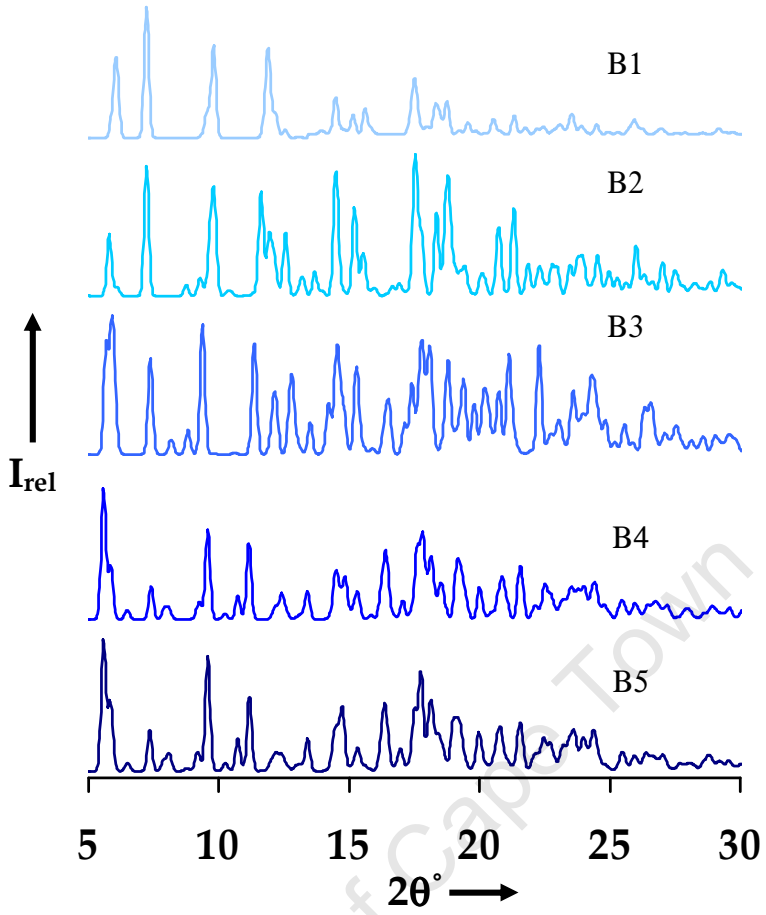

Figure 65. *Stacked calculated PXRD traces of the five 1:1 β-CD-metobromuron inclusion complexes.*

The PXRD traces for B1, B2 and B3 appear to be similar to each other. However, there are distinct differences between them which are manifested in the peak angular positions of particular peaks and their relative intensities. There remains a superficial similarity between the traces and the reasons for the similarity will be discussed here. In addition, an explanation of the similarities between the PXRD traces of complexes B4 and B5 will also be given.

The unit cells of the two monoclinic structures B1 and B2 are similar (a = ~19, c = ~24, b = ~16 Å, β = ~109˚) while the unit cell of the triclinic complex B3 requires the metric transformation a' = a + b, b' = b – a, c' = c for corresponding unit cell lengths. The angles of the new cell, however, are those of an obtuse angled triclinic cell.

B1 has a C-centred unit cell with a column of complex units located at ½ + x, ½ + y, z (Figure 66) while B2 has a column located at -x, ½ + y, -z, as shown in Figure 67. In the space group C2, the cyclodextrin dimers lie in the same plane, all dimers and the included guests having identical orientations, a C-lattice requirement. In addition, a crystallographic diad passes through the dimer interface. However, the column of complex units of B2 at –x, ½ + y, -z is generated by applying the 2_1-operation to the column near the origin. This results in the reversal of column polarity, such that alternate columns have opposite polarity, as shown schematically in Figure 67. This is in sharp contrast to the existence of the homopolar columns in B1.

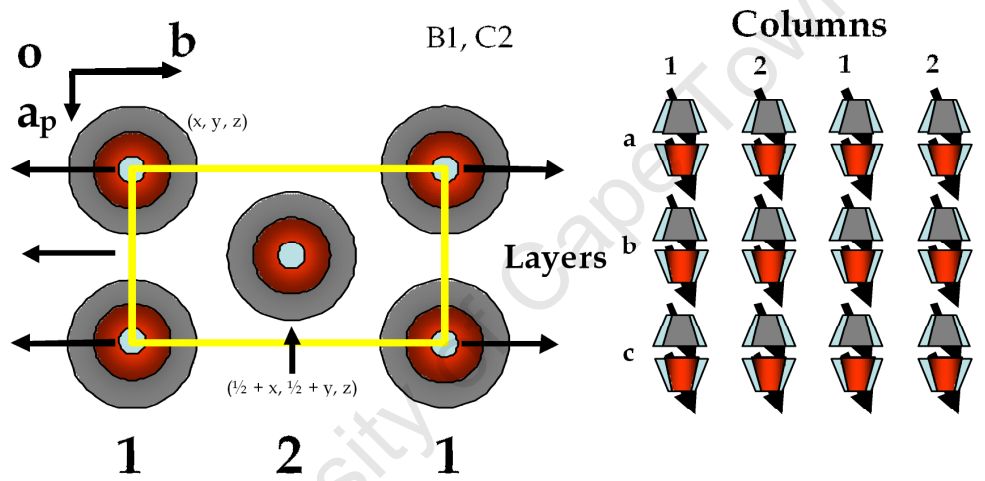

Figure 66. *The schematic diagram shows the unit cell for the complex B1 (left) crystallising in the space group C2. The image on the right shows the homopolar columns of the C2 structure.*

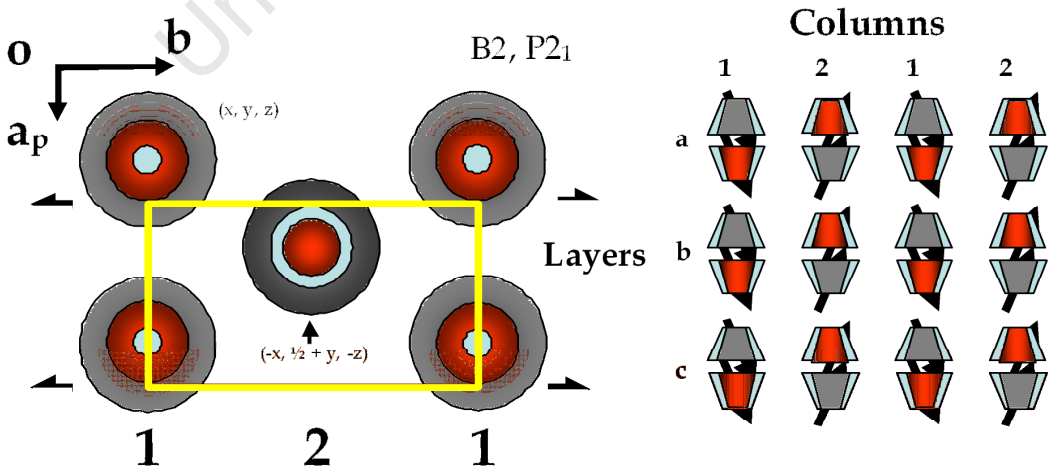

Figure 67. *The schematic diagram shows the unit cell for the complex B2 (left) crystallising in the space group $P2_1$. The image on the right shows columns of opposite orientation belonging to the $P2_1$ structure.*

After the application of the metric transformation to the unit cell of B3 (space group P1) the new cell shares a common axis (*c)* with the original triclinic cell. The dimers lie in the same plane with respect to the new cell, resulting in a pseudo-C-centred arrangement.[24] The dimers of the C2 structure (B1) have a twofold rotation axis located at the dimer interface whereas this symmetry is lacking in the P1 structure. All the columns in the new cell are homopolar as shown in Figure 68.

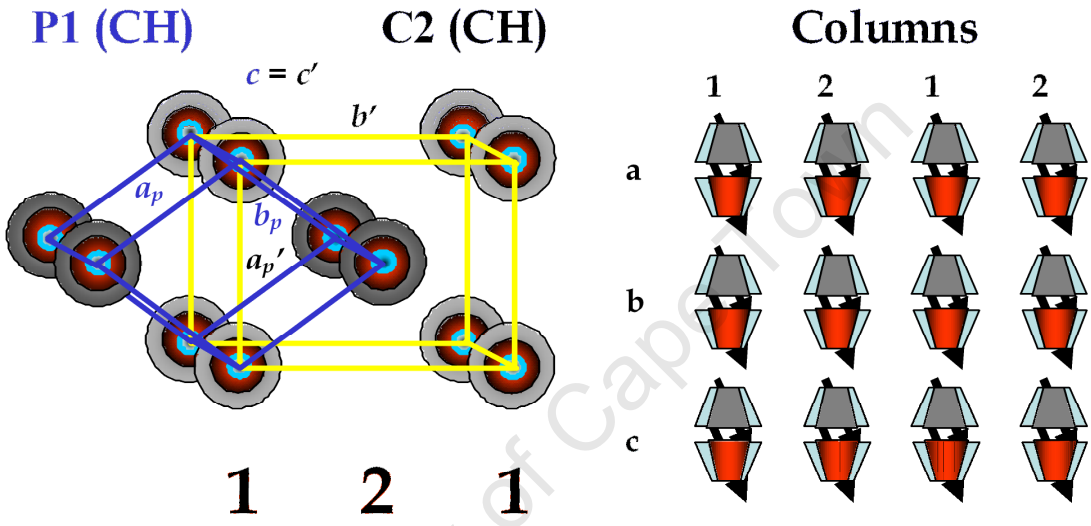

Figure 68. *The diagram on the left shows both the original P1 unit cell of B3 (blue) and the transformed unit cell (yellow) after the application of the appropriate metric transformation. The diagram on the right shows the arrangement of the columns of the new unit cell.*

The PXRD traces for inclusion complexes B4 and B5 are practically superimposable. Both structures crystallise in the space group $P2_1$ with the unit cell length of the *c*-axis in B5 double that of the *c*-axis in B4. The doubling of the *c*-axis is not due to the cooling process during data-collection but rather due to the existence of two types of dimeric β-CD complex with alternative guest conformations/orientations, an occurrence also noted elsewhere.[24] Closer inspection of the reciprocal lattice using the program LAYER revealed that for B5, the levels *hkl (h = 1, 2, 3,…)* have alternating weak and strong intensity rows normal to *c** whereas the rows of B4 have more uniform intensities, as shown in Figure 69.

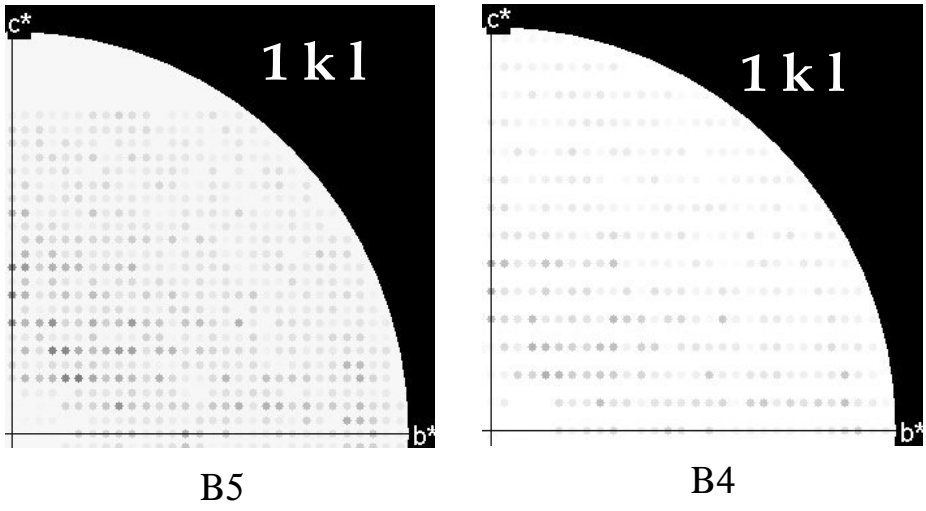

Figure 69. *Representative reciprocal lattice level 1kl for complexes **B5** and **B4**.*

The layers of weak intensity therefore result from the presence of the second (crystallographically independent) dimeric complex column with alternative guest conformations/orientations located at approximately x, y, ½ +z (*cf* Figure 62).

Conformation of the β-cyclodextrin host molecules

All the β-CD dimeric complexes formed by self-association through hydrogen bonding exhibit sevenfold symmetry.[15] The sevenfold symmetry of the five complexes described here is well maintained as the values for **r** and **l** both have narrow ranges while the glycosidic oxygen angle **a** is very close to the value for a regular heptagon (128.6˚), as shown in Table 16. For all the cyclodextrins involved in forming the five complexes, the root mean square deviations of the O4 atoms from the least-squares planes through the O4-heptagons are small. In addition, the torsion angles **t** for the five complexes are all within a narrow band implying a nearly planar conformation of the O4 heptagons. All glucopyranose rings are in the $^4C_1$ conformation.

The intramolecular O2•••O3′ hydrogen bonds stabilise the round conformation of the β-CD macrocycle.[25] The O2•••O3′ distances for the five complexes are all very similar and provide further evidence of a symmetrical cyclodextrin (Table 16). The tilt angles for the complexes are all positive and

are restricted to ranges of 0.1-17.5˚ for τ_1 and 1.0-17.9˚ for τ_2. All the cyclodextrin molecules involved in complex formation have therefore retained their truncated cone-like appearance and are not significantly distorted due to the inclusion of the guest molecules. The Φ and Ψ torsion angles are all within the accepted ranges of 102.0-123.0˚ and 112-149˚ respectively, implying that the distortion of the host molecule is negligible.[11]

Intra-dimer hydrogen bonds

Dimer formation is facilitated by hydrogen bonds reflected in O2•••O2, O2•••O3 and the O3•••O3 close contacts. The intermolecular O2•••O3 hydrogen bonds are on average the weakest of the O•••O interactions, followed by the stronger O2•••O2 interactions, with O3•••O3 interactions the strongest. However, the difference between the O2•••O2 and O2•••O3 sets is only slight with average distances of 3.04 and 3.00 Å, respectively. Instead, the average O3•••O3 distance is ~2.80 Å. It is on this basis that the O3•••O3 interactions are held responsible for dimer formation (or its maintenance). It is also thought that O3•••O3 interactions as well as the O2•••O3 interactions are responsible, to some extent, for the preservation of the round shape of the hydrogen bonded dimer.[25]

Table 16. *Tabulated geometric parameter ranges for inclusion complexes B1, B2, B3, B4 and B5.*

complex	r Å	l Å	a°	φ°	t°	τ_1°	τ_2°	O2•••O3′ Å	[b]deviation Å
B1									
A	4.70 – 5.30	4.26 – 4.47	126.1 – 131.2	112.5 – 120.1	-2.7 – 2.5	1.0 – 12.5	3.0 – 11.7	2.81 – 2.89	0.036
B2									
A	4.81 – 5.26	4.20 – 4.48	123.9 – 132.6	116.7 – 120.7	-4.7 – 3.9	2.0 – 13.6	3.0 – 13.7	2.73 – 2.88	0.032
B	4.97 – 5.18	4.28 – 4.47	125.6 – 130.6	116.6 – 121.0	-3.9 – 4.4	1.5 – 8.8	2.6 – 11.5	2.72 – 2.84	0.052
B3									
A	4.80 – 5.24	4.26 – 4.49	125.2 – 132.5	115.4 – 119.4	-3.6 – 2.5	1.1 – 9.3	1.5 – 15.6	2.67 – 2.84	0.036
B	4.72 – 5.24	4.31- 4.41	126.9 – 130.3	117.0 – 119.5	-3.4 – 4.8	0.1 – 13.2	1.8 – 14.4	2.68 – 2.81	0.045
B4									
A	4.99 – 5.12	4.31 – 4.41	127.1 – 129.7	116.9 – 1192	-4.7 – 4.1	2.3 – 7.1	1.8 – 10.7	2.71 – 2.89	0.036
B	4.70 – 5.40	4.27 – 4.54	122.0 – 132.7	116.6 – 120.2	-2.4 – 2.3	1.7 – 9.3	5.0 – 17.9	2.72 – 2.92	0.019
B5									
A	4.99 – 5.18	4.34 – 4.42	126.7 – 130.6	117.6 – 119.5	-3.3 – 2.4	2.7 – 8.6	1.9 – 11.5	2.71 – 2.94	0.028
B	4.86 – 5.23	4.30 – 4.44	124.8 – 131.6	116.7 – 119.5	-4.0 – 3.5	2.2 – 6.0	3.9 – 13.2	2.74 – 2.88	0.037
C	4.96 – 5.12	4.34 – 4.44	127.4 – 129.6	116.1 – 118.9	-3.9 – 4.2	2.3 – 9.7	1.0 – 13.0	2.71 – 2.89	0.031
D	4.94 – 5.25	4.29 – 4.52	123.7 – 131.6	116.7 – 119.4	-3.4 – 3.1	1.8 – 17.5	3.5 – 17.2	2.74 – 2.90	0.028

(b) = root mean square deviation of O4 atoms from the O4-heptagon

Inter and intra-layer interactions

Inter- and intra-layer interactions as well as the solvent (water) mediated inter- and intra-layer interactions stabilise the two-dimensional dimeric layers as well as the overall three-dimensional structure.[26] The inter- and intra-layer interactions involve O6•••O6 and O2•••O2 contacts as well as weaker C-H•••O hydrogen bonds. The average contact distance for the inter-layer O6•••O6 interactions for the five structures is 2.77 Å while the average contact distances for the intra-layer O6•••O6 and O2•••O2 interactions are 2.82 and 2.73 Å respectively. The average interaction distance for the C-H•••O hydrogen bonds is 3.34 Å and the average hydrogen bonding angle is 151˚. The O6•••O6 and O2•••O2 interactions are rather strong interactions in both the inter- and intra-layer interactions. These interactions are also the only direct link between cyclodextrin molecules. In other words they act as the 'glue' holding the crystal structure together.

Host-water interactions

Generally, the water molecules govern the organisation of the crystal structure. The water molecules are located in two sub-networks corresponding to the primary and secondary rims.[26,27] These water molecules are able to engage in hydrogen bonding with the hydroxyl groups of the primary and secondary rims, other water molecules and even the guest molecules. It was initially proposed that these sub-networks were separate from each other; this, however, is not entirely accurate. In a high-resolution low-temperature study, which used intensities measured on a synchrotron, Makedonopoulou *et al.* showed that close contacts exist between water molecules which indirectly link the primary and secondary rims.[15] In this regard, we found that the water molecules in all the complexes under study here are essentially located near the primary rim and secondary rim interfaces. All the complexes have OW•••OW (water-water) close contacts linking the primary rim to the secondary rim interface.

GUEST INTERACTIONS

Host-guest interactions

The primary host-guest interactions present in all the structures in this series are weak C-H•••O interactions. There are two types of C-H•••O hydrogen bonds, those formed between the methine hydrogens in the CD cavity and the ethereal and carbonyl oxygen atoms of the guest (Table 17). Both B4 and B5 have strong O-H•••O interactions involving the carbonyl oxygen atom of the guest and a primary hydroxyl of the host cyclodextrin. The average interaction distance and angle are ~2.80 Å and 162.0˚ respectively. These interactions are significantly absent in complexes B2 and B3. Furthermore, B2 and B3 have hydrogen bonds which involve the secondary hydroxyls of the host and methyl hydrogens of the guest. The average interaction distance is 3.36 Å and average angle is 145.0˚ Also, the guests of B2, B3 and B4 are involved in O•••O attractive close contacts made between ethereal or carbonyl oxygen atoms of the guest and the O3 or O4 atoms of their respective host cyclodextrins. We have also noted that all the structures have C-H•••Br hydrogen bonds, which further stabilise the host-guest complexes. The mean interaction distance is 3.13 Å. We are unable to make any observations regarding the host-guest interaction in complex B1, as the guest molecule is disordered to such an extent that it could not be modelled.

Table 17. *Summary of host-guest interactions for B2, B3, B4 and B5.*

Interaction	B2	B3	B4	B5
ethereal C-H•••O	3-22 - 3.31 Å 136.0 - 145.0°	3.19 - 3.36 Å 122.0 - 143.0°	3.36 Å 135.0°	3.35 - 3.51 Å 128.0 - 167.0°
carbonyl C-H•••O	3.43 Å 170.0°	3.34 - 3.54 Å 164.0 - 175.0°	2.87 - 3.54 Å 133.0 - 160.0°	3.44 Å 164.0°
hydroxyl O6-H•••O	-	-	2.81 Å, 160.0°	2.80 Å, 163.0°
hydroxyl O3-H•••O	3.20 - 3.34 Å	3.04 - 3.32 Å	-	-
O•••O contacts	3.20 Å	3.04 – 3.12 Å	3.17 – 3.24 Å	-
C-H•••Br	3.17 - 3.19 Å	2.85 – 3.18 Å	3.07 – 3.25 Å	2.92 - 3.24 Å

Guest intramolecular interactions

All the intramolecular N-H•••O and C-H•••O hydrogen bonds are retained in the complexed guest molecules. However, they are distorted with respect to those of the uncomplexed guest. The hydrogen bond distances of the uncomplexed guest for N-

H•••O and C-H•••O interactions are 2.57 and 2.93 Å and the respective hydrogen bond angles are 110.0˚ and 107.0˚. The N-H•••O hydrogen bond lengths and angles for the four structures span the range 2.48 to 2.73 Å and 100.0 to 114.0˚. The mean lengths and angles for the C-H•••O interaction range from 2.77 to 3.04 Å and 102.0 to 127.0˚ respectively. The different range for both hydrogen bond interactions reflect the observed changes in the guest conformation that accompany their inclusion in the host molecules.

Guest-guest intermolecular interactions

There are several close contacts between the included guests in this series and this is reflected in the wide range of contact distances seen. Contact distances range from 2.60 to 3.51 Å for C•••O, O•••O, C•••C and C•••Br interactions respectively. There are also three weak C-Br•••π interactions. The interactions range from 3.82 to 3.98 Å with an angular range of 121.0 to 177.0˚. These interactions are generally weak.[21,22]

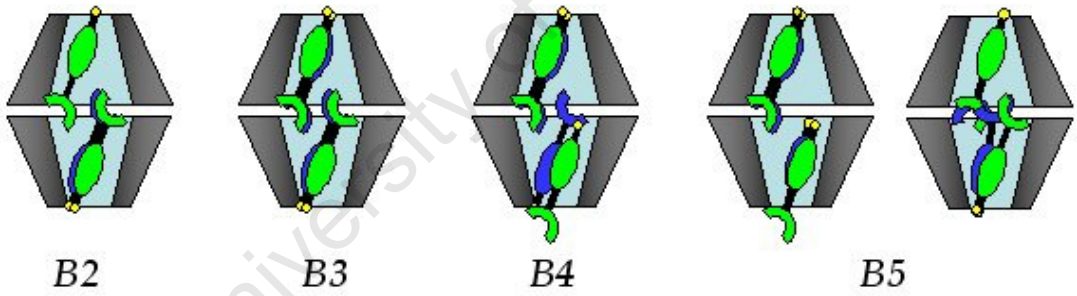

Figure 70. *The schematic diagram shows the orientations of the guest molecules in the dimeric cavity.*

Guest orientation *(modes of inclusion)*

For complexes B2 and B3 the orientations of the included guest molecules are similar. Both sets of guests are disordered over two positions, except that in B2 one of the disordered guest molecules could not be modelled (Figure 70). The guests are arranged in an anti-parallel manner. In the case of B4, the guests are also disordered over two positions but here the major components of disorder are arranged in a parallel fashion while the minor components are arranged in the usual anti-parallel manner. In B5, with two dimers in the asymmetric unit, there is a combination of arrangements. In one dimer the guests are disordered over two positions and have

the usual anti-parallel arrangement. In the second dimer, the guests are also disordered over two positions but with parallel arrangement. For continuity the arrangements are explained here. In the anti-parallel arrangement, the bromophenyl groups of the included guests are located at the primary rims of each CD. The entire bromophenyl group is located above the O4 mean plane with the bromine atom protruding from the primary rim. The more polar urea group is located at the secondary rim interface. In the parallel arrangement, one bromophenyl group is located at the primary rim of one of the CDs of the dimer while the other guest is arranged such that the bromophenyl group is located at the secondary rim interface of the dimer. Not all the atoms belonging to the phenyl ring are located above the O4 mean plane. This is an indication that the guests are not lodged as deeply as in the anti-parallel arrangement. The urea group, in this case, is lodged at the primary rim with the methoxy-1-methyl moiety protruding from the primary rim, as shown in Figure 70.

In order to explain the different guest orientations, one often considers factors such as guest size, shape and dipole moments. This is the case especially when dealing with a variety of guests. However, additional parameters need to be considered when the guest remains the same, as in complexes B1-B5. Additional parameters such as the angles of inclination, relative rotation, hydrophobicity and even crystallisation conditions contribute in some way to the variety of guest inclusion modes observed.

Inclination and rotation

In order to facilitate the accommodation of the guests inside the cavity the guests are tilted with respect to the O4 heptagon and rotated with respect to the other guest present in the cavity. This maximises the use of the available space inside the cavity and minimises abnormally close contacts and steric interference. It also affects the extent of guest protrusion which has an effect on the packing. The inclination angles of the guest with respect to the CD within which it is included as well as the angles of rotation are reported in Table 18. Inclination angles for the SC complexes (B4 and B5) are on average larger than the tilt angles for CH complexes.

Table 18. *Inclination angles (˚) between mean O4 plane and the phenyl ring of each guest.*

	A	B	C	D	E	F	G	H
B1	-	-	-	-	-	-	-	-
B2	61.7(5)	65.4(4)	58.0(2)	-	-	-	-	-
B3	59.2(6)	65.1(7)	60.0(8)	58.9(3)	-	-	-	-
B4	64.8(5)	67.5(5)	62.2(5)	65.6(5)	-	-	-	-
B5	64.0(4)	65.0(3)	60.5(2)	62.7(7)	61.8(1)	62.0(9)	60.8(1)	60.5(2)

Hydrophobicity

According to Lichtenthaler *et al.* the secondary rim of β-CD molecules is relatively hydrophilic when compared to the relatively hydrophobic primary rim.[28,29] Furthermore, secondary rim interfaces formed between head-to-head hydrogen bonded cyclodextrin molecules are hydrophilic as it is more likely that the secondary rim interacts with water molecules of crystallisation and particular polar portions of guest molecules. In other words, the polar regions of a particular guest are more likely to interact with the polar regions of the cyclodextrin host. Similarly, the hydrophobic portions of the host cavity are more likely to interact with the hydrophobic portions of the guest. However, the exact position of the hydrophobic moiety depends on its size and nature.[30] With this in mind, the anti-parallel arrangement seen in all four complexes B2-B5 is consistent with the assertions of Lichtenthaler.[28] It is clear that the anti-parallel alignment is the preferred arrangement for the guests in this series as the anti-parallel arrangement is present within each individual CD dimer. B4 and B5 also have guests with parallel orientation where the more polar moiety protrudes from the cavity. The polar moiety of the guests does not hydrogen bond with interstitial water molecules but rather hydrogen bonds via a hydroxyl group (also polar) to the carbonyl oxygen atom of the guest. This follows the conclusion of Bergeron *et al.* which states that the solvation of the polar group is the determining factor in the location and stabilisation of the guest in the cavity.[31]

Crystallisation conditions

In summary, four complex preparations were devised. The solvent medium and temperature profiles were varied in each experiment and are presented in Table 19.

(With regard to form B2, its discovery during attempts to crystallise B1 was described earlier under 'Crystallisation Conditions').

Table 19. *Preparation and crystallisation conditions of B1, B3, B4 and B5*

Preparation	Temperature profile	Solvent system	Ratio V/V %	Phase
1	slow cooling from 80˚C - RT	water	100	B1
2	elevated temperature (~ 38˚C)	water/ethanol	75/25	B3
3	low temperature (-4˚C)	water/ethanol	75/25	B4
4	slow cooling from 80˚C - RT	water/ethanol	75/25	B5

From the tabulated data, preparations 1 and 4 differed only in the make-up of the solvent medium. The solvent medium of 1 was water while the solvent medium of 4 was a water/ethanol (75/25) mixture. For these experiments 1 acts as an internal standard for 4. Preparations 2 and 3 had different temperature profiles with identical solvent media. The result of these variations was the isolation of different phases. Preparations 1 and 4 produced phases B1 and B5 respectively, while preparations 2 and 3 produced phases B3 and B4 respectively.

Both temperature and the addition of ethanol affect the polarity of the primary solvent (*viz.* water) and this must in turn influence the solvation of the guest molecules in solution. This, according to Bergeron *et al.*, influences the interaction of the guest with the host in solution.[31]

Monolinuron and metobromuron were subjected to the same experiments. However, metobromuron proved to be more prolific than monolinuron at producing new forms and it was decided to carry out a more comprehensive study of metobromuron. In pursuing this, a wide range of experimental conditions was employed, crystal forms resulting from each experiment being identified. Not all of the conditions giving rise to one specific form were reported in this thesis. Instead, a single procedure for preparing a specific form reproducibly was reported. Also, a variety of conditions was used in the pursuit of new crystal forms (inclusion complexes). Only the conditions which generated new forms were reported in the thesis.

CRYSTAL PACKING

Generally, the secondary hydroxyl groups rarely interact with the guest but they are, however, involved in an invariant network of hydrogen bonds which connects neighbouring dimers directly or via water molecules. The primary hydroxyls are involved in hydrogen bonding to adjacent dimers and are influenced by the presence of the guest. All the dimers are associated via a hydrogen bonding network either directly or through water molecules. Thus, they form endless two-dimensional C-centred or pseudo-C-centred layers, as mentioned previously.[15]

Stacking by interactions via the primary rim means that those parts of the guest which protrude from the primary rim crucially influence the two-dimensional layer interactions and how they pack to form the lattice. So, hydrophobic groups located at the primary rim favour channel formation in order to avoid contact with the aqueous environment. Polar or hydrophilic groups of the guest hydrogen bond to (polar) hydroxyl groups or to water molecules favouring a screw channel formation.[24]

With regard to complexes B2 and B3 (CH packing motif with the hydrophobic moieties located at the primary rim), the guest molecules are almost completely isolated from the aqueous environment. B4 and B5 pack in the screw channel arrangement with the more polar moiety of the included guest located at the primary rim of one of the CDs making up the dimer.

Finally, all previously reported incidences of multiplicity of forms have only dealt with two different crystal forms. It is therefore important to highlight the remarkable occurrence of as many as five structurally different inclusion complexes with the same host-guest stoichiometry reported here.

REFERENCES

1. Barbour, L.J., LAYER, A computer program for the graphic display of intensity data as simulated precession photographs, *J. Appl. Cryst.*, **1999**, 32, 351-352.
2. XPREP, *Data Preparation and Reciprocal Space Exploration*, Version 5.1, (Copyright Bruker Analytical X-ray Systems, **1997**).
3. Otwinowski, Z., Minor, W., *Processing of X-ray Diffraction Data in Oscillation Mode in Methods in Enzymology*, Vol. 276, Carter, C.W., Sweet, R.M., (eds.), Academic Press, New York, **1996**, 307-326.
4. Sheldrick, G.M., *SHELXS-97*, *Program for Crystal Structure Solution,* Institüt für Anorganische Chemie der Universität, Tammanstrasse 4, D-3400 Göttingen, Germany, **1997**.
5. Sheldrick, G.M. *SHELXH*-97, *Acta Crystallogr.,* **2008**, A64, 112-122.
6. Etter, M.C., Macdonald, J.C. and Bernstein, J., *Acta Crystallogr.,* **1990**, B46, 256-262.
7. Bernstein, J., Davis, R.E., Shimoni, L. and Chang, N-L., *Angew. Chem., Int. Ed. Engl.*, **1995**, 34, 1555-1573.
8. Caira, M.R., de Vries, E.J.C. and Nassimbeni, L.R., *Chem. Commun.,* **2003**, 16, 2058-2059.
9. Cambridge Structural Database and Cambridge Structural Database System, Version 5.29 November **2007**, Cambridge Crystallographic Centre, University Chemical Laboratory, Cambridge, England.
10. Lichtenthaler, F.W. and Immel, S., *Starch/Stärke*, **1996**, 48, 225-232.
11. Saenger, W. and Steiner, T., *Acta Crystallogr.,* **1998**, A54, 798-805.
12. Saenger, W., Betzel, C., Hingerty, B.E. and Brown, G.M., *Nature*, **1982**, 296, 581-583.
13. Saenger, W., Betzel, C., Hingerty, B.E. and Brown, G.M., *Angew. Chem., Int. Ed. Engl.,* **1983**, 22, 883-884.
14. Betzel, C., Saenger, W., Hingerty, B.E. and Brown, G.M., *J. Am. Chem. Soc.,* **1984**, 106, 7545-7557.
15. Makedonopoulou, S. and Mavridis, I.M., *Acta Crystallogr.*, **2000**, B56, 322-331.
16. Schneider, T.R. and Sheldrick, G.M., *Acta Crystallogr.,* **2002**, D58, 1772-1779.
17. Sheldrick, G.M., *Direct Methods for Solving Macromolecular Structures,* edited by Fortier, S., Dordrecht: Kluwer Academic Publishers, **1998**, 401-411.
18. Sheldrick, G.M., *Z. Kristallogr.,* **2002**, 217, 644-650.
19. Caira, M.R., and Dodds, D.R., *J. Inclusion Phenom. Macrocyclic Chem.,* **1999**, 34, 19-29.
20. Harding, M.M., MacLennan, M.J. and Paton, R.M., *Nature (London),* **1978**, 274, 621-623.
21. Nagaraj, B., Narasimhamurthy, T., Yathirajan, H.S., Nagaraja, P., Narasgowda, R.S. and Rathore, R.S., *Acta Crystallogr.,* **2005**, C61, 177-180.
22. Personal communication, Nangia, A., **2008**.
23. Hamilton, J.A. and Chen L., *J. Am. Chem. Soc.,* **1988**, 110, 4379-4391.

24. Giastas, P., Yannakopoulou, K. and Mavridis, I.M., *Acta Crystallogr.,* **2003**, B59, 287-299.

25. Mentzafos, D., Mavridis, I.M., Le Bas, G. and Tsoucaris, G., *Acta Crystallogr.,* **1991**, B47, 746-757.

26. Le Bas, G. and Tsoucaris, G., *Supramol. Chem.,* **1994**, 4, 13-16.

27. Tsorteki, F., Bethanis, K., Pinotsis, N., Giastas, P. and Mentzafos, D., *Acta Crystallogr.*, **2005**, B61, 207-217.

28. Lichtenthaler, F.W. and Immel, S., *Starch/Stärke*, **1996**, 48, 145-154.

29. Lichtenthaler, F.W. and Immel, S., *Liebigs Ann.*, **1996**, 48, 27-37.

30. Nakanishi, I., Fujiwara, T. and Tomita, K., *Acta Crystallogr.,* **1984**, A40, C78.

31. Bergeron, R., Channing, M., McGovern, K. and Roberts, W., *Bioorg. Chem.,* **1979**, 8, 263-281.

Chapter 7
ISOTRUCTURALITY OF TRIMEB COMPLEXES OF TWO PHENYLUREA GUESTS

We report the isolation of three isostructural TRIMEB inclusion complexes involving two phenylurea guest molecules and we investigate the solid-state features of the inclusion complexes using single crystal X-ray diffraction.

TRIMEB INCLUSION OF METOBROMURON AND MONOLINURON

Preparation of single crystals

TRIMEB solutions were prepared by dissolving 0.077 mmol of the cyclodextrin in cold distilled de-ionised water (1 mL) at *ca* 4°C. Once all the cyclodextrin had dissolved, equimolar amounts of **1** and **2** were added to the solutions with vigorous stirring. In order to induce different crystal forms, the preparations were carried out in duplicate. To one set of preparations a small aliquot of ethanol (0.2 mL, 96 %) was added, while the other contained only water. In the case of the preparation that contained only water, precipitation occurred as soon as the guest was added while the preparations containing ethanol remained clear. The solutions were stirred overnight. The solutions were filtered and placed in a hot water bath set to 55˚C for at least 12 h in order to induce crystallisation. The complex reactions yielded TRIMEB•metobromuron•0.5(H_2O) C1 (0.5 ± 0.1), TRIMEB•metobromuron •0.38(C_2H_5OH)•0.4(H_2O) C2 (0.4 ± 0.1) and TRIMEB•monolinuron•0.2(H_2O) C3 (0.2 ± 0.1).

Stoichiometry

The stoichiometries of the three complexes were determined by means of UV spectrophotometry (Table 1). Thermogravimetric analysis was used to determine the water content for all three crystal forms as well as the ethanol content in C2. The temperatures of evolution of H_2O and ethanol were sufficiently different allowing one to distinguish between the two solvents. The reported water content is the average of two readings.

Table 1. *Stoichiometries for complexes C1, C2 and C3.*

Complex	C1	C2	C3
Host:Guest ratio	1.00:1.03	1.00:1.01	1.00:0.98
H_2O[a]	0.5H_2O	0.4H_2O	0.2H_2O
C_2H_6O	-	0.38	-

(a) H_2O molecules per CD molecule.

X-RAY STRUCTURES OF C1, C2 AND C3

Space group determination

Forms C1, C2 and C3 are isostructural and are discussed together here. The program LAYER was used to determine the crystal symmetry. The Laue symmetry was found to be *mmm* indicating the orthorhombic crystal system.[1] From further examination of the reciprocal lattices the reflection conditions obtained were *hkl : none, h00 : h = 2n, 0k0 : k = 2n, 00l : l = 2n* confirming the space group as $P2_12_12_1$. The space group $P2_12_12_1$, common to C1, C2 and C3 was confirmed with the aid of the program XPREP.[2] From density considerations Z = 4 for all three complexes.

Structure solution and refinement

Refinement parameters and crystal data are reported in Table 2. Unit cell refinement and data reduction were performed with the program DENZO-SMN.[3] C1, C2 and C3 were found to be isostructural with the complexes (TRIMEB)•(*p*-iodophenol)•4(H_2O) (Refcode : RONWOG) and (TRIMEB)•((S)-ibuprofen) (Refcode : CAMPIP).[4,5,6] The three structures were solved by isomorphous replacement using only the host coordinates of RONWOG (C1 and C2) and CAMPIP (C3). All non-hydrogen atoms except O6, C7, C8 and C9 of each methyl glucose unit were used in the model as the input fragment. The glucopyranose units for the host were labelled G1-G7 with disordered moieties labelled A and B. The structures were refined with SHELXH-97 with successive difference Fourier maps revealing the methoxyl groups.[7] Several atoms of the host molecules were disordered over two positions; these are reported in Table 3. The site-occupancy factors (s.o.f.s) of the major components of disorder were refined as x initially set to 0.5. They refined to 0.68, 0.53 and 0.69 for C1, C2 and C3 respectively. The minor components refined as 1-x. All the non-hydrogen atoms of the hosts refined anisotropically except for the disordered atoms including C8G1, C8G5, C7G2 and C8G2 for C1 and C9G1, C7G5 for C2, which were refined isotropically. All hydrogens attached to carbon atoms were placed in idealised positions using a riding model.

Table 2. *Crystal data and data-collection parameters for C1, C2 and C3.*

parameters	*C1*	*C2*	*C3*
Formula unit	$(C_{63}H_{112}O_{35})\bullet(C_9H_{11}O_2N_2Br)\bullet 0.5H_2O$	$(C_{63}H_{112}O_{35})\bullet(C_9H_{11}O_2N_2Br)\bullet 0.38(C_2H_6O)\bullet 0.4H_2O$	$(C_{63}H_{112}O_{35})\bullet(C_9H_{11}O_2N_2Cl)\bullet 0.2H_2O$
Mr	1725.66	1713.35	1647.37
Crystal system	Orthorhombic	Orthorhombic	Orthorhombic
Space group	$P2_12_12_1$	$P2_12_12_1$	$P2_12_12_1$
***a*/Å**	15.0730(2)	15.0496(1)	14.8956(1)
***b*/ Å**	20.9788(3)	21.3449(2)	20.5348(2)
***c*/ Å**	27.5933(5)	27.4299(3)	28.0009(3)
α/°	90.00	90.00	90.00
β/°	90.00	90.00	90.00
γ/°	90.00	90.00	90.00
Vol. Å³	8725.40(2)	8811.37(1)	8564.86(1)
Z	4	4	4
ρ_{calc} g cm⁻³	1.314	1.292	1.278
μ (MoKα) mm⁻¹	0.559	0.553	0.132
F(000)	3676	3656	3534
Crystal size mm³	0.10 x 0.13 x 0.15	0.10 x 0.15 x 0.20	0.10 x 0.08 x 0.42
Temperature K	113 ± 2	113 ± 2	113 ± 2
Range scanned θ/°	$2.79 \le \theta \le 25.02$	$1.76 \le \theta \le 27.88$	$3.28 \le \theta \le 25.33$
Index range	-16 : 17; -24 : 24; -32 : 31	-19 : 18; -25 : 24; -35 : 34	-17 : 17; -24 : 24; -33 : 33
ϕ Scan angle °	1.0	1.0	1.0
ϕ Scan range °, no of frames	283.0, 283	328.0, 328	239.0, 239
ω Scan angle °	1.0	1.0	1.0
ω Scan range °, no of frames	70.0, 70	37.0, 37; 57.0, 57	120.0, 120; 129.0, 129
Dx mm	36	40	40
No. of reflections	72296	80699	89794
No. of unique reflections	15310	19315	15568
No. of reflections with I>2σ(I)	9168	13119	10779
No. of l.s. parameters	963	979	924
R_{int}, R_σ	0.0982, 0.1167	0.0382, 0.0677	0.0682, 0.0672
S	1.034	1.040	1.036
R_1 [$F_o > 4\sigma(F_o)$]	0.0925	0.0560	0.0824
wR_2	0.2713	0.1462	0.2385
No. of reflections omitted	17	12	53
Weighting scheme parameters	a = 0.1648, b = 4.7386	a = 0.0733, b = 3.1208	a = 0.1409, b = 7.0967
(Δ/σ)	<0.001	<0.001	<0.001
Δρ excursions eÅ⁻³	-0.59, 2.71	-0.79, 0.48	-0.55, 0.86

All hydrogen atoms were assigned isotropic temperature factors of 1.2 times those of their parent atoms except for methyl hydrogen atoms, which were assigned isotropic temperature factors of 1.5 times those of their parent atoms.

For complexes C1 and C2 two sites were revealed for water molecules in the electron density map while a single site was revealed in the electron density map of C3. The site-occupancies of the water molecules range from 0.24 to 0.39 while the isotropic temperature factors range from 0.04 to 0.09 Å^2. From TGA (n = 2) the two sites of C1 accounted for 0.5 water molecules while the two sites of C2 accounted for 0.4 water molecules. The single site of C3 accounted for 0.2 water molecules.

Table 3. *Disordered host atoms of complexes C1, C2 and C3.*

C1	**C5A6**	**O5A6**	**C6A6**	**O6A6**	**C9A6**					
C2	**O4A6**	**C5A6**	**O5A6**	**C6A6**	**O6A6**	**C9A6**				
C3	**C4A5**	**C5A5**	**O5A5**	**C1A5**	**C2A5**	**C3A5**	**C5A5**	**O6A5**	**C9A5**	**O4A6**
	O2A5	**C7A5**	**O3A5**	**C8A5**	**C4A6**	**C5A6**	**O5A6**	**O6A6**	**C9A6**	

Modelling of the guest

After refinement of the host our attention turned to the guest. After careful inspection of the difference map the highest peaks were assigned as bromine (C1 and C2) and chlorine (C3). This was followed by the placement of the phenyl rings which were easily identifiable by their hexagonal shape. An AFIX 66 instruction, constraining the rings as rigid hexagons, was applied once all the atoms were located in the difference map. This was followed by the careful placement and refinement of the urea moieties of the three models. Two positions for the guest molecule were determined for C1 and C2 with those positions labelled A and B. The bromine atom is shared in the disordered guest components of complexes C1 and C2. The cavity of complex C2 contains both the guest and an ethanol molecule with partial occupancy (0.65). The guest in C3 was not disordered. The site-occupancies of the major components of disorder (A) were refined as x while the minor components (B) were refined as 1-x. An initial value of x = 0.5 was set, eventually refining to 0.60 for C1 and 0.57 for C2. Each guest model was assigned a global isotropic temperature factor with a starting value of 0.05 Å^2. The values settled between 0.05 and 0.08 Å^2 for models A and B. Distance restraints were imposed to ensure reasonable geometries, as the least-squares refinements were sensitive. The standard deviation σ for restrained bond lengths was set between 0.001 and 0.008Å. Only the bromine atoms (C1 and C2) were refined anisotropically and all other atoms belonging to the guests were refined isotropically. All the atoms belonging to

the guest of complex C3 were refined anisotropically. The guest hydrogens were added in idealised positions in a riding model. Aromatic type hydrogens refined with 1.2 times the U_{iso} of their parent atoms while the methyl hydrogens refined with 1.5 times the U_{iso} of their parent atoms.

STRUCTURAL DESCRIPTION

Complex C1 consists of a single TRIMEB molecule, one disordered guest molecule and two water molecules with partial occupancy. C2 consists of a single TRIMEB molecule, a single disordered guest molecule, an ethanol molecule with partial occupancy and two water molecules also with partial occupancy. C3 consists of a single TRIMEB molecule, a guest molecule and a water molecule with partial occupancy. The labelled TRIMEB host molecule is shown in Figure 1.

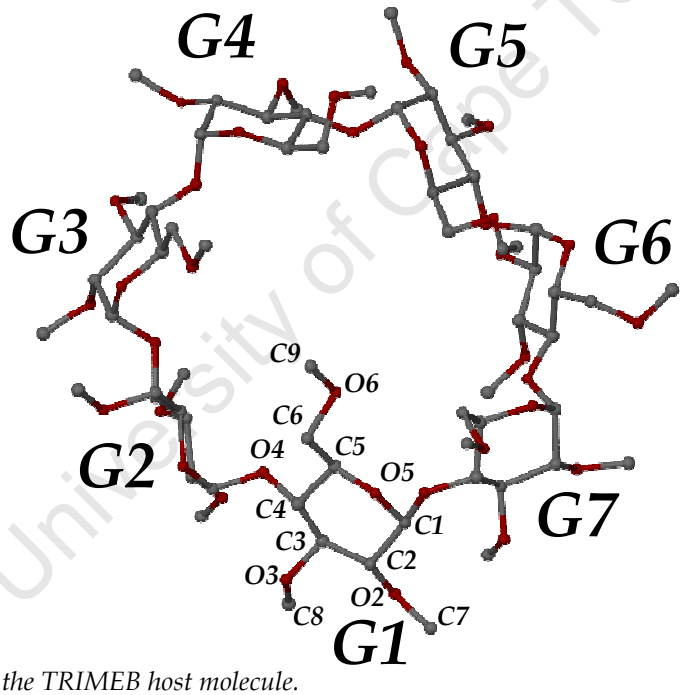

Figure 1. *Labelling of the TRIMEB host molecule.*

Host conformation

Primary hydroxyl torsion angles

All the primary hydroxyl torsion angles (**ω**) of C1, C2 and C3 correspond to the *(-)-gauche* orientation with three exceptions, namely G1, G3 and B6 (minor disordered component) having the *(+)-gauche* conformation. The **ω** torsion angles for the complexes are very similar with the largest difference between the torsion angles for C1, C2 and C3 being ~9˚ (G1). The C5-C6-O6-C9 torsion angles for the three

complexes range between -179.1 and 179.6˚. All the glucose residues are in the $^4C_1$-chair conformation.

Macrocyclic symmetry

The radii **r** for C1, C2 and C3 vary within similar narrow ranges, namely 4.65 – 5.25 Å, 4.64 – 5.25 Å and 4.63 – 5.28 Å respectively. The lengths **l** for the three complexes are also very similar and also vary within narrow bands: 4.28 – 4.49 Å, 4.27 – 4.51 Å and 4.23 – 4.48 Å for C1, C2 and C3 respectively. The average glycosidic oxygen angle **a** for the three complexes is 127.2˚ while the glycosidic oxygen angles of C1, C2 and C3 fall within the range 119.9 - 137.1˚.

Planarity of the O4-Heptagons

The root mean square deviations (**d**) for C1, C2, and C3 are 0.415 Å, 0.420 Å and 0.516 Å respectively. Each complex has four O4 atoms with negative deviations from the mean O4 plane (O4G2, O4G3, O4G5 and O4G6 for C1; O4G3, O4G4, O4G6 and O4G7 for C2 and O4G2, O4G3, O4G5 and O4G6 for C3). The torsion angle **t** ranges from -28.2 to 21.3˚ for C1, -32.6 to 19.8˚ for C2, and -45.4 to 24.5˚ for C3. The tilt angles τ_1 and τ_2 for C1, C2 and C3 are all positive with angular ranges from 10.4 to 41.3˚ for τ_1 (C1) and 12.5 to 40.4˚ for τ_2 (C1), 10.5 to 41.2˚ for τ_1 (C2) and 10.3 to 40.6˚ for τ_2 (C2), 13.4 to 46.7˚ for τ_1 (C3) and 14.0 to 41.3˚ for τ_2 (C3). The intersaccharidic angles φ for the complexes range from 115.1 to 119.6˚ for C1, 110.9 to 119.5˚for C2 and 110.2 to 119.8˚ for C3.

The parameters reported here for C1, C2 and C3 are indicative of an elliptically distorted host conformation. This is evidenced by the values for the radii. The individual O4 atoms of the O4-heptagon deviate significantly from the mean O4 plane with the extent of the deviation communicated by the values for **d** and **t**. The three cyclodextrins have a saddle-like appearance shown in Figure 2.

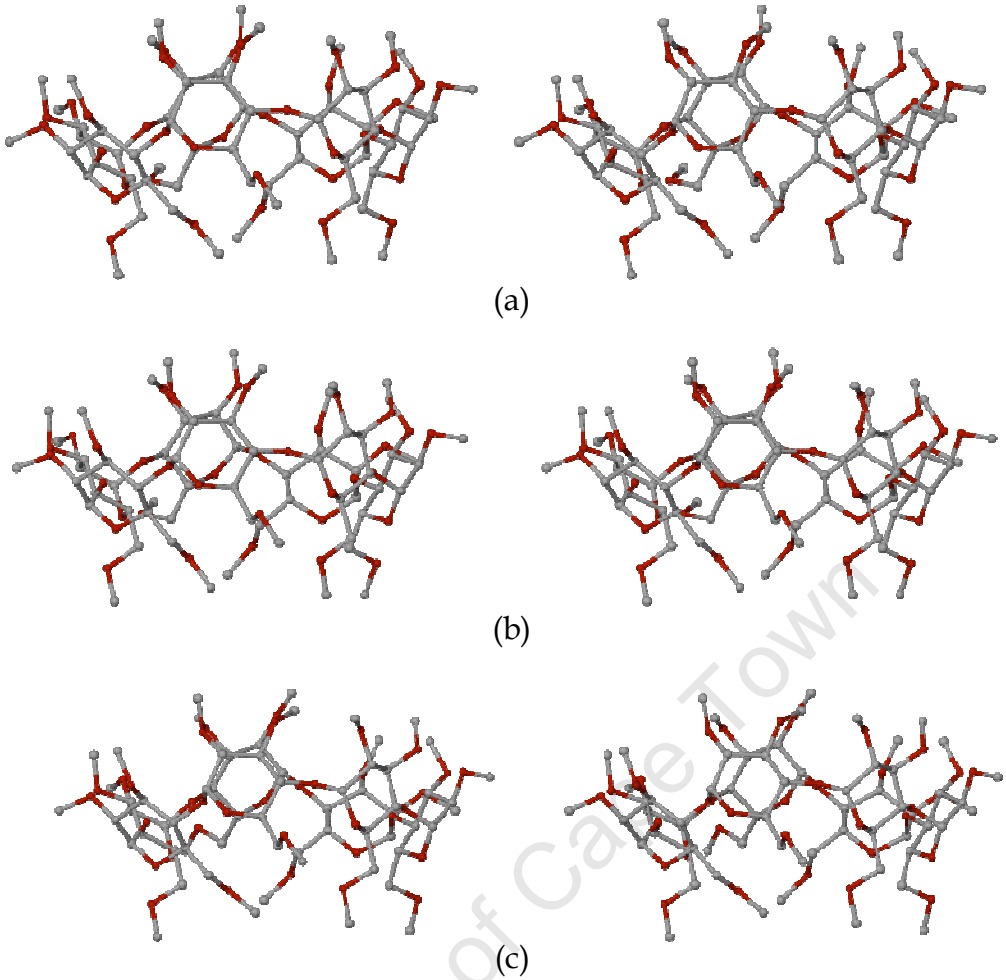

Figure 2. *Stereo view of the TRIMEB molecules belonging to complexes C1 (a), C2 (b) and C3 (c), shown side-on to illustrate the saddle-like curvature of the host molecules. Only the major components of disordered atoms are included in the figures.*

C1, C2 and C3 each have glucose units with negative torsion angles (**t**) (tabulated values for the torsion angles are reported in the appropriate appendix). The tilt angles (τ_1 and τ_2) of the three complexes are positive indicating that the glucose units lean inward toward the centre of the cavity. The extent of closure of the primary faces is similar in the three complexes. The similarity in the extent of primary face closure is illustrated in Figure 3. These complexes thus belong to the category of TRIMEB inclusion complexes in which the host cavity is cup-shaped, presenting a large hydrophobic surface to the encaged guest molecule.[8,9]

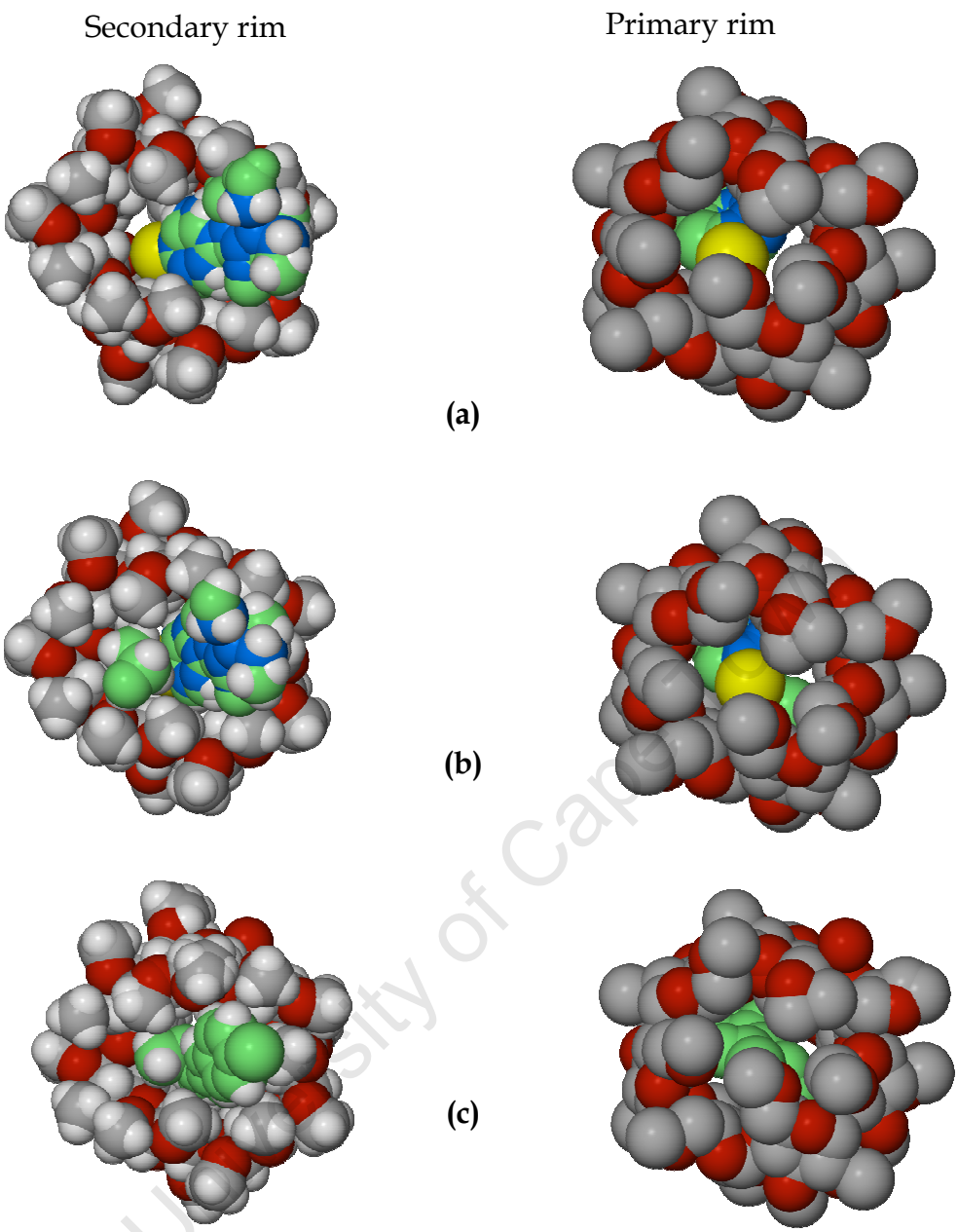

Figure 3. *Space filling diagrams of complexes C1 (a), C2 (b) and C3 (c), viewed from both secondary and primary rims. Hydrogen atoms were omitted from the primary rim for clarity.*

The remarkable similarity found in the host conformations was expected since the TRIMEB skeleton used in the refinements of C1 and C2 was the same. Even more remarkable is the similarity with C3 for which the trial model was a TRIMEB skeleton from a different structure. The TRIMEB skeletons are overlaid in Figure 4.

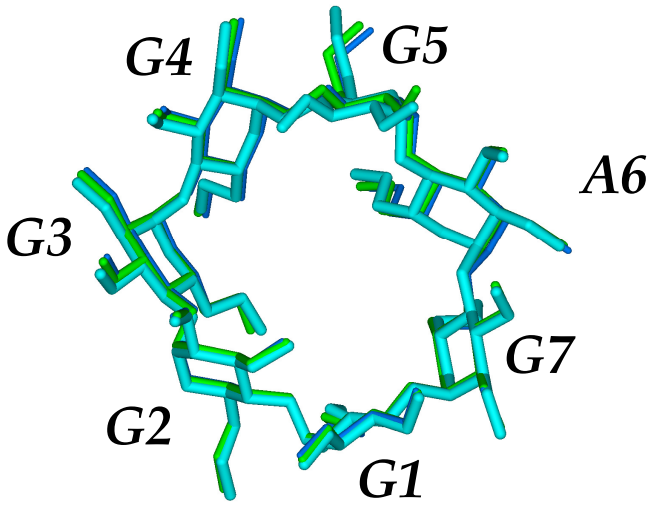

Figure 4. *An overlay of the host molecules in complexes C1 (green), C2 (blue) and C3 (cyan). Disorder and hydrogen atoms are omitted for clarity.*

Furthermore, the similarities between the structures extend to the twofold disorder manifested by the atoms listed in Table 3. However, the extent of disorder is different in each case. For instance, in C1 and C2 the disorder involves only glucose unit 6 while in C3 it involves units 5 and 6, as shown in Figure 5.

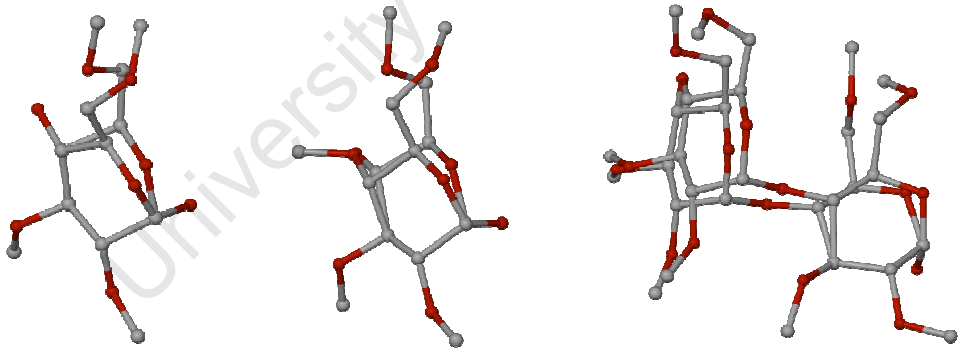

Figure 5. *Disorder of the host molecules of complexes C1 (a), C2 (b) and C3 (c).*

INTRA- AND INTERMOLECULAR INTERACTIONS

Host intramolecular interactions

The host conformations of C1, C2 and C3 are stabilised by several analogous intramolecular C-H•••O interactions.[8] The host molecule in complex C1 has 13 intramolecular C-H•••O hydrogen bonds which can be divided into seven different

types. There are five C6-H•••O5, two each of C8-H•••O2 and C1-H•••O3 and one each of C8-H•••O4, C1-H•••O6, C9-H•••O3 and C6-H•••O6 interactions. 12 interactions stabilise the host conformation while one occurs within a methyl glucose unit (C8-H•••O4). The mean bond length for the C-H•••O interactions is 3.17 Å (range 3.01 – 3.48 Å) while the mean bond angle is 132.0˚ (range 117.0 – 158.0˚).

The host molecule in complex C2 has 15 intramolecular C-H•••O hydrogen bonds consisting of eight different types. Six are C6-H•••O5 interactions, two each of the C1-H•••O3 and C7-H•••O3 type interactions and one each of C1-H•••O6, C6-H•••O6, C8-H•••O2, C8-H•••O4 and C9-H•••O5 type hydrogen bonds. Eleven of the intramolecular interactions stabilise the host conformation while four are found within methyl glucose units (C8-H•••O2, C8-H•••O4 and two C7-H•••O3). The mean hydrogen bond length is 3.17 Å (range 3.01 – 3.43 Å). The mean hydrogen bond angle is 131.0˚ and the range is 111.0 to 155.0˚.

Complex C3 has ten intramolecular hydrogen bonds made up of four C6-H•••O5 interactions, two each of C8-H•••O2 and C1-H•••O3 interactions and one each of C7-H•••O3 and C6-H•••O6 hydrogen bonds. Seven intramolecular interactions stabilise the host conformation while three occur within methyl glucose units (C7-H•••O3 and two C8-H•••O2 hydrogen bonds). The mean interaction distance for the C-H•••O hydrogen bonds is 3.17 Å (range 3.01 – 3.48 Å) while the mean hydrogen bond angle is 134.0˚ (range 124.0 – 167.0˚).

Host-Host intermolecular interactions

Complexes C1 and C2 both have five intermolecular hydrogen bonds while complex C3 has six. The intermolecular interactions of C1 can be divided into three different C-H•••O interactions. There are three C2-H•••O6 interactions, one C9-H•••O3 and one C7-H•••O2 interaction present in C1. The mean hydrogen bond distance is 3.39 Å (range 3.29 – 3.46 Å) while the mean hydrogen bond angle is 152.0˚ ranging from 131.0 to 167.0˚. The intermolecular hydrogen bonds of complex C2 can also be divided into three types. There are three C2-H•••O6 hydrogen bonds, one C2-H•••O3 interaction and one C7-H•••O2 hydrogen bond. The mean distance for

the five C-H•••O bonds is 3.42 Å (range 3.37 – 3.48 Å). The mean bond angle is 156.0˚ and ranges from 151.0 to 167.0˚. The six C-H•••O hydrogen bonds of C3 consist of two C7-H•••O2 interactions, two C2-H•••O6 interactions and two C9-H•••O3 hydrogen bonds. The mean distance is 3.34 Å (range 3.19 – 3.53 Å) while the mean angle is 149.0˚ (range 124.0 – 167.0˚).

Host-Water interactions

Complexes C1 and C2 each have five host-water interactions while C3 has only three such interactions. For C1, two of the interactions are OW-H•••O hydrogen bonds with a mean hydrogen bond distance of 2.74 Å (range 2.71 – 2.77 Å) and a mean hydrogen bond angle of 158.0˚ (range 152.0 – 164.0˚). The three remaining interactions are O•••OW close contacts with a mean distance of 3.04 Å (2.74 - 3.37 Å). In the case of C2 the two OW-H•••O hydrogen bonds have a mean distance of 2.82 Å (range 2.77 – 2.87 Å) with a mean hydrogen bond angle of 165.0˚ (range 151.0 – 179.0˚). The three remaining interactions are O•••OW close contacts with a mean interaction distance of 3.01 Å (range 2.67 – 3.41 Å). Complex C3 has a single C-H•••OW hydrogen bond with a bond distance of 3.21 Å and a hydrogen bond angle of 161.0˚. The two remaining interactions are close contacts and have a mean interaction distance of 2.83 Å (2.83 – 2.84 Å).

GUEST INCLUSION

Guest disorder and location

The C1 complex consists of a single host molecule, a single guest molecule and two water molecules with partial occupancy located in the cavity. The guest molecule is disordered over two positions with Br1 shared between the two positions (Figure 6). The major component of disorder A is shown in green while the minor component is shown in blue. The shared atom is shown in cyan. Both water molecules have partial occupancy linked to the twofold disorder of the guest molecule.

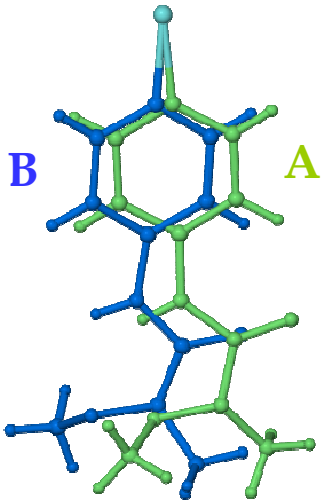

Figure 6. *Twofold disorder of the guest belonging to C1. The shared bromine atom is shown in cyan.*

The guest is orientated with the bromophenyl moiety buried deep within the TRIMEB cavity while the urea group protrudes from the secondary rim, as shown in Figure 7 (a).

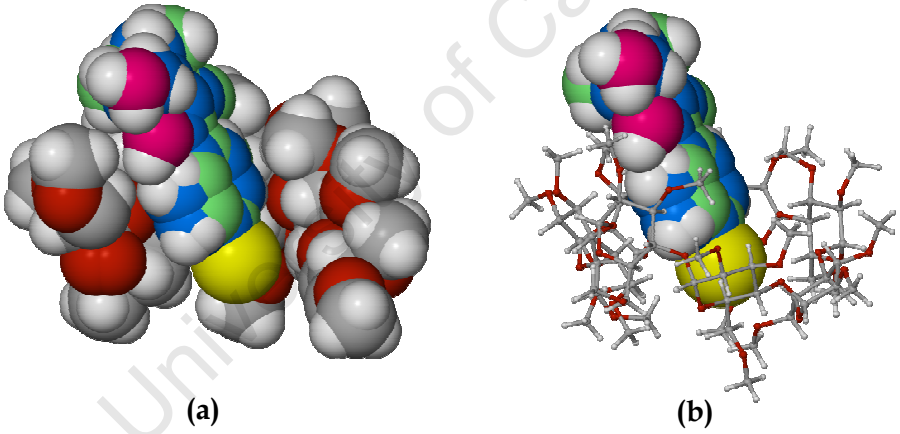

Figure 7. *(a) A cutaway image of the complex C1. (b) shows how the guest molecule is tilted with respect to the host molecule of complex C1.*

The guest is tilted so as to maximally occupy the TRIMEB cavity (Figure 7 (b)). The two water molecules (shown in pink) are hydrogen bonded to both the host and guest serving to stabilise the complex. The amount of tilt of the guest molecule is measured by the angle between the phenyl ring (mean plane) of the guest molecule and the O4 mean plane of the cyclodextrin in which it is included. For guest A the angle is 59.6(5)˚ and for guest B the angle is 60.7(5)˚. Furthermore, the guest

molecules are rotated with respect to each other such that the angle between the mean planes of molecules A and B is ~17˚, as shown in Figure 8.

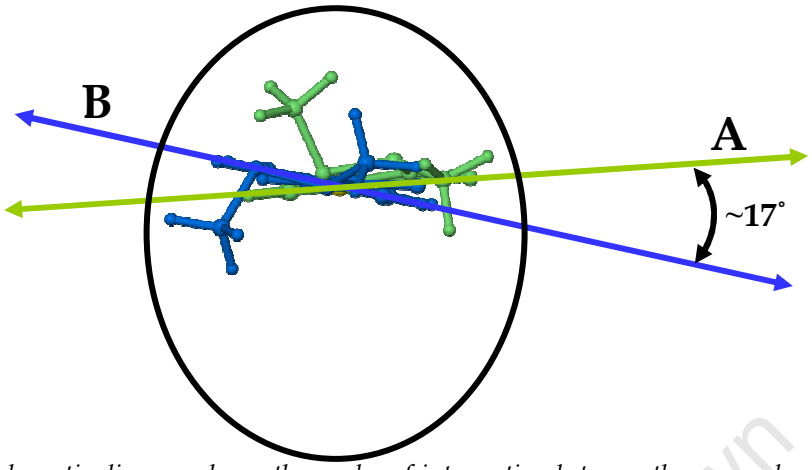

Figure 8. *The schematic diagram shows the angles of intersection between the mean planes of the disordered guest molecules.*

In the case of C2, the complex consists of a single host molecule, a twofold disordered guest molecule, two water molecules with partial occupancy and an ethanol molecule also with partial occupancy. As with complex C1 the twofold disordered guest molecule shares a common bromine atom (Br1 – cyan coloured atom in Figure 9).

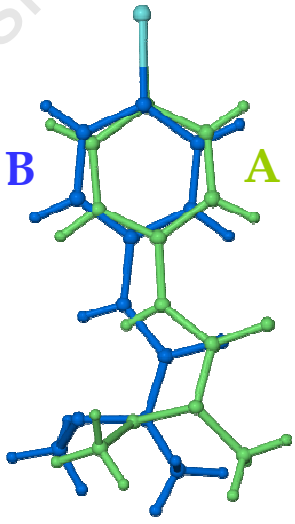

Figure 9. *Twofold disorder of the guest belonging to C2. The shared bromine atom is shown in cyan.*

The guest is also orientated with the bromophenyl moiety buried deep within the cavity while the urea group protrudes from the secondary rim, as shown in Figure 10 (a). The two water molecules are also hydrogen bonded to both the host and

guest and act in the same manner as in C1. The ethanol molecule is also included in the cavity of the TRIMEB host molecule and is hydrogen bonded via its hydroxyl group to a secondary methoxyl group of the host (2.80 Å, 156.0˚) (Figure 10 (b)).

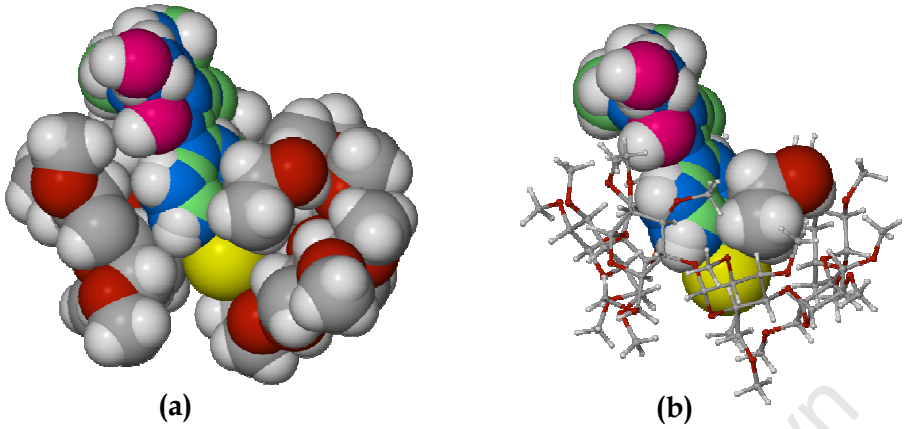

Figure 10. *(a) A cutaway image of the complex C2. (b) shows how the guest molecule is tilted with respect to the host molecule of complex C2. Also shown in (b) is the ethanol molecule which shares the cavity with the guest molecule.*

The guest is tilted with respect to the mean O4 plane such that the major component of the twofold disorder guest A makes an angle of 58.8(1)˚ with the mean O4 plane while the minor component B makes an angle of 64.6(3)˚. Similarly to C1, the guest molecules are rotated such that the angle between the mean planes of molecules A and B is ~7˚(Figure 11).

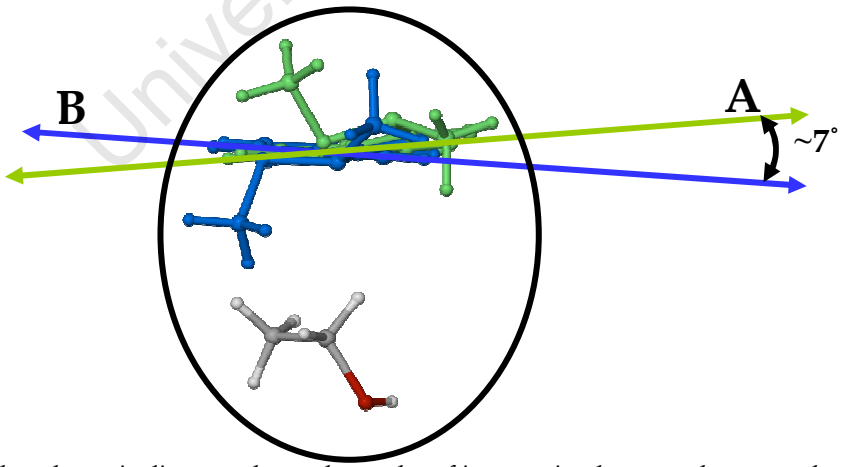

Figure 11. *The schematic diagram shows the angles of intersection between the mean planes of the disordered guest molecules.*

The asymmetric unit of complex C3 consists of a single host molecule, a guest molecule and a water molecule with partial occupancy. Unlike the situation in complexes C1 and C2 the guest is not disordered (Figure 12).

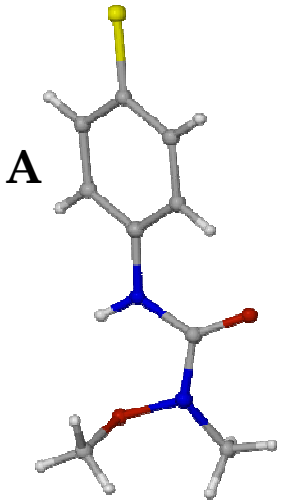

Figure 12. *The guest molecule of complex C3.*

The guest molecule is oriented with the urea group buried deep within the cavity while the chlorophenyl moiety protrudes from the secondary rim, as shown in Figure 13 (a) and (b).

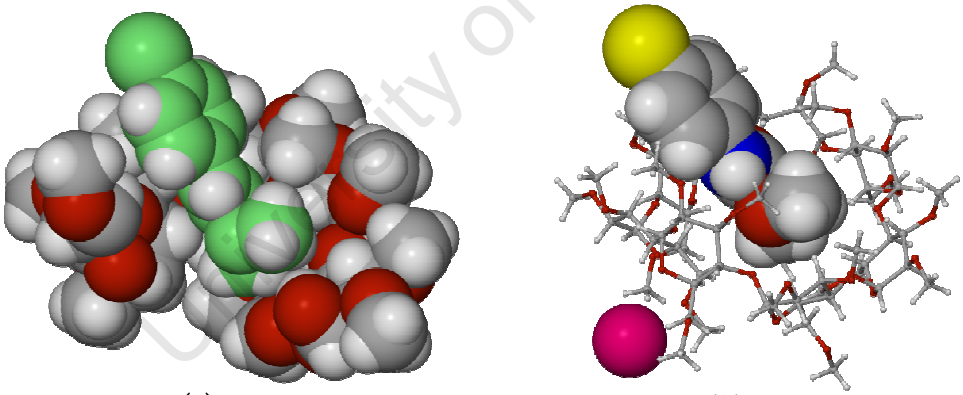

Figure 13. *(a) A cutaway image of the complex C3. (b) shows the tilt of the guest with respect to the host of complex C3.*

The water molecule is located outside the cavity and hydrogen bonds to both the host and guest molecules (Figure 13 (b)). The guest is tilted with respect to the mean O4 plane of the cyclodextrin making an angle of 47.2(2)˚ with it.

Guest conformations

The values reported for the torsion angles of the guests of C1 have small deviations from those reported for the uncomplexed guest. τ_1 ranges from -171(1)˚ to -176(2)˚ while τ_2 ranges from -13(3)˚ to +1(2)˚. τ_3 ranges from -175(1)˚ to +172(1)˚ indicating an 'extended' conformation of the two guests. The relative conformations of the included guests of C1 are compared with those of the uncomplexed guest (Figure 14 (a), (b), (c) and (d)).

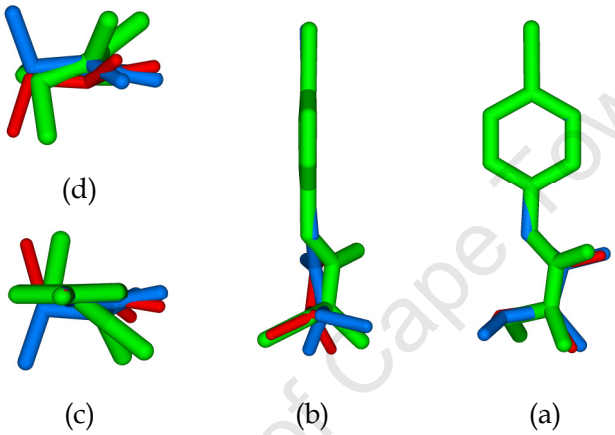

Figure 14. *Relative conformations of the included guests in complex C1 as compared with that of the uncomplexed guest. Guest A - blue, guest B - red, and uncomplexed guest - green.*

The torsion angle τ_4 ranges from -17(1)˚ to +11(1)˚ and τ_6 ranges from -22(4)˚ to +28(1)˚. τ_5 and τ_7 have ranges from -156(1)˚ to +153(1)˚ and from -164(1)˚ to +167(1)˚ respectively. The ranges for τ_8 and τ_9 are -115(3)˚ to +122(9)˚ and -95(1)˚ to +100(1)˚ respectively. The disposition of bond C13-O12 is nearly perpendicular to the mean plane through C9, O10, N11, O12 and C14.

In complex C2 the torsion angle τ_1 equals -170˚. τ_2 ranges from -13(7)˚ to -3(4)˚, a narrow range of values close to the value of τ_2 for the uncomplexed guest. τ_3 ranges from -175(1)˚ to +164(6)˚ indicating an 'extended' conformation for the two disordered guest components. The 'extended' conformation is also owing to the *trans*-planar conformation of the amide group. τ_4 ranges between -14(2)˚ and +17(4)˚. τ_5 spans the range -149(4)˚ to +152(7)˚ and is close to -180/180˚. τ_6 ranges from -32(1)˚ to 33(2)˚ while τ_7 ranges from -168(3)˚ to -166(3)˚. The conformations of the

included guests of C2 are compared with those of the uncomplexed guest (Figure 15 (a), (b), (c) and (d)).

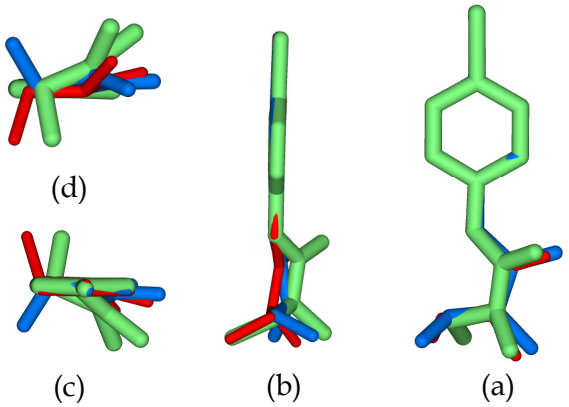

Figure 15. *Relative conformations of the included guests in complex C2 as compared with that of the uncomplexed guest. Guest A - blue, guest B - red, and uncomplexed guest - green.*

τ_8 and τ_9 range from -127(6)˚ to +125(1)˚ and -97(2)˚ to +98(6)˚ respectively, an indication that the disposition of bond C13-O12 is nearly perpendicular to the mean plane passing through C9, O10, N11, O12 and C14.

For complex C3 the torsion angle τ_1 has a value of 155(6)˚. The value of τ_2 is -10(1)˚. As with the uncomplexed guest, τ_3 is very close to -180/180˚ having a value of -176(2)˚. This indicates an 'extended' conformation as with the uncomplexed guest. τ_4 and τ_6 have values of 3(1)˚ and -23(1)˚ respectively. The conformations of the included guest of C3 and the uncomplexed guest are compared in Figure 16 (a), (b), (c) and (d).

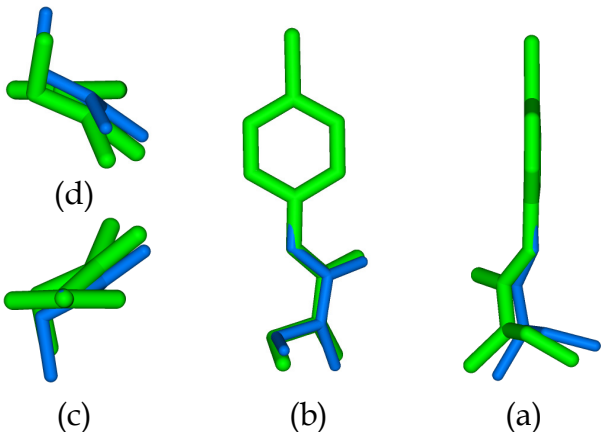

Figure 16. *Relative conformations of the included guest in complex C3 as compared with that of the uncomplexed guest. Guest A – blue and uncomplexed guest - green.*

The values for τ_5 and τ_7 are 150(8)˚ and +171(7)˚ respectively. The values for τ_8 and τ_9 are -103(8)˚ and +101(7)˚ indicative of the C13-O12 bond being almost perpendicular to the mean plane through C9, O10, N11, O12 and C14.

HYDROGEN BONDING INTERACTIONS OF THE GUEST

Host-guest intermolecular interactions

There are three host-guest hydrogen bonds in the structure of C1. All three are C-H•••O hydrogen bonds with a mean C•••O distance of 3.38 Å (range 3.17 – 3.52 Å) and a mean hydrogen bond angle of 138.0˚ (range 120.0 – 173.0˚). A single C-Br•••H(C) interaction was observed with a Br•••H distance of 3.13 Å. There are also several host-guest close contacts. The mean close contact distance is 3.17 Å and the range is 2.98 to 3.30 Å. The host-guest interactions are shown in Figure 17.

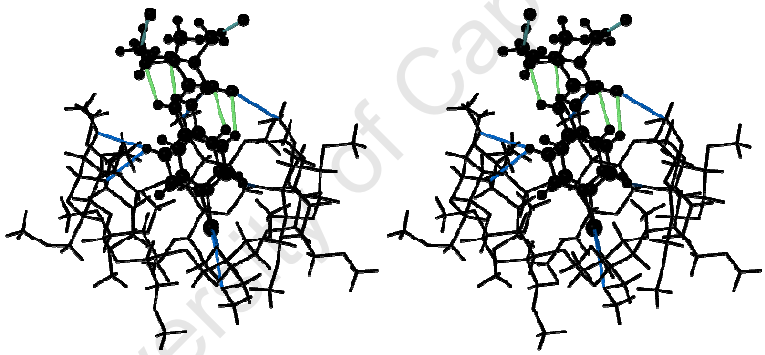

Figure 17. *Stereo view of the intermolecular hydrogen bonds (blue) between the host and guest in the cavity in complex C1. Also shown are the intramolecular hydrogen bonds (green) of the guest molecule. The hydrogen bonds indicated in cyan are those of the guest hydrogen bonding to an adjacent host molecule.*

A single host-guest C-H•••O hydrogen bond is observed in the structure of complex C2. The hydrogen bond length is 3.26 Å with a hydrogen bond angle of 152.0˚. Two C-Br•••H interactions were observed with a mean interaction distance of 3.23 Å (range 3.23 - 3.24 Å). There are also several close contacts between host and guest present in the structure. The mean distance for the close contact interactions is 3.30 Å in the range 3.06 – 3.54 Å. All the host-guest interactions are shown in Figure 18. There is a single ethanol-host hydrogen bond present in the structure. The hydrogen bond length is 2.80 Å while the hydrogen bond angle is 156.0˚.

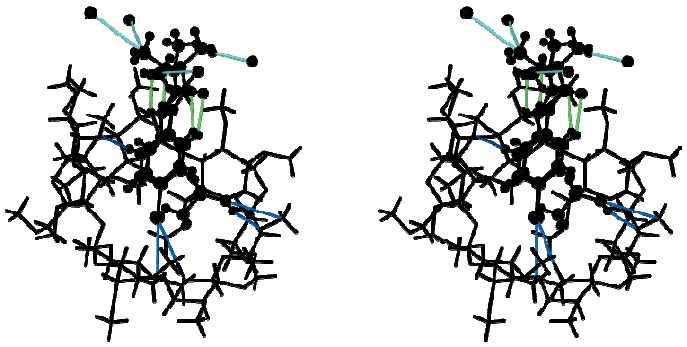

Figure 18. *Stereo view of the intermolecular hydrogen bonds (blue) between the host and guest in the cavity in complex C2. Also shown are the intramolecular hydrogen bonds (green) of the guest molecule. The hydrogen bonds indicated in cyan are those of the guest hydrogen bonding to an adjacent host molecule.*

There are two C-H•••O hydrogen bonds in the structure of complex C3. They have a mean hydrogen bond distance of 3.41 Å (range 3.32 – 3.50 Å) and a mean hydrogen bond angle of 155.0˚ (range 150.0 – 160.0˚). Four C-Cl•••H(C) interactions were observed with a mean Cl•••H interaction distance of 2.99 Å and a range of 2.85 to 3.10 Å. There are also two close contacts present in the structure. The mean close contact distance is 3.27 Å (range 3.17 – 3.37 Å) (Figure 19).

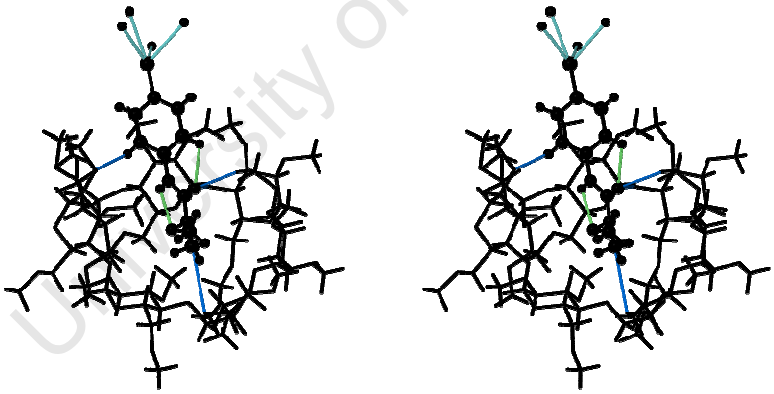

Figure 19. *Stereo view of the intermolecular hydrogen bonds (blue) between the host and guest in the cavity in complex C3. Also shown are the intramolecular hydrogen bonds (green) of the guest molecule. The hydrogen bonds indicated in cyan are those of the guest hydrogen bonding to an adjacent host molecule.*

Guest intramolecular interactions

In complex C1 four intramolecular hydrogen bonds were observed for the guest and its disordered counterpart. Two are N-H•••O hydrogen bonds with N•••O lengths in the range 2.54 - 2.57 Å (mean = 2.55 Å) and the hydrogen bond angle ranging from 110.0 to 111.0° (mean = 110.5˚). For the uncomplexed guest the N•••O distance is 2.57 Å while the angle is 110.0˚. The two remaining bonds are C-H•••O

bonds spanning a narrow range of 2.82 - 2.89 Å (mean = 2.85 Å) while the angular range is 120.0 - 124.0° (mean = 122.0˚). The C•••O bond length for the uncomplexed guest is 2.93 Å while the hydrogen bonding angle is 107.0˚ (Figure 17).

Four intramolecular hydrogen bonds are also observed for the disordered guest of complex C2. The mean N•••O hydrogen bond length for the two N-H•••O interactions is 2.54 Å (range 2.51 – 2.58 Å) while the mean hydrogen bond angle is 110.5˚ (range 109.0 – 112.0˚). The C-H•••O hydrogen bonds have a mean C•••O bond length of 2.87 Å (range 2.85 – 2.88 Å). The mean hydrogen bond angle is 121.5˚ in the range 121.0 to 122.0˚ (Figure 18).

Two intramolecular hydrogen bonds were observed for the guest of complex C3. The N•••O hydrogen bond distance is 2.55 Å while the hydrogen bond angle is 109.0˚. The C•••O hydrogen bond distance is 2.87 Å while the hydrogen bonding angle is 113.0˚ (Figure 19).

The intermolecular bonds serve to stabilise the host-guest interaction while the guest intramolecular interactions stabilise the guest conformation.

Guest-Water interactions

In C1, two close contacts between the guest and included water molecules were observed along with a single N-H•••OW (water) hydrogen bond and a single OW-H•••O hydrogen bond. The length of the N-H•••OW hydrogen bond is 2.93 Å while the angle is 157.0˚. The length of the OW-H•••O hydrogen bond is 3.00 Å while the hydrogen bond angle is 134.0˚. The mean OW•••O close contact distance is 3.28 Å (range 3.12 – 3.44 Å). There is also a single water-to-water (OW-H•••OW) hydrogen bond with a length of 2.87 Å and a hydrogen bond angle of 135.0˚ (Figure 20).

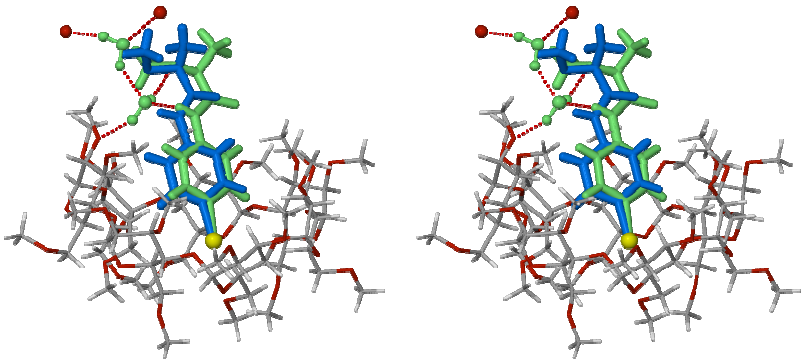

Figure 20. *Stereo view showing the guest-water hydrogen bonds of complex C1. The atoms shown in red belong to an adjacent host molecule.*

In the structure of complex C2 there are two water-guest close contacts and a single N-H•••OW hydrogen bond as well as two OW-H•••O hydrogen bonds, as shown in Figure 21. The N-H•••OW hydrogen bond length is 2.88 Å while the angle is 158.0˚. The two OW-H•••O hydrogen bonds have a mean distance of 3.08 Å (range 2.79 – 3.37 Å) while the mean angle is 141.0˚ (range 128.0 – 155.0˚). The hydrogen bond distance for the C•••OW close contact is 3.22 Å. As with complex C1 there is a single OW-H•••OW hydrogen bond with a length of 2.82 Å and an angle of 144.0˚.

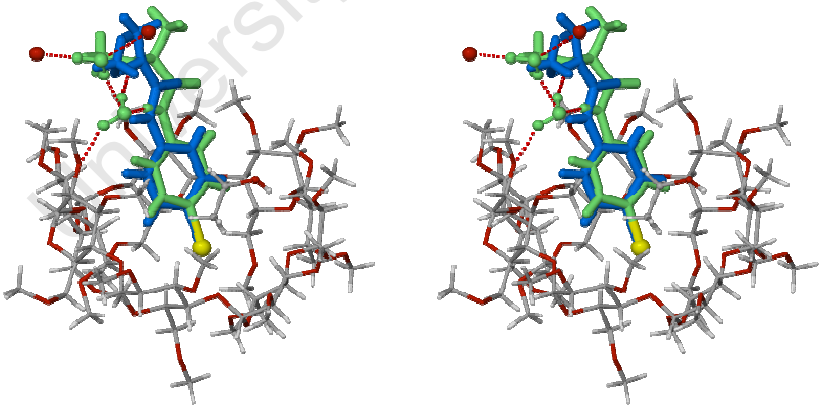

Figure 21. *Stereo view showing the guest-water hydrogen bonds of complex C2. The atoms shown in red belong to an adjacent host molecule.*

A single C-H•••OW hydrogen bond was observed in the structure of C3. The hydrogen bond length is 3.30 Å with a hydrogen bond angle of 136.0˚ (Figure 22).

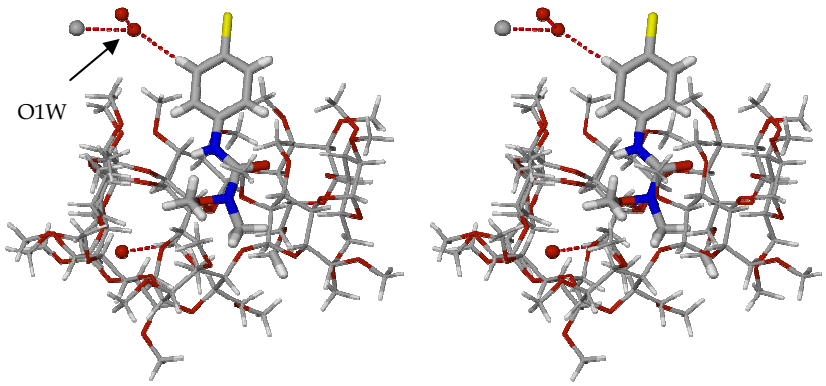

Figure 22. *Stereo view showing the guest-water hydrogen bonds of complex C3.*

CRYSTAL PACKING

Complexes C1, C2 and C3 (Figure 23) pack in the same arrangement adopted by the TRIMEB inclusion complexes of (S)-naproxen and (S)-ibuprofen.[6,8] The complex units pack in a screw channel mode and are arranged in a head-to-tail manner parallel to the *b*-axis. The mean O4 plane is parallel to the *ac*-plane. The packing diagrams serve as visual confirmation that the guests are isolated from neighbouring guest molecules although the protruding guest residues are in contact with methoxyl groups of the neighbouring host molecules.

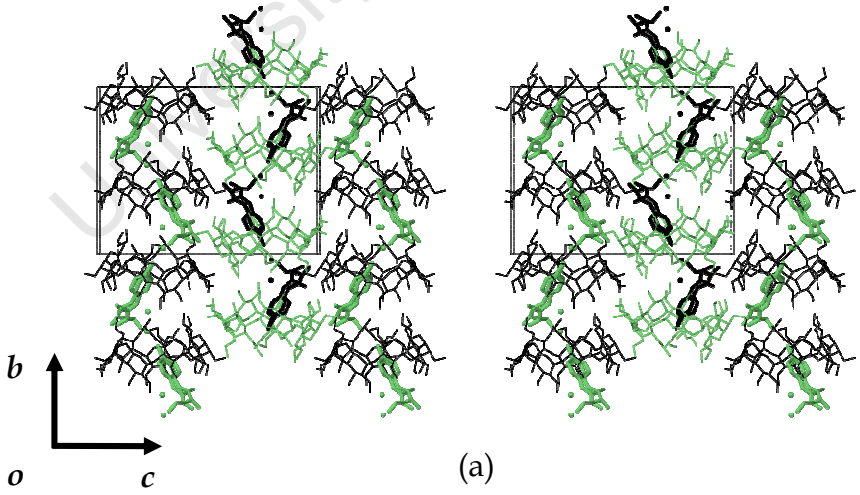

Figure 23. *Packing diagrams of complexes C1 (a), C2 (b) and C3 (c). Hosts and guests are shown in different colours for clarity. (b) and (c) continue on the next page.*

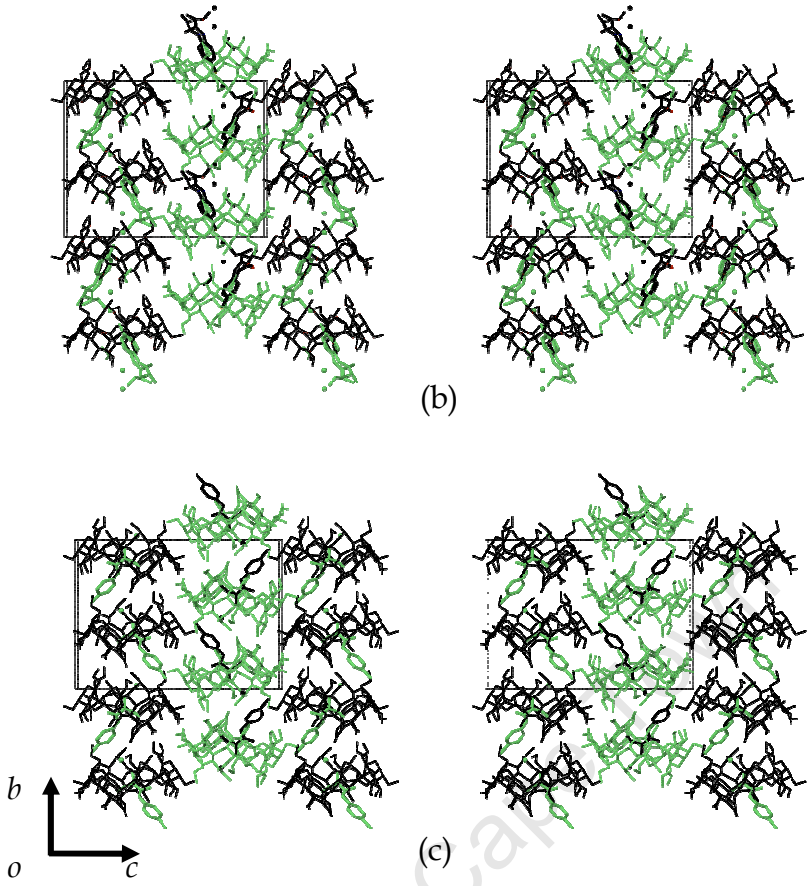

Figure 23. *Packing diagrams of complexes C1 (a), C2 (b) and C3 (c). Hosts and guests are shown in different colours for clarity.*

Comparative PXRDs

The calculated and experimental PXRD traces for complexes C1, C2 and C3 are shown in Figure 24. There is a very close match in peak positions between the traces, differences in peak intensities being due to varying degrees of preferred orientation in the powdered samples.

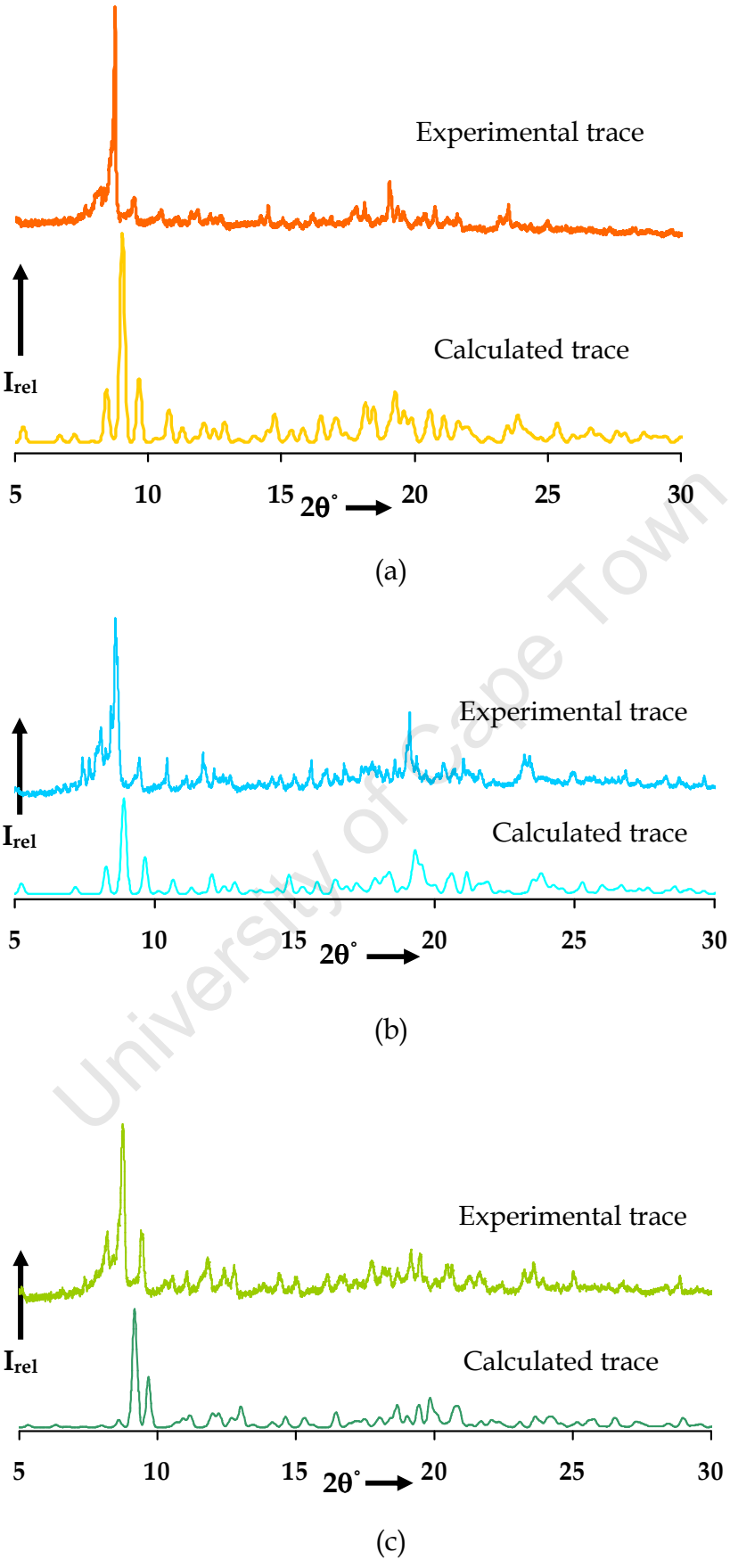

Figure 24. *The experimental and calculated PXRD traces of complexes C1 (a), C2 (b) and C3 (c).*

Each experimental PXRD pattern is in very close agreement with its respective computed pattern. Shifts to slightly higher 2θ angles in the calculated patterns are attributed to the different temperature conditions, namely 293 K (experimental) and 113 K (calculated). The match between the PXRD patterns confirms the phase of the bulk material and that of the single crystal selected for data-collection as being the same.

DISCUSSION

Isostructurality

The complexes C1, C2 and C3 crystallise in the same space group ($P2_12_12_1$), have similar unit cell dimensions (a = ~15, b = ~21, c = ~27 Å, α = β = γ = 90˚) and have PXRD patterns that are similar (Figure 25). In addition, the three - dimensional packing arrangements are the same, implying that the atomic co-ordinates of the host molecules are the same or similar. Furthermore, the host molecules of the three complexes are superimposable (*cf* Figure 4). It therefore follows that C1, C2 and C3 are isostructural. The small differences in the PXRD patterns are primarily due to different guest orientations (C1, C2 *vs* C3) and differences in solvent content.

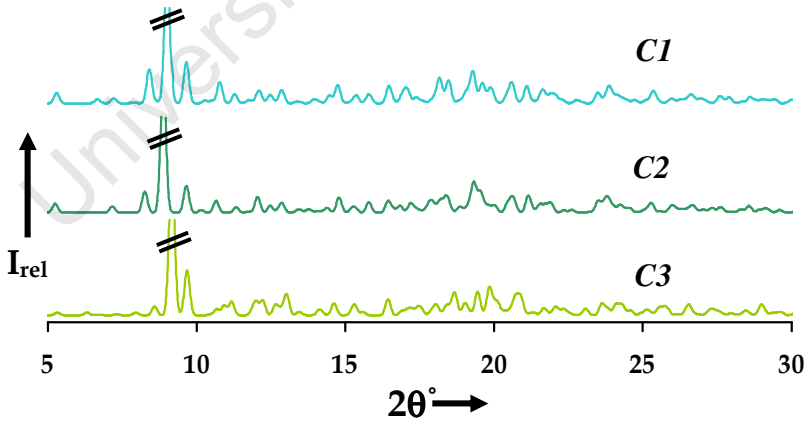

Figure 25. *Stacked calculated PXRD traces of the 1:1 TRIMEB inclusion complexes C1, C2 and C3.*

Conformation of TRIMEB host molecules

The similarity of the hosts of C1, C2 and C3 is reflected in the parameters that describe the conformation of the host, such as those listed in Table 4.

Table 4. *Tabulated geometric parameter ranges for inclusion complexes C1, C2 and C3.*[⊥]

complex	r Å	l Å	a˚	φ˚	t˚	τ_1˚	τ_2˚	[b]d Å
C1	4.65 - 5.25	4.28 – 4.49	121.0 – 136.9	115.1 – 119.6	-28.7 – 21.3	10.4 – 41.3	12.5 – 40.4	0.415
C2	4.64 – 5.25	4.27 – 4.51	121.2 – 137.1	110.9 – 119.5	-32.6 – 19.8	10.5 – 41.2	10.3 – 40.6	0.420
C3	4.63 – 5.28	4.23 – 4.48	119.9 – 136.5	110.2 – 119.8	-45.4 – 23.8	13.4 – 46.7	14.0 – 41.3	0.516

(b) = root mean square deviation of O4 atoms from the O4-heptagon.

Values for **r** and **l** reflect an elliptical distortion of the host for the complexes while the average value of **a** (127.2˚) is smaller than the value for a regular heptagon (128.5). The root mean square deviations of the O4 atoms from the least-squares planes through the O4-heptagons are substantial (Table 4). The torsion angles for complexes C1, C2 and C3 span a wide range and confirm the large deviations reflected by **d** (Table 4). The O4-heptagons have a saddle-like appearance, as mentioned previously. All glucopyranose rings are in the $^4C_1$ conformation.

The tilt angles (τ_1 and τ_2) for the hosts are all positive with τ_1 ranging from 10.4 to 46.7˚ and τ_2 ranging from 10.3 to 41.3˚. The positive tilt angles indicate that the glucose units tilt toward the cavity effectively closing off the primary rim, as mentioned previously.

Table 5. *Close contacts and intra- and intermolecular hydrogen bond distances.*

complex	Intramolecular C-H•••O	Intermolecular C-H-•••O	Host-Water hydrogen bonds	Host-Water close contacts
C1	3.01 – 3.48 Å	3.29 – 3.48 Å	2.71 – 2.77 Å	2.74 - 3.37 Å
	117.0 – 158.0˚	131.0 – 167.0˚	152.0 – 164.0˚	-
C2	3.01 – 3.43 Å	3.37 – 3.48 Å	2.77 – 2.87 Å	2.67 - 3.41 Å
	111.0 – 155.0˚	151.0 – 167.0˚	151.0 – 179.0˚	-
C3	3.01 – 3.48 Å	3.19 – 3.53 Å	3.21 Å	2.83 – 2.84 Å
	124.0 – 167.0˚	124.0 – 167.0˚	161.0˚	-

Intramolecular hydrogen bonds

Several different C-H•••O hydrogen bonds are responsible for the stabilisation of the TRIMEB structure. The average C-H•••O hydrogen bond distance (C•••O) for all three complexes is 3.17 Å while the average for the hydrogen bond angle for all

[⊥] Individual values for parameters reported here appear in the relevant appendix.

three complexes is 132.0˚ (hydrogen bond distance and angular ranges are reported in Table 5).

Intermolecular hydrogen bonds

The function of the host-guest intermolecular hydrogen bonds is to stabilise the three - dimensional structure in the absence of water molecules, which normally perform this function (*i.e.* in hydrated species). The average C-H•••O hydrogen bond distance for the three complexes is 3.38 Å while the average hydrogen bond angle is 152.0˚ (hydrogen bond distance and angular ranges are reported in Table 5).

Water interactions

Complexes C1 and C2 have very similar water contents; both have two water molecules with partial occupancy located within hydrogen bonding distance of the guest in the cavity. These water molecules are involved in hydrogen bonding between the host and guest forming 'water bridges'. In C1, the water molecules are involved in a N-H•••OW hydrogen bond and a OW-H•••O hydrogen bond with the guest. The water molecules also form two OW-H•••O hydrogen bonds with the host molecule. C2 has a single N-H•••OW hydrogen bond and two OW-H•••O hydrogen bonds between the guest and water molecules. There are also two OW-H•••O hydrogen bonds with the host molecule. C3 has only a single water molecule with partial occupancy located outside the cavity. The water molecule is involved in a C-H•••OW hydrogen bond with both the host and the guest. The water molecules of all three complexes are involved in C•••OW and O•••OW close contacts with both the host and guest molecules. The presence of the N-H•••OW and OW-H•••O interactions must contribute to the overall stabilisation of the amido residues inside the cavity.[6,10,11]

GUEST INTERACTIONS

Host-guest interactions

The primary interactions for the series of TRIMEB inclusion complexes are the C-H•••O hydrogen bonds. The mean C-H•••O hydrogen bond distance for the three complexes is 3.37 Å while the mean hydrogen bonding angle is 146.0˚. Several close

contacts have also been observed in the structures. These are C•••C, C•••O and O•••O close contacts. All three structures also have C-Halogen•••H(C) interactions (halogen = Br or Cl). Furthermore, complexes C1 and C2 have C-Br•••O interactions formed between the host and guest. The mean distance for the C-Br•••O interaction is 3.19 Å. A summary of the host-guest interactions occurring in the complexes is provided in Table 6.

Table 6. *Summary of host-guest interactions for C1, C2 and C3.*

Interaction	*C1*	*C2*	*C3*
C-H•••O	3.17 – 3.52 Å 120.0 – 173.0˚	3.26 Å 152˚	3.32 – 3.50 Å 150.0 – 160.0˚
C•••O contacts	2.98 Å	3.06 – 3.36 Å	3.37 Å
C•••C contacts	3.26 Å	3.54 Å	-
O•••O contacts	-	-	3.17 Å
C-Hal•••H(C)[c]	3.13 Å	3.23 - 3.24Å	2.85 - 3.10 Å
C-Br•••O	3.16 Å	3.23 Å	-

(c) Hal = Br or Cl

Guest intramolecular interactions

The intramolecular N-H•••O and C-H•••O hydrogen bonds are retained in the complexed guest molecules. The hydrogen bond distances and angles have undergone some distortion as a result of the inclusion (Table 7).

Table 7. *Intramolecular hydrogen bond distances.*

Complex	*N•••O Å*	*C•••O Å*
C1 and C2	2.51 - 2.58 Å 109.0 - 112.0°	2.82 - 2.89 Å 120.0 - 124.0°
C3	2.55 Å, 109.0°	2.87 Å, 113.0°
uncomplexed guest 1	2.57 Å, 110.0°	2.93 Å, 107.0°
uncomplexed guest 2	2.56 Å, 107.0°	2.92 Å, 106.0°

The different ranges for the hydrogen bond interactions reflect the observed changes in the guest conformation that accompany their inclusion in the host molecules.

Guest Orientation (*modes of inclusion)*

C1 and C2 have similar orientations of the included guest molecules and as it turns out both guest molecules are disordered over two positions. Even the water molecules of both complexes are located in almost identical positions in the cavity. The guest molecules are arranged such that the hydrophobic bromophenyl moiety is

located deep within the hydrophobic cavity of the TRIMEB molecule. The polar urea moiety protrudes from the secondary rim into the interstitial spaces interacting with the included water molecules. The primary methoxyl groups close off the primary rim. The orientations of the guest in C1 and C2 are consistent with the assertions of Lichtenthaler.[12,13] For complex C3, the orientation of the guest molecule is reversed. The more polar urea moiety is located deep within the hydrophobic cavity while the more hydrophobic chlorophenyl moiety protrudes from the secondary rim into the interstitial space. As with complexes C1 and C2 the primary hydroxyl groups close off the primary rim. The orientation of the guest molecule in C3 behaves in a contrary manner to the assertions of Lichtenthaler. However, the origin of the 'inversion' phenomenon must be associated with the small differences in the physical properties of the halogen substituents on the two guests metobromuron (Br) and monolinuron (Cl), but theoretical calculations would be necessary to substantiate this and these were not pursued due to time constraints. On the other hand, to complicate matters, one could also pose the question as to whether different preparative conditions might not produce different complex crystals with opposing guest orientations of e.g. the monolinuron molecule.

CRYSTAL PACKING

Despite the fact that chemically different moieties protrude from the secondary faces, the TRIMEB complexes C1, C2 and C3 crystallise in the space group $P2_12_12_1$. The complex units are arranged in head-to-tail manner along the *b*-direction; the arrangement isolates the guest molecules from other guest molecules.

REFERENCES

1. Barbour, L.J., LAYER, A computer program for the graphic display of intensity data as simulated precession photographs, *J. Appl. Cryst.*, **1999**, 32, 351-352.
2. XPREP, *Data Preparation and Reciprocal Space Exploration*, Version 5.1, (Copyright Bruker Analytical X-ray Systems, **1997**).
3. Otwinowski, Z., Minor, W., *Processing of X-ray Diffraction Data in Oscillation Mode in Methods in Enzymology*, Vol. 276, Carter, C.W., Sweet, R.M., (eds.), Academic Press, New York, **1996**, 307-326.
4. Harata, K., Uekama, K., Otagiri, M., Hirayama, F., *Bull. Chem. Soc. Jpn.*, **1983**, 56, 1732-1736.
5. Harata, K., Uekama, K., Otagiri, M., Hirayama, F., *J. Inclusion Phenom. Mol. Recognit. Chem.*, **1984**, 1, 279-293.
6. Brown, G.R., Caira, M.R., Nassimbeni, L.R. and van Oudtshoorn, B., *J. Inclusion Phenom. Mol. Recognit. Chem.*, **1996**, 26, 281-294.
7. Sheldrick, G.M. SHELXH, *Acta Crystallogr.*, **2008**, *A*64, 112-122.
8. Caira, M.R., Griffith, V.J., Nassimbeni, L.R. and van Oudtshoorn, B., *J. Incl. Phenom. Mol. Recognit. Chem.*, **1994**, 20, 277-290.
9. Harata, K. *Chem. Rev.*, **1998**, 98, 1803-1827.
10. Harding, M.M., MacLennan, M.J. and Paton, R.M., *Nature (London)*, **1978**, 274, 621-623.
11. Caira, M.R., and Dodds, D.R., *J. Inclusion Phenom. Macrocyclic Chem.*, **1999**, 34, 19-29.
12. Lichtenthaler, F.W. and Immel, S., *Starch/Stärke*, **1996**, 48, 145-154.
13. Lichtenthaler, F.W. and Immel, S., *Liebigs Ann.*, **1996**, 48, 27-37.

Chapter 8
THERMAL ANALYSIS OF THE CYCLODEXTRIN INCLUSION COMPLEXES OF 1, 2 AND 3

In this chapter we describe the thermal behaviour of the cyclodextrin inclusion complexes reported in this thesis.

THERMAL STABILITY OF PHENYLUREAS

The relative thermal instability of phenylureas is well documented.[1,2,3,4] With low melting points (95°C for **1**, 81.5°C for **2** and 174.6°C for **3**),[5] the thermal behaviour of the three phenylureas may well be enhanced by their cyclodextrin inclusion. Inside the CD cavity guest molecules are isolated from each other. Therefore, in the absence of the crystalline guest, energy cannot be absorbed and no melt is observed for the guest molecules.[6] The guest molecules are therefore thermally stabilized by their cyclodextrin inclusion.

Isostructural complexes A1 and B1

(β-CD•monolinuron•7.4H_2O and β-CD•metobromuron•8.3H_2O)

HSM

After removal from their mother liquor the crystals of both complexes were dried on filter paper, covered with silicone oil and placed between cover slips. This was done to detect gas evolution (dehydration) through the formation of bubbles upon heating. At the start of the HSM experiment (RT = 25°C) the crystals of both complexes A1 and B1 were clear and translucent (Figure 1, RT). The HSM results shown are for complex B1 and serve only as representative of the behaviour of A1 and B1.

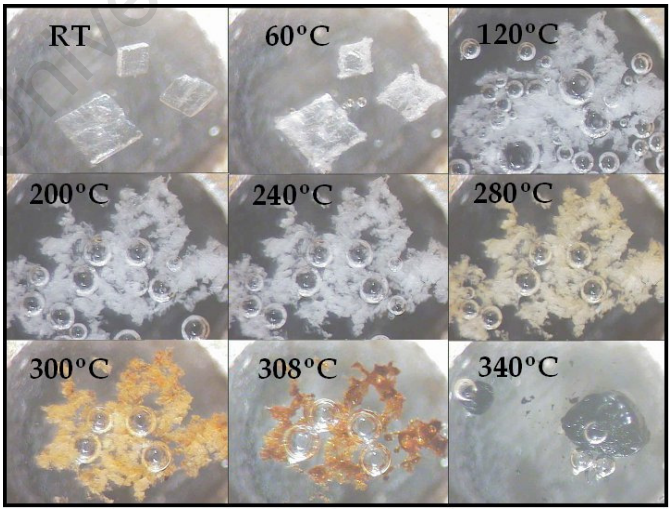

Figure 1. *Representative HSM micrographs of complex B1 recorded at various temperatures.*

The onset of dehydration of both complexes started between 60.0 and 90.0°C, evidenced by bubble formation. The bubbling continued until ~120.0°C and then

ceased. At ~240.0°C the crystals of both complexes underwent a colour change indicating the onset of decomposition. Both complexes melted in the range 300.0 - 315.0°C with complete decomposition by 340.0°C. It is noteworthy that the onset temperatures obtained from HSM are higher than those obtained from TGA and DSC measurements.

TGA

Figures 2 and 3 show the TGA and DSC traces for complexes A1 and B1. The TGA trace for A1 (Figure 2, top) showed a significant mass loss of ~8.9% (for n = 2, where n is the number of measurements taken) in the temperature range 30.0 to 130.0°C♦, represented by **A** in the Figure. The mass loss is equivalent to approximately 7.4 water molecules per complex unit. The second thermal event in the TGA trace is the decomposition of the complex, indicated by **B** in Figure 2 (top) with an onset temperature of ~290.0°C.

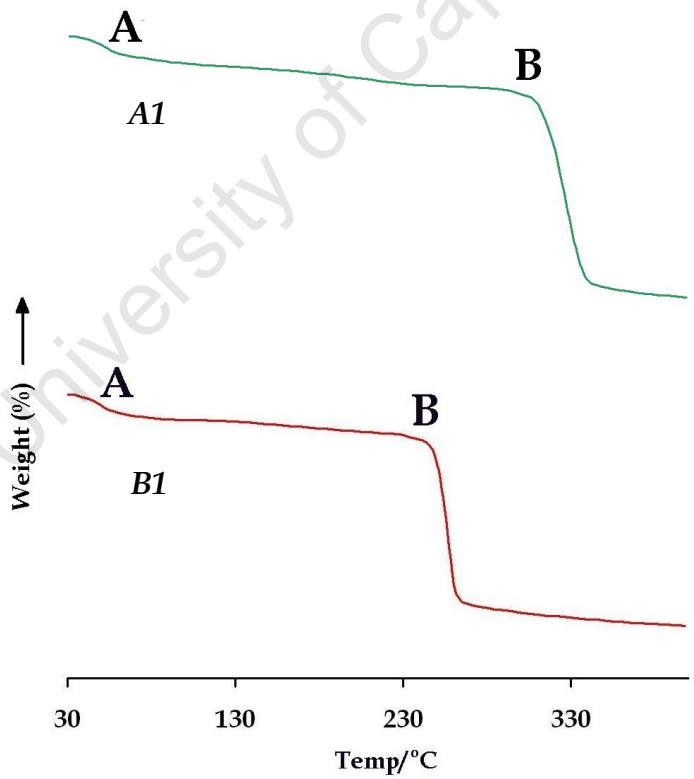

Figure 2. *Stacked TGA traces for isostructural β-CD complexes A1 (top) and B1 (bottom).*

♦ It is noted that the reported range for complex dehydration of 30-130˚C is based on the fact that no major dehydration endotherms occur beyond 130˚C in the DSC traces of the complexes discussed here and throughout. Furthermore, the decreasing gradient of the TGA trace beyond this range may be indicative of early decomposition or evidence of guest loss prior to complete decomposition.

The TGA trace for B1 (Figure 2, bottom) showed a mass loss of ~9.7% in the temperature range 30.0 to 130.0°C, represented by **A**. The mass loss is equal to approximately 8.3 water molecules per complex unit. **B** (Figure 2) indicates decomposition of the complex with an onset temperature of ~230°C.

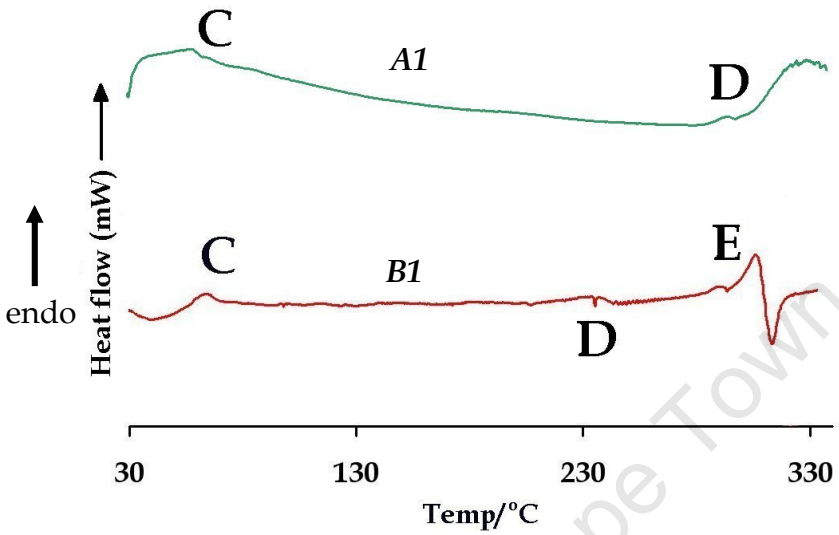

Figure 3. *DSC traces for isostructural β-CD complexes A1 (top) and B1 (bottom).*

DSC

The DSC trace for complex A1 (Figure 3, top) showed two thermal events **C** and **D** with **C** indicating the dehydration of the complex (onset temperature 51.2°C, peak = 60.4°C) followed by the melt and decomposition of the complex indicated by **D** (melt onset = 282.9°C). The trace for complex B1 showed three thermal events namely **C**, **D** and **E**. Event **C** indicates the dehydration of the complex (onset = 59.9°C, peak = 71.6°C) while the exotherm indicated by **D** (exotherm peak temperature = 242.0°C) correlates with the onset of decomposition shown in the TGA trace (Figure 2, bottom). The final thermal event indicated by **E** is the melt and associated exothermic decomposition of the complex (melt onset = 285.3°C, decomposition onset = 315.3°C). The differences in temperature at which the thermal events are observed are due to differences in crystal size, geometry and the conditions under which the HSM and the thermal analyses were performed.

Isostructural complexes A2, A3 and B3

((β-CD)$_2$•(monolinuron)$_2$•22H$_2$O, (β-CD)$_2$•(monuron)$_2$•19.4H$_2$O and (β-CD)$_2$•(metobromuron)$_2$• 21(H$_2$O) respectively)

HSM

Micro-fissures appear in the crystals at ~60.0°C with the first bubbles forming at about 75°C indicating dehydration of complexes A2, A3 and B3. This continued for *ca* 100.0°C with few or no bubbles being formed after 200.0°C. At ~240.0°C the crystals experiences a colour change indicating the onset of decomposition. All three complexes melted in the range 300.0 to 315.0°C with complete decomposition by 340.0°C as shown in Figure 4.

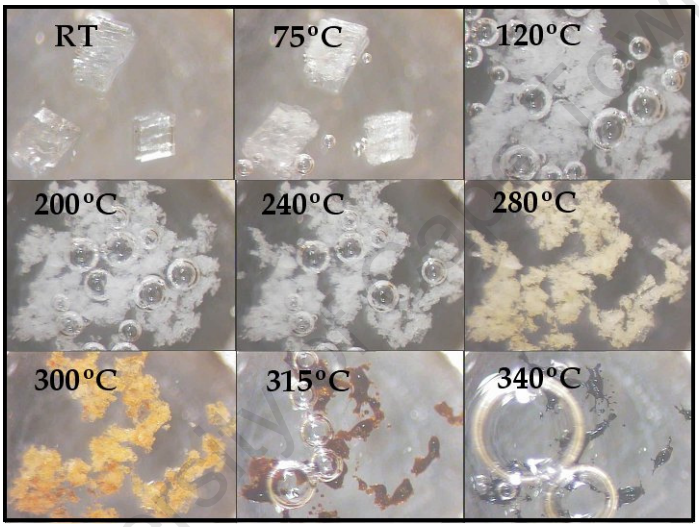

Figure 4. *Representative HSM micrographs of complex B3 recorded at various temperatures.*

TGA

The TGA traces for complexes A2, A3 and B3 each have two thermal events **A** and **B**. In each case, **A** indicates the dehydration of the complexes while **B** indicates the onset of decomposition. The dehydration of complexes A2, A3 and B3 (Figure 5, top, middle and bottom respectively) occur in the temperature range 30.0 to 130.0°C with mass losses of 12.8, 11.7 and 11.9% respectively. The mass losses account for 11 water molecules per complex unit for complex A2, 9.7 water molecules per complex unit for A3 and 10.5 water molecules per complex unit for B3. The decomposition of complexes A2 and A3 occurs at ~290.0°C while the decomposition for complex B3 occurs at ~230.0°C.

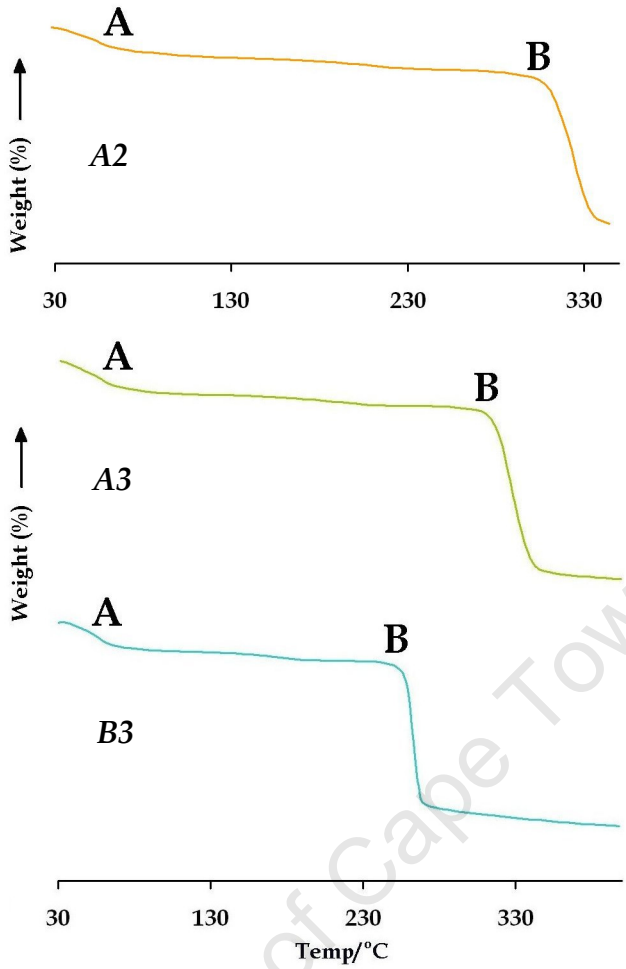

Figure 5. *TGA traces for isostructural β-CD complexes A2 (top), A3 (middle) and B3 (bottom).*

DSC

The DSC traces for the complexes A2, A3 and B3 each showed two thermal events. Event **C** indicates the endotherm for dehydration while **D** indicates the melt and subsequent decomposition of each complex. The broad dehydration endotherm **C** of complex A2 (Figure 6, top) has an onset temperature of ~62.5°C and consists of two peaks which indicate the staggered release of included water molecules. The larger of the two peaks occurs at 77.5°C. The melt endotherm **D** has an onset temperature of 293.8°C and is immediately followed by decomposition. The dehydration endotherm **C** for complex A3 (Figure 6, middle) consists of three peaks and has an onset temperature of 52.1°C. The largest of the three peaks occurs at 68.5°C. Similarly to complex A2 the three peaks indicate staggered release of included water molecules. The onset temperature of the melt indicated by **D** is 281.7°C. The melt is immediately followed by decomposition (Figure 6, middle). For complex B3 (Figure

6, bottom), the dehydration endotherm **C** has an onset temperature of 32.0°C. The multiple peaks present in the dehydration endotherm are indicative of the staggered release of included water molecules.

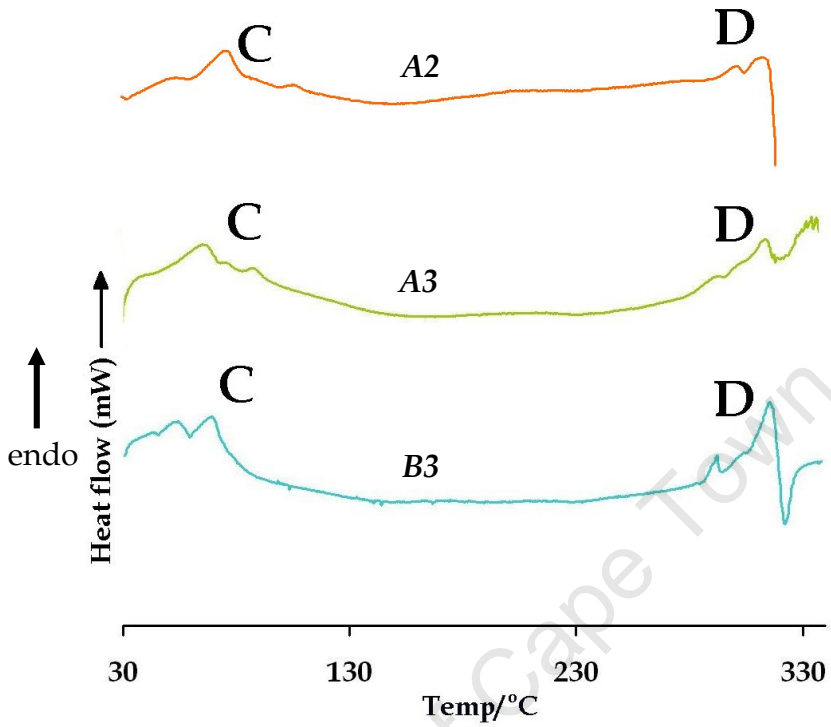

Figure 6. *DSC traces for isostructural β-CD complexes A2 (top), A3 (middle) and B3 (bottom).*

The melt endotherm **D** (B3) has an onset temperature of 288.5°C and is directly followed by a decomposition exotherm with peak temperature 324.0°C.

Complexes B2, B4 and B5

((β-CD)$_2$•(metobromuron)$_2$•20(H_2O), (β-CD)$_2$•(metobromuron)$_2$•25(H_2O) and (β-CD)$_2$•(metobromuron)$_2$•25H_2O respectively)

HSM

The crystals of complexes B2, B4 and B5 are clear and translucent at room temperature (Figure 7, RT). Dehydration of the three complexes occurs in the range from ~60.0 to 200°C while the crystals also become opaque.

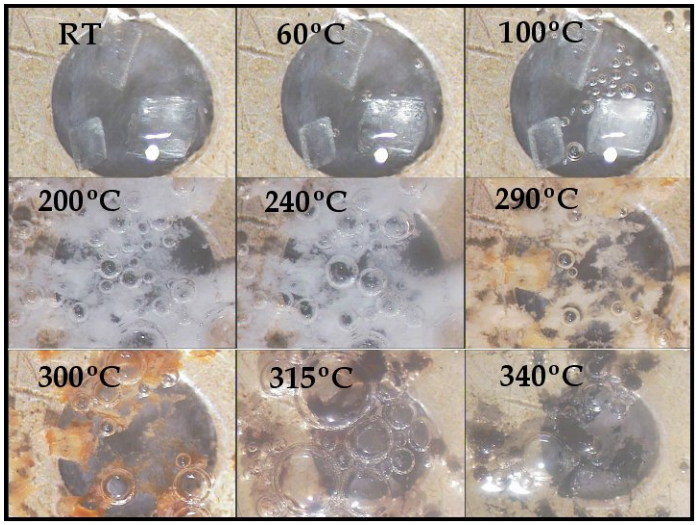

Figure 7. *Representative HSM micrographs of complex B5 recorded at various temperatures.*

Similarly to the other complexes the crystals undergo a colour change from approximately 240.0°C onwards. The crystals melt between 300.0 and 315.0°C and are completely decomposed by 340.0°C.

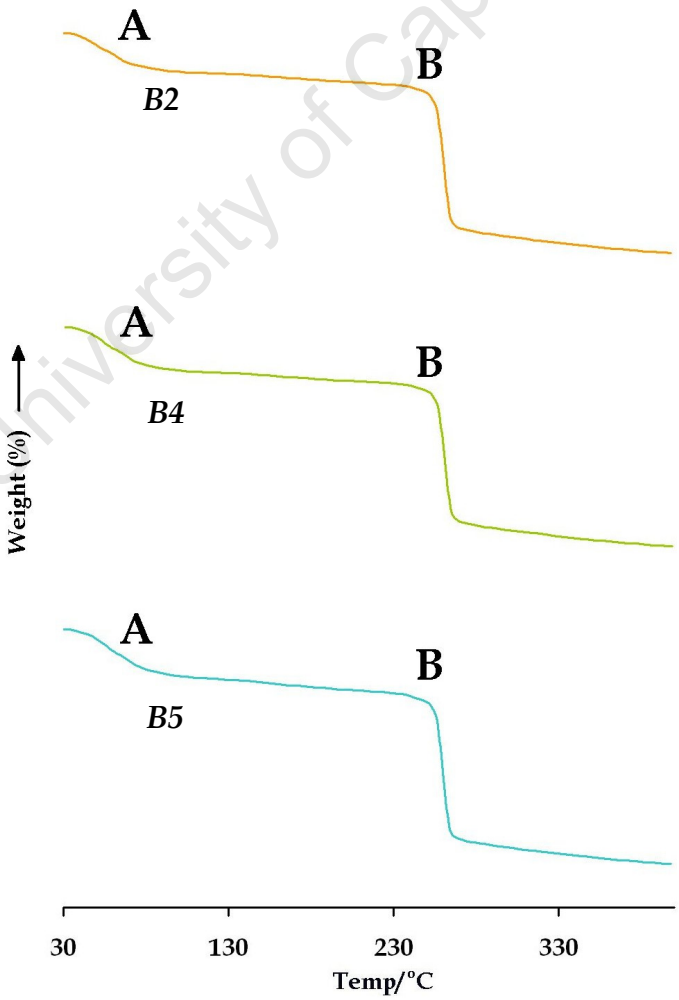

Figure 8. *TGA traces for β-CD complexes B2 (top), B4 (middle) and B5 (bottom).*

TGA

The TGA traces for complexes B2, B4 and B5 (Figure 8) showed mass losses of 11.4% for B2 and 13.9% for both B4 and B5. This is equivalent to 10 water molecules per complex unit for B2 and 12.5 water molecules for both B4 and B5. The dehydration mass loss for complexes B2, B4 and B5 indicated by **A** (Figure 8) occurs in the range 30.0 to 130.0°C. The onset of decomposition indicated by **B** in all three traces occurs at ~230.0°C.

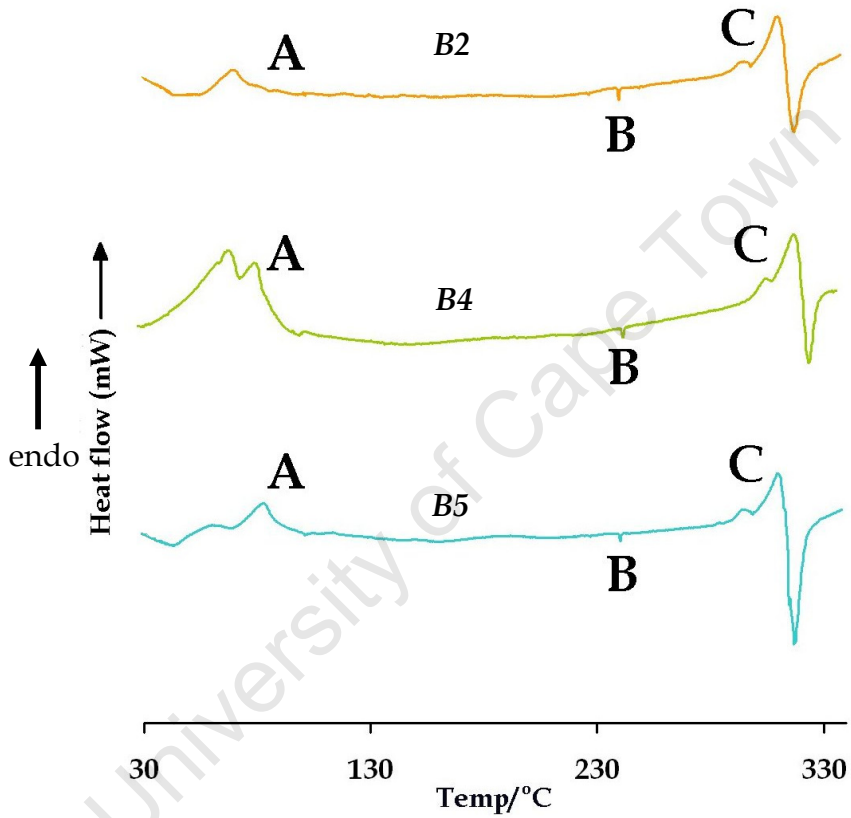

Figure 6. *DSC traces for β-CD complexes B2 (top), B4 (middle) and B5 (bottom).*

DSC

Apart from the dehydration endotherms of complexes B2, B4 and B5, their DSC traces have very similar profiles. The dehydration endotherm **A** of complex B2 (Figure 9, top) consists of a single peak with an onset temperature of 62.2°C. Endotherm **A** for complex B4 (Figure 9, middle) consists of two peaks indicating staggered release of water molecules. The onset temperature of endotherm **A** is 32.3°C and the peak is at 71.3°C. Endotherm **A** for complex B5 (Figure 9, bottom) consists of two peaks and indicates the staggered release of water molecules. The

onset of dehydration for complex B5 is 45.3°C. All three DSC traces have an exotherm **B** at 242.0°C. This exotherm, as previously stated, correlates with the onset of decomposition shown in the TGA traces in Figure 8. Thermal event **C** indicates the melt endotherms of each complex (melt onset temperatures for B2, B4 and B5 are 289.5, 301.3 and 292.2°C respectively). All the melt endotherms are followed by decomposition exotherms having peak temperatures 320.2, 327.2 and 318.4 °C for complexes B1, B2 and B3 respectively.

Isostructural complexes C1, C2 and C3

(TRIMEB•metobromuron•0.5H_2O, TRIMEB•metobromuron•0.38(C_2H_5OH)•0.4(H_2O) and TRIMEB•monolinuron•0.2H_2O respectively)

HSM

The crystals of C1, C2 and C3 (Figure 10) showed the formation of micro-fissures between the temperatures of 40.0 and 120.0°C with simultaneous dehydration. The single bubble present at the top of the micrographs labelled 40.0, 80.0 and 120°C (Figure 10), evidences this. The melt onset of C1, C2 and C3 on HSM was observed at 160.0°C.

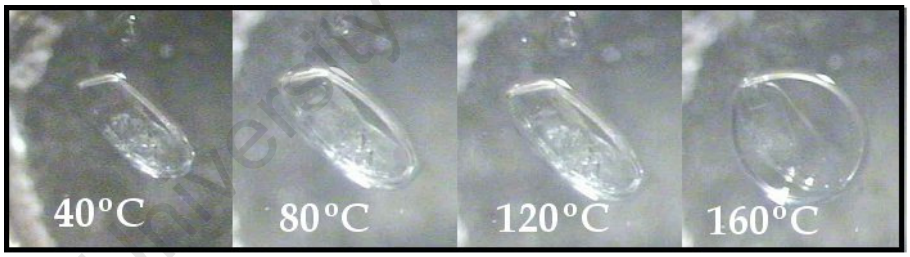

Figure 10. *Representative HSM micrographs of complexes C1 and C3 recorded at various temperatures.*

TGA

The TGA traces for complexes C1 and C3 each have three thermal events **A**, **B** and **C** while the trace for complex C2 has four events namely **A**, **B**, **C** and **D** (Figure 11). Thermal event **A** for traces C1, C2 and C3 indicates the mass loss due to dehydration (range 30 - 50°C). C1, C2 and C3 experience mass losses on dehydration of 0.5, 0.4 and 0.2% respectively. These are equivalent to 0.5 water molecules per complex unit for C1, 0.4 water molecules per complex unit for C2 and 0.2 water molecules per complex unit for C3.

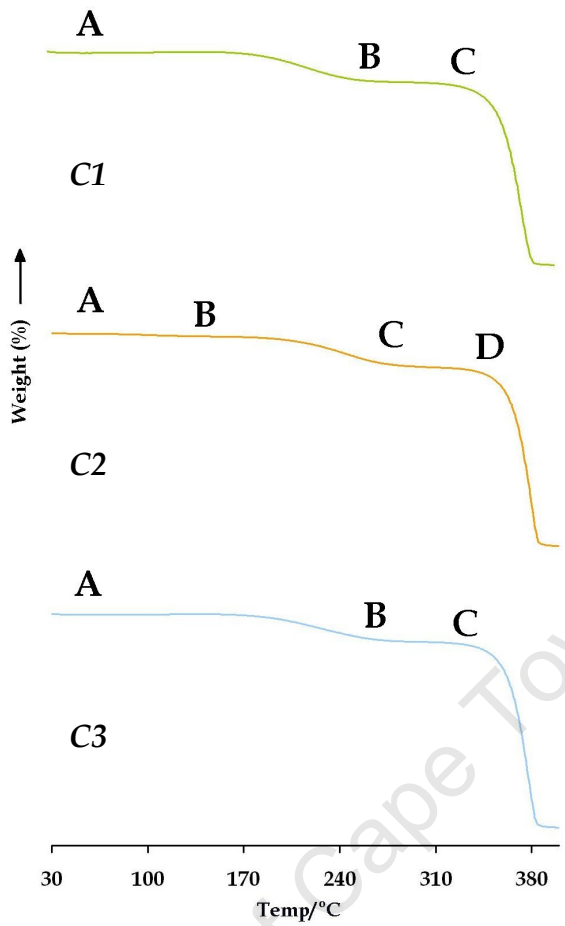

Figure 11. *TGA traces for isostructural TRIMEB complexes C1 (top), C2 (middle) and C3 (bottom).*

In addition, complex C2 experiences a mass loss of 2.8% in the range 60.0 to 170.0°C indicated by **B** (Figure 11, middle). The mass loss is equivalent to 0.4 molecules of ethanol per complex unit. Thermal events **B**, **C** and **B** for complexes C1, C2 and C3 indicate mass losses of ~12.7, 13.2 and 11.3% respectively. These values correlate reasonably with the loss of the included guest molecules.[♣] Events **C**, **D** and **C** indicate the onset of decomposition of C1, C2 and C3 at 290.5, 319.8 and 290.0°C respectively.

DSC

The DSC traces for complexes C1, C2 and C3 all show a single melt endotherm labelled **E** (Figure 12). The onset temperatures for complexes C1 and C3 are 149.3 and 148.6°C respectively while the onset temperature for the melt of complex C2 is

[♣] The mass percentages determined from the TG analysis for the loss of the guest molecules are not equal to the calculated values owing to the thermal events of decomposition and guest loss leading in to each other and partially overlapping.

142.8°C, slightly advanced compared to the same events in C1 and C3. The endotherm also appears broader than those for C1 and C3.

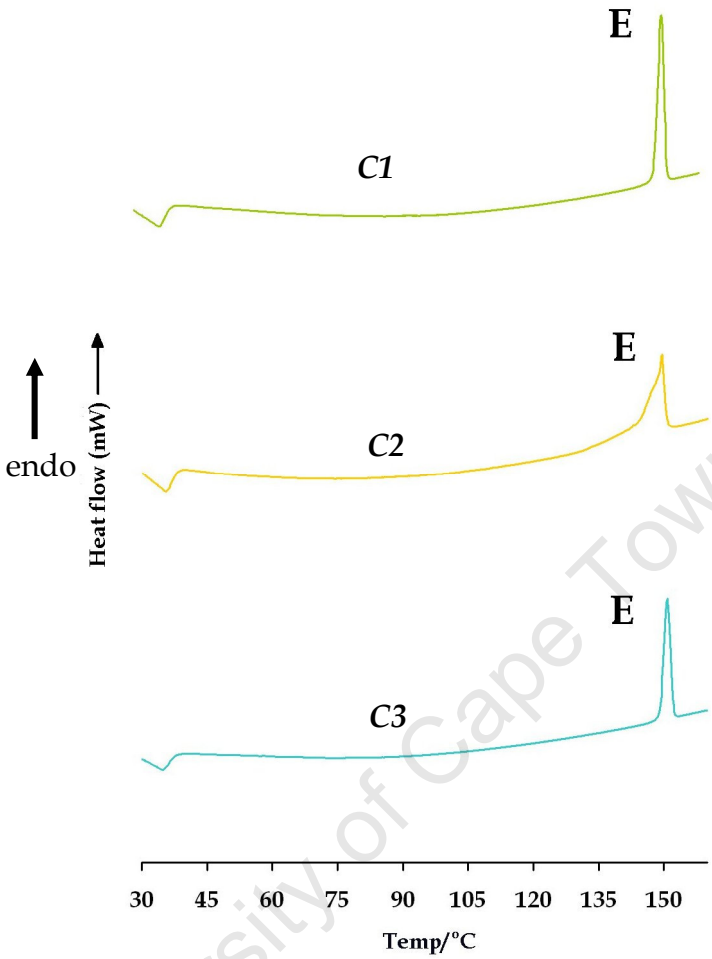

Figure 12. *DSC traces for isostructural TRIMEB complexes C1 (top), C2 (middle) and C3 (bottom).*

This is possibly owing to the simultaneous melt of the complex and the evolution of included ethanol.

DISCUSSION

Generally, the thermo-analytical profile of the cyclodextrin inclusion complexes described here can be divided into three parts, namely a) dehydration, b) melt and c) decomposition.

a) Dehydration - From TGA data (Table 1) dehydration of the β-CD inclusion complexes occurs in the range 30.0 to 130.0°C while the onset temperatures determined from DSC (Table 2) range between 30.0 and 65.0°C. The profile of the dehydration endotherm, in many cases, shows the staggered release of included

water molecules. This can be attributed to the wide range of hydrogen bonding strengths that they experience in different environments in the complex crystals. Dehydration of the TRIMEB inclusion complexes occurs within a smaller temperature range, namely 30.0 to 50.0°C. The smaller range is probably due to the presence of significantly fewer water molecules present in the structure and hence a more restricted range of hydrogen bond strengths.

Table 1. *Thermo-analytical data obtained from TGA for the cyclodextrin inclusion complexes.*

Complex	Mass loss range (°C)	% loss	Mass loss range (°C)	% loss	Mass loss range (°C)	% loss	Decomposition onset (°C)
A1	30.0 - 130.0	8.9	-	-	-	-	250.0
B1	30.0 - 130.0	9.7	-	-	-	-	230.0
A2	30.0 - 130.0	12.8	-	-	-	-	290.0
A3	30.0 - 130.0	11.7	-	-	-	-	290.0
B3	30.0 - 130.0	11.9	-	-	-	-	230.0
B2	30.0 - 130.0	11.4	-	-	-	-	230.0
B4	30.0 - 130.0	13.9	-	-	-	-	230.0
B5	30.0 - 130.0	13.9	-	-	-	-	230.0
C1	30.0 - 50.0	0.5	-	-	148.0 - 290.0	12.7	290.0
C2	30.0 - 50.0	0.4	60.0 - 170.0	2.8	170.0 - 319.8	13.2	319.8
C3	30.0 - 50.0	0.2	-	-	142.0 - 290.0	11.3	290.0

The exothermic event, which occurs between 130.0 and 280.0°C (peak ≈ 242.0°C) for complexes B1, B2, B4 and B5, has been attributed to several different reversible and irreversible phenomena in the literature.[7] Here however, it coincides with the irreversible phenomenon of thermal decomposition.

b) Melt - The onset temperatures for the melting of the β-CD complexes determined from DSC lie within the range 281.7 to 301.3°C while the melt peaks range from 311.0 to 321.0°C. The TRIMEB complexes showed a single endotherm for the melt (DSC) of the inclusion complex with an onset temperature range of 142.8 to 149.3°C. The melt peaks range from 149.4 to 151.3°C. The TGA traces of the three TRIMEB complexes showed a mass loss in the range 142.0 to 319.8°C. The correspondence

between the melt onset on DSC and the onset of the mass loss on TGA further supports the assumption of guest loss during the TG analysis.

Table 2. *Thermo-analytical data obtained from DSC for the cyclodextrin inclusion complexes.*

Complex	Dehydration onset (°C)	Peak (°C)	Exotherm range (°C)	Melt onset (°C)	Melt peak (°C)	Decomposition onset (°C)	Decomp. peak (°C)
A1	51.2	60.4	-	285.3	-	-	-
B1	59.9	71.6	241.0 - 245.0	282.9	313.0	315.3	319.0
A2	62.5	77.5	-	288.5	313.7	-	-
A3	52.1	68.5	-	281.7	316.5	-	-
B3	32.0	70.7	-	293.8	316.3	317.3	324.0
B2	62.2	76.9	241.0 - 244.9	289.5	312.2	317.1	320.2
B4	32.3	71.3	241.0 - 245.0	301.3	321.0	324.5	327.2
B5	45.3	84.4	241.2 - 244.7	292.2	311.7	315.0	318.4
C1	-	-	-	149.3	151.3	-	-
C2	-	-	-	142.8	149.4	-	-
C3	-	-	-	148.6	150.9	-	-

c) Decomposition - The decomposition of complexes A1, A2 and A3 proceeded directly from the melt and are therefore not distinct events. Complexes B1, B2, B3, B4 and B5 have distinct melt endotherms; this is followed by exotherms of decomposition. The TRIMEB complexes were not heated to decomposition. The approximate temperatures of decomposition that were determined using the TGA are reported in Table 1.

Series B1-B5

The only distinction that can be made between the complexes B1-B5 based on their thermal behaviour is the fact that complex B3 does not display an exotherm in the region 240.0-245.0˚C. The absence of the exotherm in this region may be used to identify complex B3. The large differences in onset temperatures for dehydration may result from the differences in particle size and crystal quality since the O•••OW interaction distance ranges are similar for the five complexes. On the other hand the remarkable similarity in the thermal events following dehydration may be related to the fact that all five structures are either C-centred or pseudo-C-centred.

REFERENCES

1. Mahedero, M.C., Muñoz De La Peña, A., Bautista, A. and Aaron, J.J., *J. Inclusion. Phenom. Macrocyclic Chem.*, **2002**, 42, 61-70.
2. Mattern, G.C., Singer, G.M., Louis, J., Robson, M. and Rosen, J.D., *J. Assoc. Off. Anal. Chem.* **1989**, 72, 970-974.
3. Berrada, H., Font, G. and Moltó, J.C., *Chromatographia,* **2001**, 253-262.
4. Escuderos-Morenas, M.L., Santos-Delgado, M.J., Rubio-Barroso, S. and Polo-Díez, L.M., *J. Chromatogr. A.*, **2003**, 1011, 143-153.
5. THE MERCK INDEX, *Thirteenth edition*, **2001**, Merck & Co., Inc., Whitehouse Station, New Jersey, USA.
6. Hedges, A.R., *Chem. Rev.,* **1998**, 98, 2035 - 2044.
7. Giordano, F., Novak, C. and Moyano, J.R., *Thermochimica Acta,* **2001**, 380, 123 - 151.

Chapter 9
CONCLUSION

CONCLUSION

The initial intention of this project was to prepare and characterise inclusion complexes between the phenylureas (**1**, **2**, **3** and **4**) and selected cyclodextrins.

COMPLEX PREPARATION

Preparation of solid-state complexes

The preparation of complexes of **1**, **2**, **3**, and **4** with β- and γ-CD using the kneading method produced cyclodextrin inclusion complexes β-CD•**1**, β-CD•**2**, β-CD•**3**, β-CD•**4**, γ-CD•**1**, γ-CD•**2**, γ-CD•**3** and γ-CD•**4**. α-CD did not complex with any of the guests in the solid-state. The reaction of **1**, **2**, and **3** with β-CD and TRIMEB by means of co-precipitation yielded the cyclodextrin inclusion complexes A1, A2, A3, B1, B2, B3, B4, B5, C1, C2 and C3. Each of these complexes produced crystals suitable for single crystal X-ray diffraction. Compound **4** did not complex using the method of co-precipitation.

Preparation of solution-state complexes

1, **2**, **3**, and **4** formed complexes in solution with α- and β-cyclodextrin. γ-CD does not complex with **1**, **2**, **3**, and **4** in solution.

CHARACTERISATION AND IDENTIFICATION

The physicochemical characterisation of the cyclodextrin inclusion complexes in the solid-state proceeded via single crystal X-ray diffraction, powder X-ray diffraction (PXRD), TGA, DSC, HSM, UV spectrophotometry and elemental analysis. The complexes formed in solution were characterised by means of NMR spectroscopy. HSM, TGA and DSC provided evidence for the thermal stability of the complexes while UV spectroscopy and elemental analysis was used to establish the stoichiometry of the solid-state complexes as 1:1. PXRD provided proof that the bulk material was the same phase as the crystals selected for single crystal X-ray diffraction. For the solution-state complexes, ^{1}H-NMR spectroscopy was used to establish the stoichiometry as 1:1. This technique also provided direct evidence of inclusion through the altered resonances/chemical shifts of characteristic protons upon complexation with α- and β-CD. The information obtained from the

chemically induced shifts permitted the calculation of the stability constants for the complexes in solution. The values obtained for the stability constants lie well below 10 000 M^{-1} which represents the upper limit for ease of guest release, in application of drug complexes in the pharmaceutical industry. By analogy, the cyclodextrin-herbicide complexes reported here should readily release the included guests when employed in agrochemical applications.

SIGNIFICANCE OF THE REPORTED RESULTS

Literature reports of structures of cyclodextrin inclusion complexes of pesticides are rare. It is thus important to emphasize the significance of the crystal structures reported here. We report the isolation of 11 new cyclodextrin inclusion complexes including eight β-CD complexes and three TRIMEB complexes. Amongst the eight β-CD structures we report the remarkable occurrence of as many as five structurally different inclusion complexes with the same host and guest and moreover, the same host-guest stoichiometry (B1, B2, B3, B4 and B5). In addition, we have isolated two forms of a TRIMEB complex, one of which is a quaternary complex consisting of the cyclodextrin host, pesticide guest, a water molecule with partial occupancy and an ethanol molecule with partial occupancy (C1 and C2 respectively). This work has highlighted the importance of strictly maintaining crystallisation conditions in order to generate the same forms consistently. We also report the isolation of a new packing arrangement (CH channel type packing) for complexes crystallising in the space group $P2_1$. Other significant results include α-CD forming complexes with **1**, **2**, **3** and **4** in solution but not in the solid-state while γ-CD forms complexes with **1**, **2**, **3** and **4** in the solid-state but not in solution.

CRYSTAL STRUCTURES

All the crystal structures reported here except for one (C3) display considerable guest disorder, the resolution of which presented significant challenges. The host cyclodextrin molecules also exhibit disorder, to an extent not reported previously. Structures B1 to B5 as well as structures C1, C2 and C3 display different modes of guest inclusion. This work has also resulted in the isolation of isostructural complexes A1 and B1 which crystallise in the space group C2 (a ~ 19 Å, b ~ 24 Å, c ~

16 Å, β ~ 108.0°), isostructural complexes A2, A3 and B3 crystallising in the space group P1 (a ~ b ~ c ~ 15 Å, α ~ 87.0°, β ~ 97.0°, γ ~ 103.0°) and isostructural complexes C1, C2 and C3 belonging to the space group $P2_12_12_1$ (a ~ 15 Å, b ~ 21 Å, c ~ 27 Å, α = β = γ = 90.0°).

Isostructurality

The principles of isostructurality were used in the identification of kneaded complexes of β-CD and γ-CD with **1**, **2**, **3**, and **4**. It enabled the determination of the space group as well as approximate unit cell dimensions of the complexes in the absence of single crystal X-ray data.

ONGOING WORK

The investigation of other cyclodextrin inclusion complexes also displaying the phenomenon of crystal multiplicity is currently underway at the Centre for Supramolecular Chemistry Research at the University of Cape Town.

FUTURE WORK

Future work includes testing the soil mobility of the pesticide-cyclodextrin inclusion complexes against that of the free uncomplexed pesticide. Another goal is the determination of the degradation products of the included guest under conditions of acid and base hydrolysis. We also intend determining the effectiveness of the complex at inhibiting its target pest versus the effectiveness of the uncomplexed guest. Furthermore, the most important aspect of this type of study would be the determination of the bioavailability of the guest when administered in the form of the cyclodextrin inclusion complex.

FINAL COMMENTS

The author believes that the intended aims of this thesis have been achieved, namely the preparation of cyclodextrin inclusion complexes of the phenylurea herbicides via kneading and co-precipitation methods as well as their physicochemical characterisation. We have amply demonstrated the thermal stabilities of the inclusion complexes as superior to those of the respective uncomplexed guests by

means of HSM, TGA and DSC. We have established with the aid of PXRD and the principles of isostructurality the formation of inclusion complexes, determined the space groups of these complexes and obtained their approximate unit cell dimensions. Furthermore, we have established complex formation between selected cyclodextrins and the phenylurea pesticides in solution using ^{1}H-NMR spectroscopy. We have also determined the complex stoichiometries and their stability constants in solution using a specialised program for this purpose. We have isolated multiple crystal forms of CD inclusion complexes by changing the conditions of crystallisation such as temperature and the solvent medium. We have also examined the solid-state features of the inclusion complexes using single crystal X-ray diffraction. The structural and thermal data reported here will be of crucial significance in any future development of these inclusion complexes for practical applications.

Supplementary crystallographic information on each solved structure in this thesis has been saved in the folder Appendix on the disk attached to the inside back cover of this thesis. Files relating to a particular structure are saved in a subfolder named according to the name used in this thesis. The files may be viewed with WORDPAD or NOTEPAD.